Towards macrocyclic ionic liquids: novel ammonium salts based on tetrasubstituted *p-tert*-butylthiacalix[4]arenes

Pavel L. Padnya,[a,b] Elena A. Andreyko,[a] Polina A. Gorbatova,[c] Viktor V. Parfenov,[c] Ildar Kh. Rizvanov[d] and Ivan I. Stoikov*[a]

[a]*Kazan Federal University, A.M. Butlerov Chemical Institute, 420008 Kremlevskaya, 18, Kazan, Russian Federation*
[b]*RUDN University, Faculty of Science, Organic Chemistry Department, 117198 Miklukho-Maklaya St., 6, Moscow, Russian Federation*
[c]*Kazan Federal University, Institute of Physics 420008, Kremlevskaya, 18, Kazan, Russian Federation*
[d]*A. E. Arbuzov Institute of Organic and Physical Chemistry, Kazan Scientific Centre of the Russian Academy of Sciences, 420088 Kazan, Russian Federation*

Electronic Supplementary Information

Table S1. Characteristic chemical shifts of protons in ^{1}H NMR spectra of compounds **5-72**.

thiacalixarene	*t*-Bu	O-CH_2CO	Ar-H	CONH
5 [a]	1.11	4.99	7.35	8.49
6 [a]	1.11	4.99	7.35	8.53
7 [a]	1.10	4.91	7.38	9.13
8 [a]	1.11	4.99	7.36	8.75
9 [a]	1.08	4.82	7.39	8.56
10 [a]	1.12	5.03	7.36	8.68
11 [b]	1.08	4.84	7.40	8.54
12 [a]	1.07	4.82	7.39	8.53
13 [a]	1.10	4.81	7.33	8.63
14 [a]	1.11	4.97	7.34	8.74
15 [a]	1.11	4.99	7.34	8.82
16 [a]	1.10	5.03	7.32	9.08
17 [a]	1.10	4.97	7.33	9.03
18 [a]	1.09	4.93	7.30	9.01
19 [a]	1.12	4.98	7.35	8.94
20 [b]	1.08	4.86	7.40	8.94
21 [b]	1.08	4.87	7.40	8.81
22 [b]	1.21	3.98	7.60	8.01
23 [b]	1.21	3.99	7.60	8.03
24 [b]	1.20	4.01	7.60	8.10
25 [b]	1.20	4.00	7.60	8.05
26 [b]	1.20	3.98	7.60	8.06
27 [a]	1.20	3.99	7.60	8.04
28 [b]	1.19	3.96	7.59	8.04
29 [b]	1.20	3.99	7.59	8.06
30 [b]	1.20	3.99	7.60	8.05
31 [b]	1.22	4.05	7.61	8.18
32 [b]	1.22	4.03	7.61	8.13
33 [b]	1.19	4.20	7.60	8.38
34 [b]	1.22	4.04	7.60	8.27
35 [b]	1.21	4.08	7.60	8.29
36 [b]	1.21	4.08	7.60	8.27
37 [b]	1.21	4.05	7.60	8.23
38 [b]	1.22	4.09	7.60	8.27
39 [b]	1.08	4.82	7.40	8.49
40 [b]	1.08	4.82	7.40	8.49
41 [a]	1.10	4.91	7.35	8.29
42 [a]	1.11	4.89	7.35	8.23
43 [b]	1.08	4.79	7.39	8.47
44 [a]	1.11	4.89	7.35	8.23
45 [b]	1.08	4.80	7.40	8.50
46 [b]	1.08	4.80	7.39	8.50
47 [b]	1.07	4.80	7.38	8.50
48 [a]	1.11	4.91	7.36	8.38
49 [a]	1.11	4.91	7.36	8.40
50 [a]	1.10	4.95	7.35	8.51
51 [a]	1.11	4.90	7.36	8.36
52 [b]	1.08	4.85	7.40	8.78

53 [b]	1.07	4.83	7.39	8.76
54 [b]	1.07	4.83	7.45	8.87
55 [b]	1.08	4.84	7.40	8.81
56 [b]	1.21	4.00	7.60	8.03
57 [b]	1.21	4.00	7.60	8.03
58 [b]	1.20	4.03	7.60	8.07
59 [b]	1.20	4.00	7.59	8.02
60 [b]	1.20	3.99	7.61	8.06
61 [b]	1.20	3.99	7.59	8.03
62 [b]	1.20	3.97	7.59	8.02
63 [b]	1.20	4.01	7.59	8.03
64 [b]	1.21	3.99	7.60	8.04
65 [b]	1.22	4.05	7.60	8.17
66 [b]	1.21	4.04	7.60	8.14
67 [b]	1.19	4.20	7.61	8.34
68 [b]	1.21	4.08	7.61	8.22
69 [b]	1.21	4.07	7.69	8.22
70 [b]	1.21	4.05	7.60	8.22
71 [b]	1.21	4.04	7.59	8.21
72 [b]	1.21	4.07	7.60	8.23

[a] $CDCl_3$, [b] DMSO-d_6

Fig. S1. ^{1}H NMR spectrum of 5,11,17,23-tetra-*tert*-butyl-25,26,27,28-tetrakis[(N-(3',3'-dimethyl-3'-(pentoxycarbonylmethyl)-ammoniumpropyl)carbomoylmethoxy]-2,8,14,20-tetrathiacalix[4]arene tetrabromide (*cone* **9**), **$CDCl_3$, 298 K, 400 MHz**

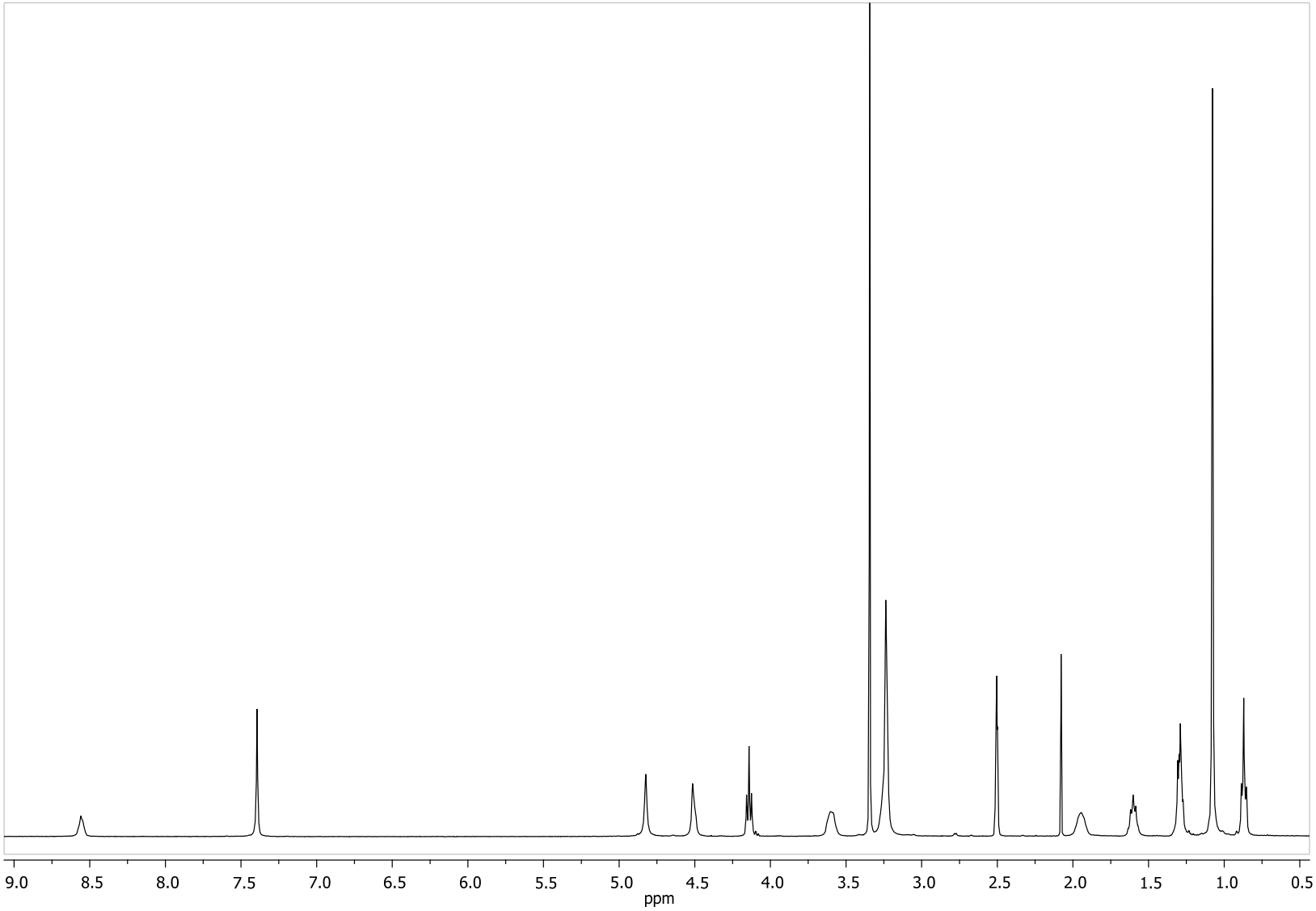

Fig. S2. ^{1}H NMR spectrum of 5,11,17,23-tetra-*tert*-butyl-25,26,27,28-tetrakis[(N-(2',2',2'-triethyl)ammoniumethyl)carbomoylmethoxy]-2,8,14,20-tetrathiacalix[4]arene tetraiodide (*cone* **15**), **$CDCl_3$, 298 K, 400 MHz**

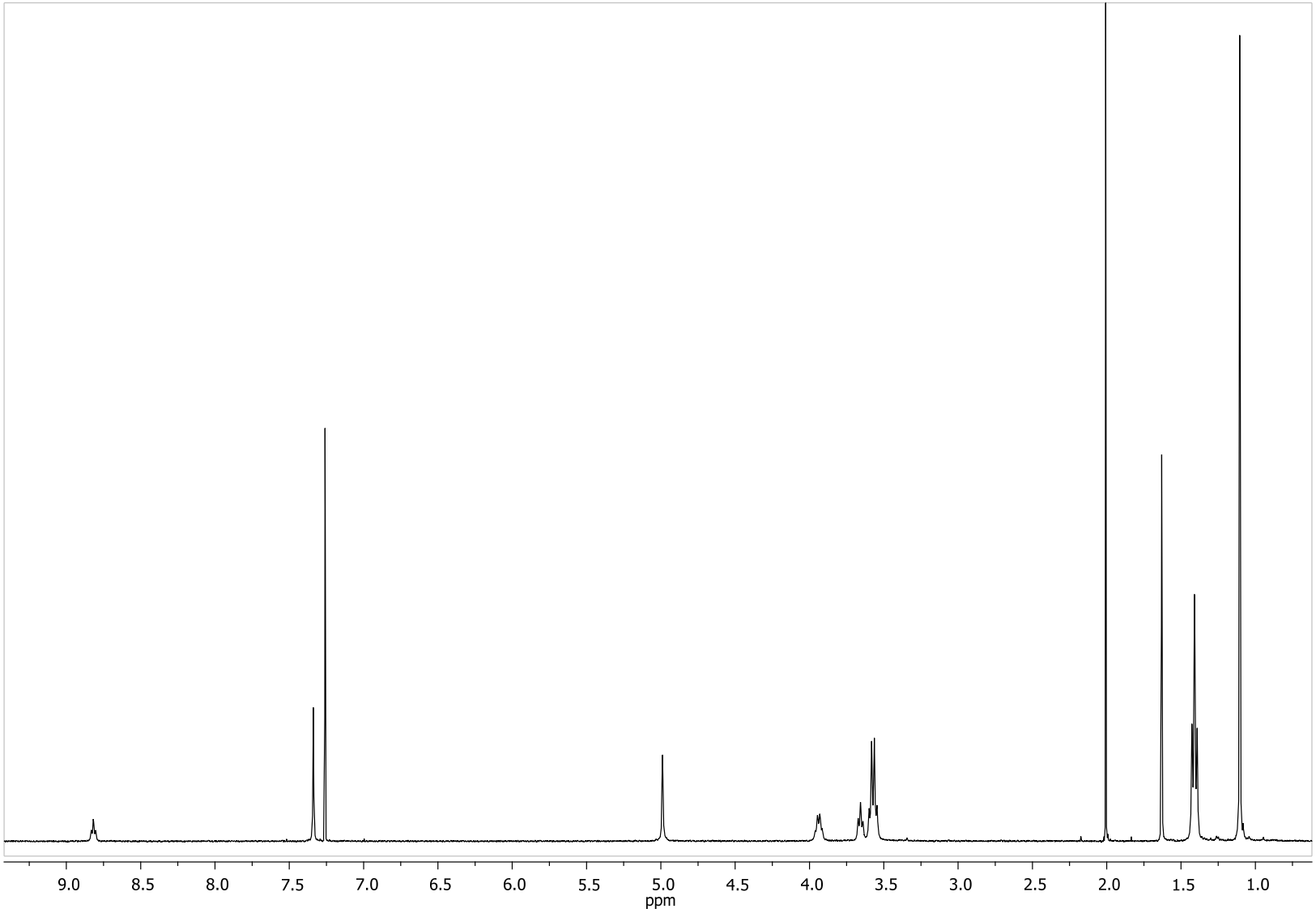

Fig. S3. ^{1}H NMR spectrum of 5,11,17,23-tetra-*tert*-butyl-25,26,27,28-tetrakis[(N-(2',2'-diethyl-2'-benzyl)ammoniumethyl)carbomoylmethoxy]-2,8,14,20-tetrathiacalix[4]arene tetrabromide (*cone* **16**), **$CDCl_3$, 298 K, 400 MHz**

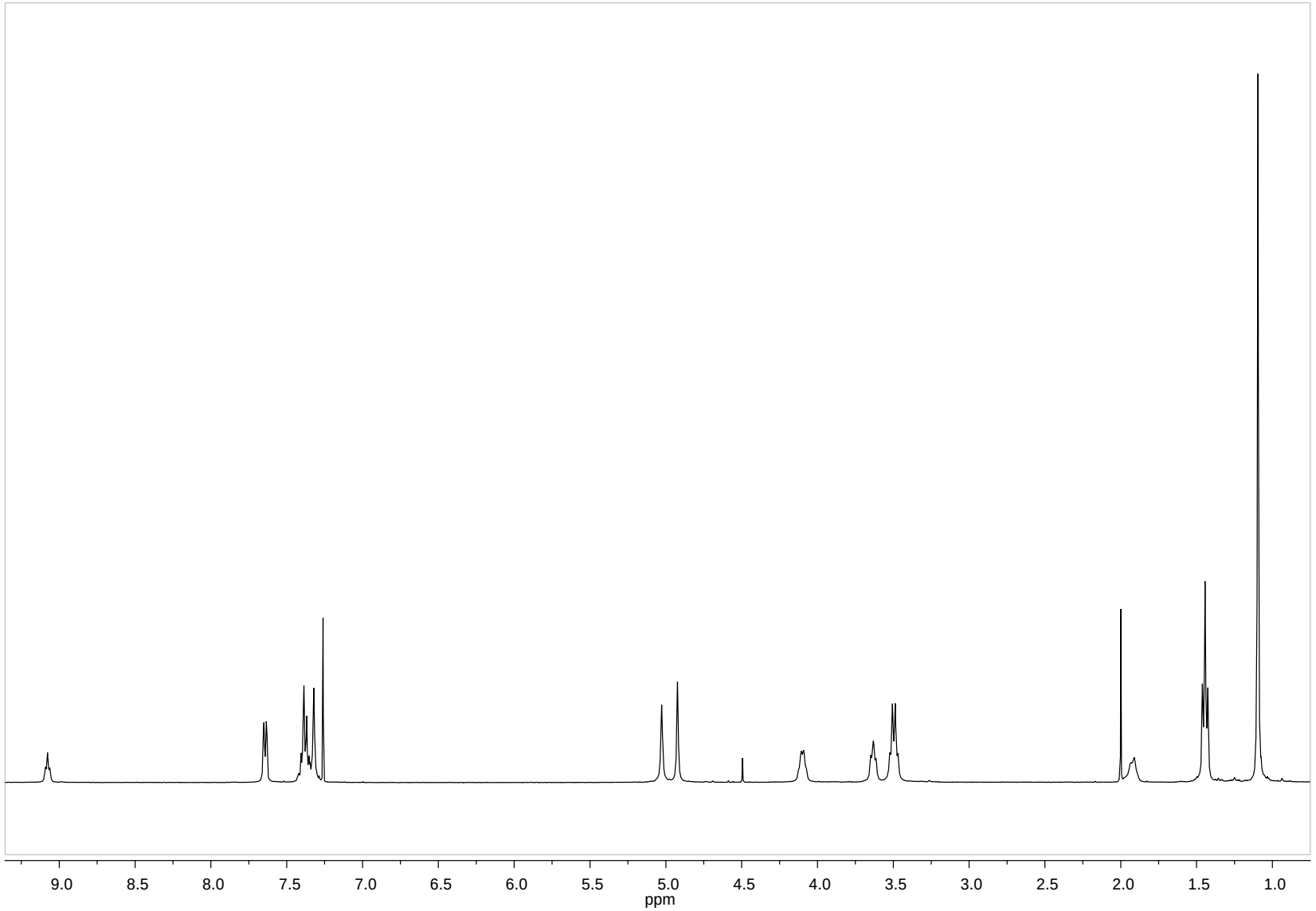

Fig. S4. ^{1}H NMR spectrum of 5,11,17,23-tetra-*tert*-butyl-25,26,27,28-tetrakis[(N-(2',2'-diethyl-2'-(ethoxycarbonylmethyl)-ammoniumethyl)carbomoylmethoxy]-2,8,14,20-tetrathiacalix[4]arene tetrabromide (*cone* **17**), **$CDCl_3$, 298 K, 400 MHz**

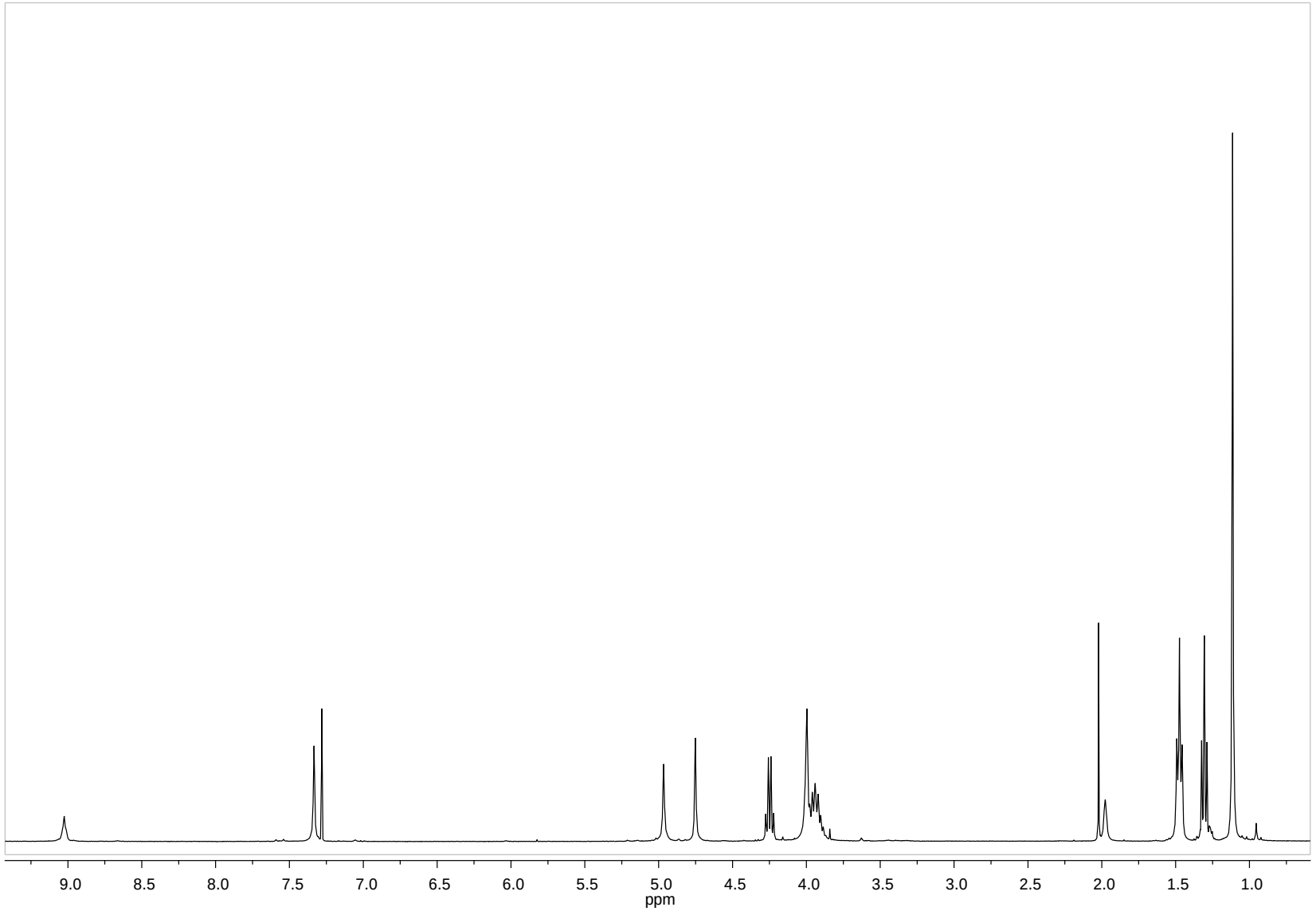

Fig. S5. ^{1}H NMR spectrum of 5,11,17,23-tetra-*tert*-butyl-25,26,27,28-tetrakis[(N-(2',2'-diethyl-2'-(pentoxycarbonylmethyl)-ammoniumethyl)carbomoylmethoxy]-2,8,14,20-tetrathiacalix[4]arene tetrabromide (*cone* **18**), **$CDCl_3$, 298 K, 400 MHz**

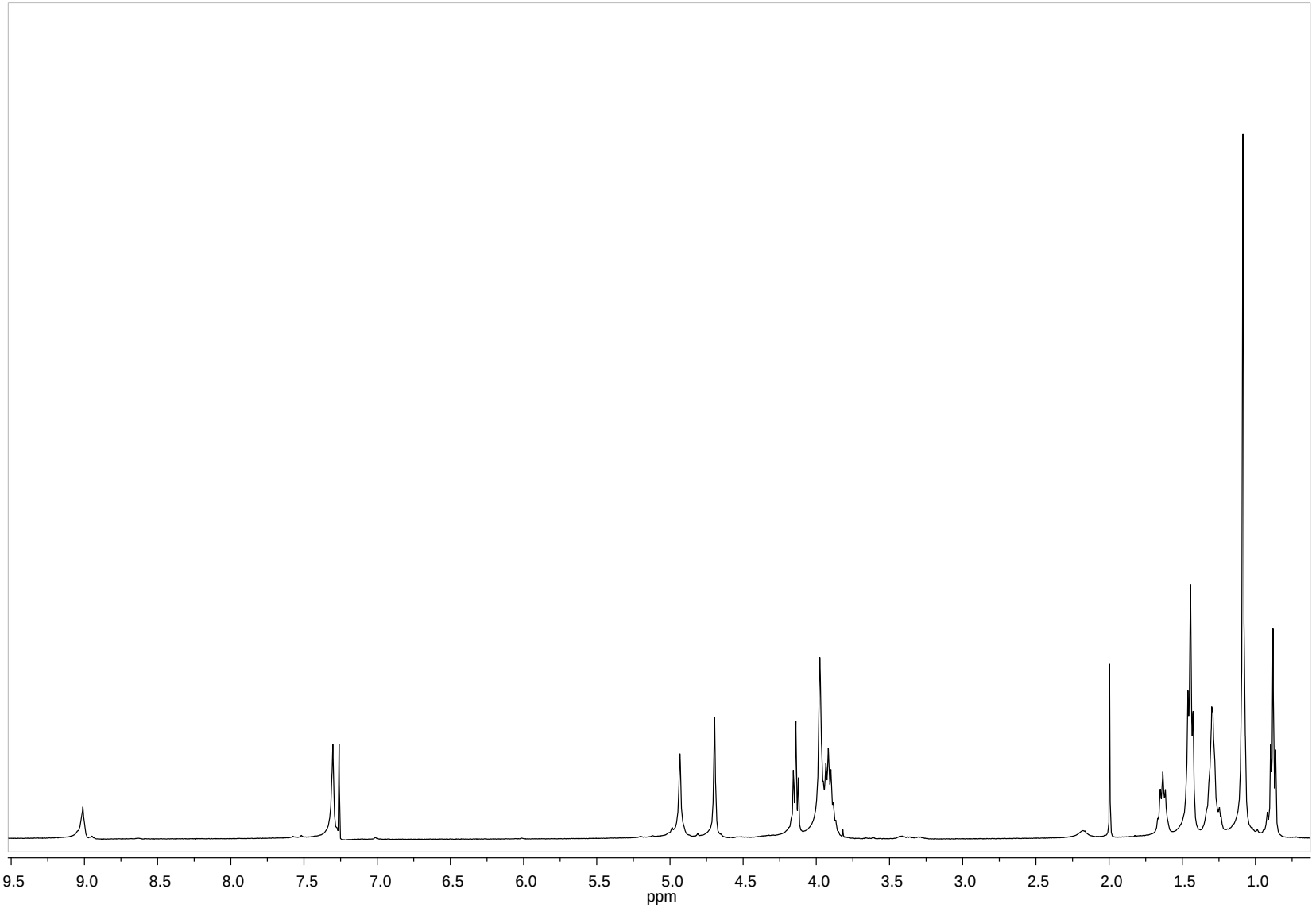

Fig. S6. ^{1}H NMR spectrum of 5,11,17,23-tetra-*tert*-butyl-25,26,27,28-tetrakis[(N-(3',3',3'-trimethyl)ammoniumpropyl)carbomoylmethoxy]-2,8,14,20-tetrathiacalix[4]arene tetraiodide (*1,3-alternate* **22**), **DMSO-d_6, 298 K, 400 MHz**

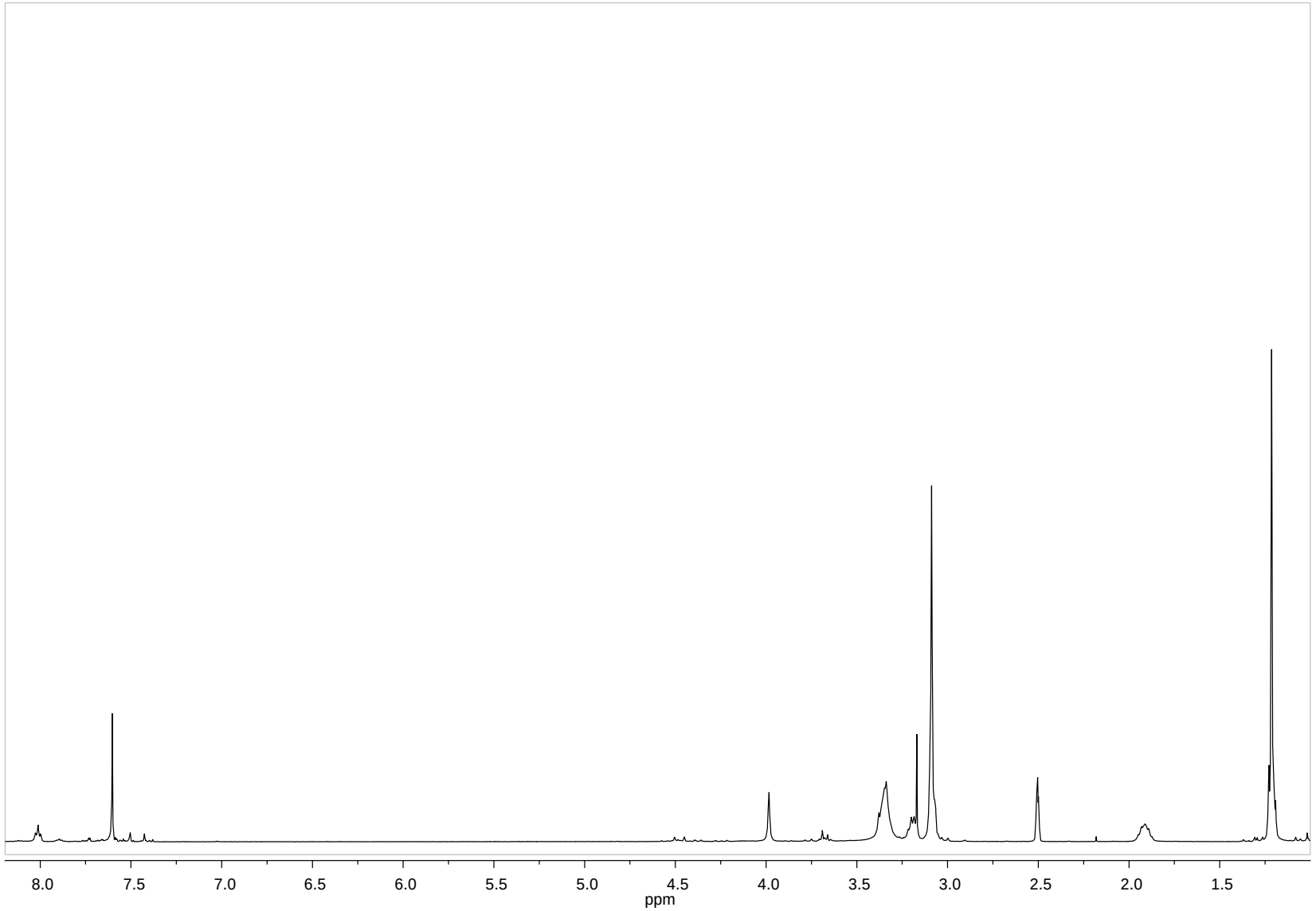

Fig. S7. ^{1}H NMR spectrum of 5,11,17,23-tetra-*tert*-butyl-25,26,27,28-tetrakis[(N-(3',3'-dimethyl-3'-ethyl)ammoniumpropyl)carbomoylmethoxy]-2,8,14,20-tetrathiacalix[4]arene tetraiodide (*1,3-alternate* **23**), **DMSO-d_6, 298 K, 400 MHz**

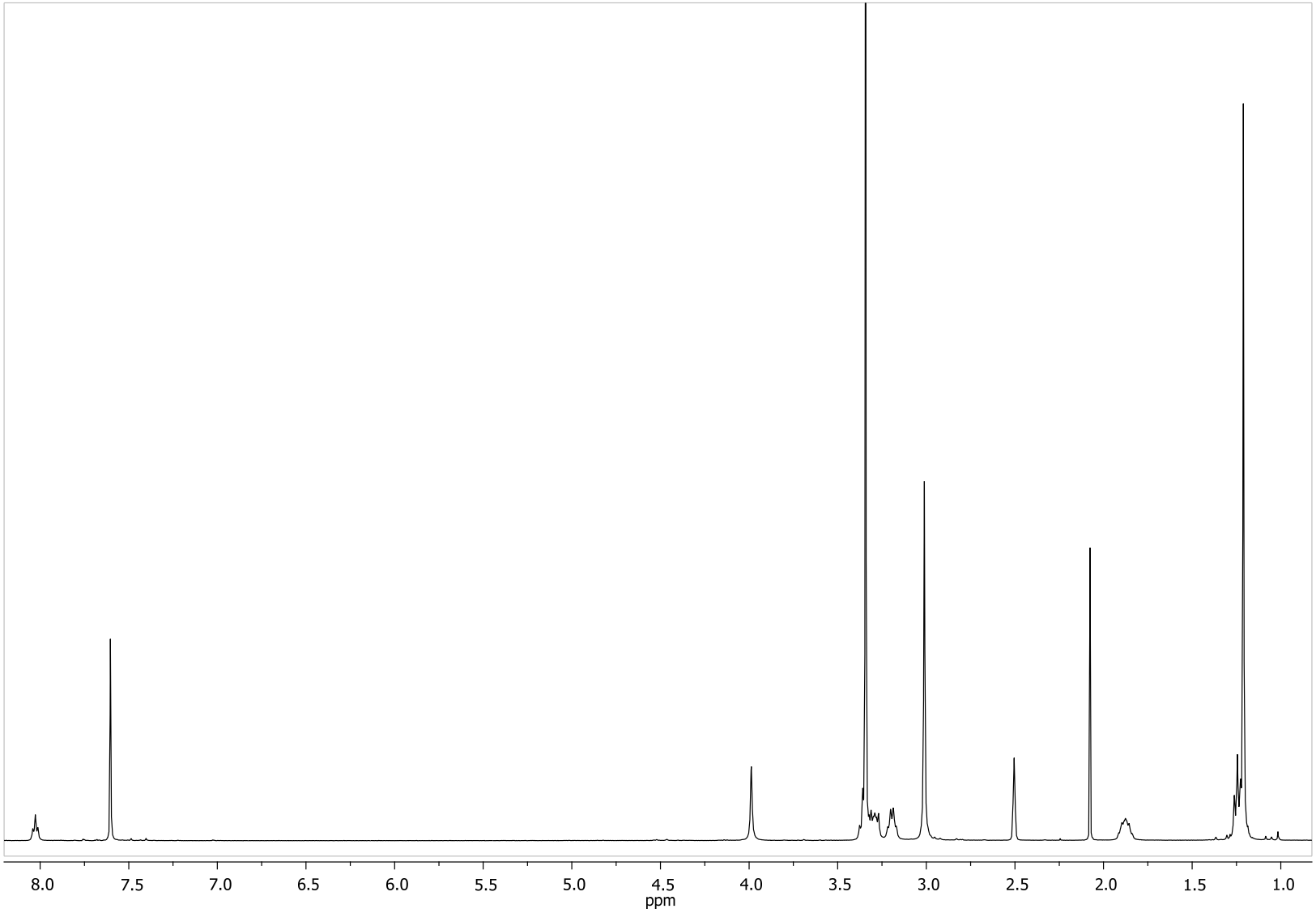

Fig. S8. ^{1}H NMR spectrum of 5,11,17,23-tetra-*tert*-butyl-25,26,27,28-tetrakis[(N-(3',3'-dimethyl-3'-benzyl)ammoniumpropyl)carbomoylmethoxy]-2,8,14,20-tetrathiacalix[4]arene tetrabromide (*1,3-alternate* **24**), **DMSO-d_6, 298 K, 400 MHz**

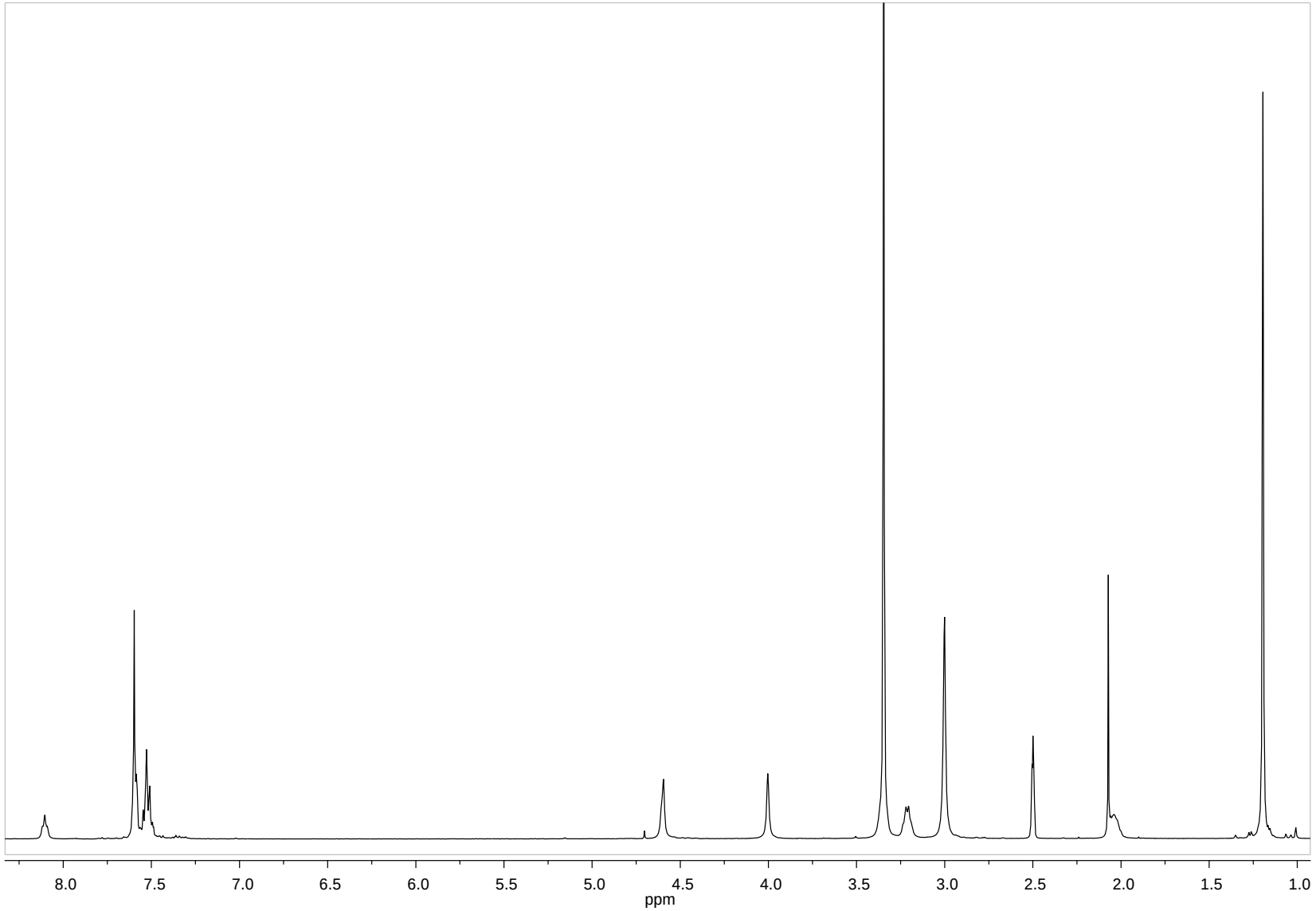

Fig. S9. ^{1}H NMR spectrum of 5,11,17,23-tetra-*tert*-butyl-25,26,27,28-tetrakis[(N-(3',3'-dimethyl-3'-(ethoxycarbonylmethyl)-ammoniumpropyl)carbomoylmethoxy]-2,8,14,20-tetrathiacalix[4]arene tetrabromide (*1,3-alternate* **25**), **DMSO-d_6, 298 K, 400 MHz**

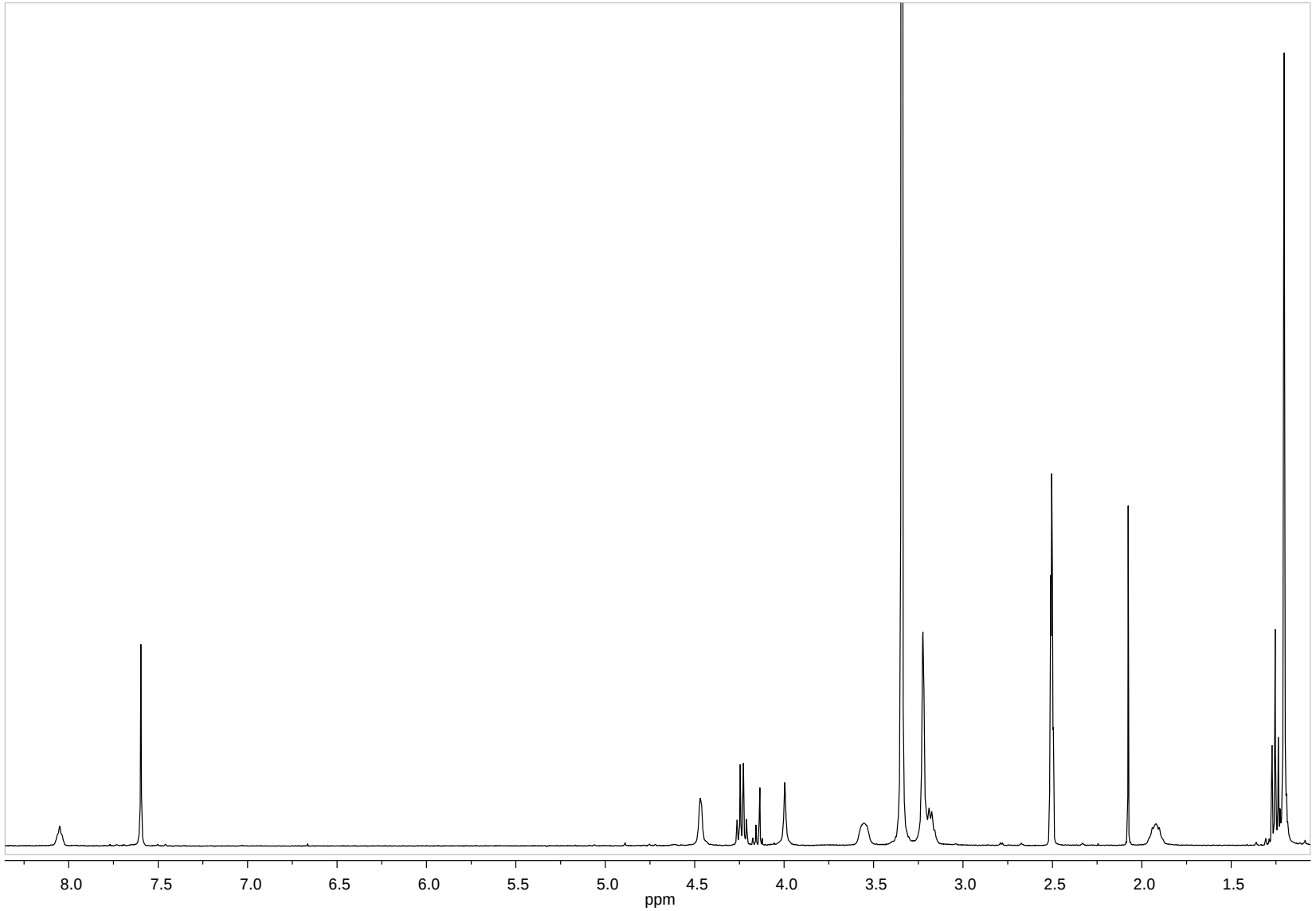

Fig. S10. ^{1}H NMR spectrum of 5,11,17,23-tetra-*tert*-butyl-25,26,27,28-tetrakis[(N-(3',3'-dimethyl-3'-(pentoxycarbonylmethyl)-ammoniumpropyl)carbomoylmethoxy]-2,8,14,20-tetrathiacalix[4]arene tetrabromide (*1,3-alternate* **26**), **DMSO-d_6, 298 K, 400 MHz**

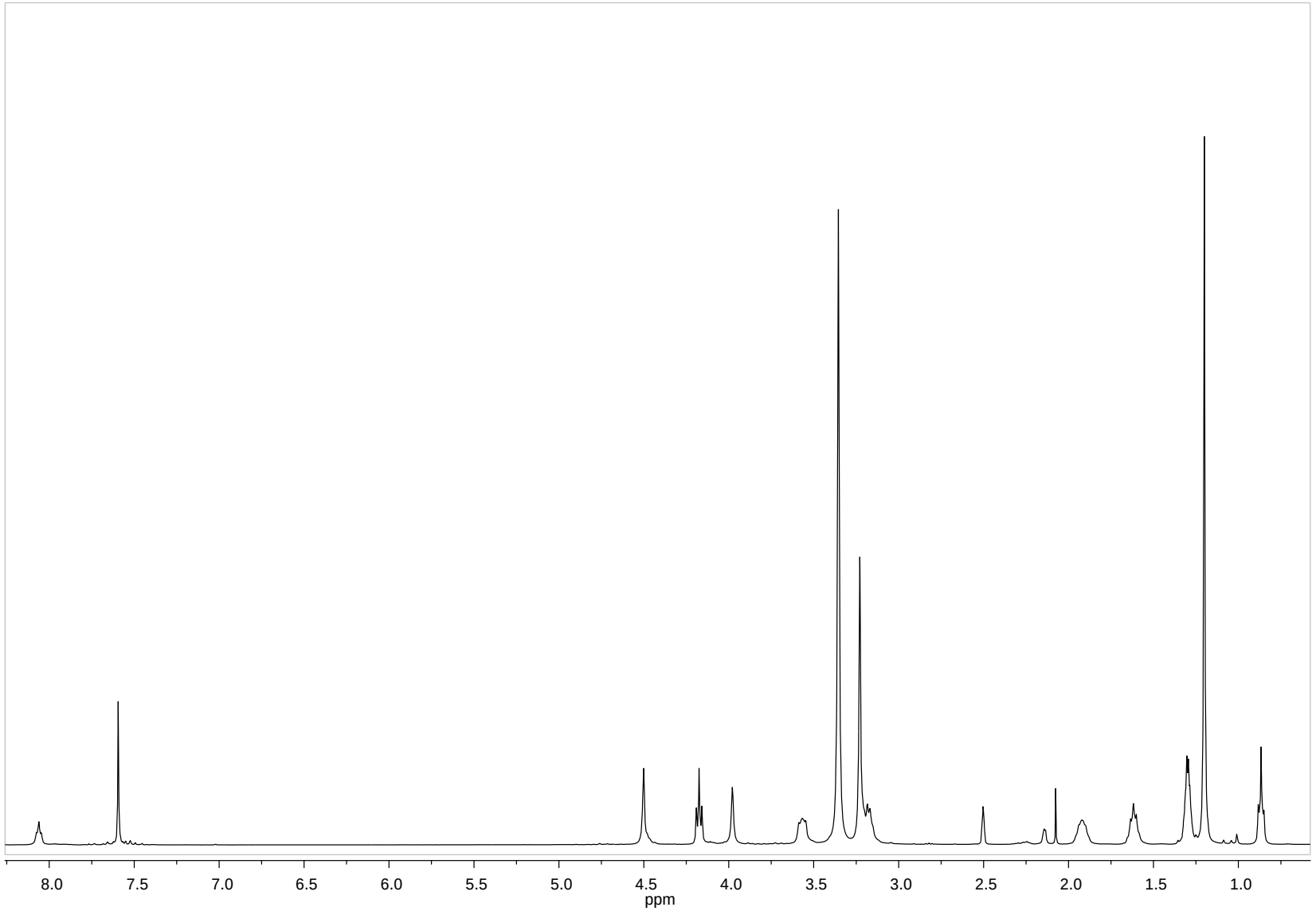

Fig. S11. ^{1}H NMR spectrum of 5,11,17,23-tetra-*tert*-butyl-25,26,27,28-tetrakis[(N-(3',3'-dimethyl-3'-{3''-propylphtalimide}-ammoniumpropyl)carbomoylmethoxy]-2,8,14,20-tetrathiacalix[4]arene tetrabromide (*1,3-alternate* **30**), **DMSO-d_6, 298 K, 400 MHz**

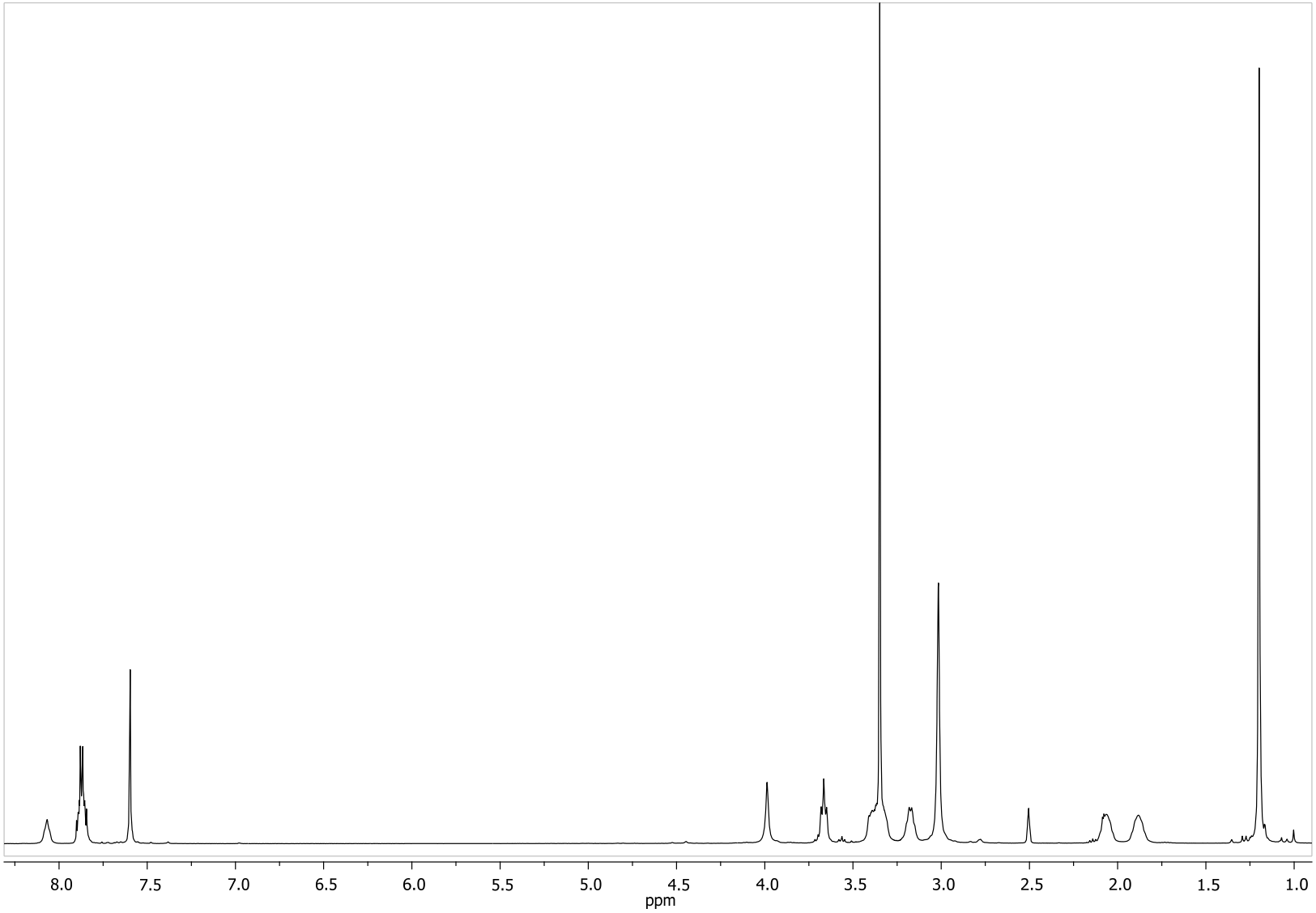

Fig. S12. ^{1}H NMR spectrum of 5,11,17,23-tetra-*tert*-butyl-25,26,27,28-tetrakis[(N-(2'-methyl-2',2'-diethyl)ammoniumethyl)carbomoylmethoxy]-2,8,14,20-tetrathiacalix[4]arene tetraiodide (*1,3-alternate* **31**), **DMSO-d_6, 298 K, 400 MHz**

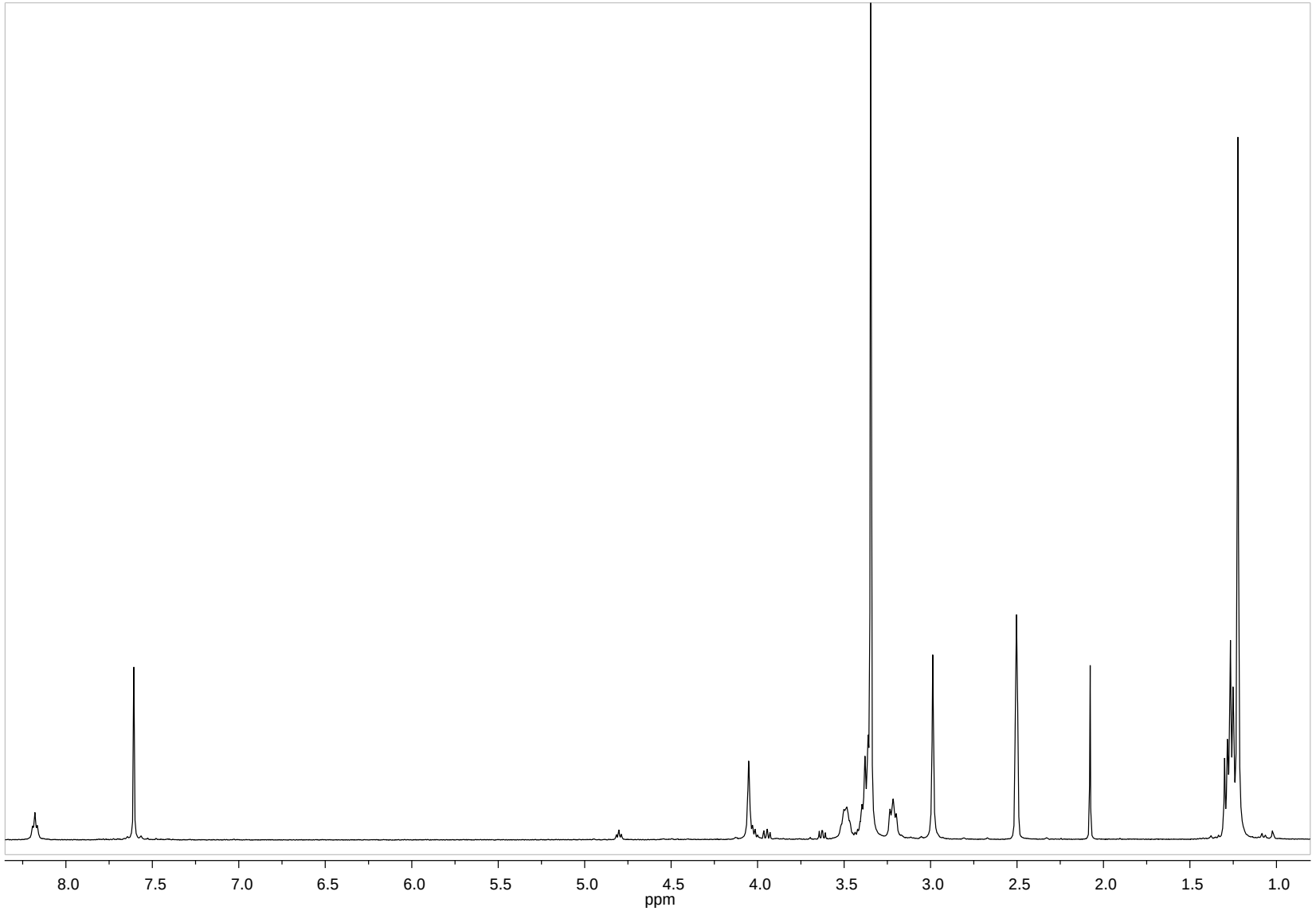

Fig. S13. ^{1}H NMR spectrum of 5,11,17,23-tetra-*tert*-butyl-25,26,27,28-tetrakis[(N-(2',2',2'-triethyl)ammoniumethyl)carbomoylmethoxy]-2,8,14,20-tetrathiacalix[4]arene tetraiodide (*1,3-alternate* **32**), **DMSO-d_6, 298 K, 400 MHz**

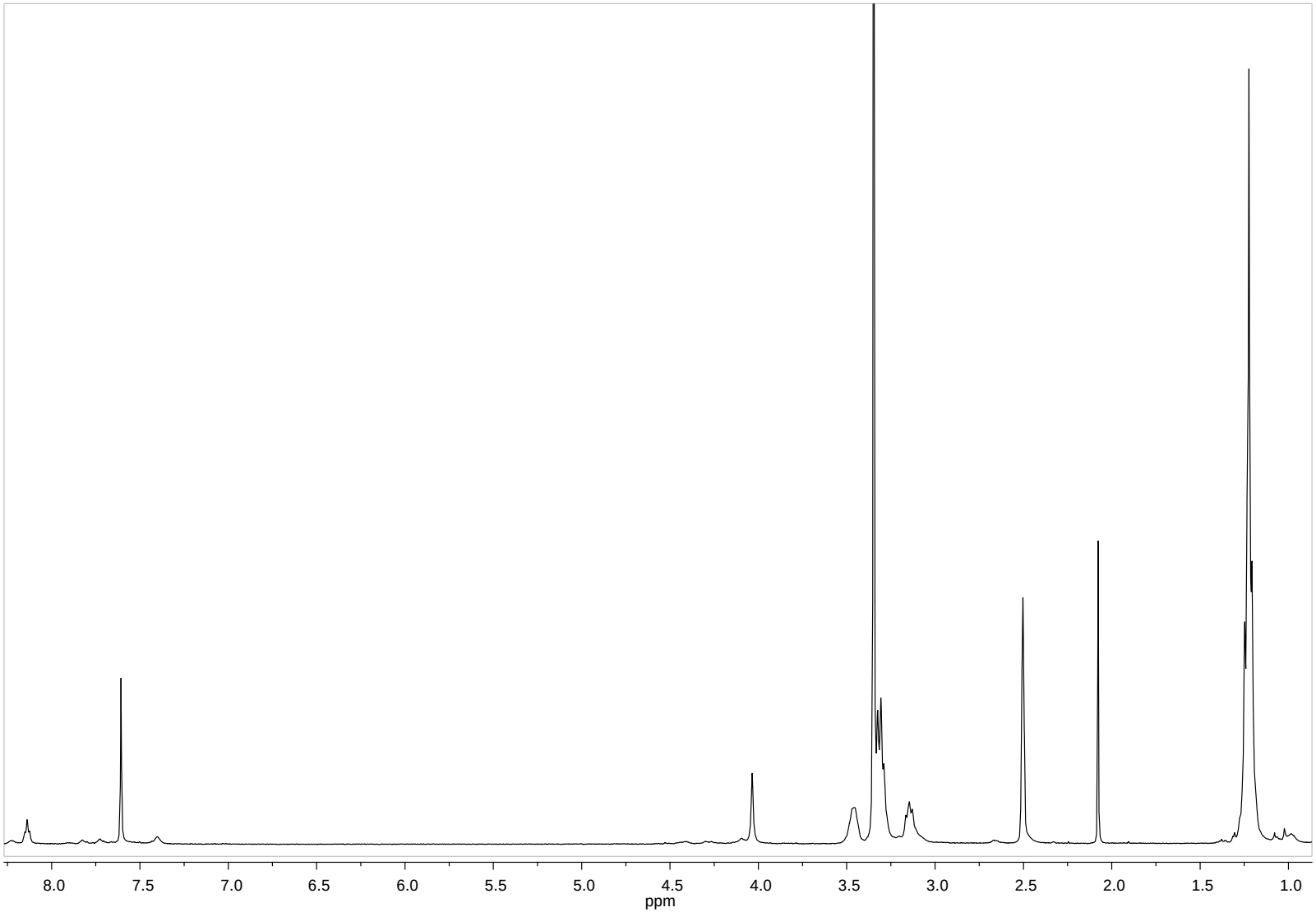

Fig. S14. ^{1}H NMR spectrum of 5,11,17,23-tetra-*tert*-butyl-25,26,27,28-tetrakis[(N-(2',2'-diethyl-2'-(benzyl)ammoniumpropyl)carbomoylmethoxy]-2,8,14,20-tetrathiacalix[4]arene tetrabromide (*1,3-alternate* **33**), **DMSO-d$_6$, 298 K, 400 MHz**

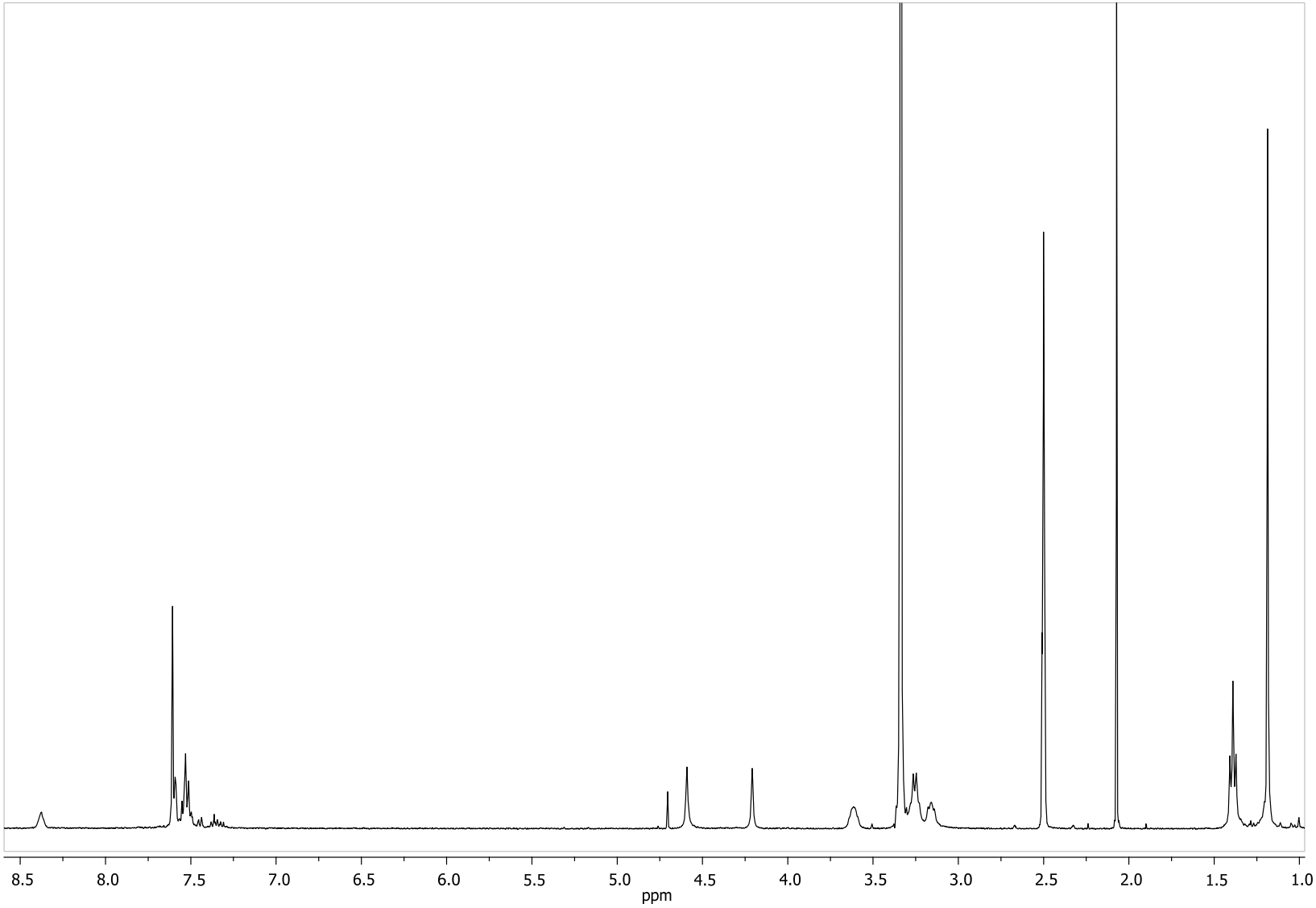

Fig. S15. ^{1}H NMR spectrum of 5,11,17,23-tetra-*tert*-butyl-25,26,27,28-tetrakis[(N-(2',2'-diethyl-2'-(ethoxycarbonylmethyl)-ammoniumethyl)carbomoylmethoxy]-2,8,14,20-tetrathiacalix[4]arene tetrabromide (*1,3-alternate* **34**), **DMSO-d$_6$, 298 K, 400 MHz**

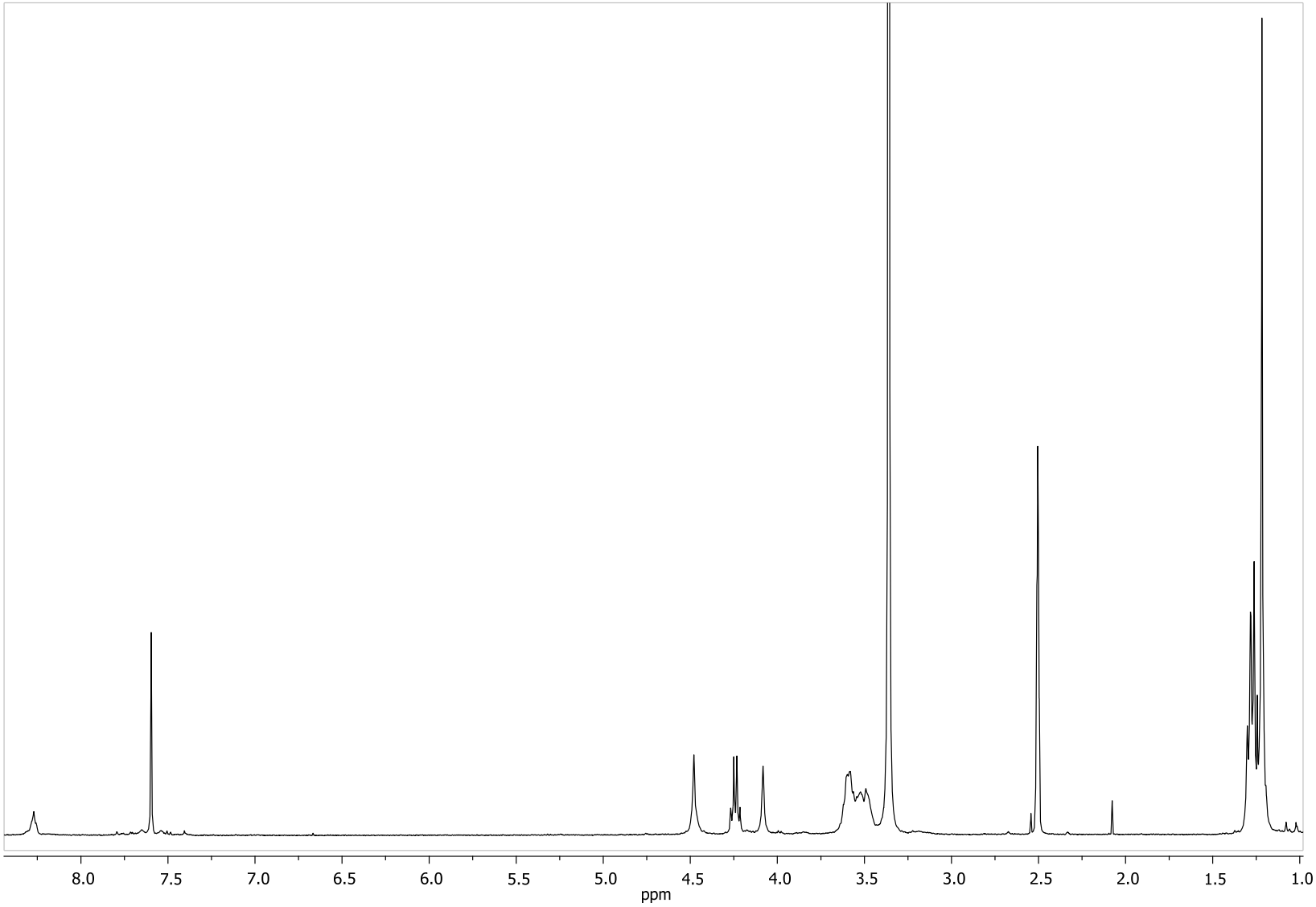

Fig. S16. ^{1}H NMR spectrum of 5,11,17,23-tetra-*tert*-butyl-25,26,27,28-tetrakis[(N-(2',2'-diethyl-2'-(pentoxycarbonylmethyl)-ammoniumethyl)carbomoylmethoxy]-2,8,14,20-tetrathiacalix[4]arene tetrabromide (*1,3-alternate* **35**), **DMSO-d$_6$, 298 K, 400 MHz**

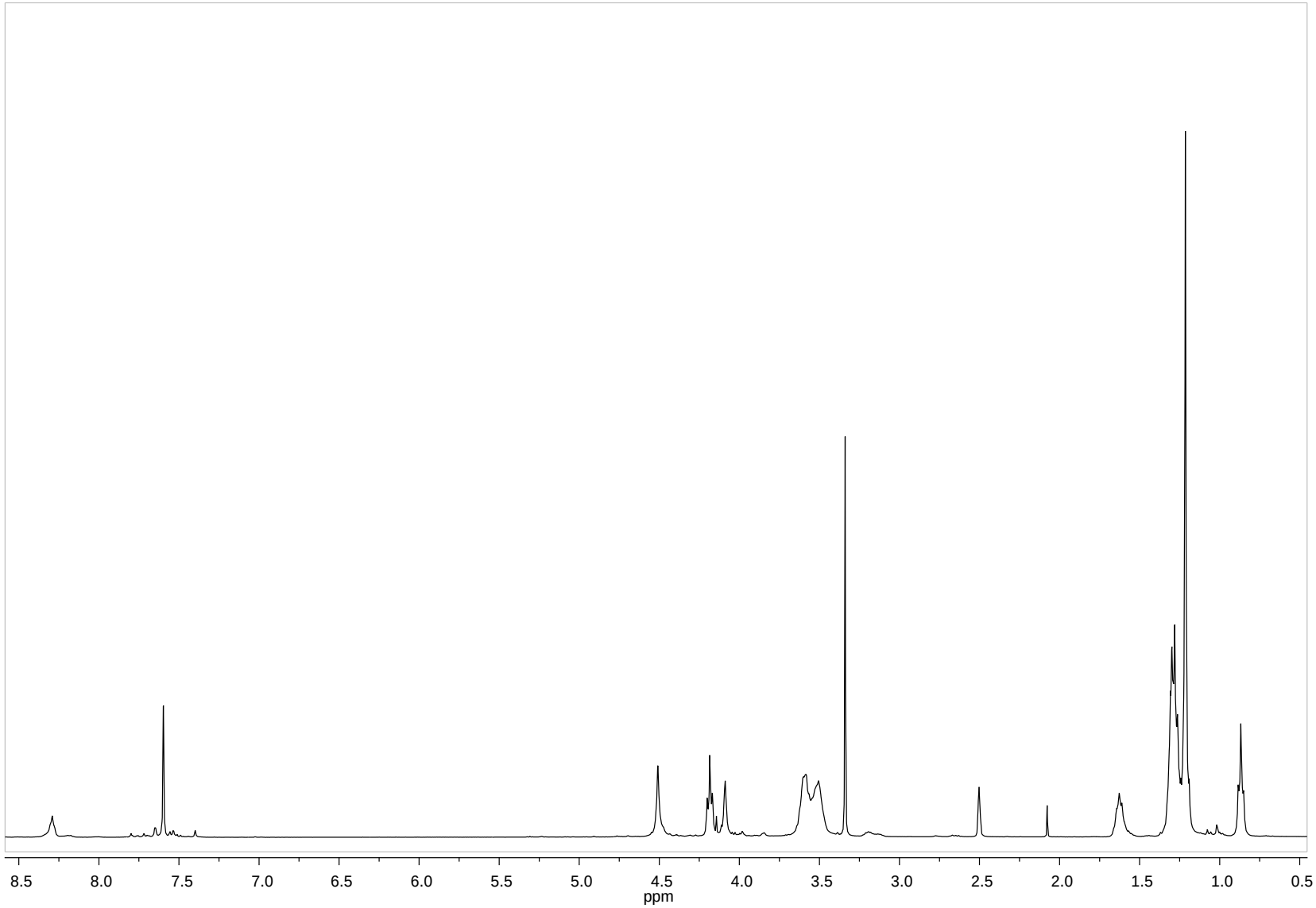

Fig. S17. ^{1}H NMR spectrum of 5,11,17,23-tetra-*tert*-butyl-25,26,27,28-tetrakis[(N-(3',3',3'-trimethyl)ammoniumpropyl)carbomoylmethoxy]-2,8,14,20-tetrathiacalix[4]arene tetra[bis(trifluoromethylsulfonyl)imide] (*cone* **39**), **DMSO-d_6, 298 K, 400 MHz**

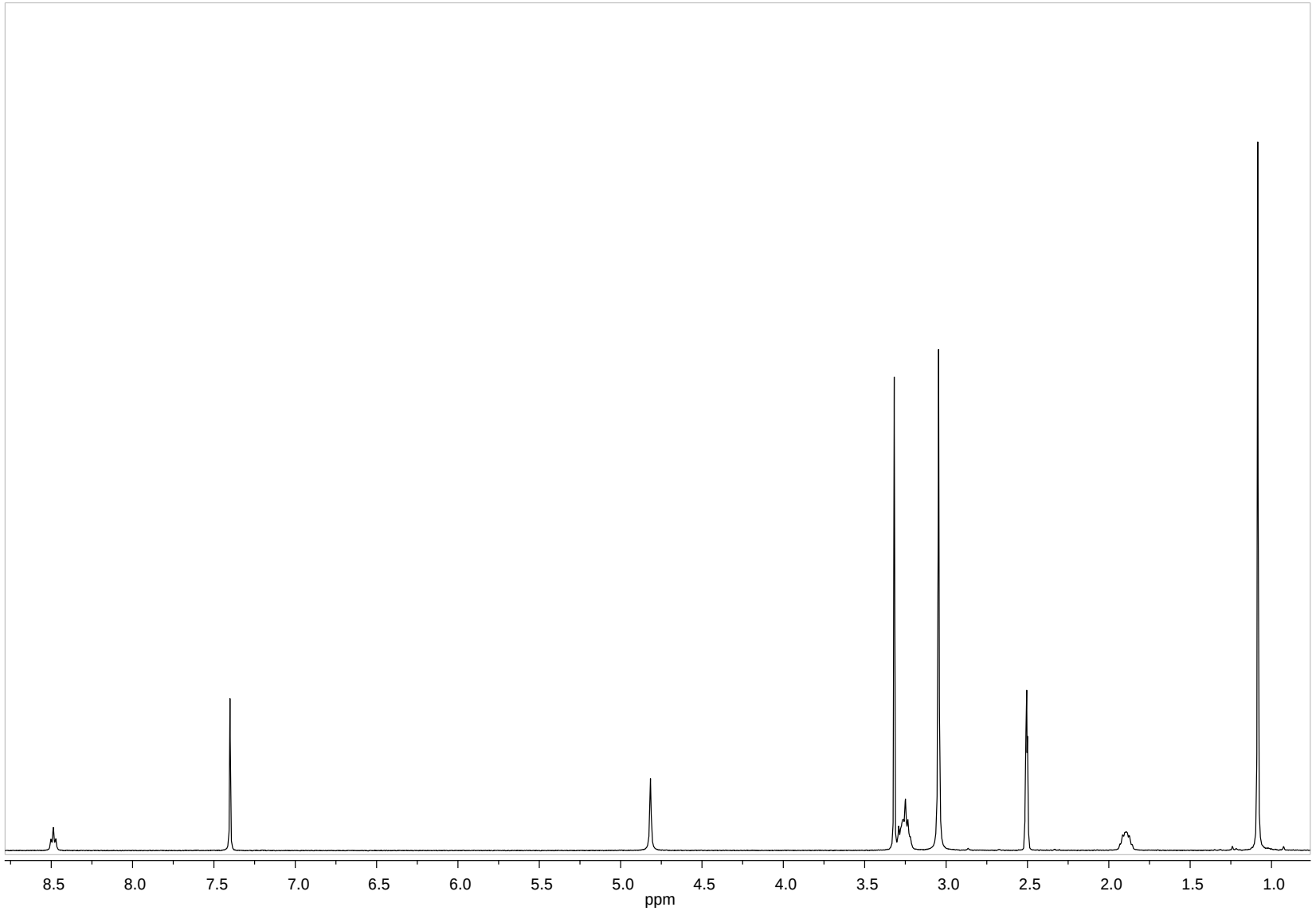

Fig. S18. ^{1}H NMR spectrum of 5,11,17,23-tetra-*tert*-butyl-25,26,27,28-tetrakis[(N-(3',3'-dimethyl-3'-ethyl)ammoniumpropyl)-carbomoylmethoxy]-2,8,14,20-tetrathiacalix[4]arene tetra[bis(trifluoromethylsulfonyl)imide] (*cone* **40**), **DMSO-d_6, 298 K, 400 MHz**

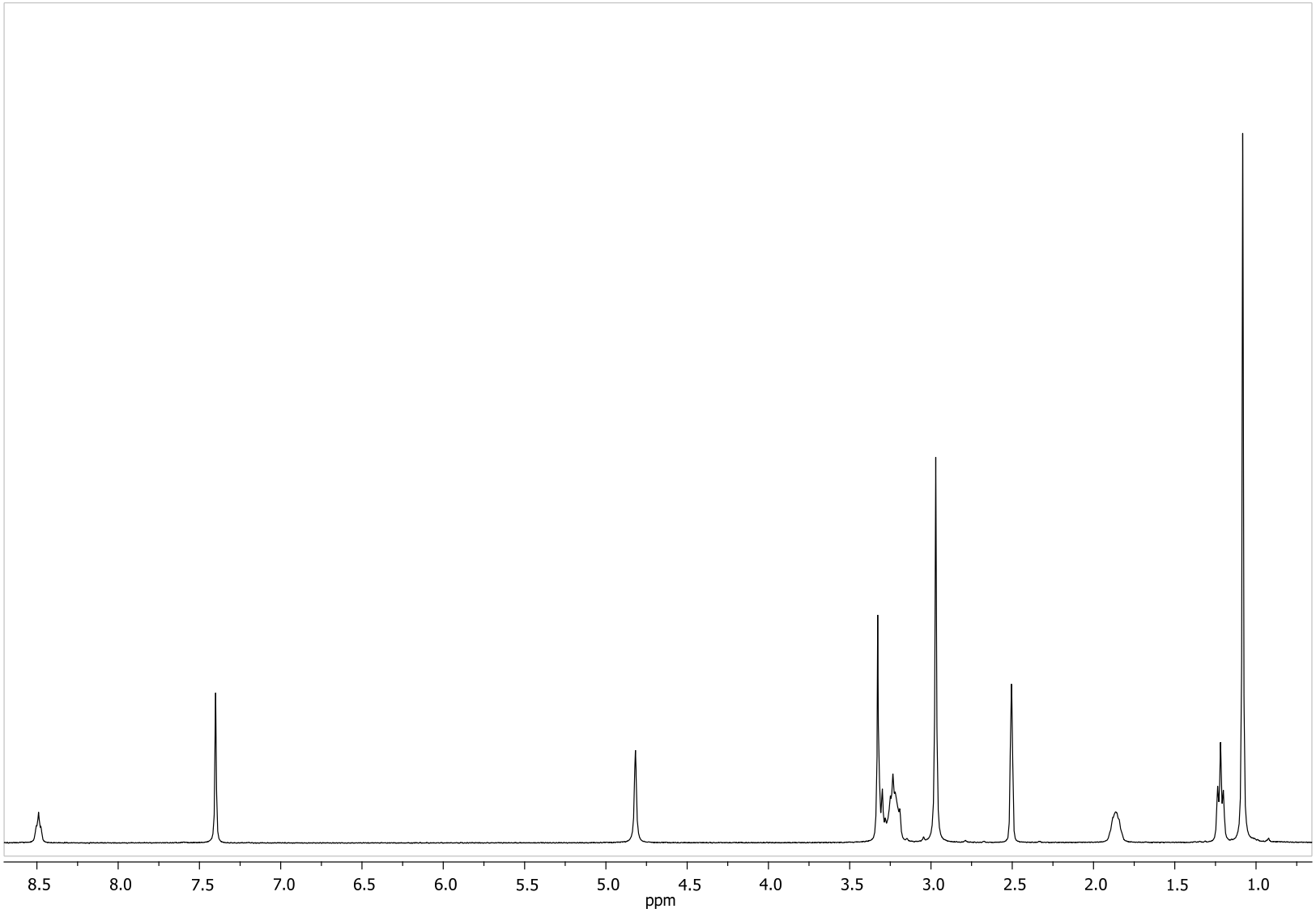

Fig. S19. ^{1}H NMR spectrum of 5,11,17,23-tetra-*tert*-butyl-25,26,27,28-tetrakis[(N-(3',3'-dimethyl-3'-benzyl)ammoniumpropyl)-carbomoylmethoxy]-2,8,14,20-tetrathiacalix[4]arene tetra[bis(trifluoromethylsulfonyl)imide] (*cone* **41**), **$CDCl_3$, 298 K, 400 MHz**

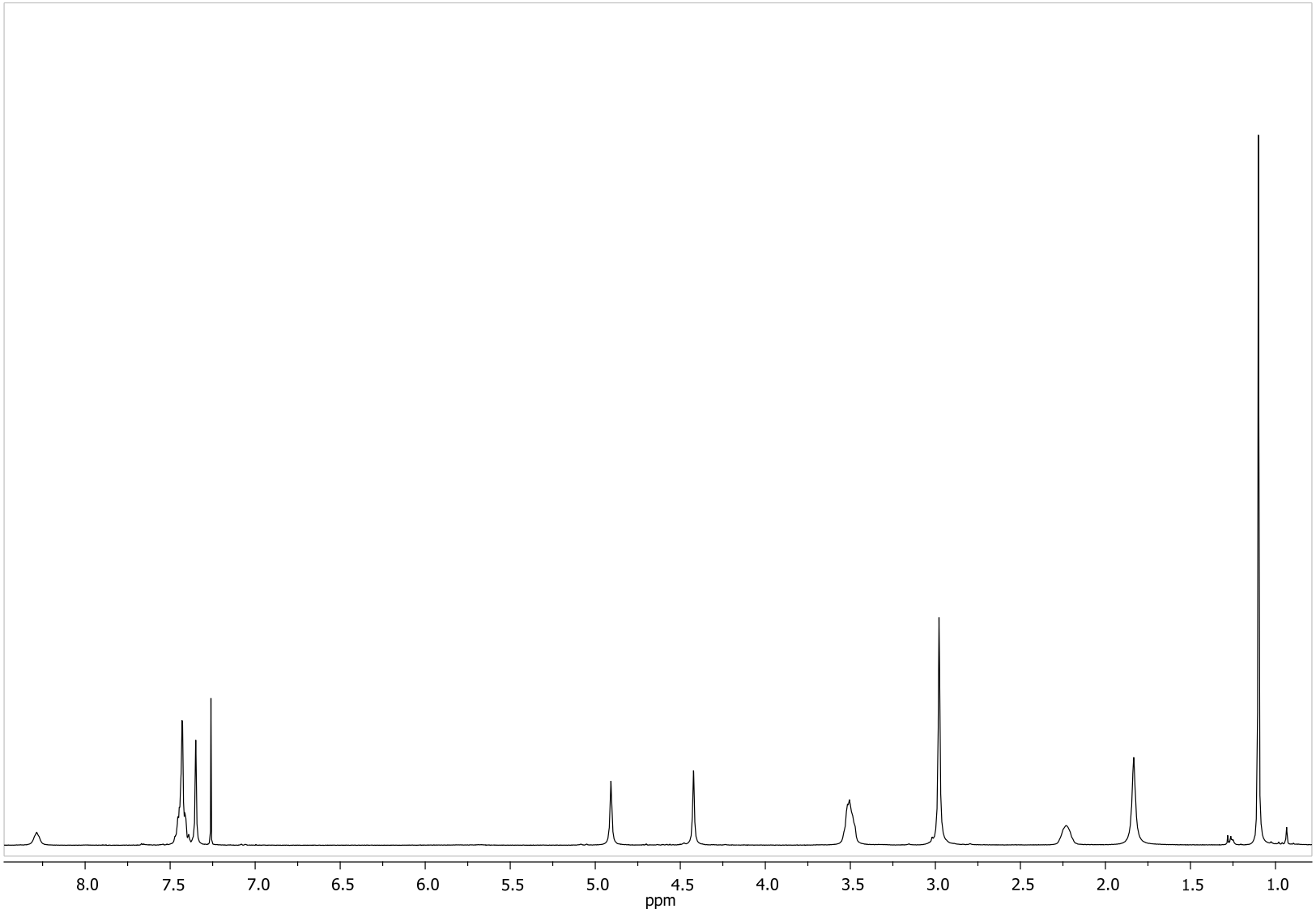

Fig. S20. ^{1}H NMR spectrum of 5,11,17,23-tetra-*tert*-butyl-25,26,27,28-tetrakis[(N-(3',3'-dimethyl-3'-(ethoxycarbonylmethyl)ammoniumpropyl)carbomoylmethoxy]-2,8,14,20-tetrathiacalix[4]arene tetra[bis(trifluoromethylsulfonyl)imide] (*cone* **42**), **$CDCl_3$, 298 K, 400 MHz**

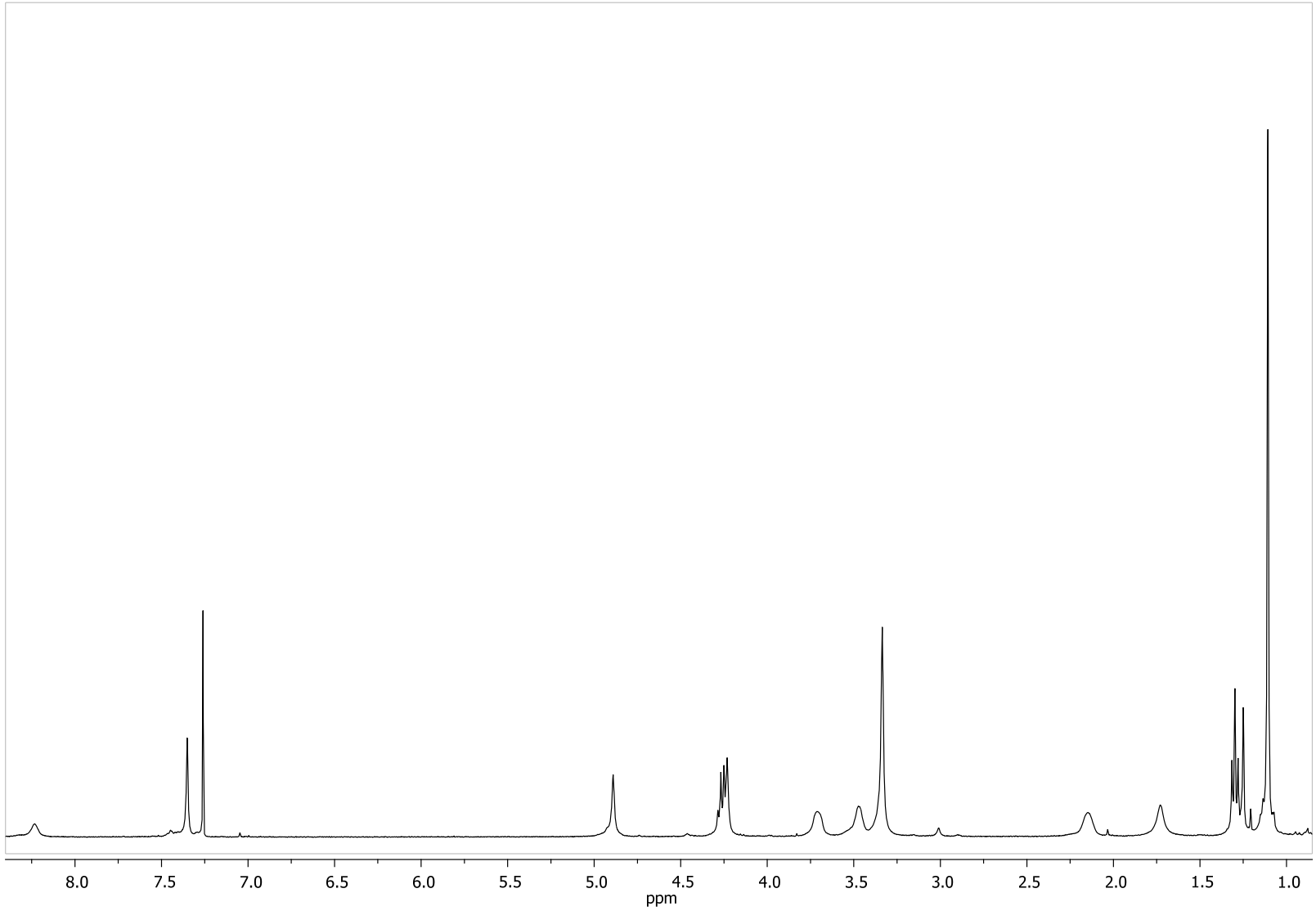

Fig. S21. ^{1}H NMR spectrum of 5,11,17,23-tetra-*tert*-butyl-25,26,27,28-tetrakis[(N-(3',3'-dimethyl-3'-(pentoxycarbonylmethyl)ammoniumpropyl)carbomoylmethoxy]-2,8,14,20-tetrathiacalix[4]arene tetra[bis(trifluoromethylsulfonyl)imide] (*cone* **43**), **DMSO-d_6, 298 K, 400 MHz**

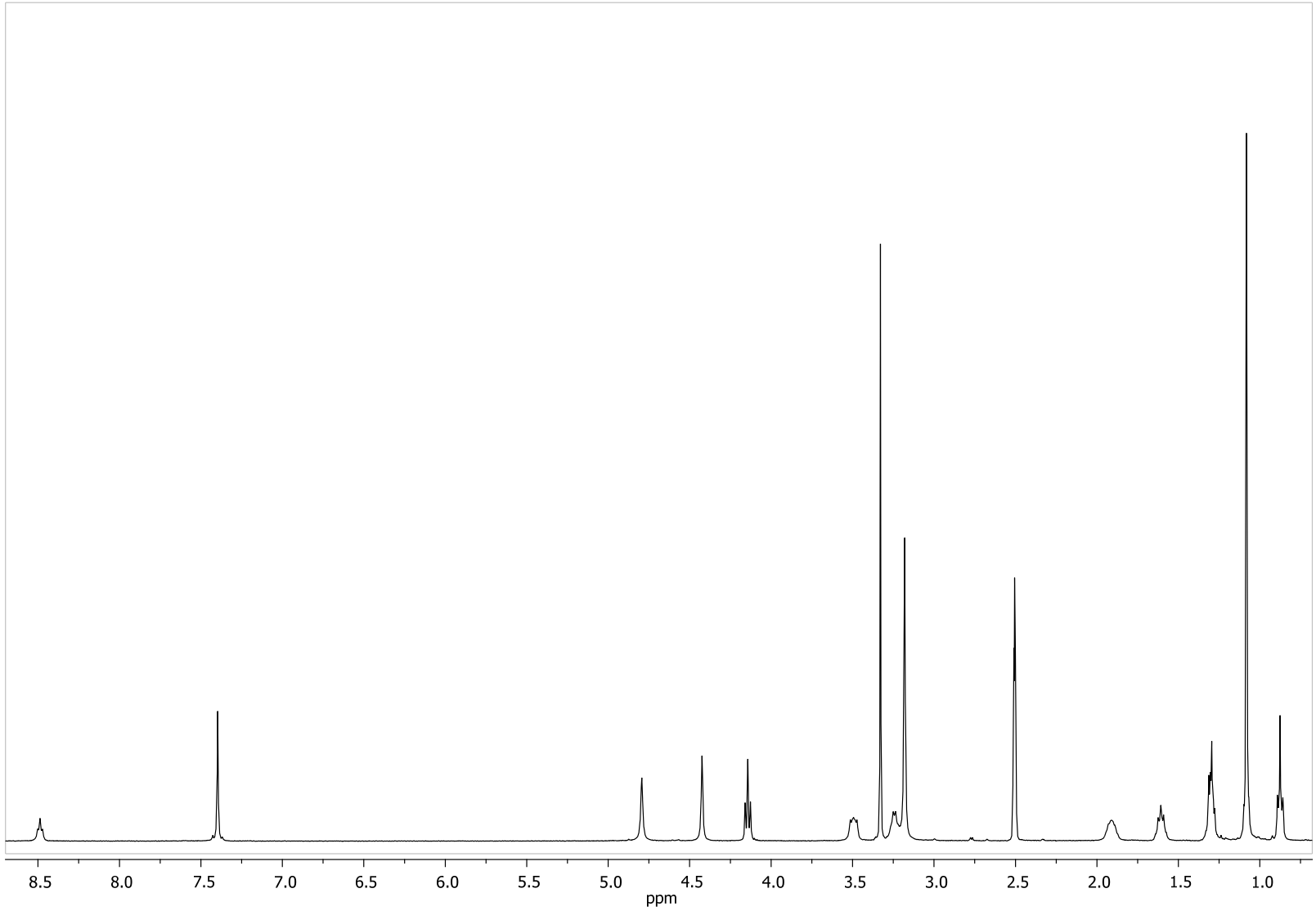

Fig. S22. ^{1}H NMR spectrum of 5,11,17,23-tetra-*tert*-butyl-25,26,27,28-tetrakis[(N-(3',3'-dimethyl-3'-{(ethoxycarbonylmethyl)amidocarbonylmethyl}ammoniumpropyl)carbomoylmethoxy]-2,8,14,20-tetrathiacalix[4]arene tetra[bis(trifluoromethylsulfonyl)imide] (*cone* 44), $CDCl_3$, 298 K, 400 MHz

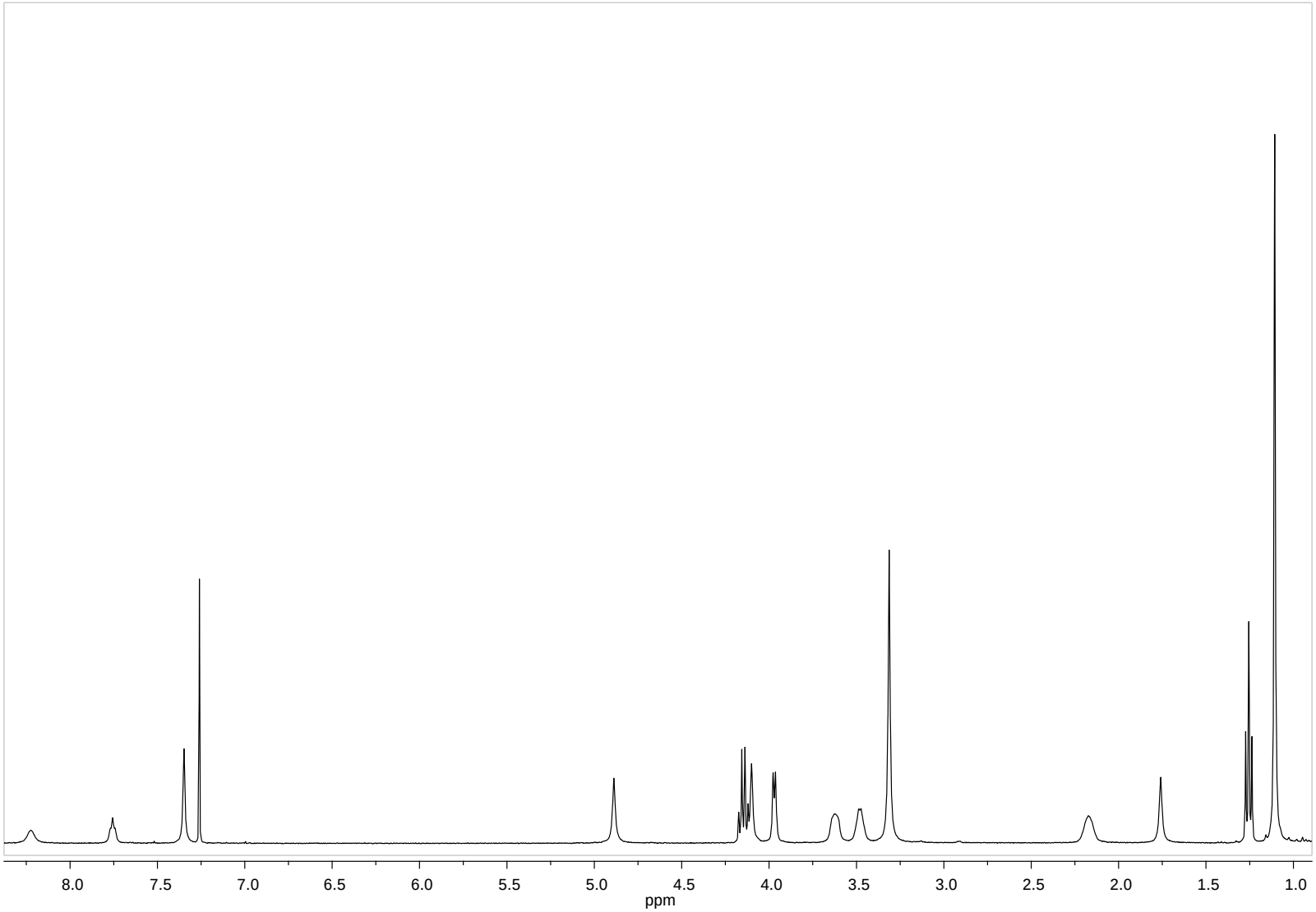

Fig. S23. ^{1}H NMR spectrum of 5,11,17,23-tetra-*tert*-butyl-25,26,27,28-tetrakis[(N-(3',3'-dimethyl-3'-{([ethoxycarbonylmethyl]-amidocarbonylmethyl)amidocarbonylmethyl}ammoniumpropyl)carbomoylmethoxy]-2,8,14,20-tetrathiacalix[4]arene tetra[bis(trifluoromethylsulfonyl)imide] (*cone* **45**), **DMSO-d_6, 298 K, 400 MHz**

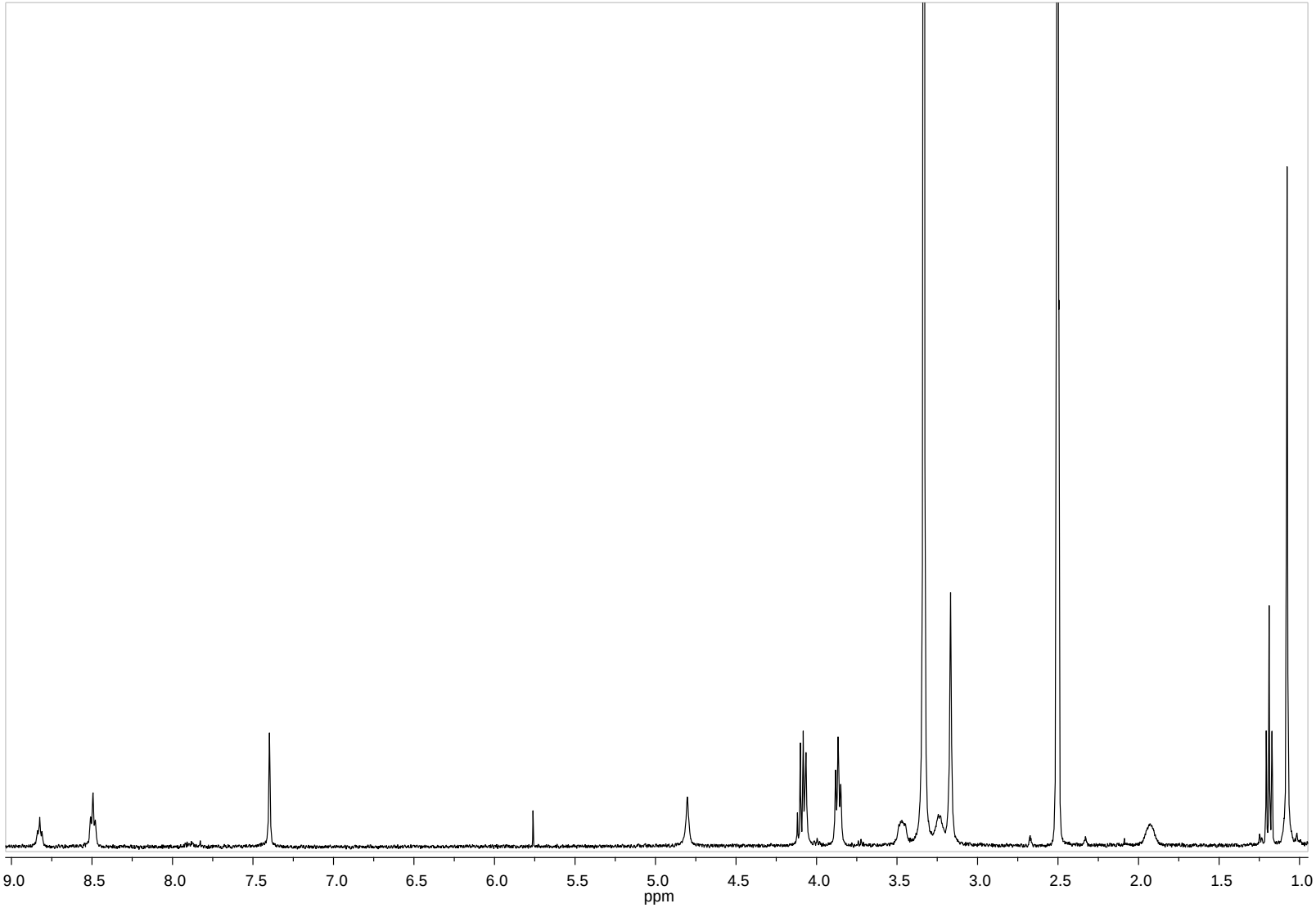

Fig. S24. ^{1}H NMR spectrum of 5,11,17,23-tetra-*tert*-butyl-25,26,27,28-tetrakis[(N-(3',3'-dimethyl-3'-{(ethoxycarbonyl[S-methyl]methyl)amidocarbonylmethyl}ammoniumpropyl)carbomoylmethoxy]-2,8,14,20-tetrathiacalix[4]arene tetra[bis(trifluoromethylsulfonyl)imide] (*cone* **46**), **DMSO-d_6, 298 K, 400 MHz**

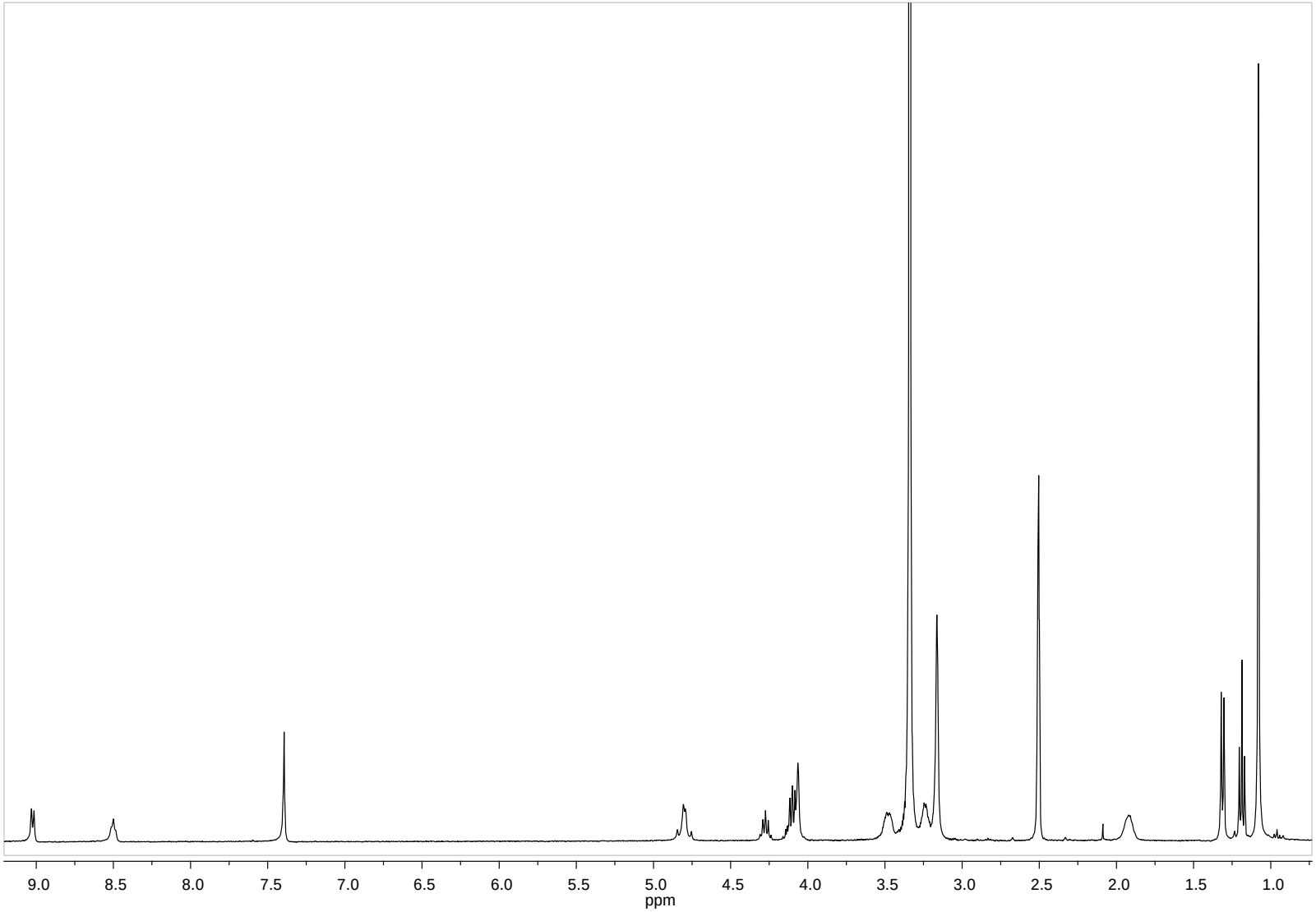

Fig. S25. ^{1}H NMR spectrum of 5,11,17,23-tetra-*tert*-butyl-25,26,27,28-tetrakis[(N-(3',3'-dimethyl-3'-{3''-propylphtalimide}ammoniumpropyl)-carbomoylmethoxy]-2,8,14,20-tetrathiacalix[4]arene tetra[bis(trifluoromethylsulfonyl)imide] (*cone* **47**), **DMSO-d$_6$, 298 K, 400 MHz**

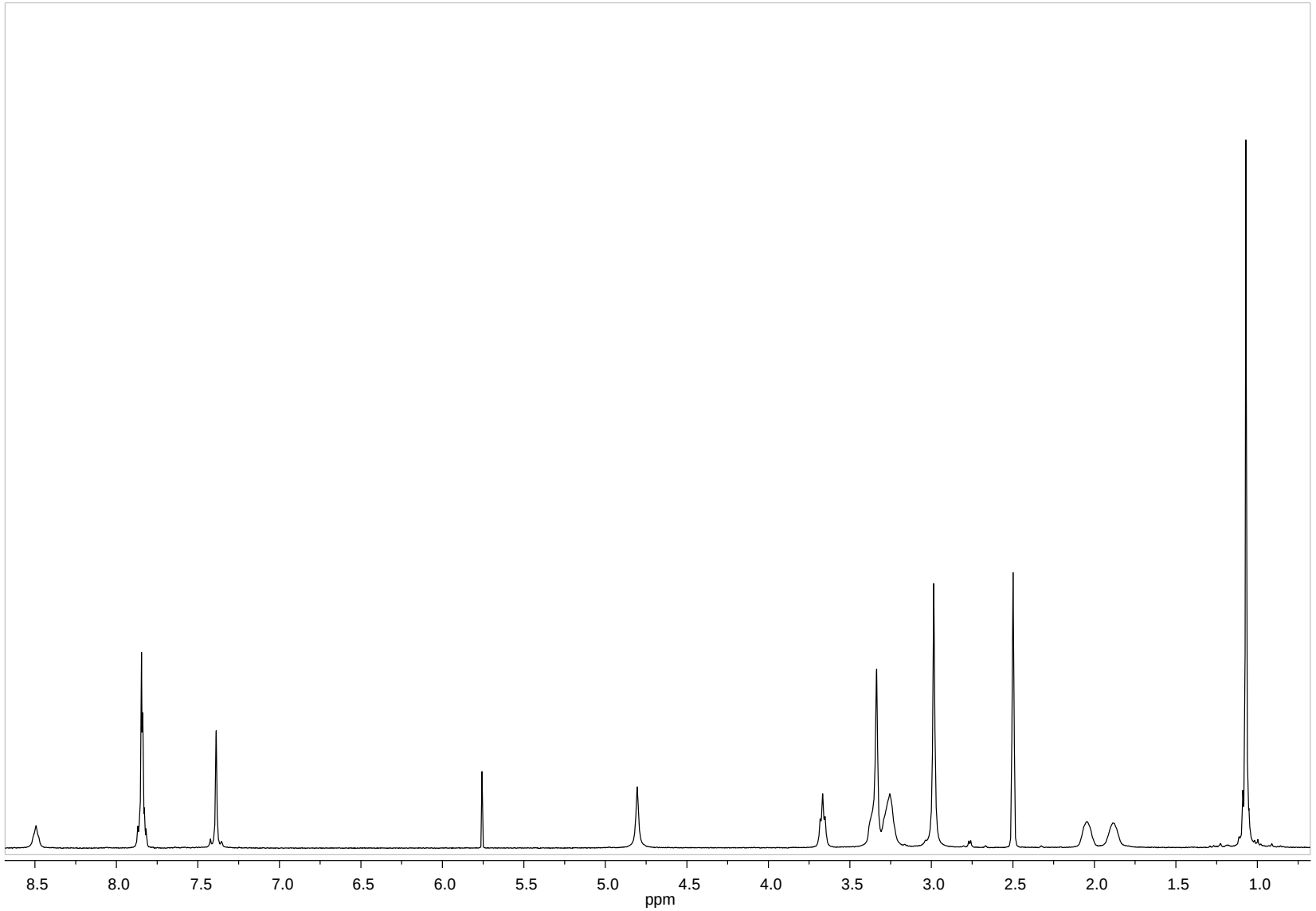

Fig. S26. ^{1}H NMR spectrum of 5,11,17,23-tetra-*tert*-butyl-25,26,27,28-tetrakis[(N-(2'-methyl-2',2'-diethyl)ammoniumethyl)carbomoylmethoxy]-2,8,14,20-tetrathiacalix[4]arene tetra[bis(trifluoromethylsulfonyl)imide] (*cone* **48**), **$CDCl_3$, 298 K, 400 MHz**

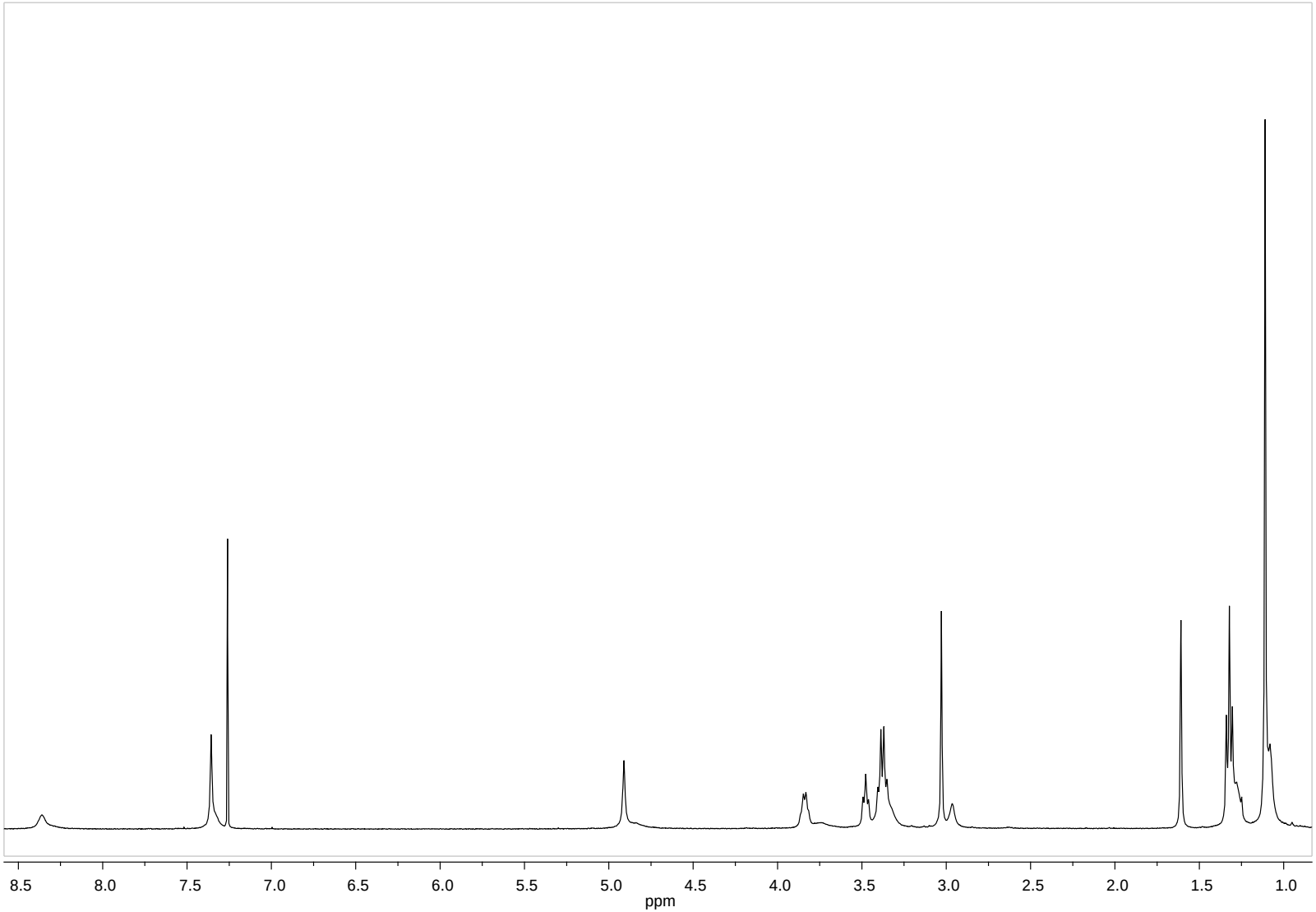

Fig. S27. ^{1}H NMR spectrum of 5,11,17,23-tetra-*tert*-butyl-25,26,27,28-tetrakis[(N-(2',2',2'-triethyl)ammoniumethyl)carbomoylmethoxy]-2,8,14,20-tetrathiacalix[4]arene tetra[bis(trifluoromethylsulfonyl)imide] (*cone* **49**), **$CDCl_3$, 298 K, 400 MHz**

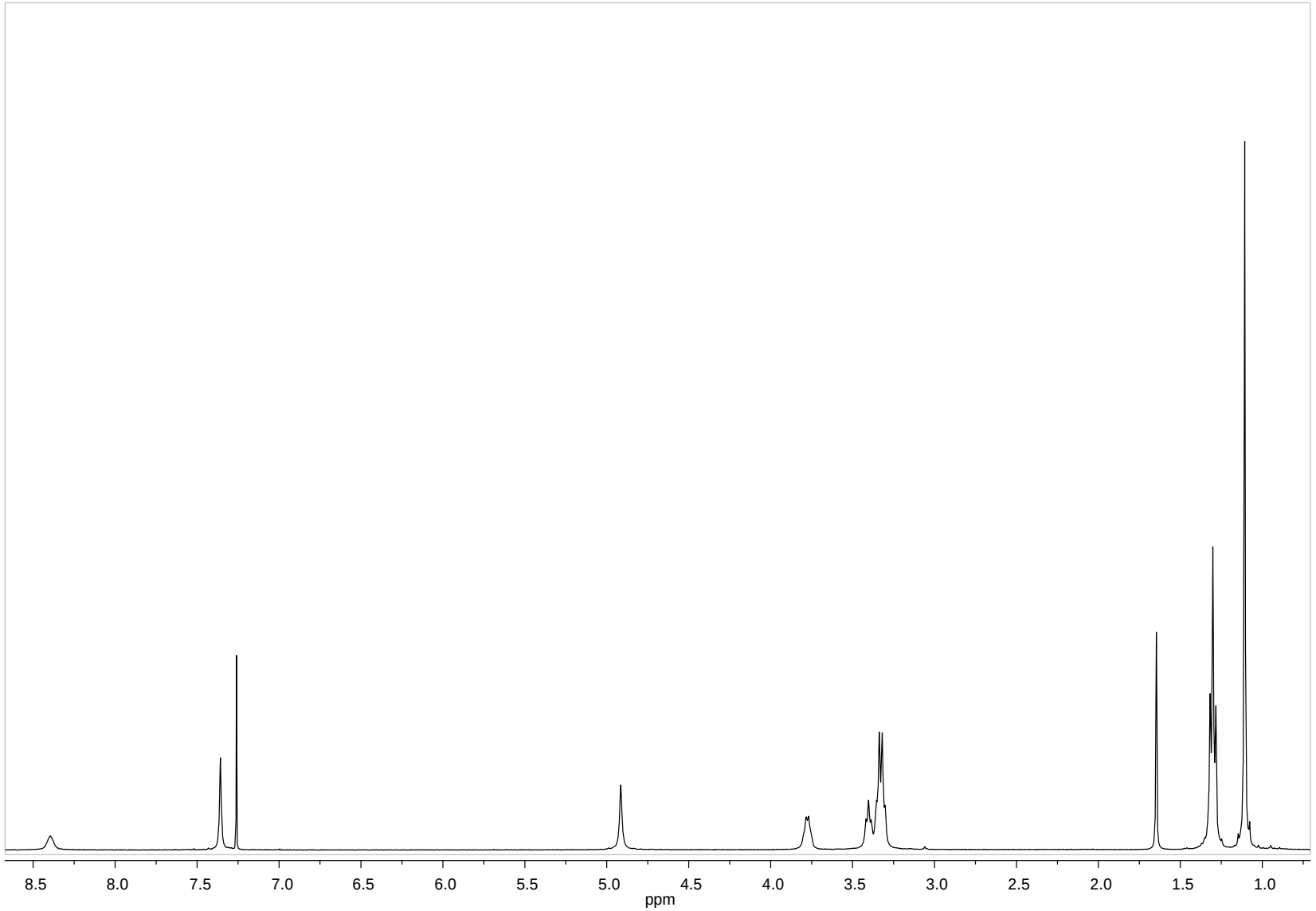

Fig. S28. ^{1}H NMR spectrum of 5,11,17,23-tetra-*tert*-butyl-25,26,27,28-tetrakis[(N-(2',2'-diethyl-2'–benzyl)ammoniumethyl)carbomoylmethoxy]-2,8,14,20-tetrathiacalix[4]arene tetra[bis(trifluoromethylsulfonyl)imide] (*cone* **50**), **$CDCl_3$, 298 K, 400 MHz**

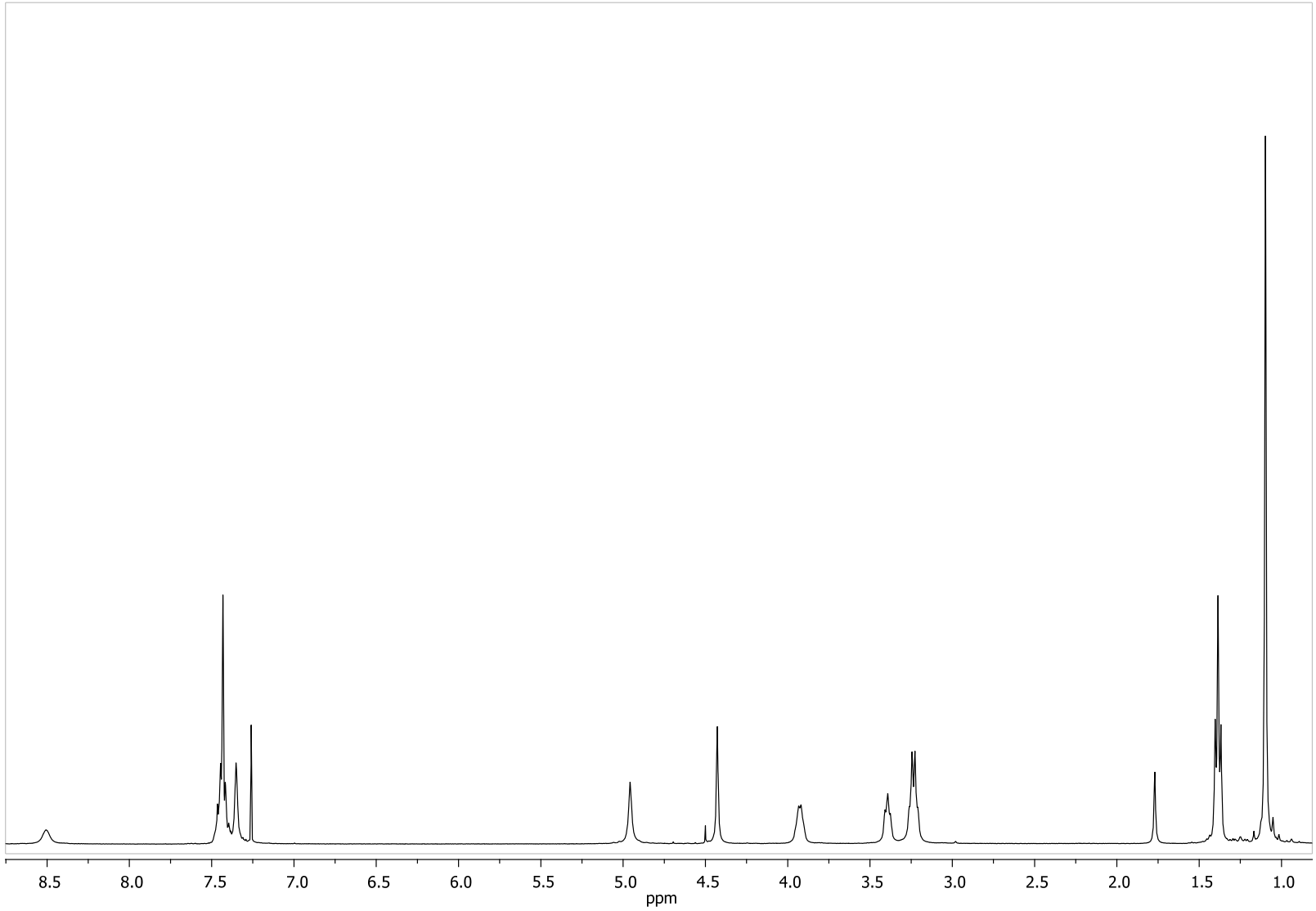

Fig. S29. ^{1}H NMR spectrum of 5,11,17,23-tetra-*tert*-butyl-25,26,27,28-tetrakis[(N-(2',2'-diethyl-2'-(ethoxycarbonylmethyl)ammoniumethyl)-carbomoylmethoxy]-2,8,14,20-tetrathiacalix[4]arene tetra[bis(trifluoromethylsulfonyl)imide] (*cone* **51**), **$CDCl_3$, 298 K, 400 MHz**

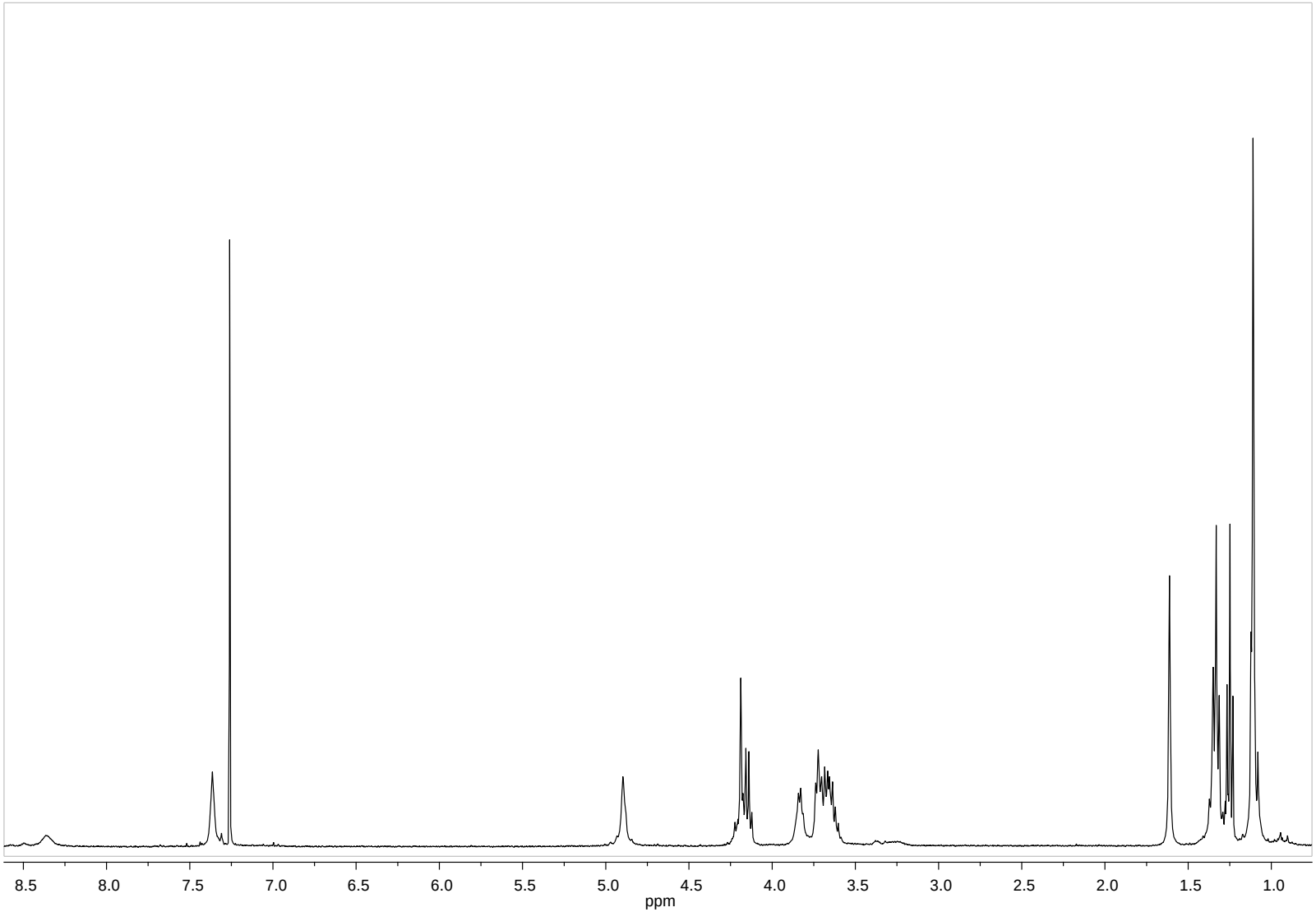

Fig. S30. ^{1}H NMR spectrum of 5,11,17,23-tetra-*tert*-butyl-25,26,27,28-tetrakis[(N-(2',2'-diethyl-2'-(pentoxycarbonylmethyl)ammoniumethyl)-carbomoylmethoxy]-2,8,14,20-tetrathiacalix[4]arene tetra[bis(trifluoromethylsulfonyl)imide] (*cone* **52**), **DMSO-d_6, 298 K, 400 MHz**

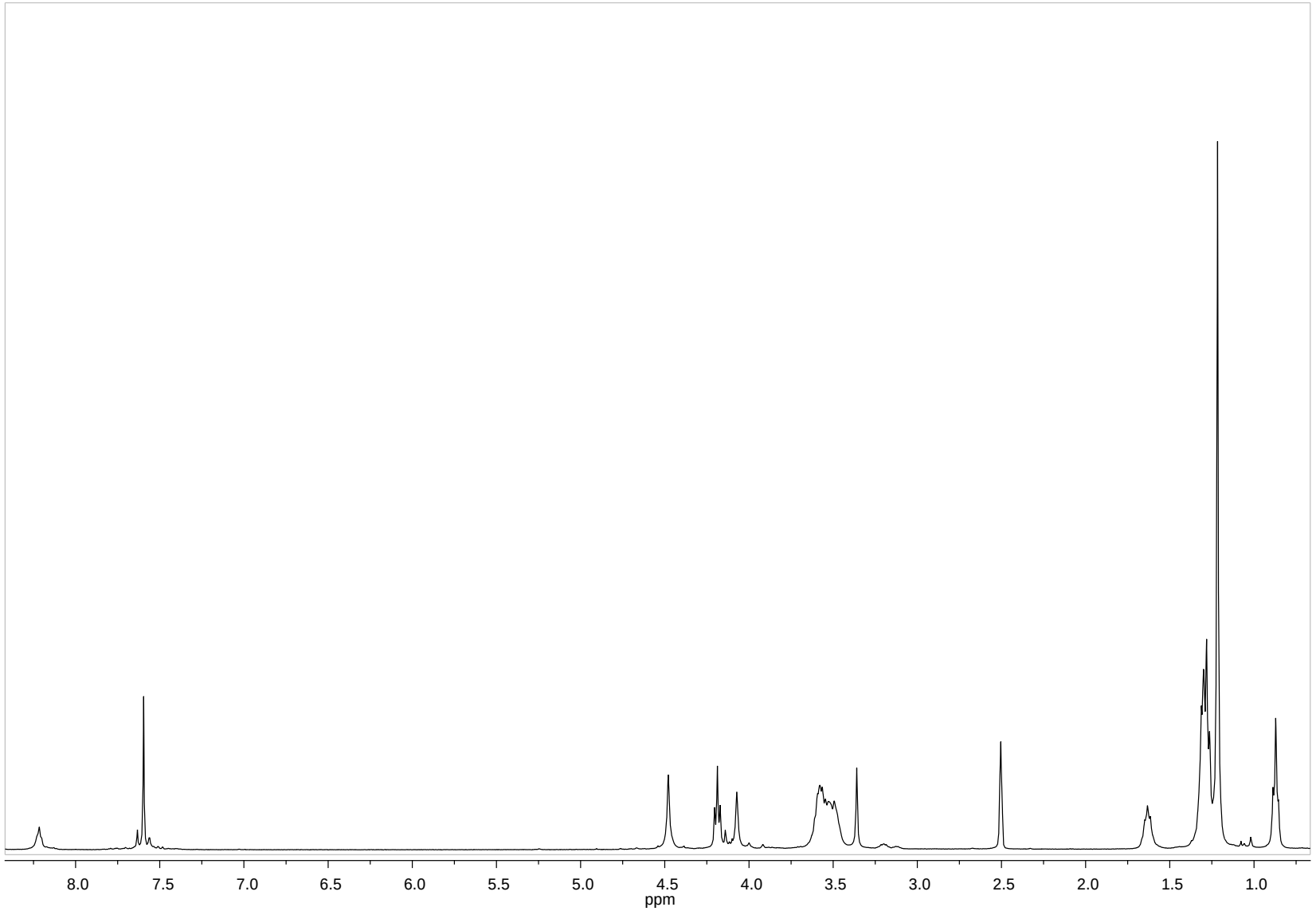

Fig. S31. ^{1}H NMR spectrum of 5,11,17,23-tetra-*tert*-butyl-25,26,27,28-tetrakis[(N-(2',2'-diethyl-2'-{(ethoxycarbonylmethyl)amidocarbonylmethyl})ammoniumethyl)carbomoylmethoxy]-2,8,14,20-tetrathiacalix[4]arene tetra[bis(trifluoromethylsulfonyl)imide] (*cone* **53**), **DMSO-d_6, 298 K, 400 MHz**

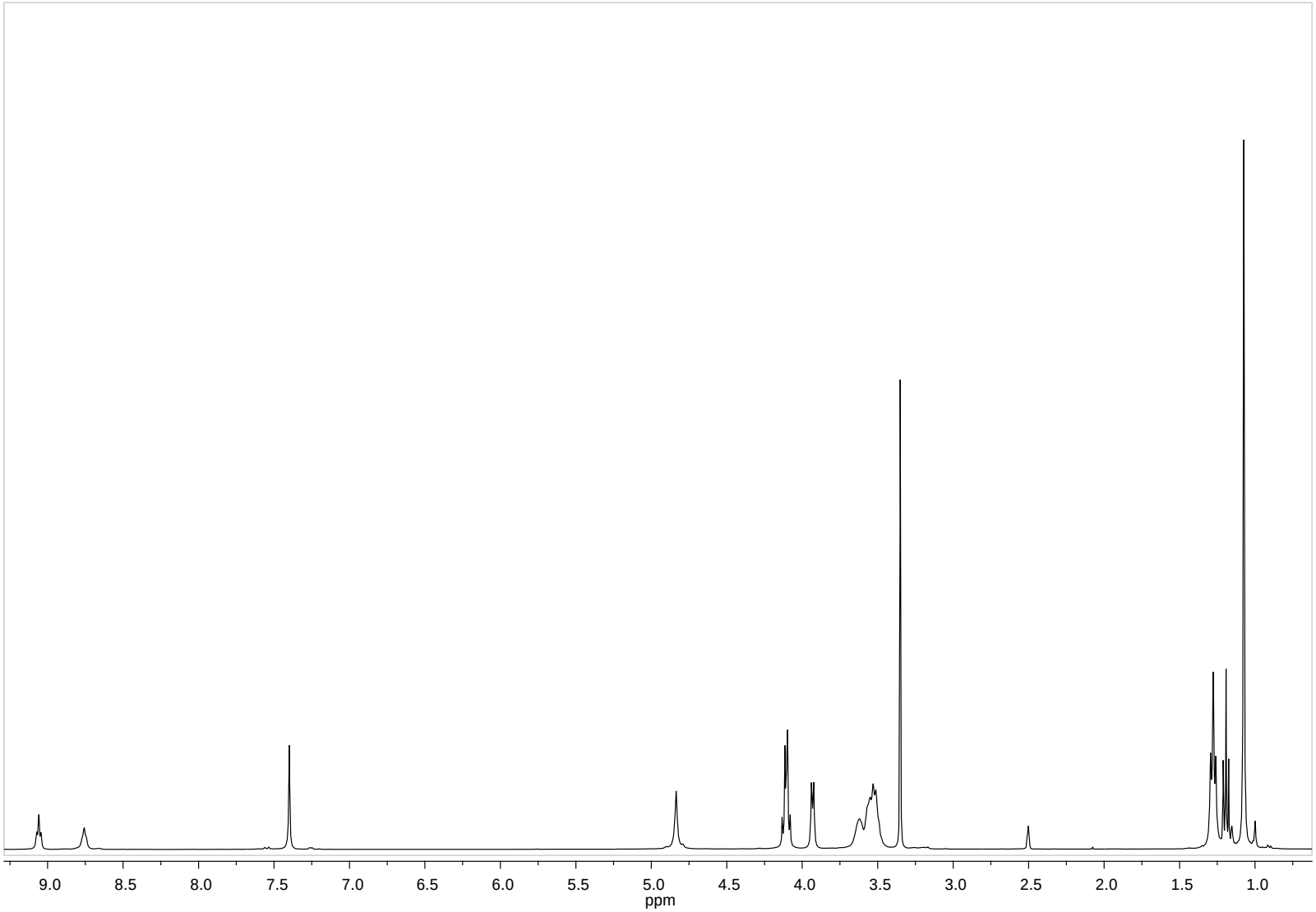

Fig. S32. ^{1}H NMR spectrum of 5,11,17,23-tetra-*tert*-butyl-25,26,27,28-tetrakis[(N-(2',2'-diethyl-2'-{([ethoxycarbonylmethyl]-amidocarbonylmethyl)amidocarbonylmethyl}ammoniumethyl)carbomoylmethoxy]-2,8,14,20-tetrathiacalix[4]arene tetra[bis(trifluoromethylsulfonyl)imide] (*cone* **54**), **DMSO-d$_6$, 298 K, 400 MHz**

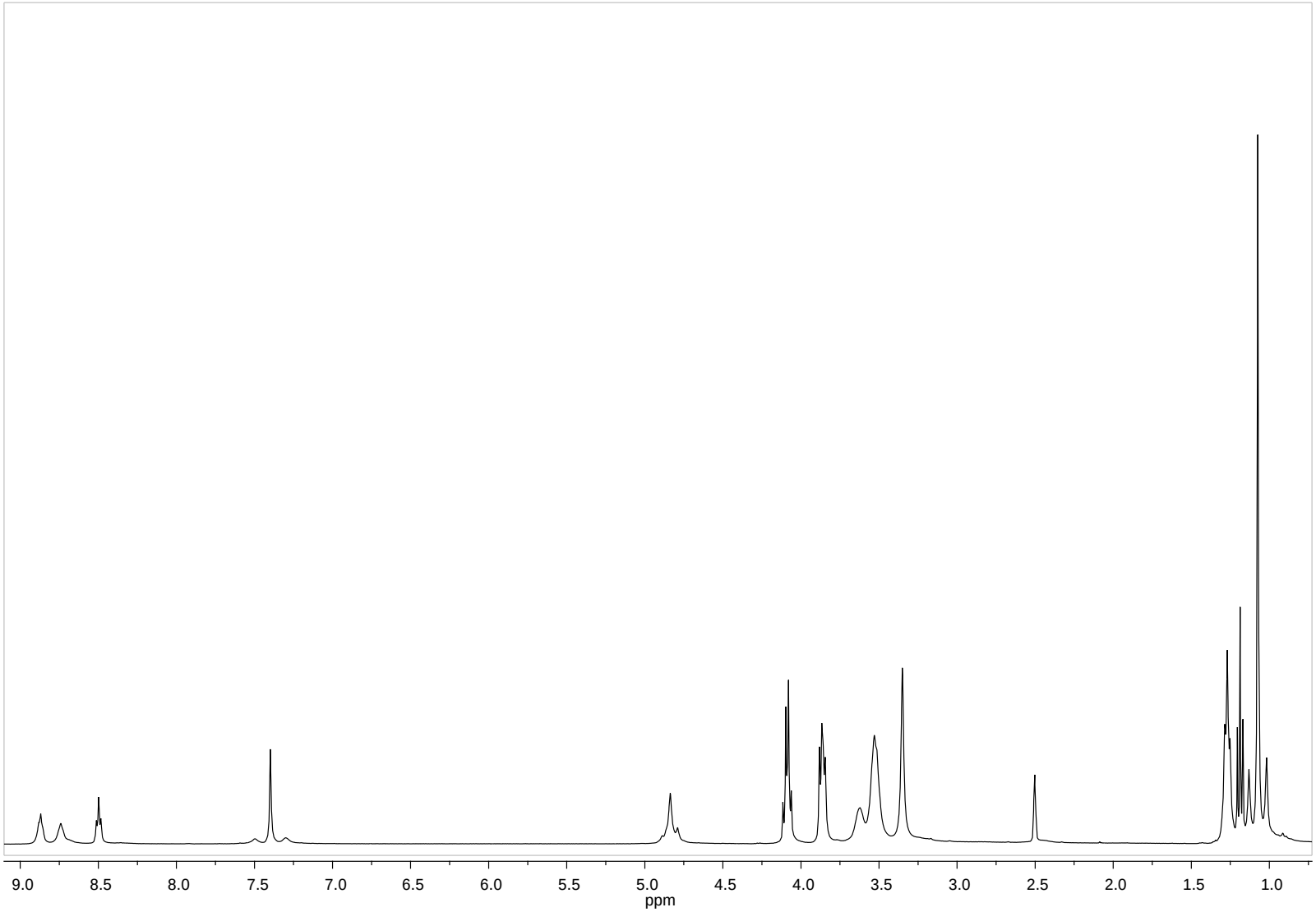

Fig. S33. ^{1}H NMR spectrum of 5,11,17,23-tetra-*tert*-butyl-25,26,27,28-tetrakis[(N-(2',2'-diethyl-2'-{(ethoxycarbonyl[S-methyl]methyl)amidocarbonylmethyl}ammoniumethyl)carbomoylmethoxy]-2,8,14,20-tetrathiacalix[4]arene tetra[bis(trifluoromethylsulfonyl)imide] (*cone* **55**), **DMSO-d$_6$, 298 K, 400 MHz**

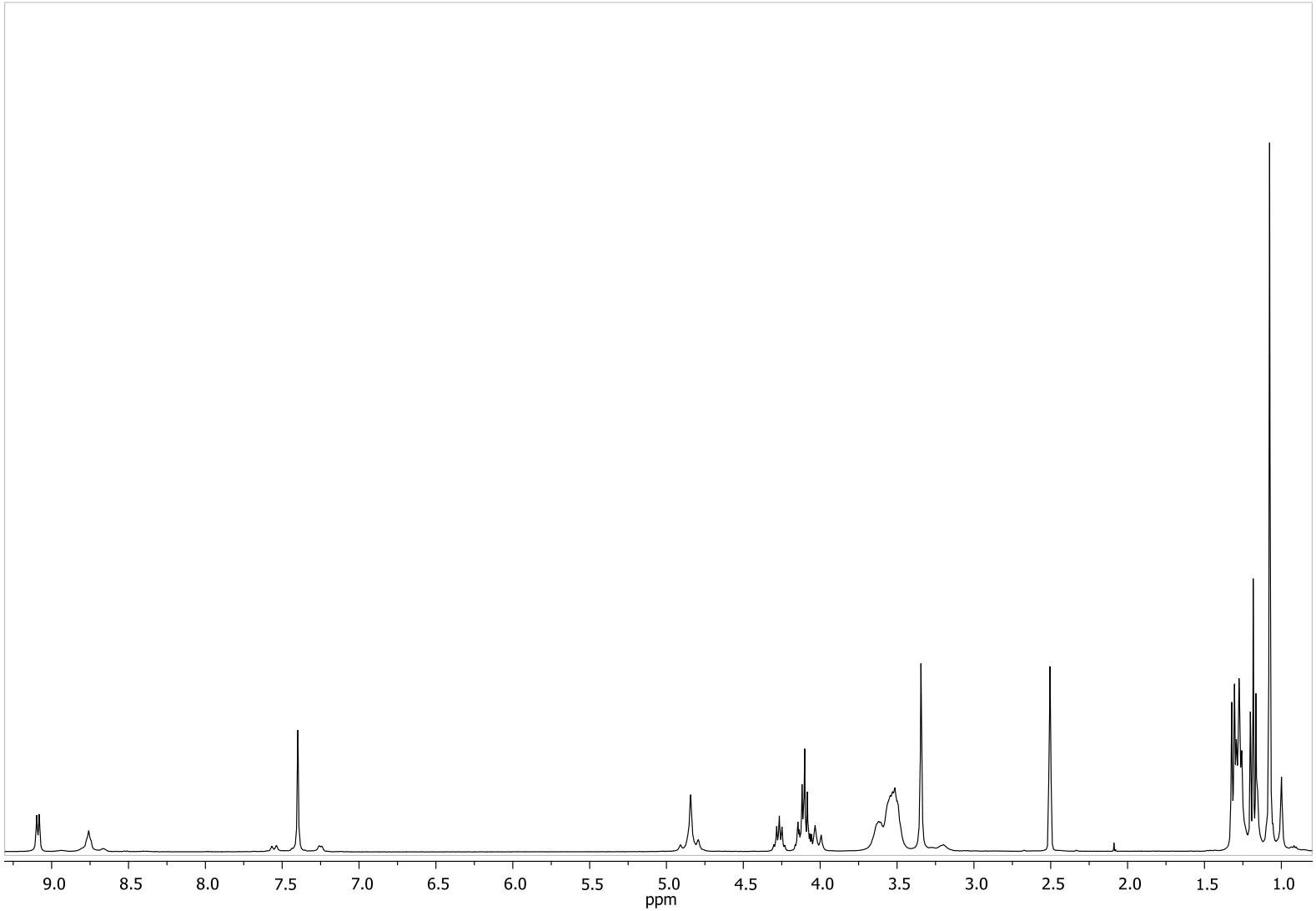

Fig. S34. ^{1}H NMR spectrum of 5,11,17,23-tetra-*tert*-butyl-25,26,27,28-tetrakis[(N-(3',3',3'-trimethyl)ammoniumpropyl)carbomoylmethoxy]-2,8,14,20-tetrathiacalix[4]arene tetra[bis(trifluoromethylsulfonyl)imide] (*1,3-alternate* **56**), **DMSO-d$_6$, 298 K, 400 MHz**

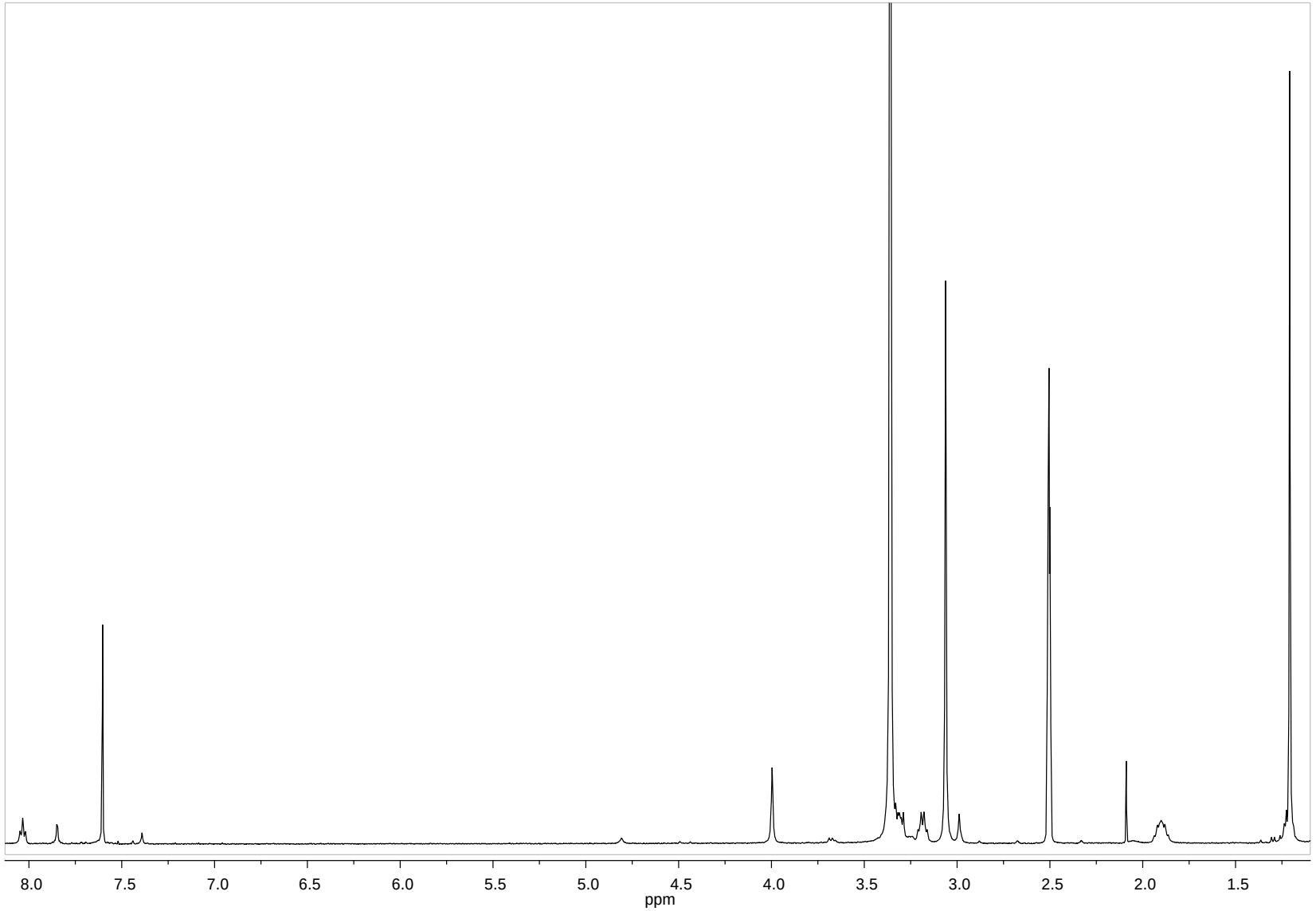

Fig. S35. ^{1}H NMR spectrum of 5,11,17,23-tetra-*tert*-butyl-25,26,27,28-tetrakis[(N-(3',3'-dimethyl-3'-ethyl)ammoniumpropyl)-carbomoylmethoxy]-2,8,14,20-tetrathiacalix[4]arene tetra[bis(trifluoromethylsulfonyl)imide] (*1,3-alternate* **57**), **DMSO-d_6, 298 K, 400 MHz**

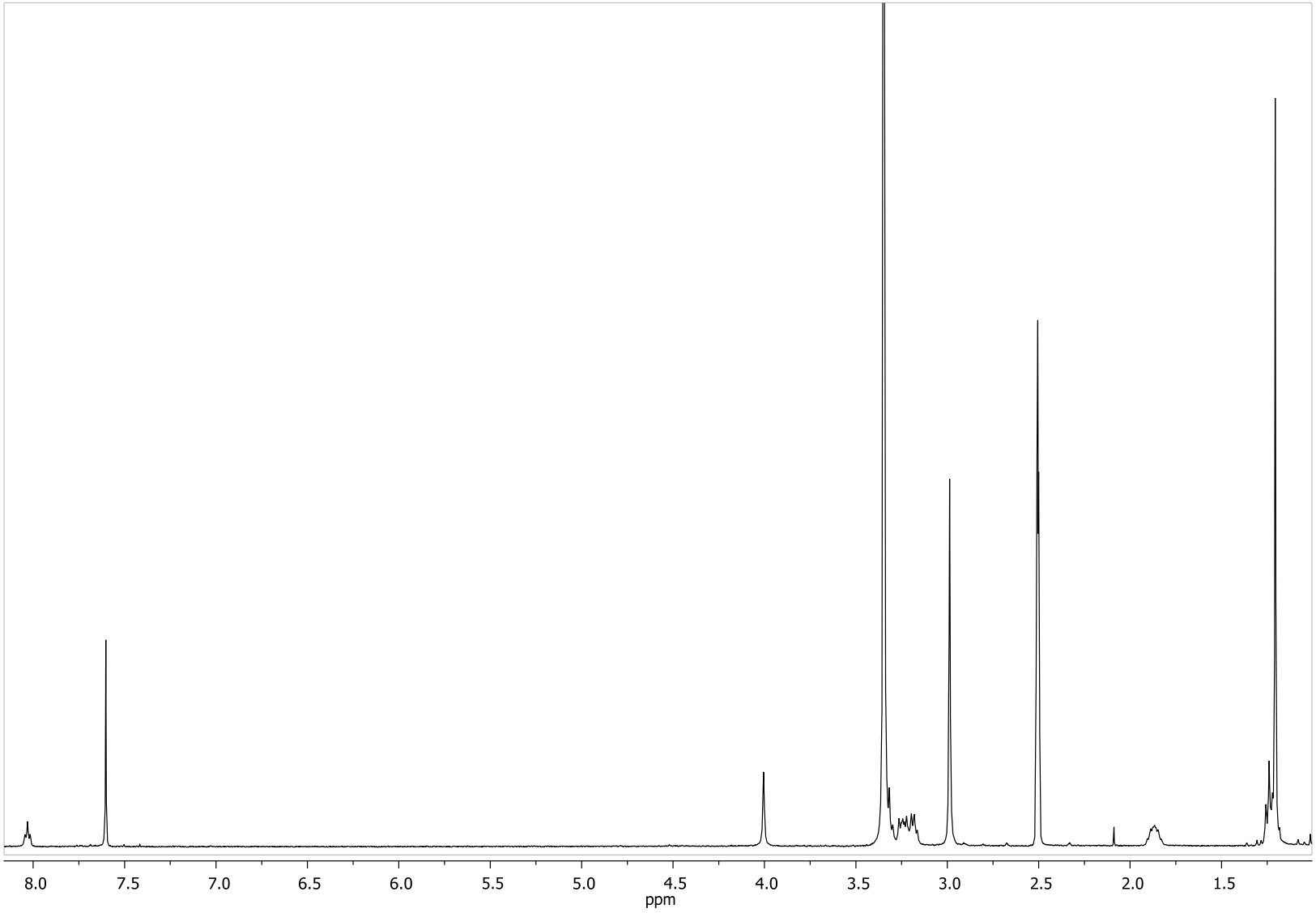

Fig. S36. ^{1}H NMR spectrum of 5,11,17,23-tetra-*tert*-butyl-25,26,27,28-tetrakis[(N-(3',3'-dimethyl-3'-benzyl)ammoniumpropyl)-carbomoylmethoxy]-2,8,14,20-tetrathiacalix[4]arene tetra[bis(trifluoromethylsulfonyl)imide] (*1,3-alternate* **58**), **DMSO-d_6, 298 K, 400 MHz**

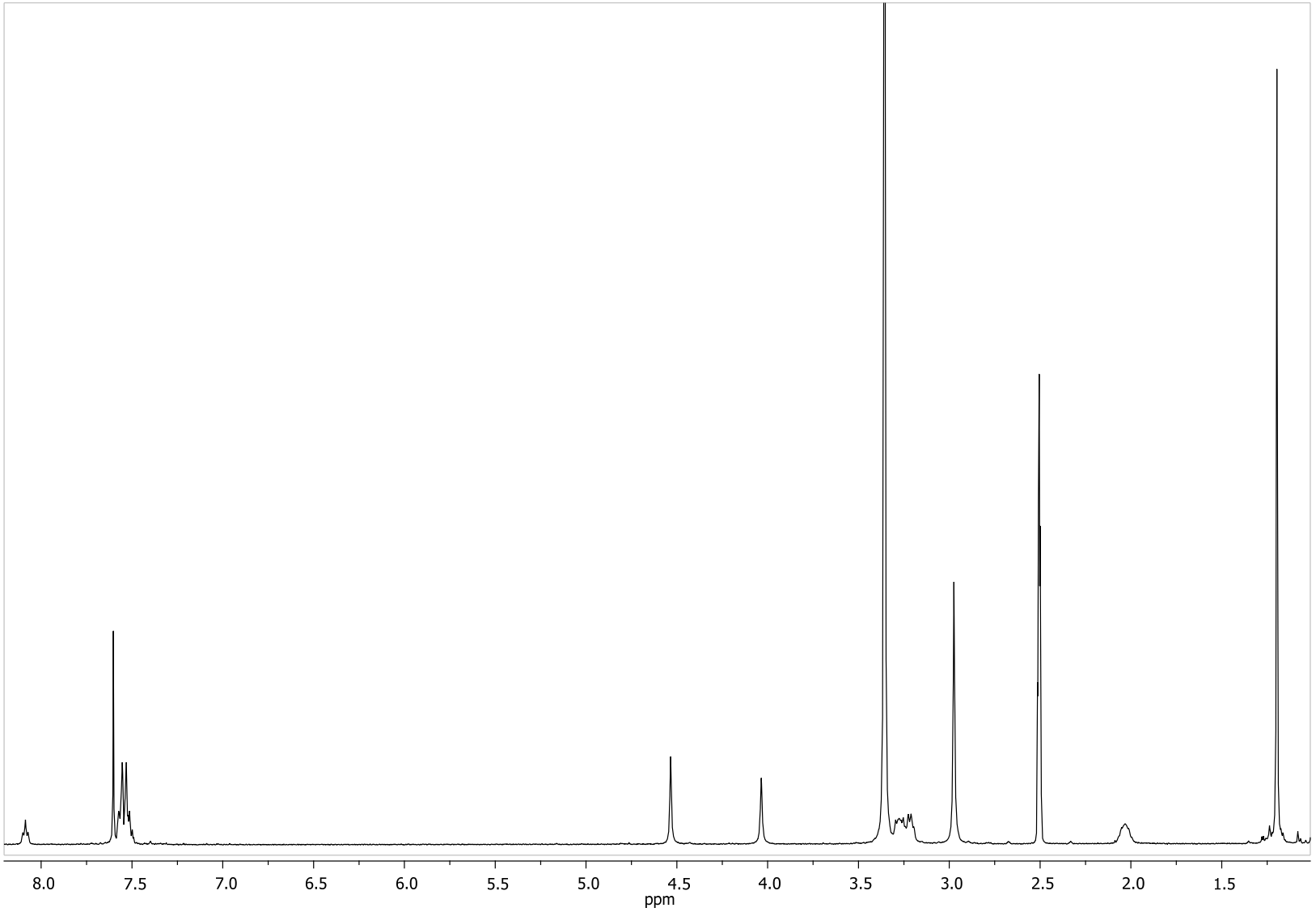

Fig. S37. ^{1}H NMR spectrum of 5,11,17,23-tetra-*tert*-butyl-25,26,27,28-tetrakis[(N-(3',3'-dimethyl-3'-(ethoxycarbonylmethyl)ammoniumpropyl)carbomoylmethoxy]-2,8,14,20-tetrathiacalix[4]arene tetra[bis(trifluoromethylsulfonyl)imide] (*1,3-alternate* **59**), **DMSO-d$_6$, 298 K, 400 MHz**

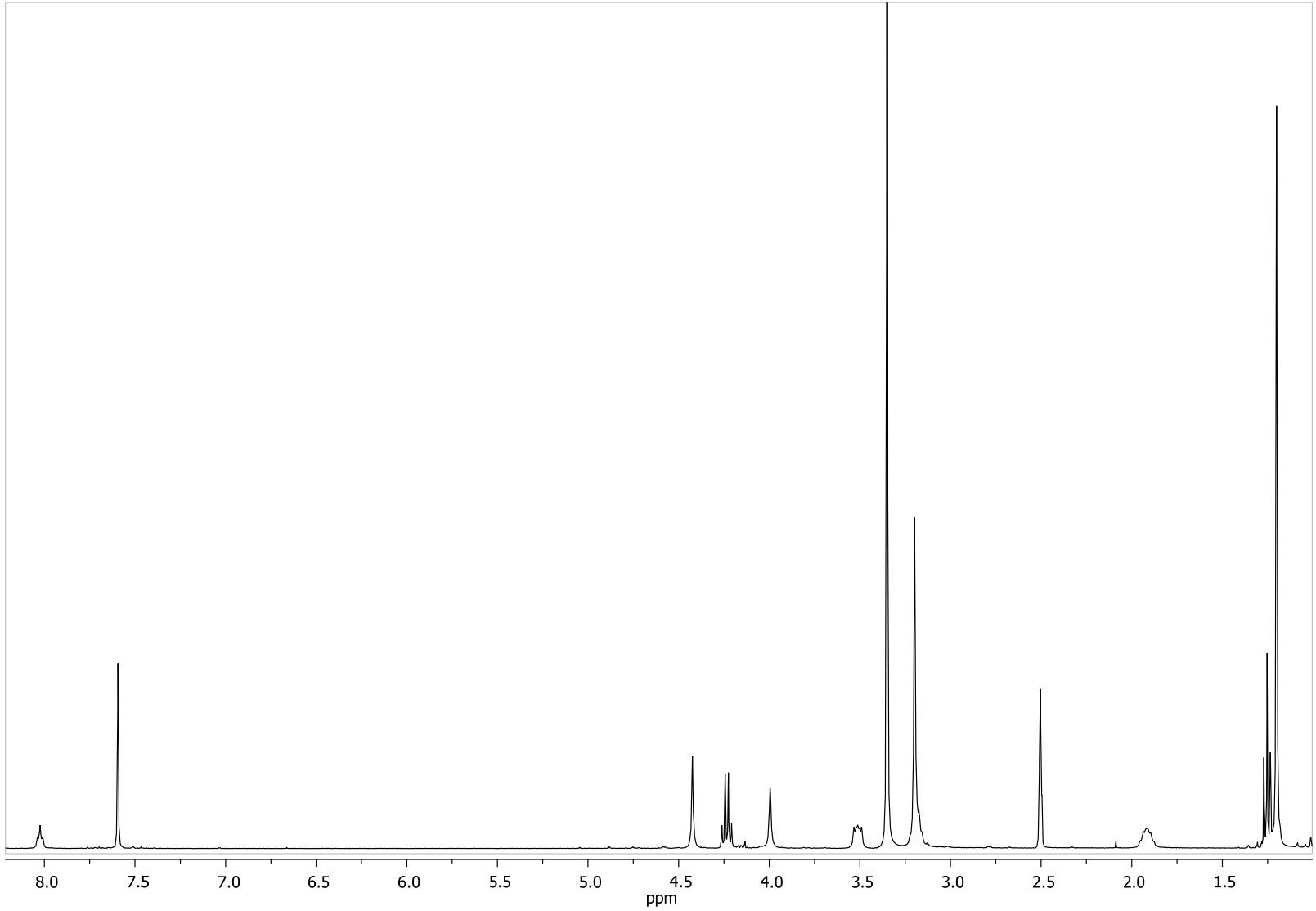

Fig. S38. ^{1}H NMR spectrum of 5,11,17,23-tetra-*tert*-butyl-25,26,27,28-tetrakis[(N-(3',3'-dimethyl-3'-(pentoxycarbonylmethyl)ammoniumpropyl)carbomoylmethoxy]-2,8,14,20-tetrathiacalix[4]arene tetra[bis(trifluoromethylsulfonyl)imide] (*1,3-alternate* **60**), **DMSO-d_6, 298 K, 400 MHz**

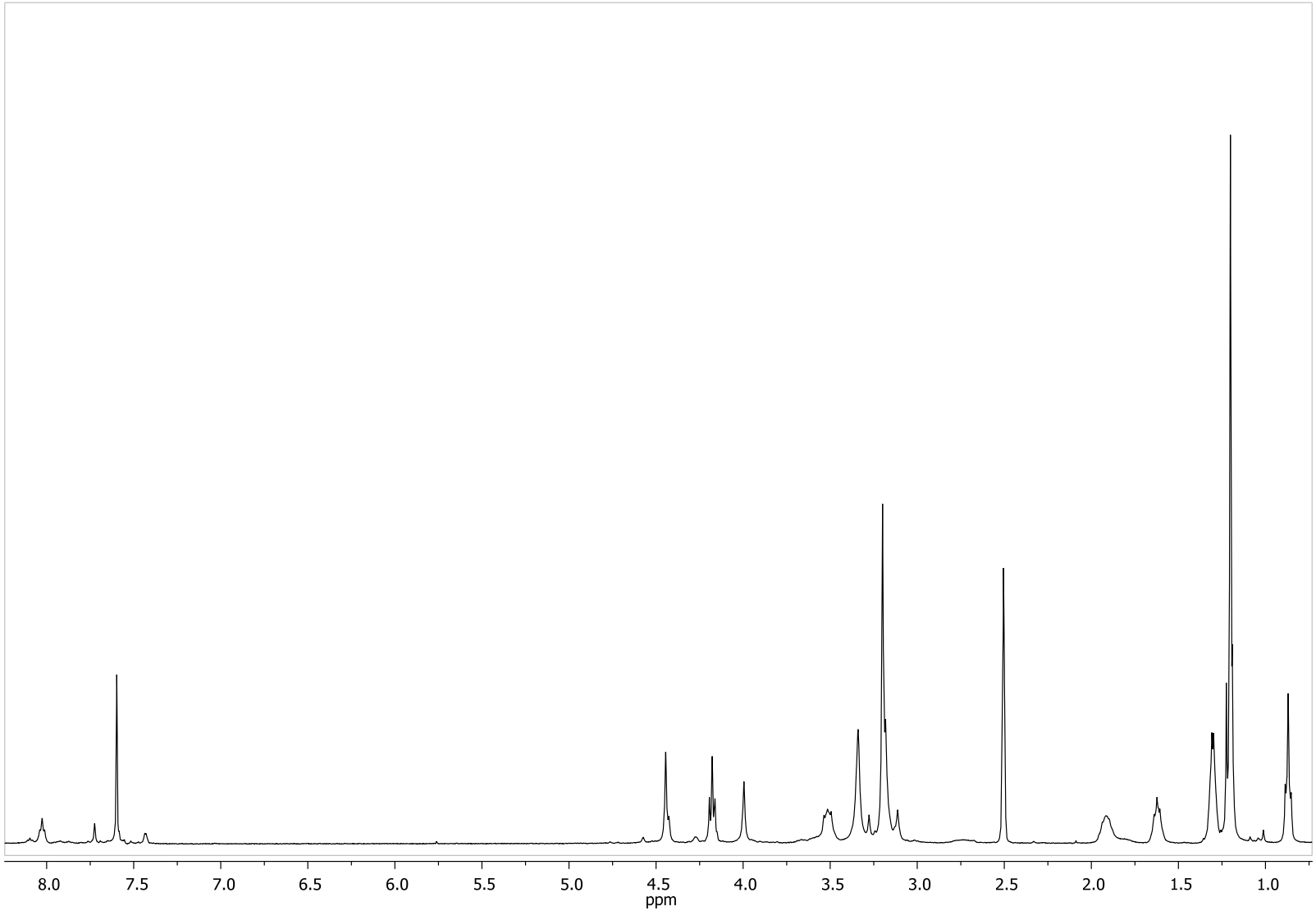

Fig. S39. ^{1}H NMR spectrum of 5,11,17,23-tetra-*tert*-butyl-25,26,27,28-tetrakis[(N-(3',3'-dimethyl-3'-{(ethoxycarbonylmethyl)amidocarbonylmethyl}ammoniumpropyl)carbomoylmethoxy]-2,8,14,20-tetrathiacalix[4]arene tetra[bis(trifluoromethylsulfonyl)imide] (*1,3-alternate* **61**), **DMSO-d$_6$, 298 K, 400 MHz**

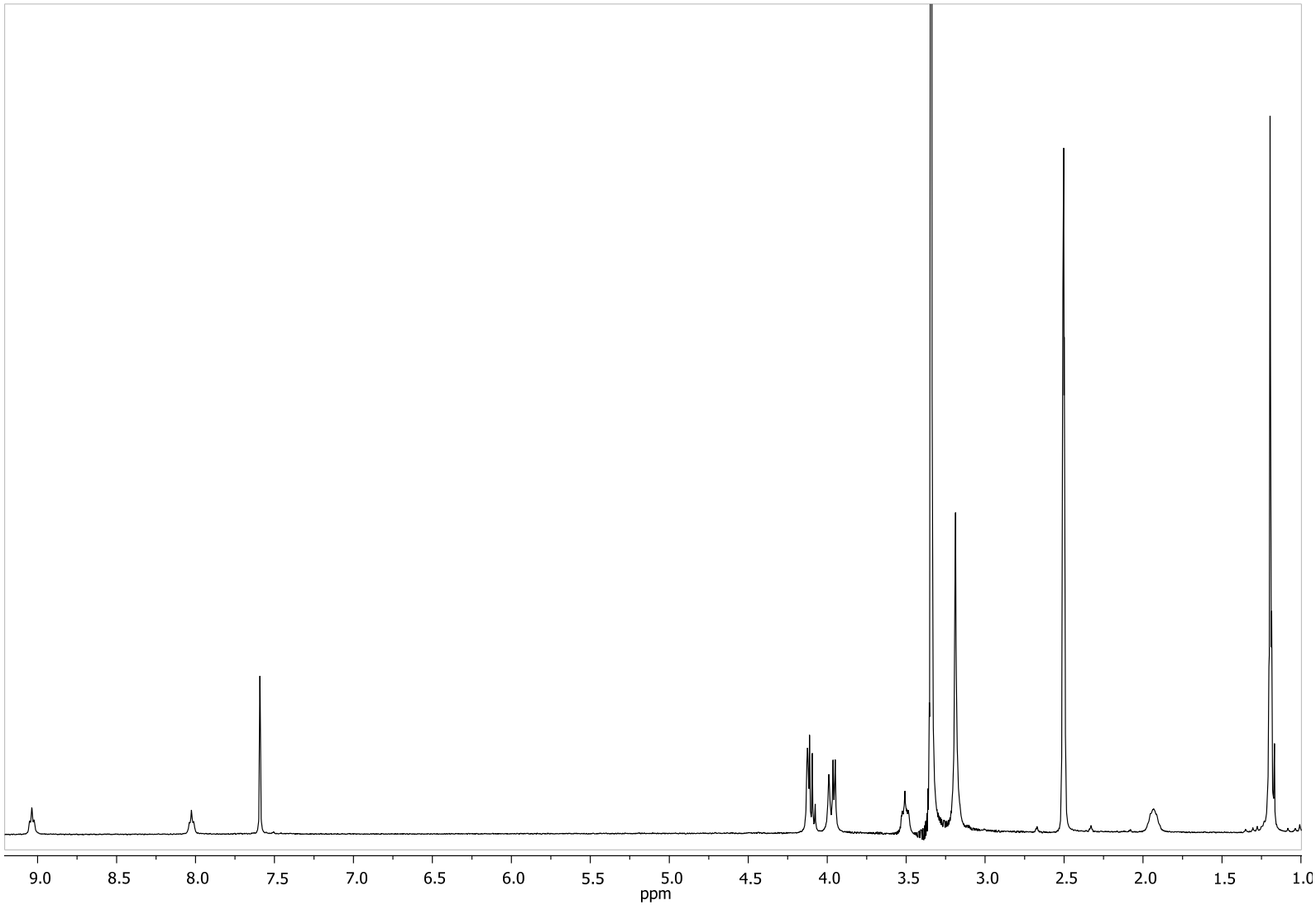

Fig. S40. ^{1}H NMR spectrum of 5,11,17,23-tetra-*tert*-butyl-25,26,27,28-tetrakis[(N-(3',3'-dimethyl-3'-{([ethoxycarbonylmethyl]amidocarbonylmethyl)amidocarbonylmethyl}ammoniumpropyl)carbomoylmethoxy]-2,8,14,20-tetrathiacalix[4]arene tetra[bis(trifluoromethylsulfonyl)imide] (*1,3-alternate* **62**), **DMSO-d$_6$, 298 K, 400 MHz**

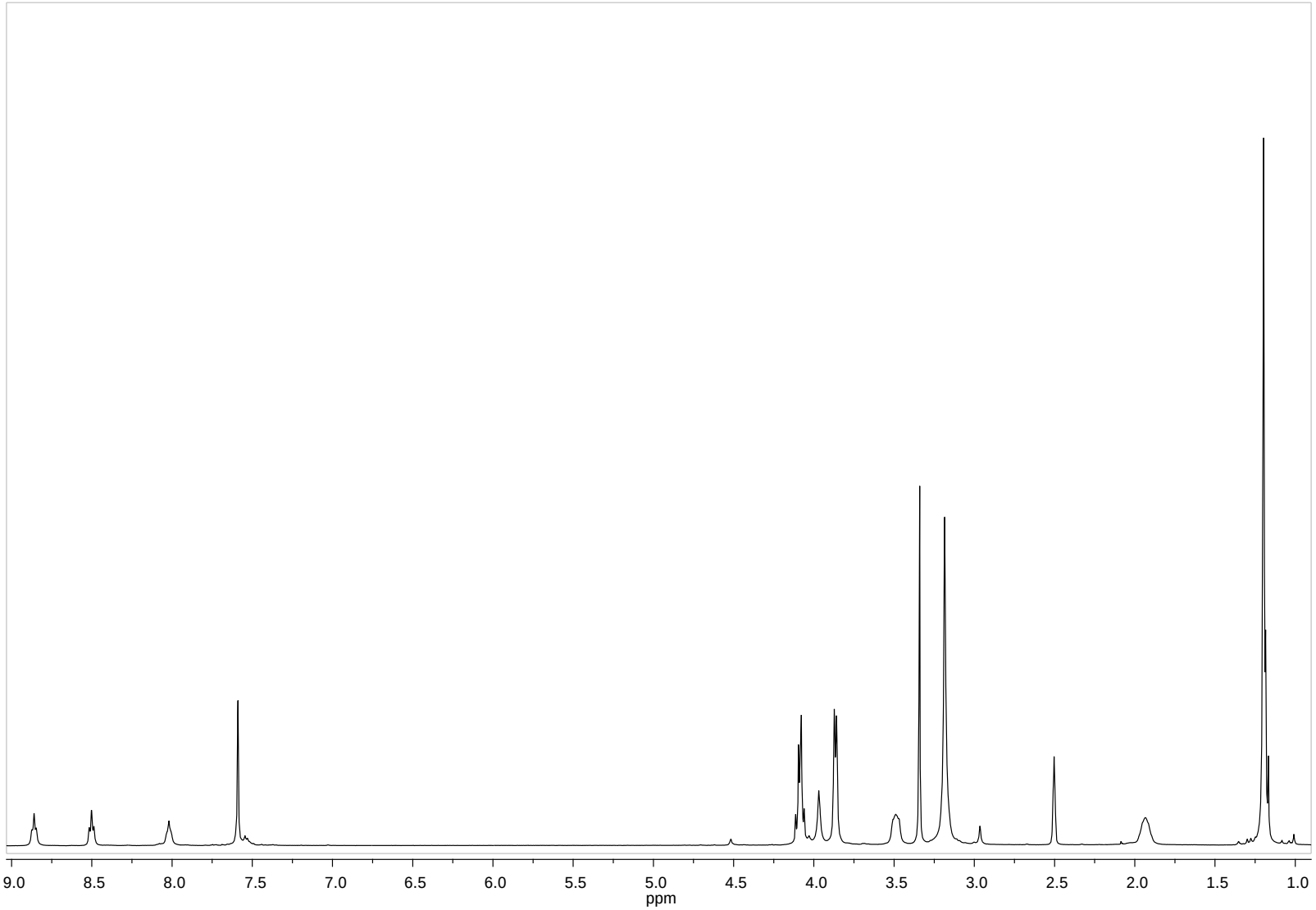

Fig. S41. ^{1}H NMR spectrum of 5,11,17,23-tetra-*tert*-butyl-25,26,27,28-tetrakis[(N-(3',3'-dimethyl-3'-{(ethoxycarbonyl[S-methyl]methyl)amidocarbonylmethyl}ammoniumpropyl)carbomoylmethoxy]-2,8,14,20-tetrathiacalix[4]arene tetra[bis(trifluoromethylsulfonyl)imide] (*1,3-alternate* **63**), **DMSO-d$_6$, 298 K, 400 MHz**

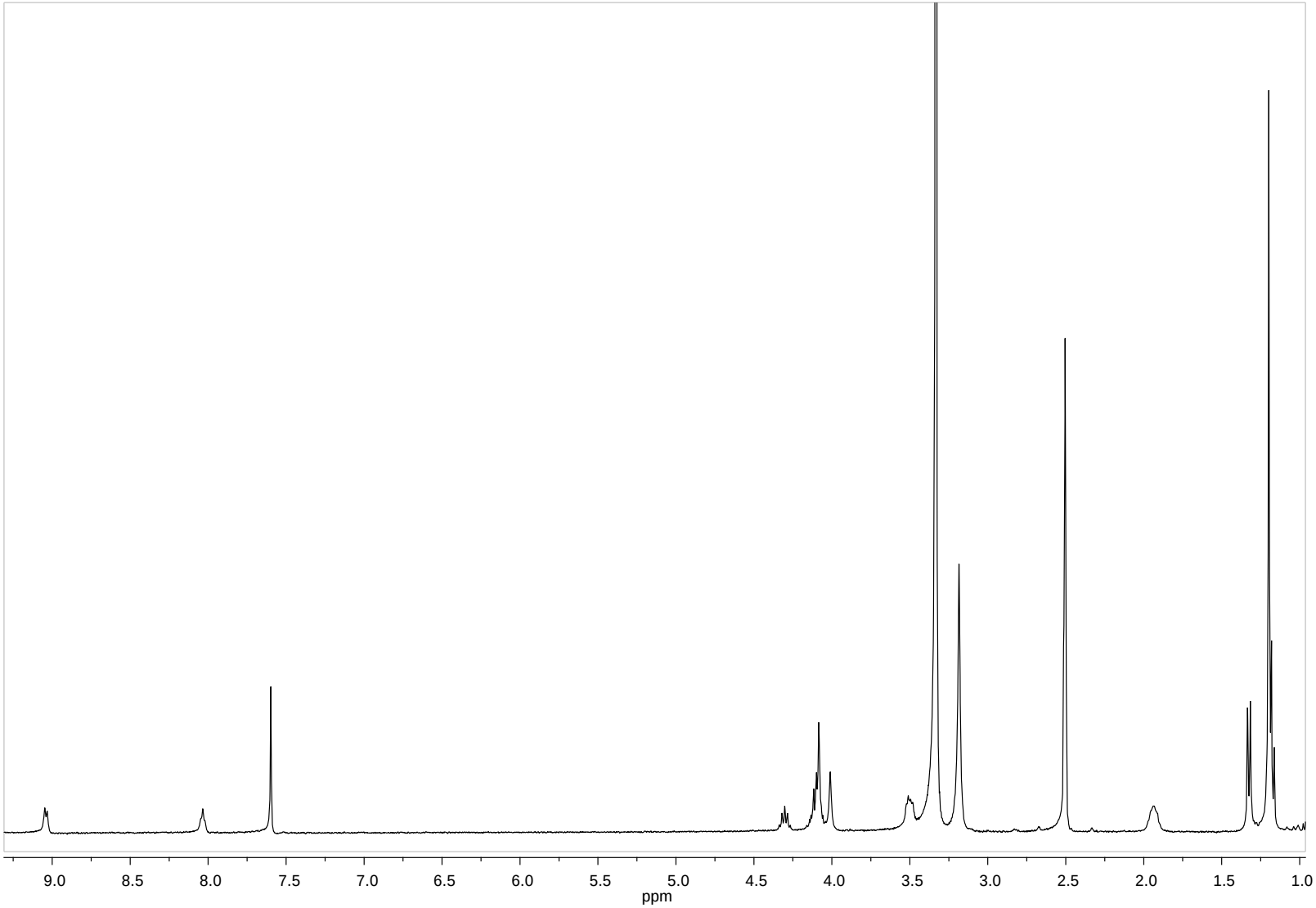

Fig. S42. ^{1}H NMR spectrum of 5,11,17,23-tetra-*tert*-butyl-25,26,27,28-tetrakis[(N-(3',3'-dimethyl-3'-{3''-propylphtalimide}ammoniumpropyl)-carbomoylmethoxy]-2,8,14,20-tetrathiacalix[4]arene tetra[bis(trifluoromethylsulfonyl)imide] (*1,3-alternate* **64**), **DMSO-d$_6$, 298 K, 400 MHz**

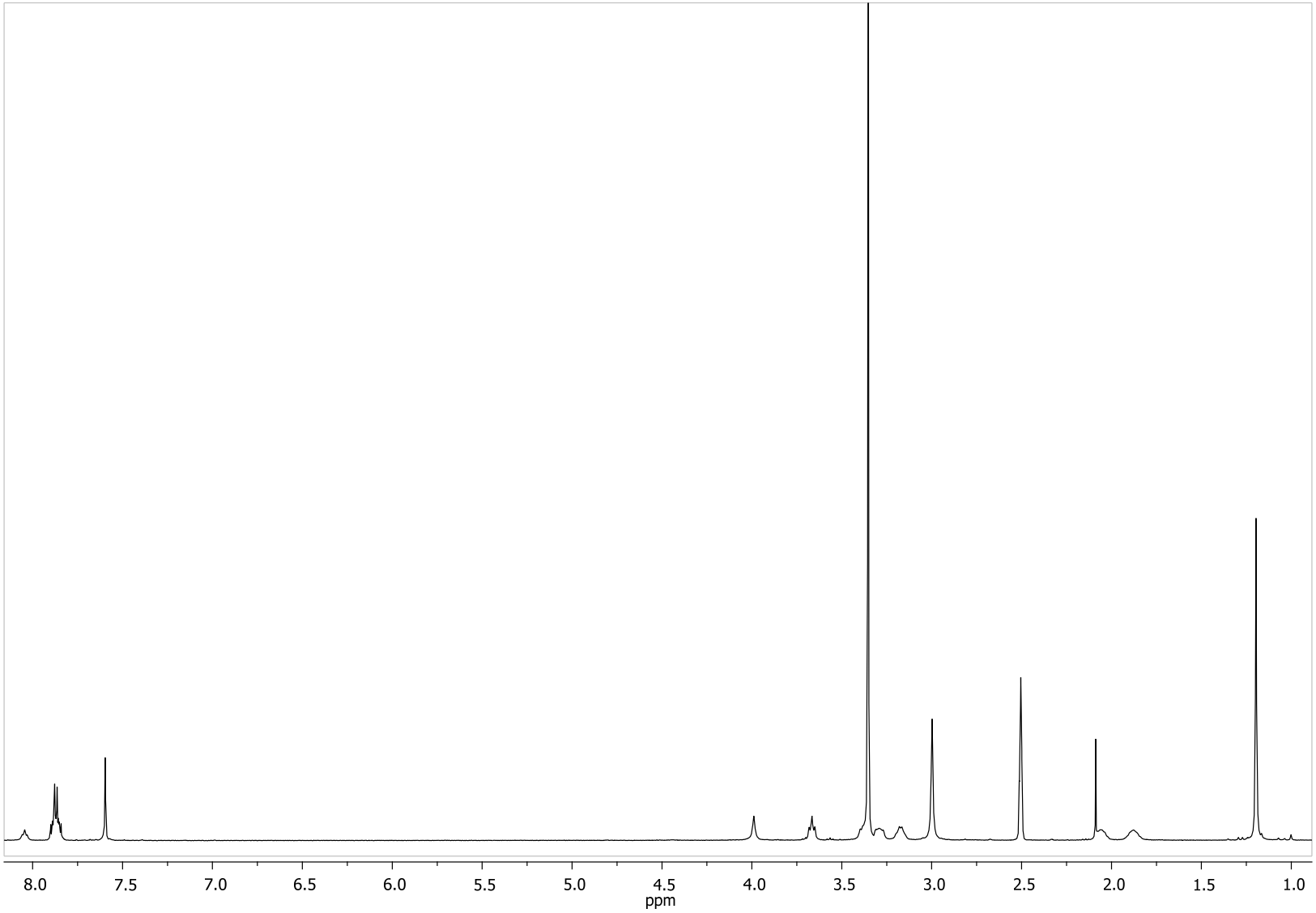

Fig. S43. ^{1}H NMR spectrum of 5,11,17,23-tetra-*tert*-butyl-25,26,27,28-tetrakis[(N-(2'-methyl-2',2'-diethyl)ammoniumethyl)-carbomoylmethoxy]-2,8,14,20-tetrathiacalix[4]arene tetra[bis(trifluoromethylsulfonyl)imide] (*1,3-alternate* **65**), **DMSO-d$_6$, 298 K, 400 MHz**

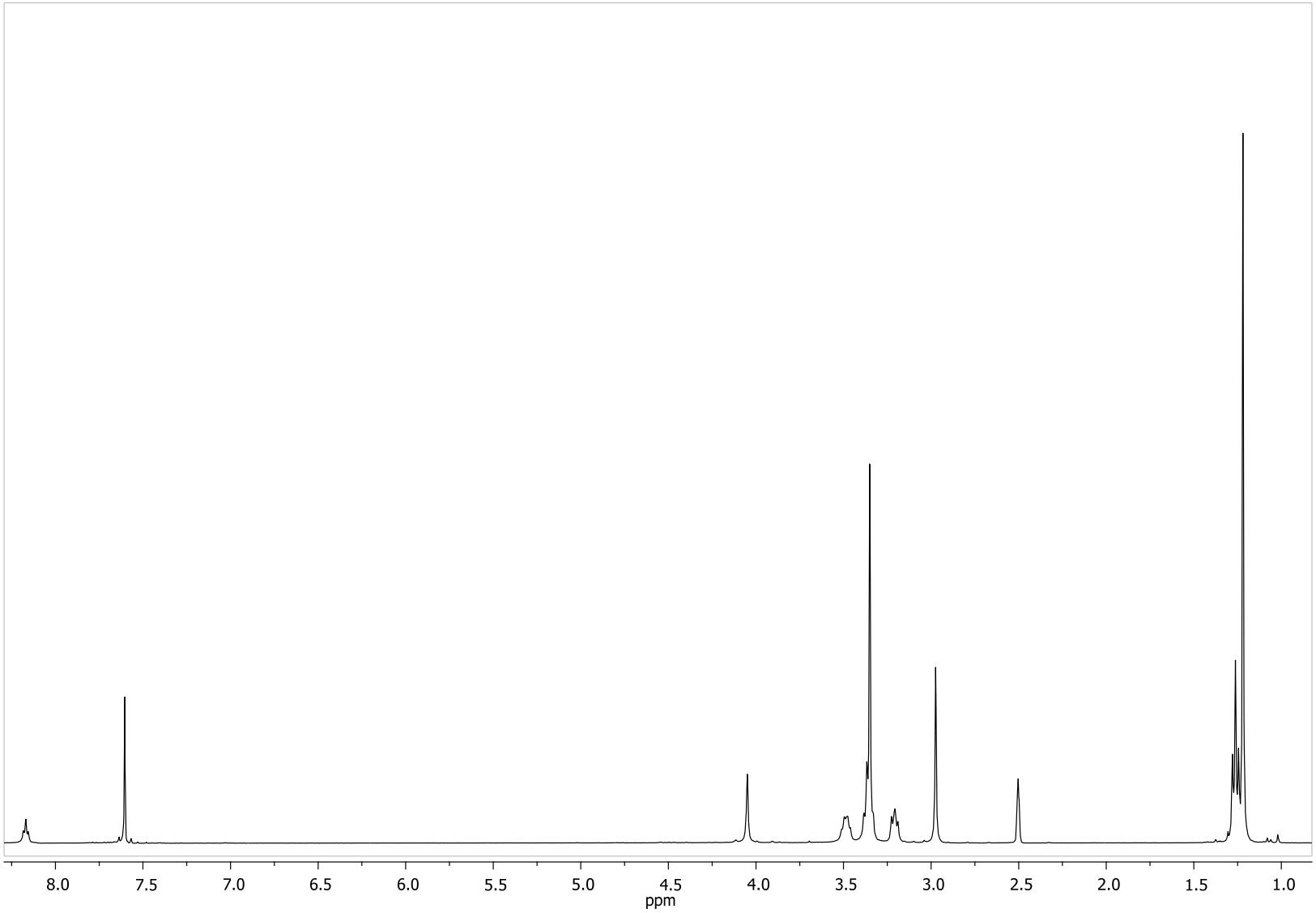

Fig. S44. ^{1}H NMR spectrum of 5,11,17,23-tetra-*tert*-butyl-25,26,27,28-tetrakis[(N-(2',2',2'-triethyl)ammoniumethyl)carbomoylmethoxy]-2,8,14,20-tetrathiacalix[4]arene tetra[bis(trifluoromethylsulfonyl)imide] (*1,3-alternate* **66**), **DMSO-d_6, 298 K, 400 MHz**

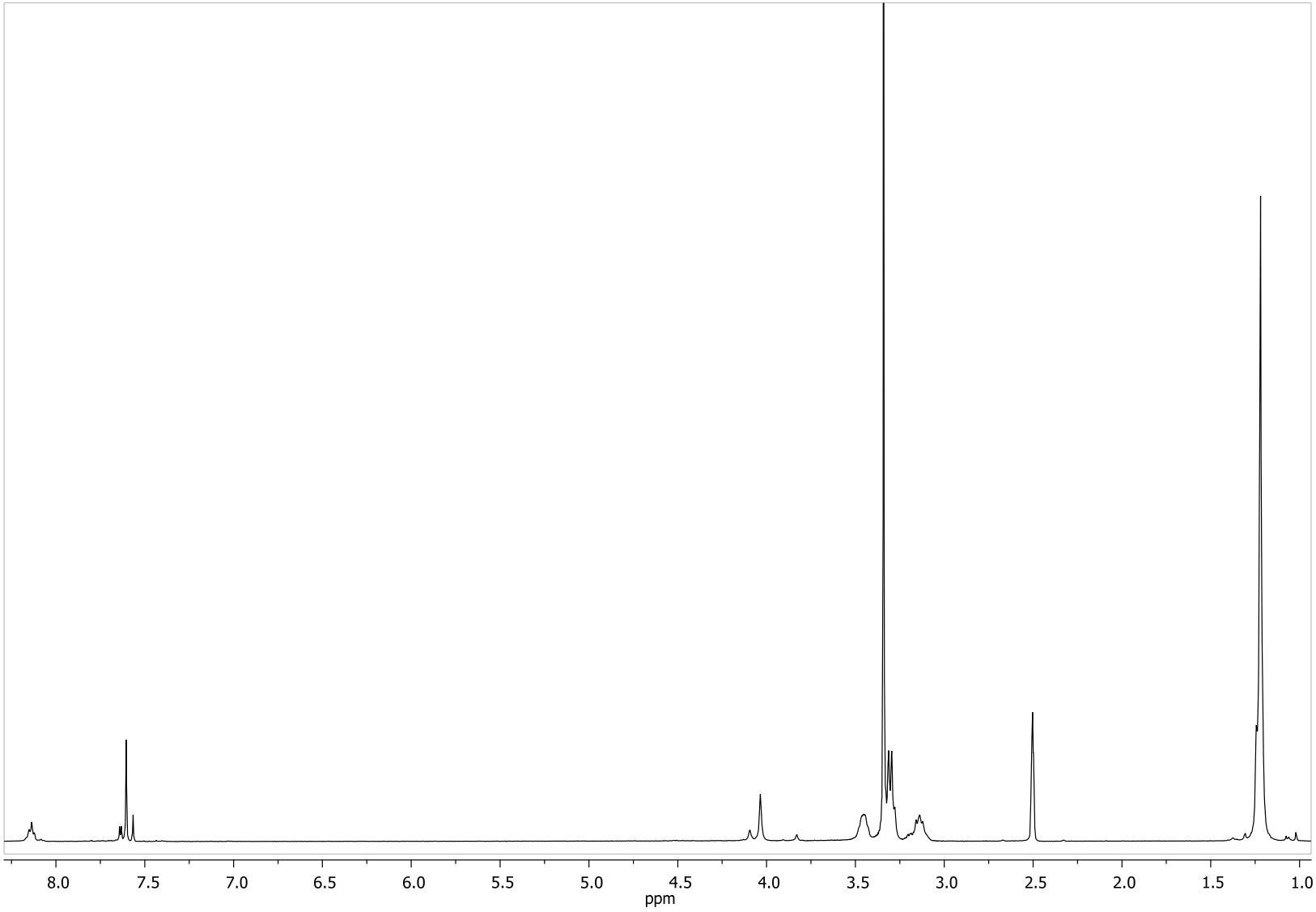

Fig. S45. ^{1}H NMR spectrum of 5,11,17,23-tetra-*tert*-butyl-25,26,27,28-tetrakis[(N-(2',2'-diethyl-2'-benzyl)ammoniumethyl)-carbomoylmethoxy]-2,8,14,20-tetrathiacalix[4]arene tetra[bis(trifluoromethylsulfonyl)imide] (*1,3-alternate* **67**), **DMSO-d$_6$, 298 K, 400 MHz**

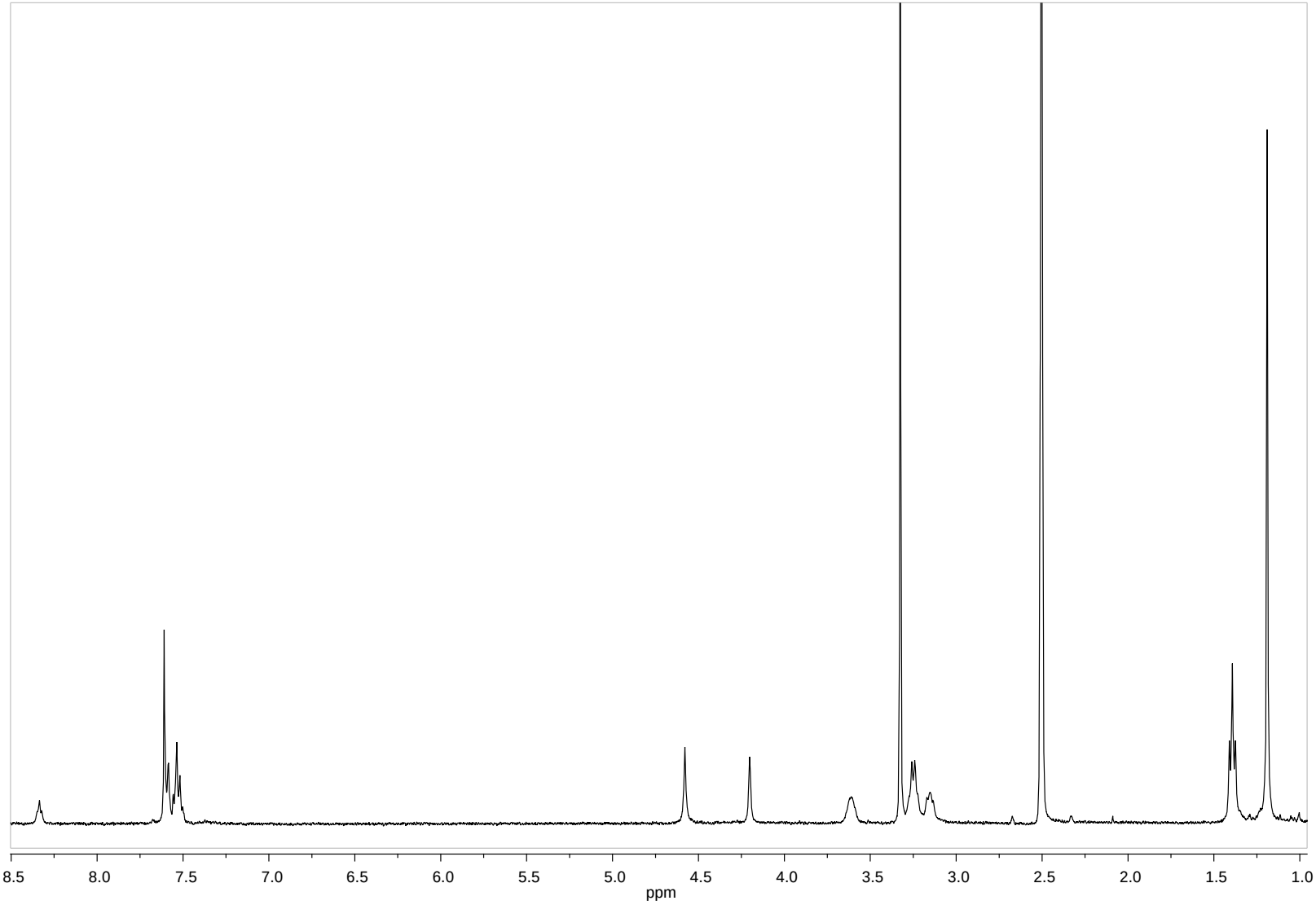

Fig. S46. ^{1}H NMR spectrum of 5,11,17,23-tetra-*tert*-butyl-25,26,27,28-tetrakis[(N-(2',2'-diethyl-2'-(ethoxycarbonylmethyl)ammoniumethyl)-carbomoylmethoxy]-2,8,14,20-tetrathiacalix[4]arene tetra[bis(trifluoromethylsulfonyl)imide] (*1,3-alternate* **68**), **DMSO-d_6, 298 K, 400 MHz**

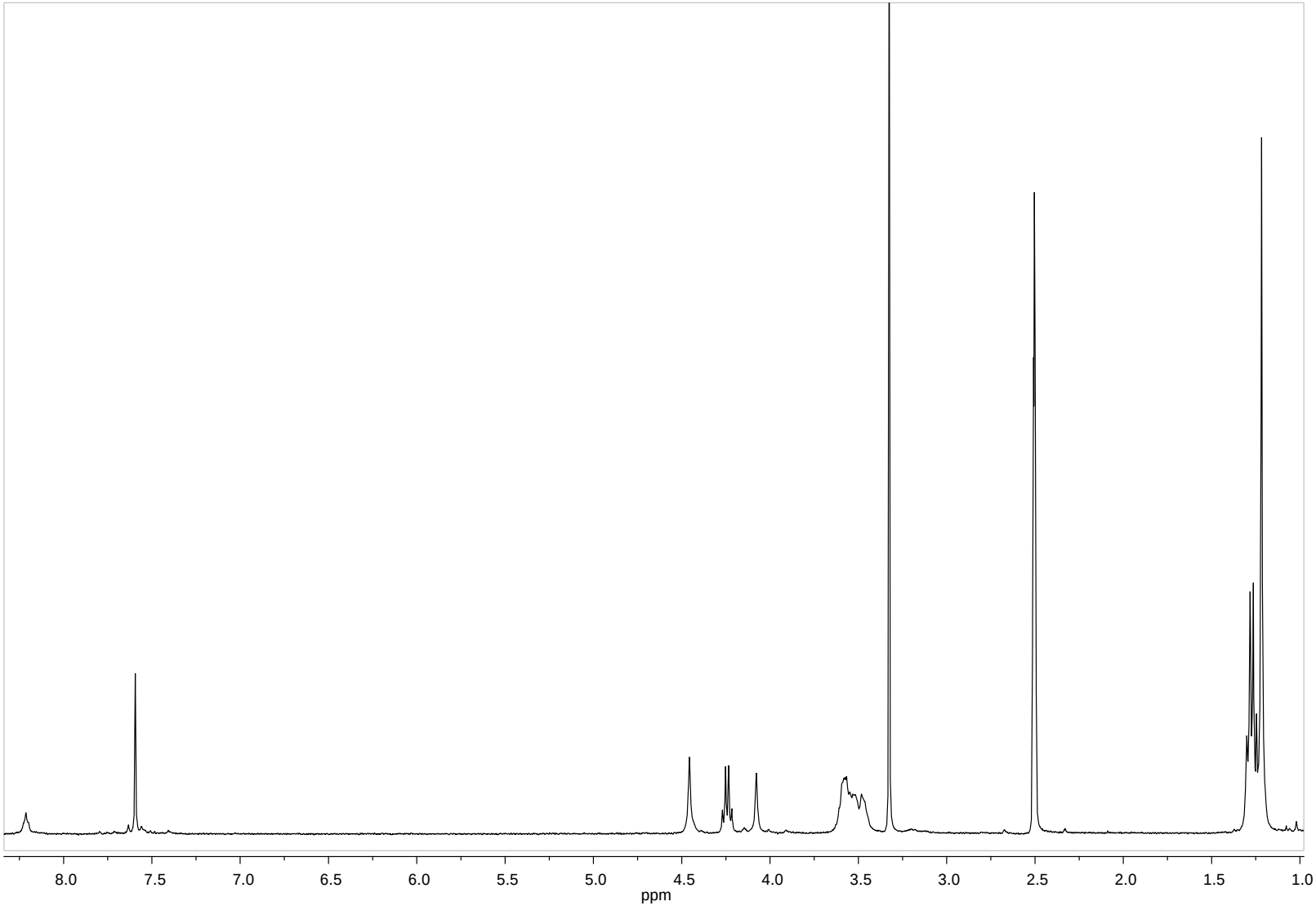

Fig. S47. ^{1}H NMR spectrum of 5,11,17,23-tetra-*tert*-butyl-25,26,27,28-tetrakis[(N-(2',2'-diethyl-2'-(pentoxycarbonylmethyl)ammoniumethyl)-carbomoylmethoxy]-2,8,14,20-tetrathiacalix[4]arene tetra[bis(trifluoromethylsulfonyl)imide] (*1,3-alternate* **69**), **DMSO-d$_6$, 298 K, 400 MHz**

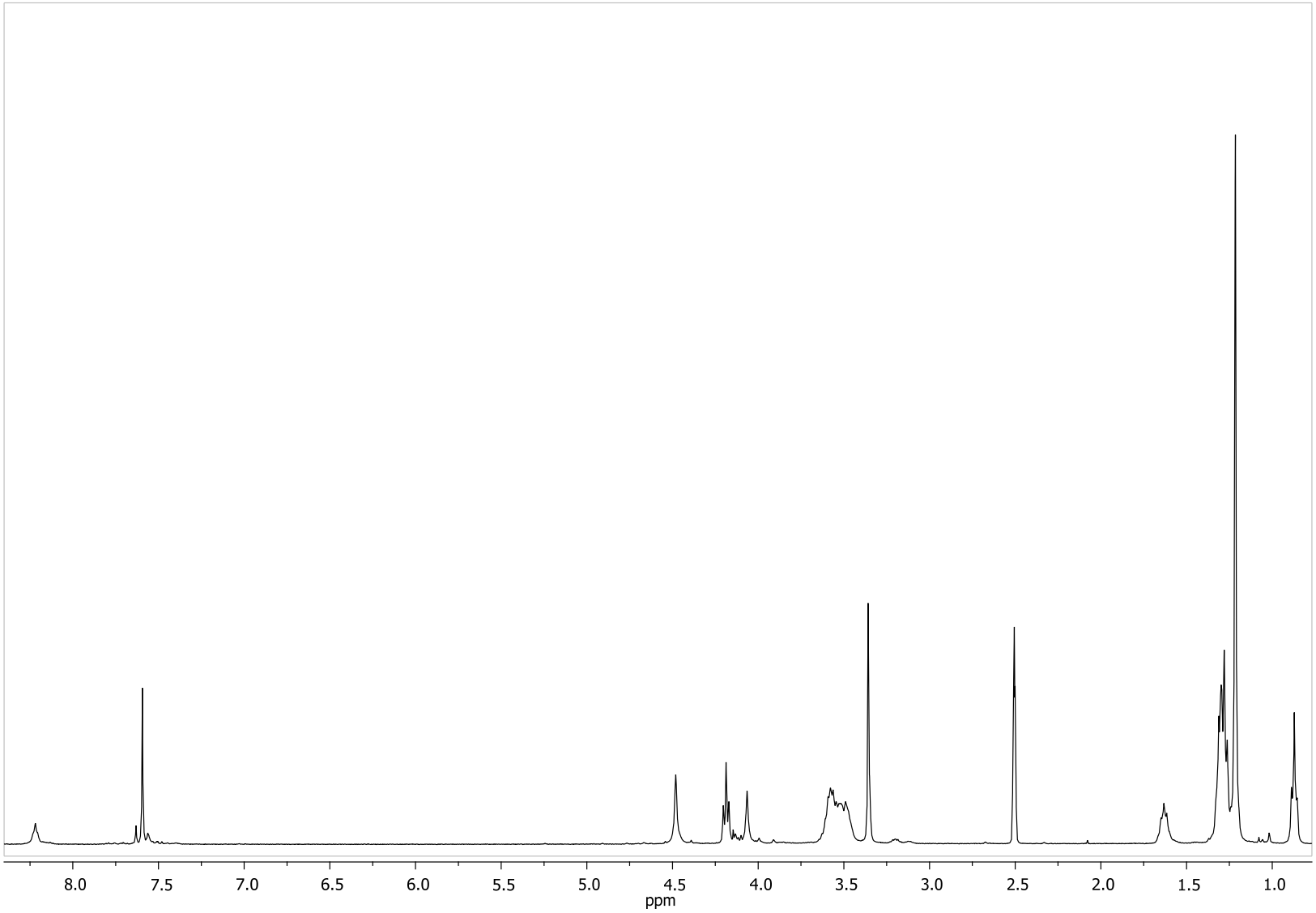

Fig. S48. ^{1}H NMR spectrum of 5,11,17,23-tetra-*tert*-butyl-25,26,27,28-tetrakis[(N-(2',2'-diethyl-2'-{(ethoxycarbonylmethyl)amidocarbonylmethyl})ammoniumethyl)carbomoylmethoxy]-2,8,14,20-tetrathiacalix[4]arene tetra[bis(trifluoromethylsulfonyl)imide] (*1,3-alternate* **70**), **DMSO-d$_6$, 298 K, 400 MHz**

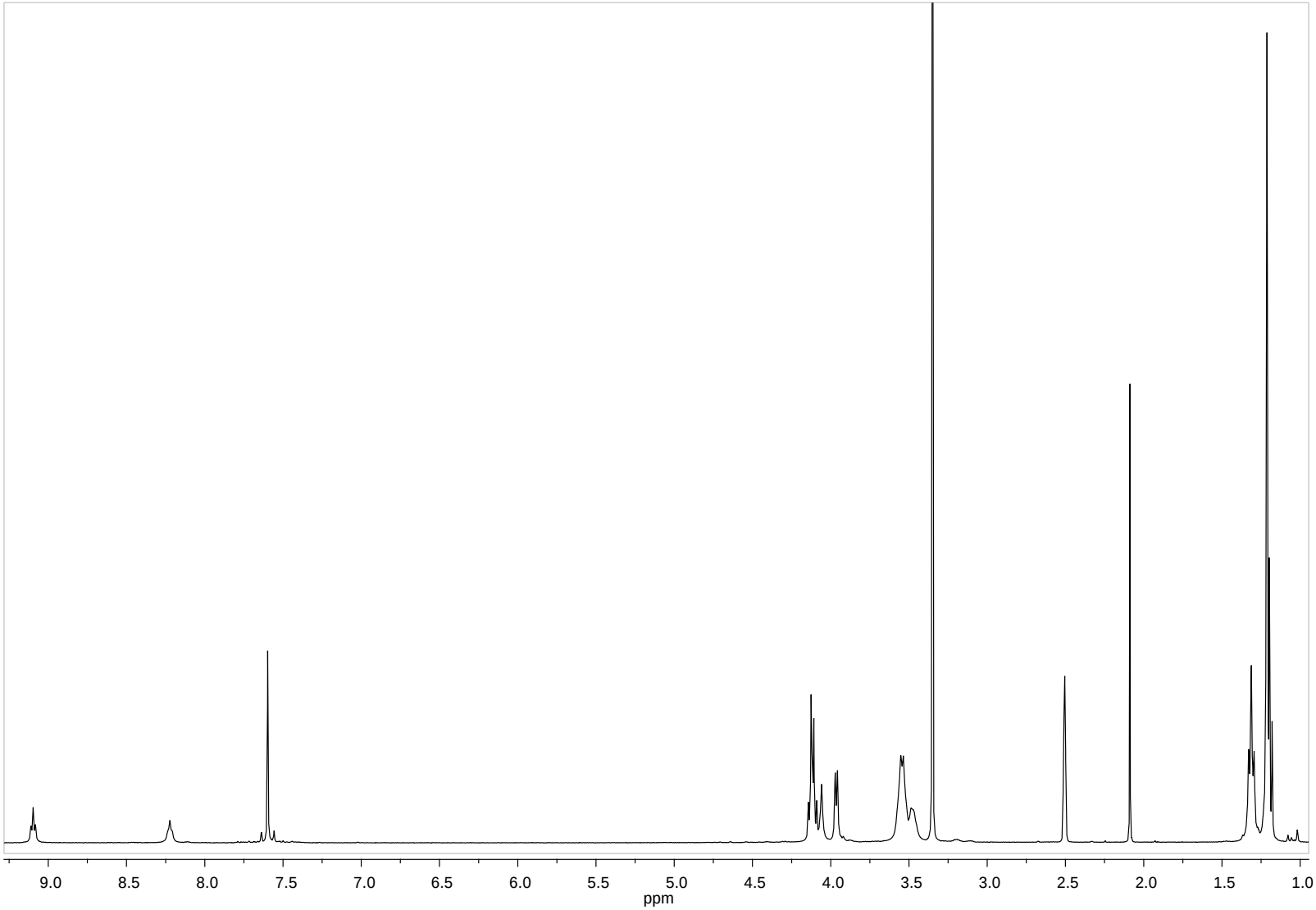

Fig. S49. ^{1}H NMR spectrum of 5,11,17,23-tetra-*tert*-butyl-25,26,27,28-tetrakis[(N-(2',2'-diethyl-2'-{([ethoxycarbonylmethyl]amidocarbonylmethyl)amidocarbonylmethyl}ammoniumethyl)carbomoylmethoxy]-2,8,14,20-tetrathiacalix[4]arene tetra[bis(trifluoromethylsulfonyl)imide] (*1,3-alternate* **71**), **DMSO-d$_6$, 298 K, 400 MHz**

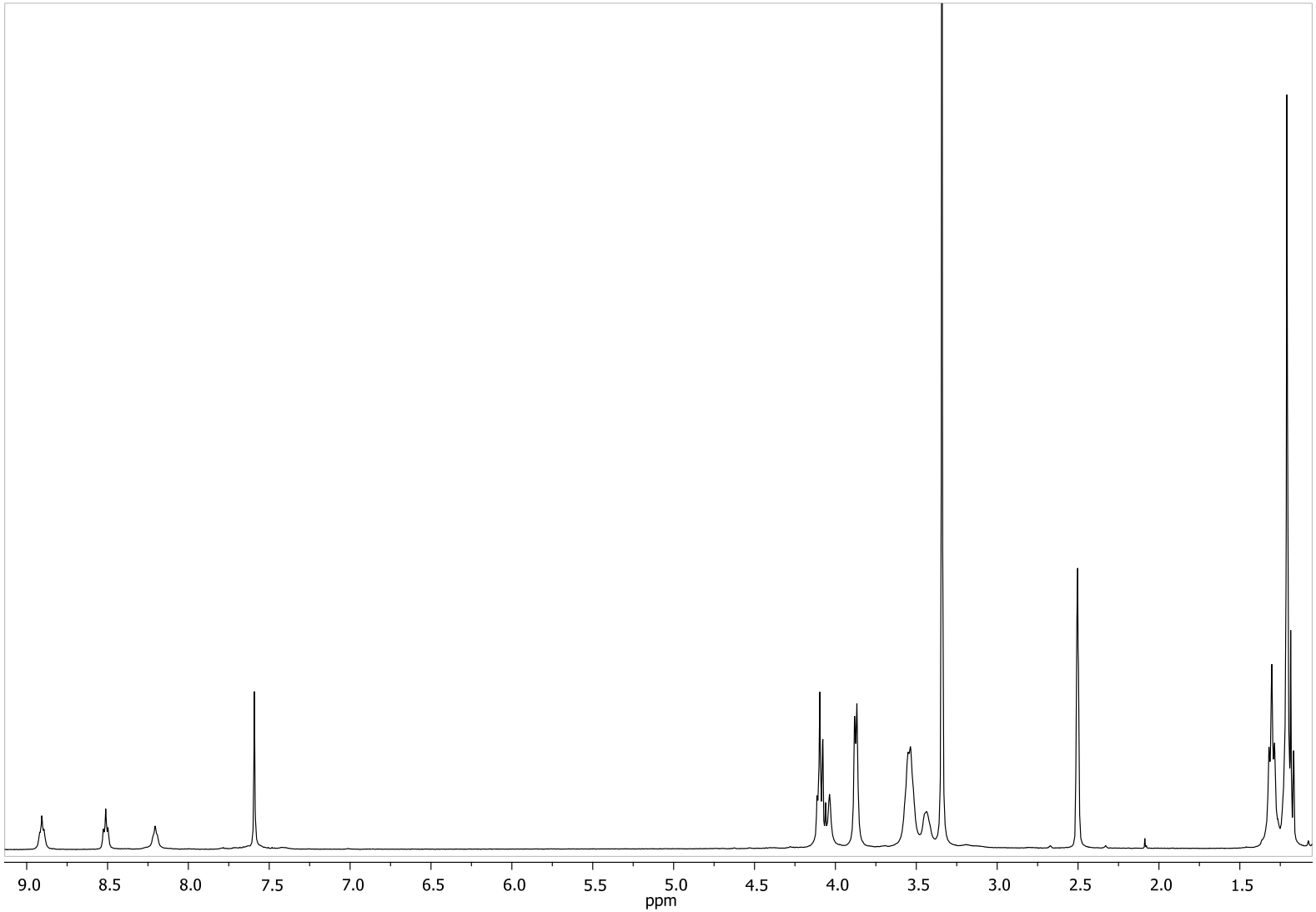

Fig. S50. ^{1}H NMR spectrum of 5,11,17,23-tetra-*tert*-butyl-25,26,27,28-tetrakis[(N-(2',2'-diethyl-2'-{(ethoxycarbonyl[S-methyl]methyl)amidocarbonylmethyl}ammoniumethyl)carbomoylmethoxy]-2,8,14,20-tetrathiacalix[4]arene tetra[bis(trifluoromethylsulfonyl)imide] (*1,3-alternate* **72**), **DMSO-d$_6$, 298 K, 400 MHz**

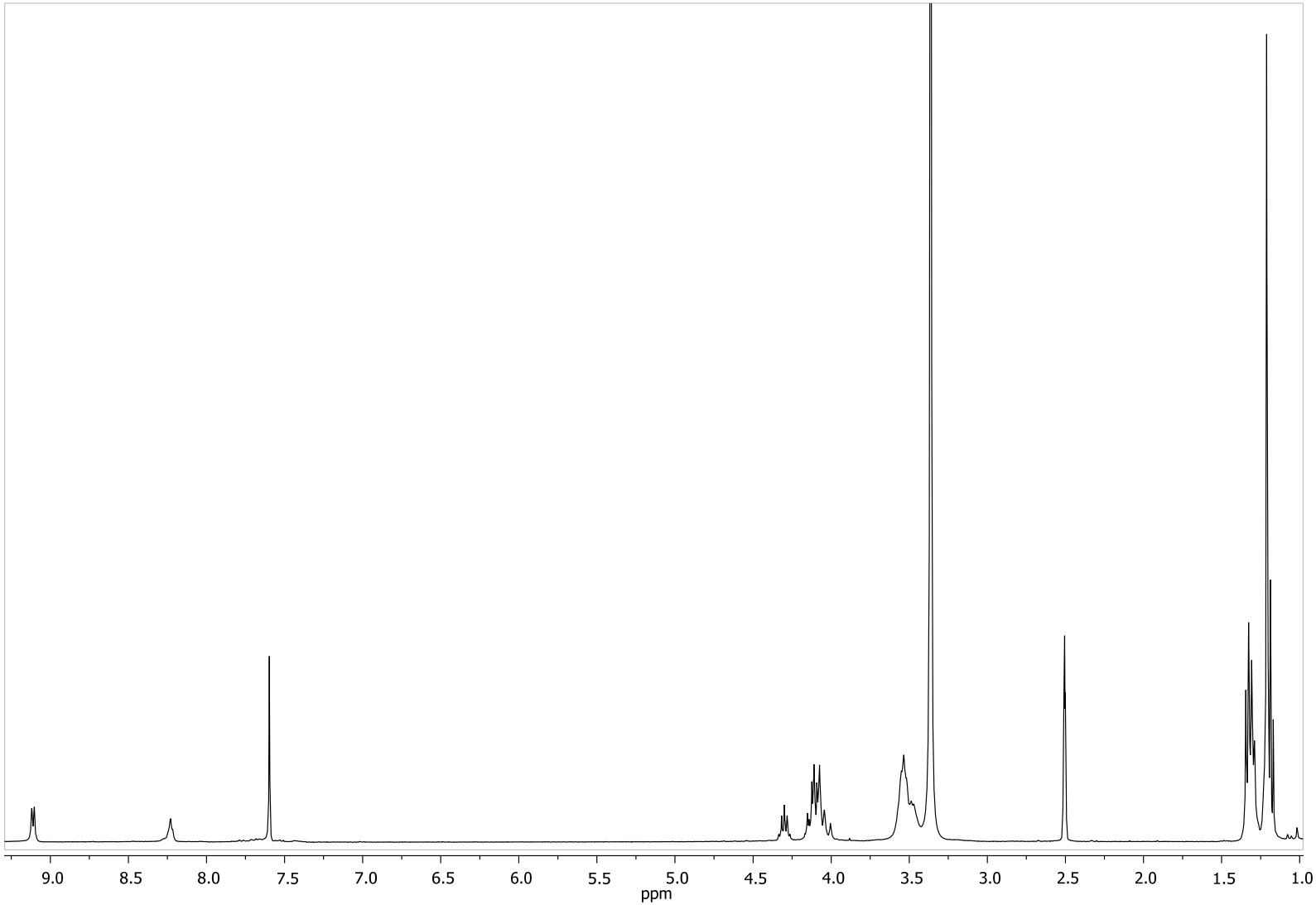

Fig. S51. ^{13}C NMR spectrum of 5,11,17,23-tetra-*tert*-butyl-25,26,27,28-tetrakis[(N-(3',3'-dimethyl-3'-(pentoxycarbonylmethyl)-ammoniumpropyl)carbomoylmethoxy]-2,8,14,20-tetrathiacalix[4]arene tetrabromide (*cone* **9**), **DMSO-d$_6$, 298 K, 100 MHz**

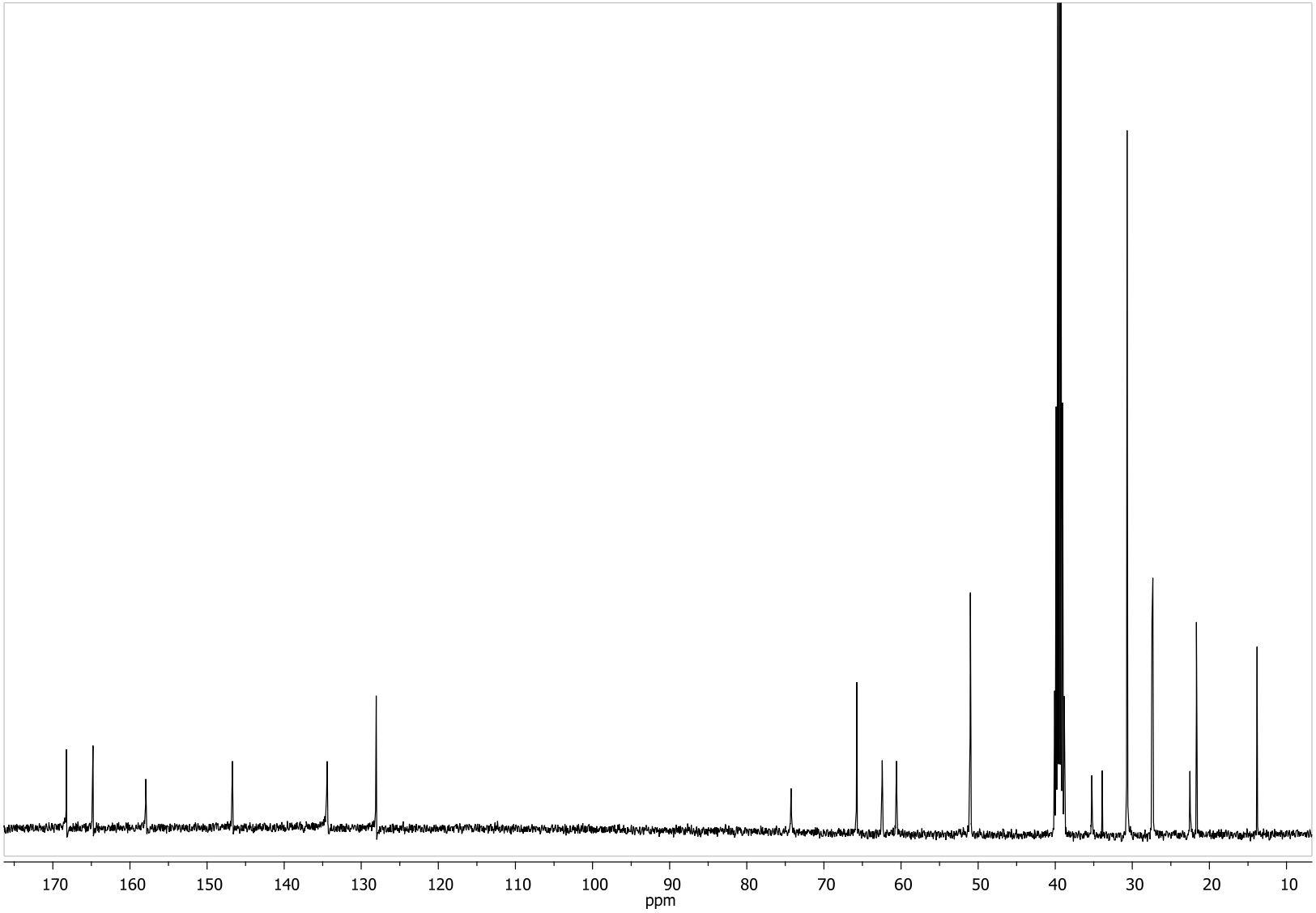

Fig. S52. ^{13}C NMR spectrum of 5,11,17,23-tetra-*tert*-butyl-25,26,27,28-tetrakis[(N-(2',2',2'-triethyl)ammoniumethyl)carbomoylmethoxy]-2,8,14,20-tetrathiacalix[4]arene tetraiodide (*cone* **15**), **$CDCl_3$, 298 K, 100 MHz**

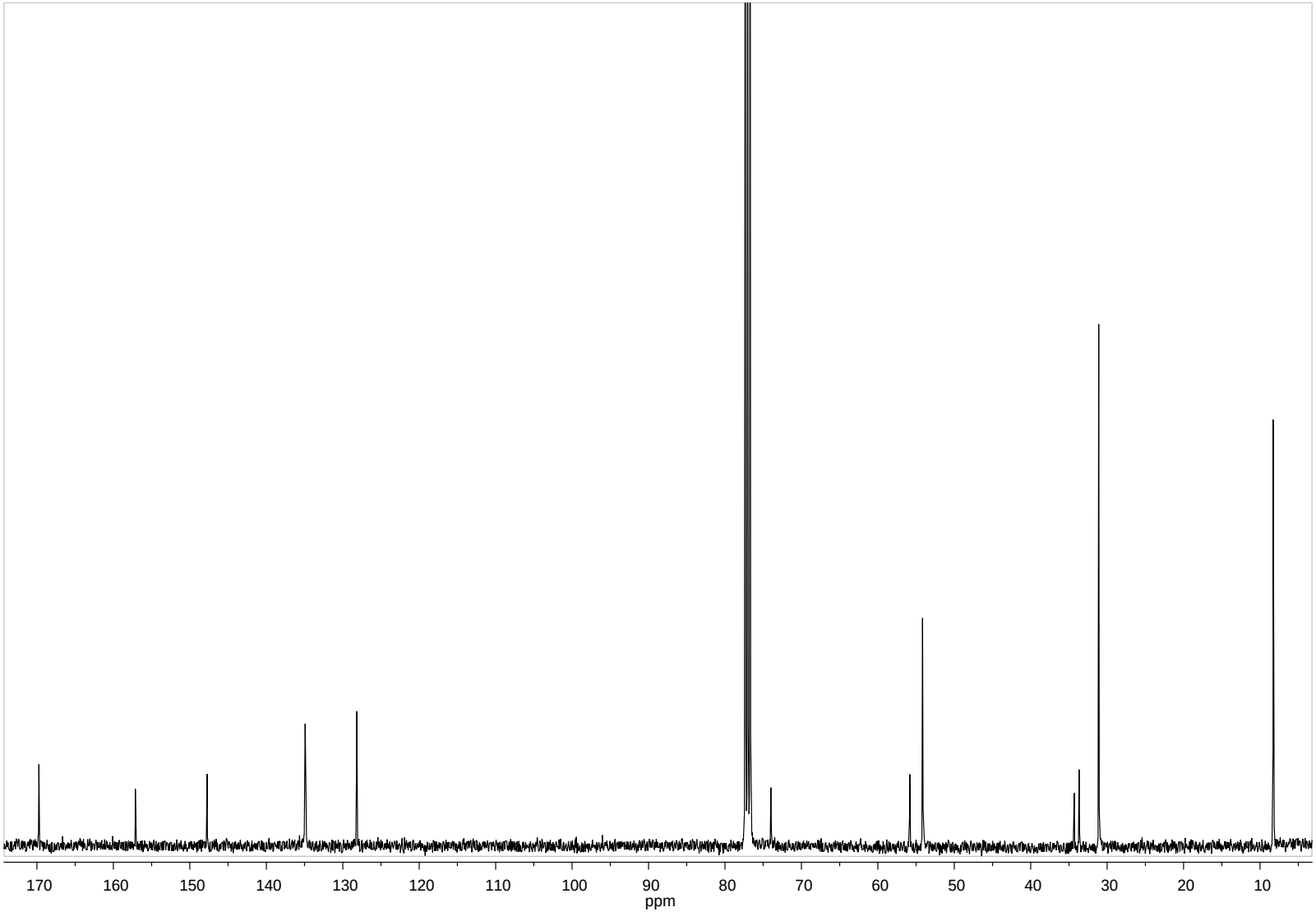

Fig. S53. ^{13}C NMR spectrum of 5,11,17,23-tetra-*tert*-butyl-25,26,27,28-tetrakis[(N-(2',2'-diethyl-2'-benzyl)ammoniumethyl)carbomoylmethoxy]-2,8,14,20-tetrathiacalix[4]arene tetrabromide (*cone* **16**), **$CDCl_3$, 298 K, 100 MHz**

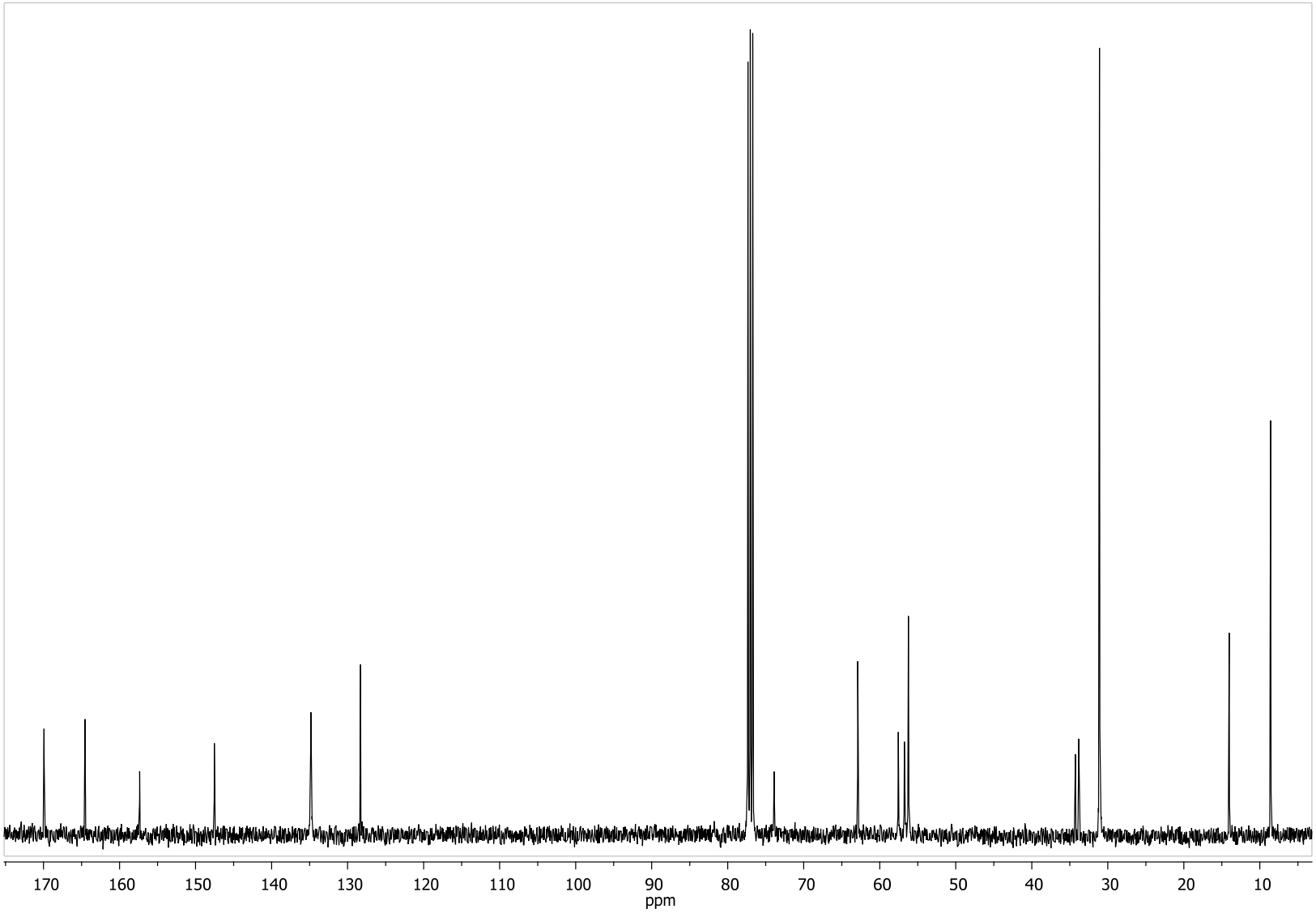

Fig. S54. ^{13}C NMR spectrum of 5,11,17,23-tetra-*tert*-butyl-25,26,27,28-tetrakis[(N-(2',2'-diethyl-2'-(ethoxycarbonylmethyl)-ammoniumethyl)carbomoylmethoxy]-2,8,14,20-tetrathiacalix[4]arene tetrabromide (*cone* **17**), **$CDCl_3$, 298 K, 100 MHz**

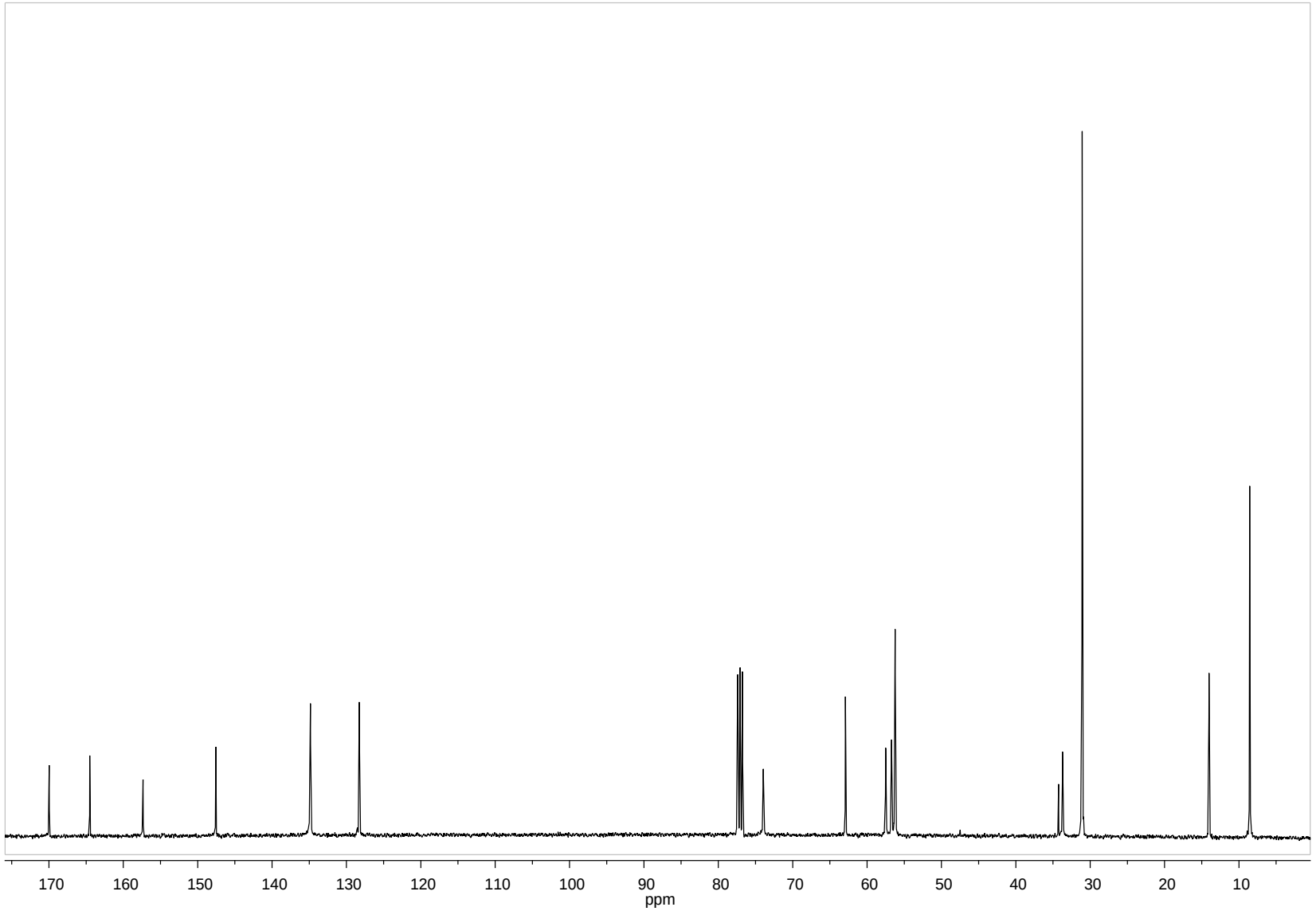

Fig. S55. ^{13}C NMR spectrum of 5,11,17,23-tetra-*tert*-butyl-25,26,27,28-tetrakis[(N-(2',2'-diethyl-2'-(pentoxycarbonylmethyl)-ammoniumethyl)carbomoylmethoxy]-2,8,14,20-tetrathiacalix[4]arene tetrabromide (*cone* **18**), **$CDCl_3$, 298 K, 100 MHz**

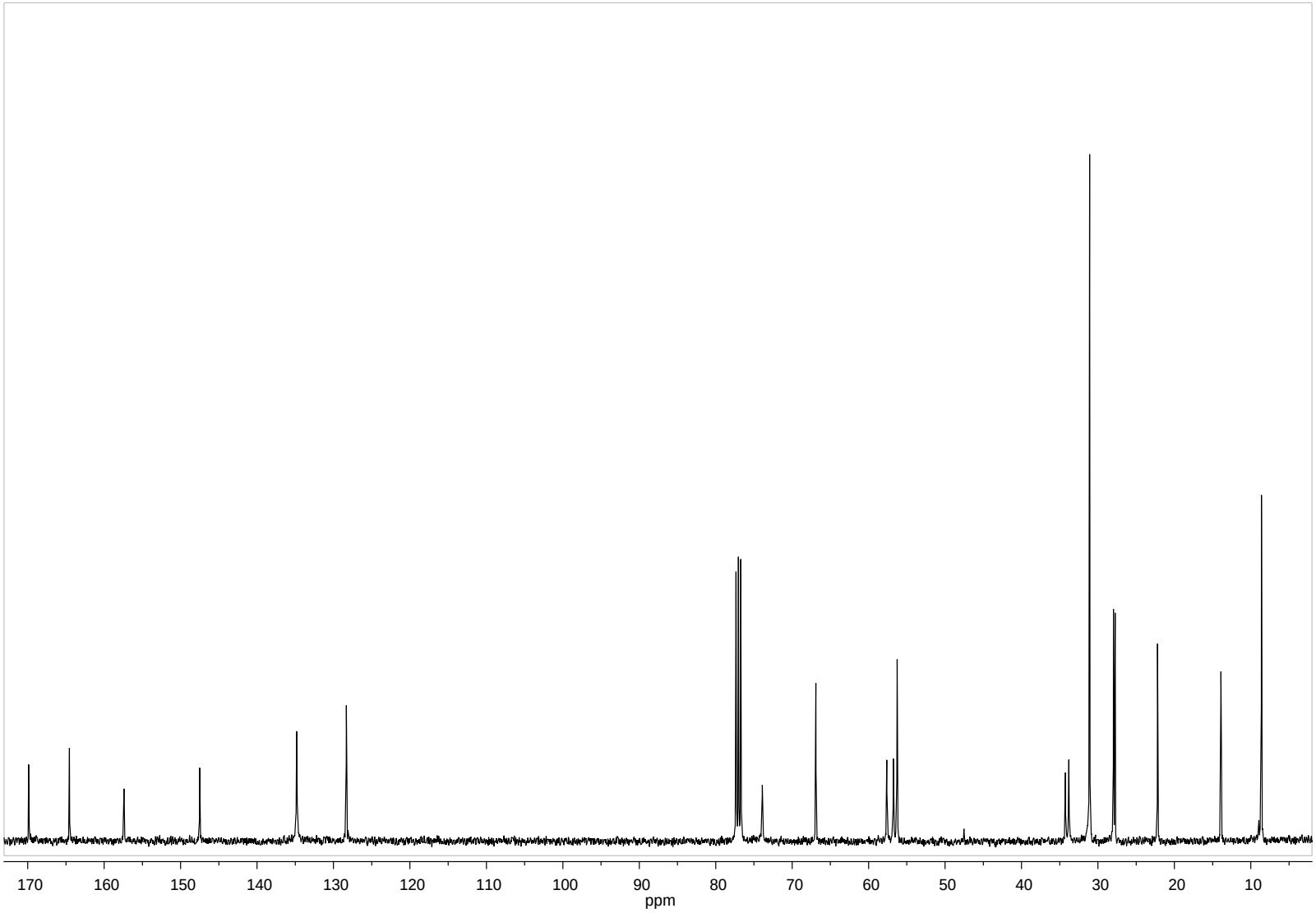

Fig. S56. ^{13}C NMR spectrum of 5,11,17,23-tetra-*tert*-butyl-25,26,27,28-tetrakis[(N-(3',3',3'-trimethyl)ammoniumpropyl)carbomoylmethoxy]-2,8,14,20-tetrathiacalix[4]arene tetraiodide (*1,3-alternate* **22**), **DMSO-d_6, 298 K, 100 MHz**

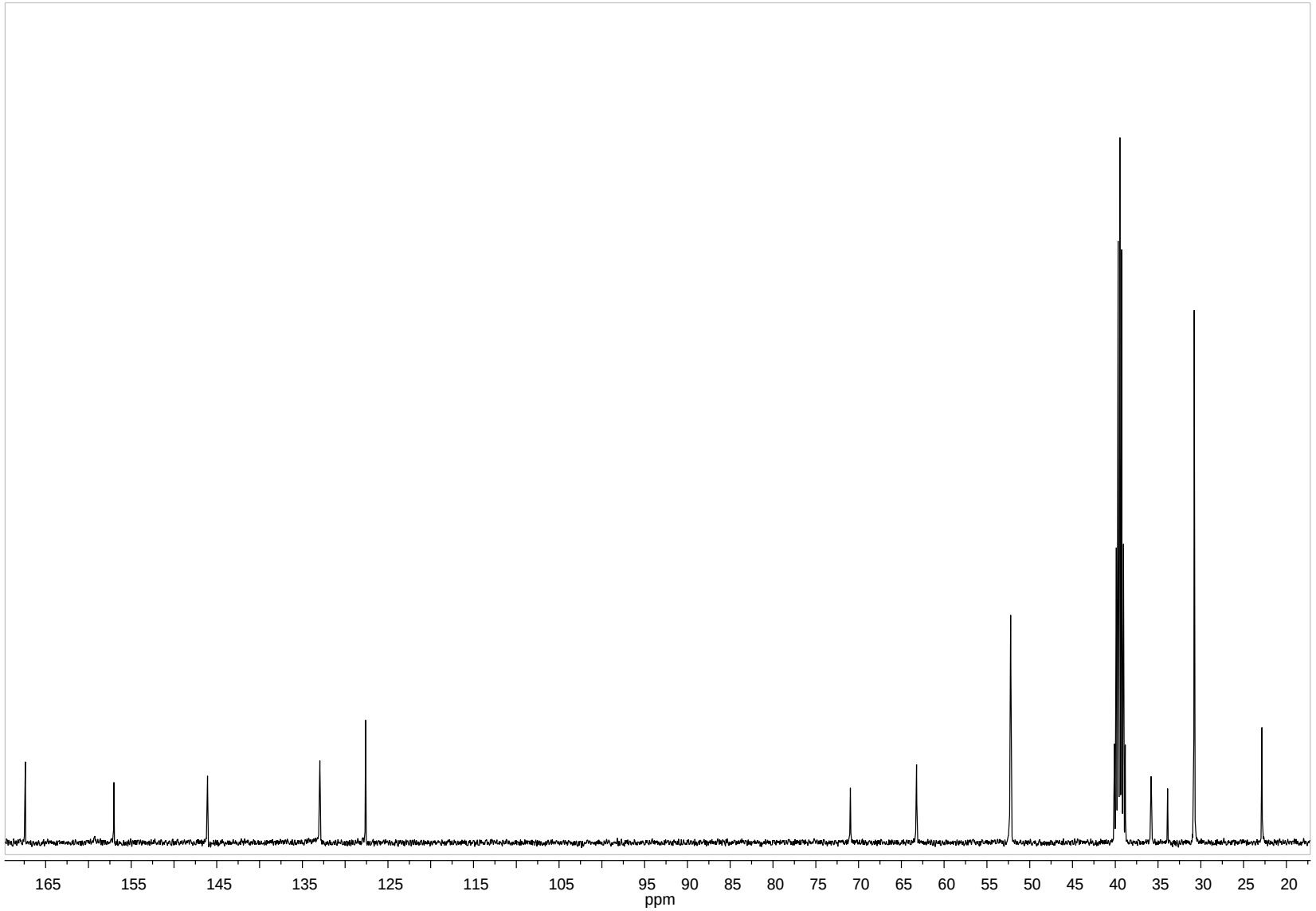

Fig. S57. ^{13}C NMR spectrum of 5,11,17,23-tetra-*tert*-butyl-25,26,27,28-tetrakis[(N-(3',3'-dimethyl-3'-ethyl)ammoniumpropyl)carbomoylmethoxy]-2,8,14,20-tetrathiacalix[4]arene tetraiodide (*1,3-alternate* **23**), **DMSO-d_6, 298 K, 100 MHz**

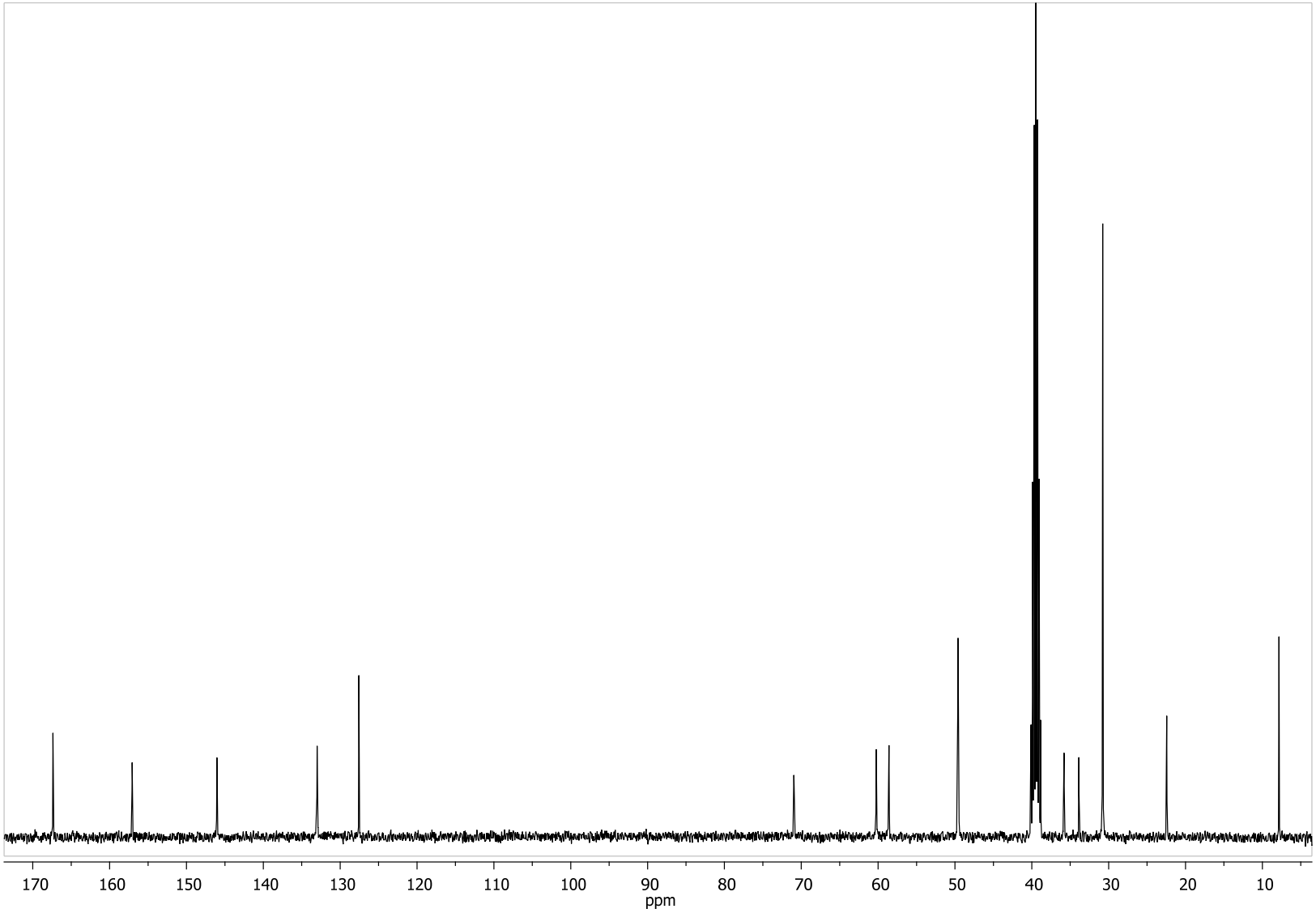

Fig. S58. ^{13}C NMR spectrum of 5,11,17,23-tetra-*tert*-butyl-25,26,27,28-tetrakis[(N-(3',3'-dimethyl-3'-benzyl)ammoniumpropyl)carbomoylmethoxy]-2,8,14,20-tetrathiacalix[4]arene tetrabromide (*1,3-alternate* **24**), **DMSO-d_6, 298 K, 100 MHz**

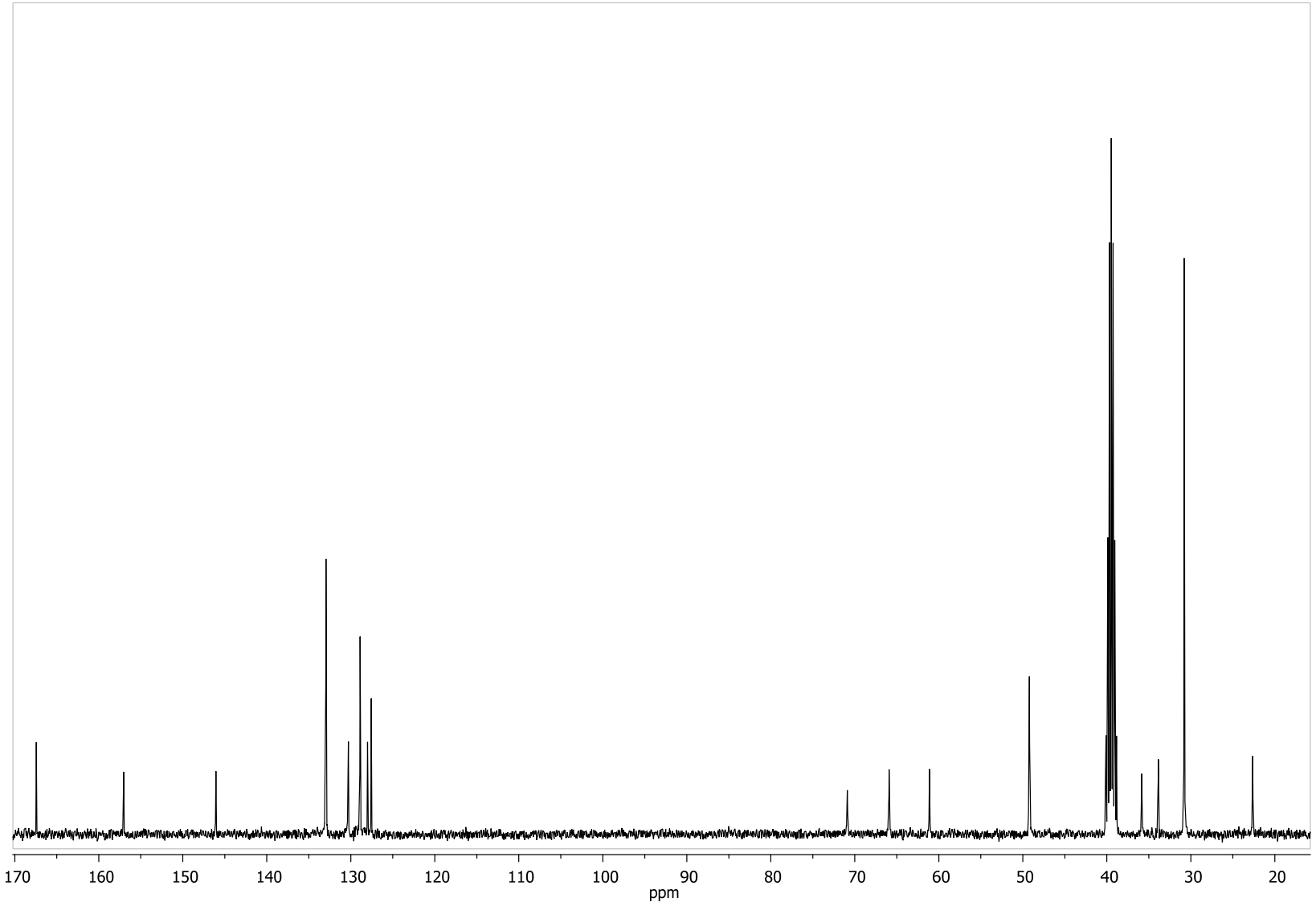

Fig. S59. ^{13}C NMR spectrum of 5,11,17,23-tetra-*tert*-butyl-25,26,27,28-tetrakis[(N-(3',3'-dimethyl-3'-(ethoxycarbonylmethyl)-ammoniumpropyl)carbomoylmethoxy]-2,8,14,20-tetrathiacalix[4]arene tetrabromide (*1,3-alternate* **25**), **DMSO-d$_6$, 298 K, 100 MHz**

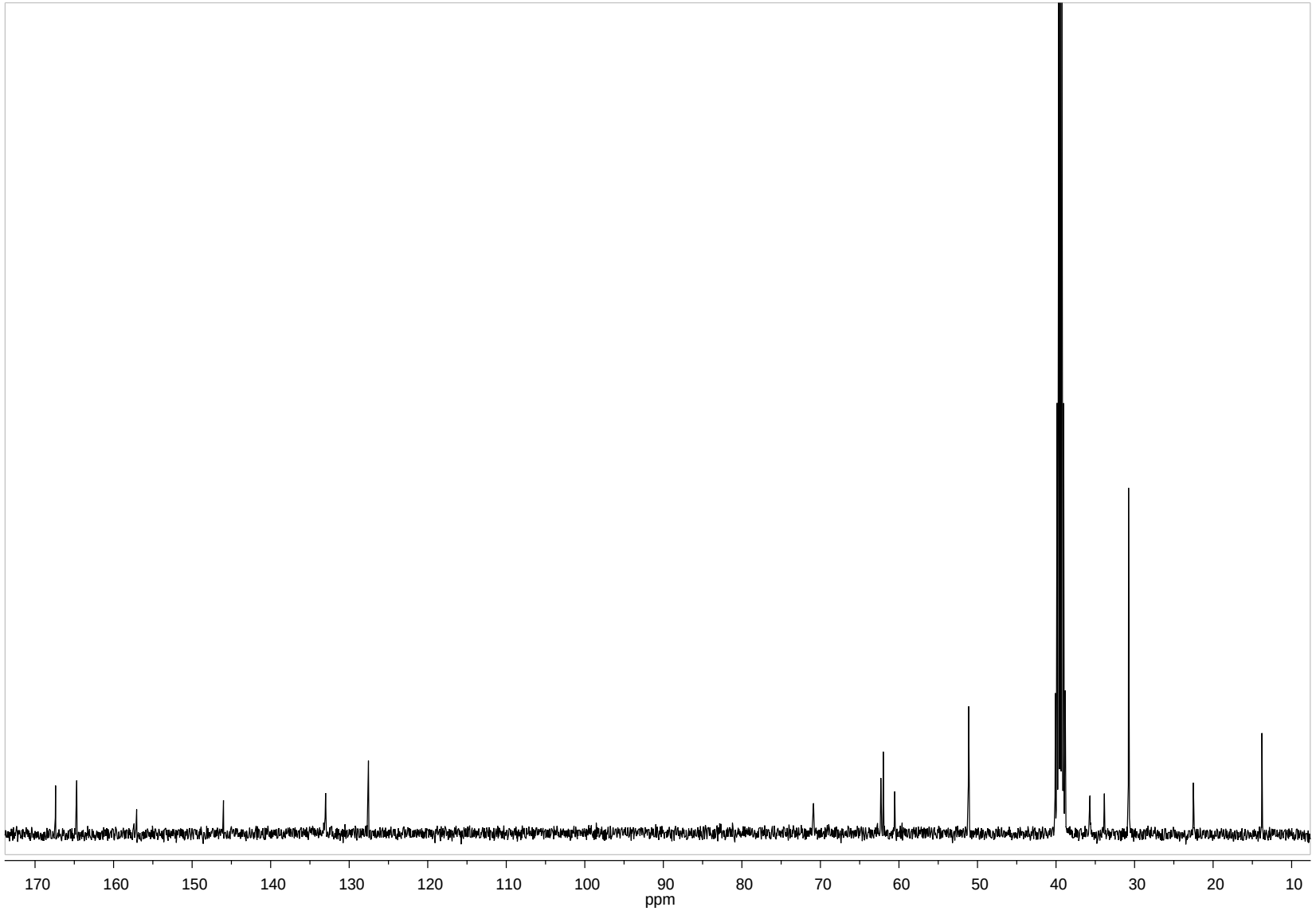

Fig. S60. ^{13}C NMR spectrum of 5,11,17,23-tetra-*tert*-butyl-25,26,27,28-tetrakis[(N-(3',3'-dimethyl-3'-(pentoxycarbonylmethyl)-ammoniumpropyl)carbomoylmethoxy]-2,8,14,20-tetrathiacalix[4]arene tetrabromide (*1,3-alternate* **26**), **DMSO-d$_6$, 298 K, 100 MHz**

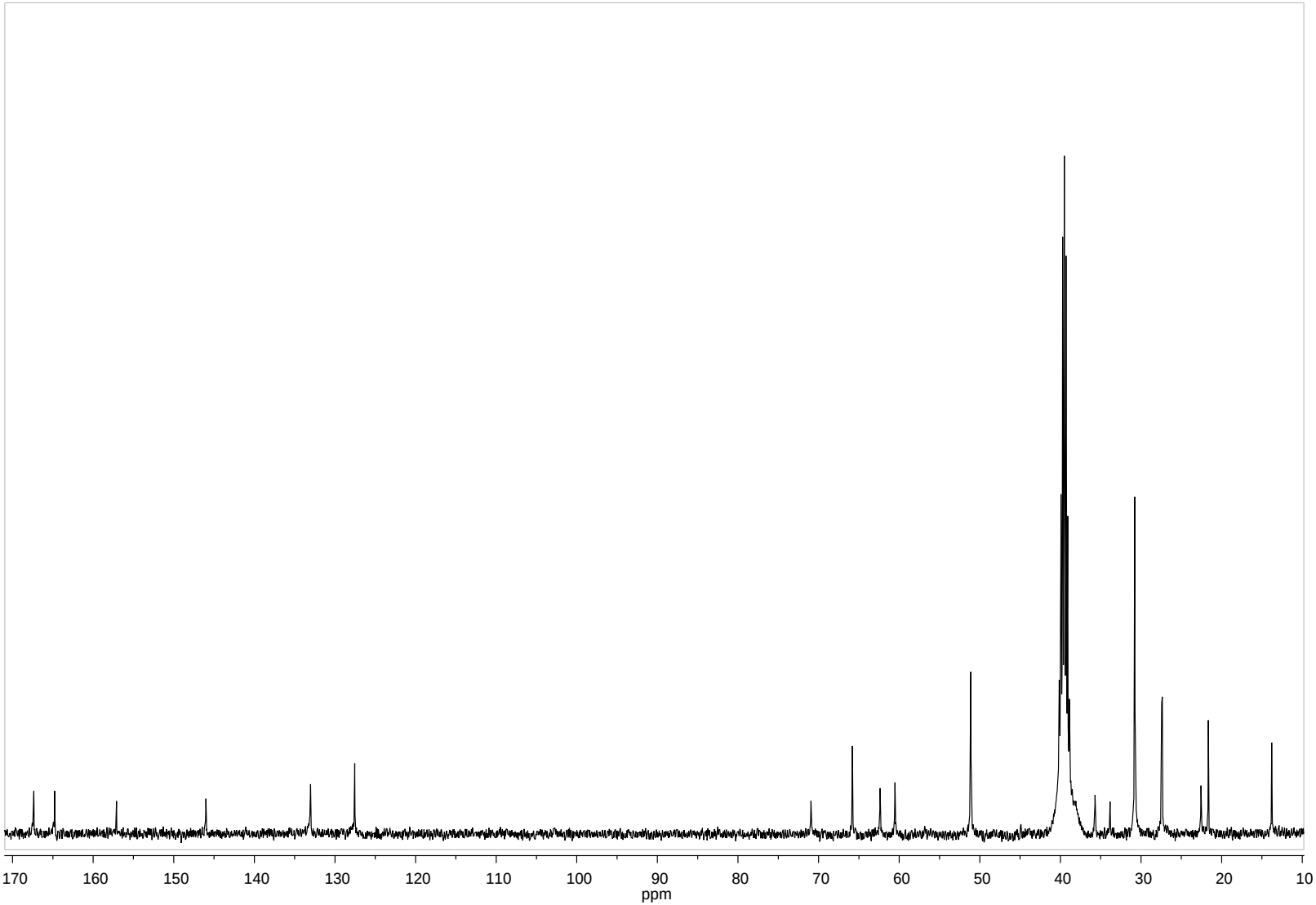

Fig. S61. ^{13}C NMR spectrum of 5,11,17,23-tetra-*tert*-butyl-25,26,27,28-tetrakis[(N-(3',3'-dimethyl-3'-{3''-propylphtalimide}-ammoniumpropyl)carbomoylmethoxy]-2,8,14,20-tetrathiacalix[4]arene tetrabromide (*1,3-alternate* **30**), **DMSO-d_6, 298 K, 100 MHz**

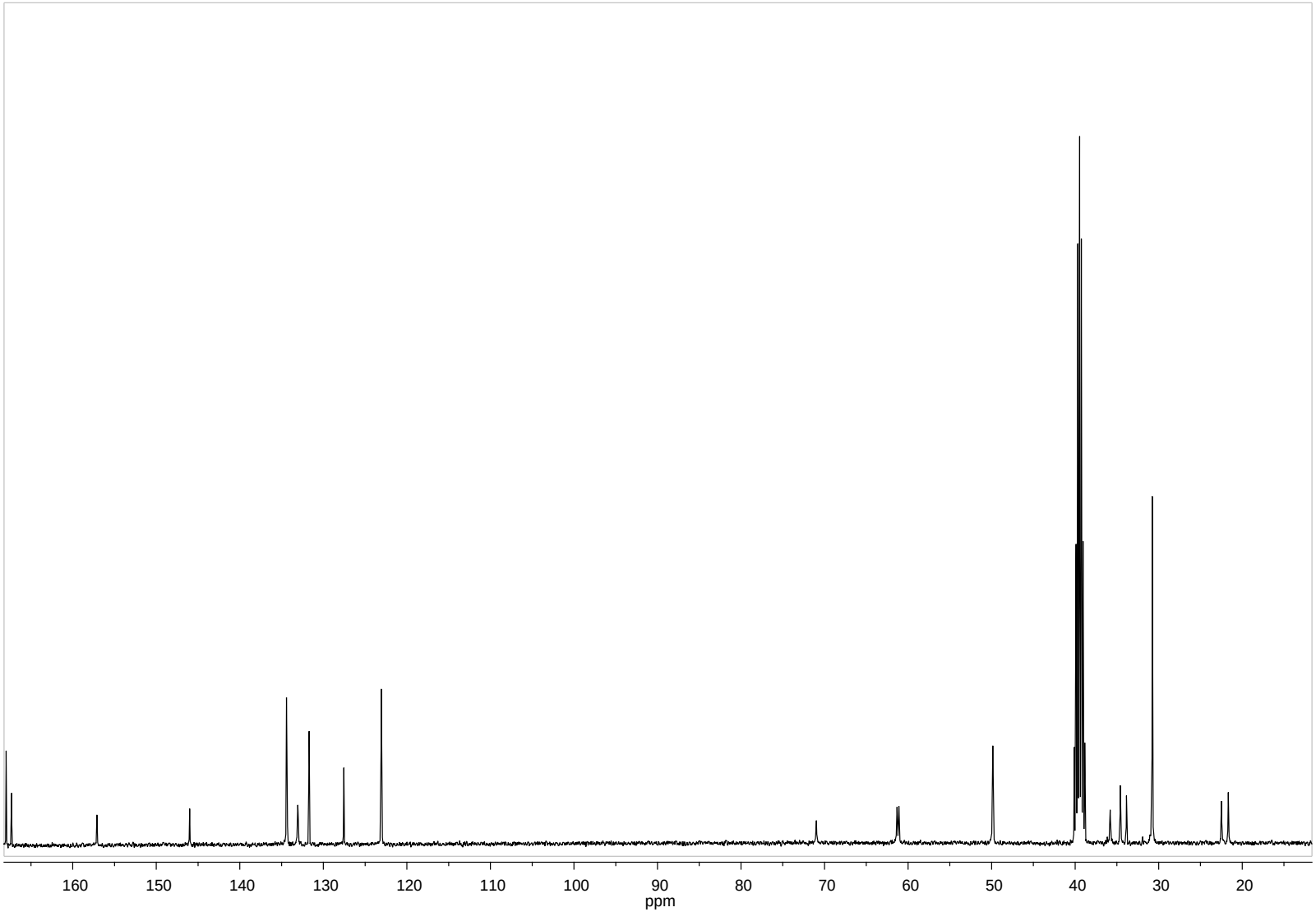

Fig. S62. ^{13}C NMR spectrum of 5,11,17,23-tetra-*tert*-butyl-25,26,27,28-tetrakis[(N-(2'-methyl-2',2'-diethyl)ammoniumethyl)carbomoylmethoxy]-2,8,14,20-tetrathiacalix[4]arene tetraiodide (*1,3-alternate* **31**), **DMSO-d_6, 298 K, 100 MHz**

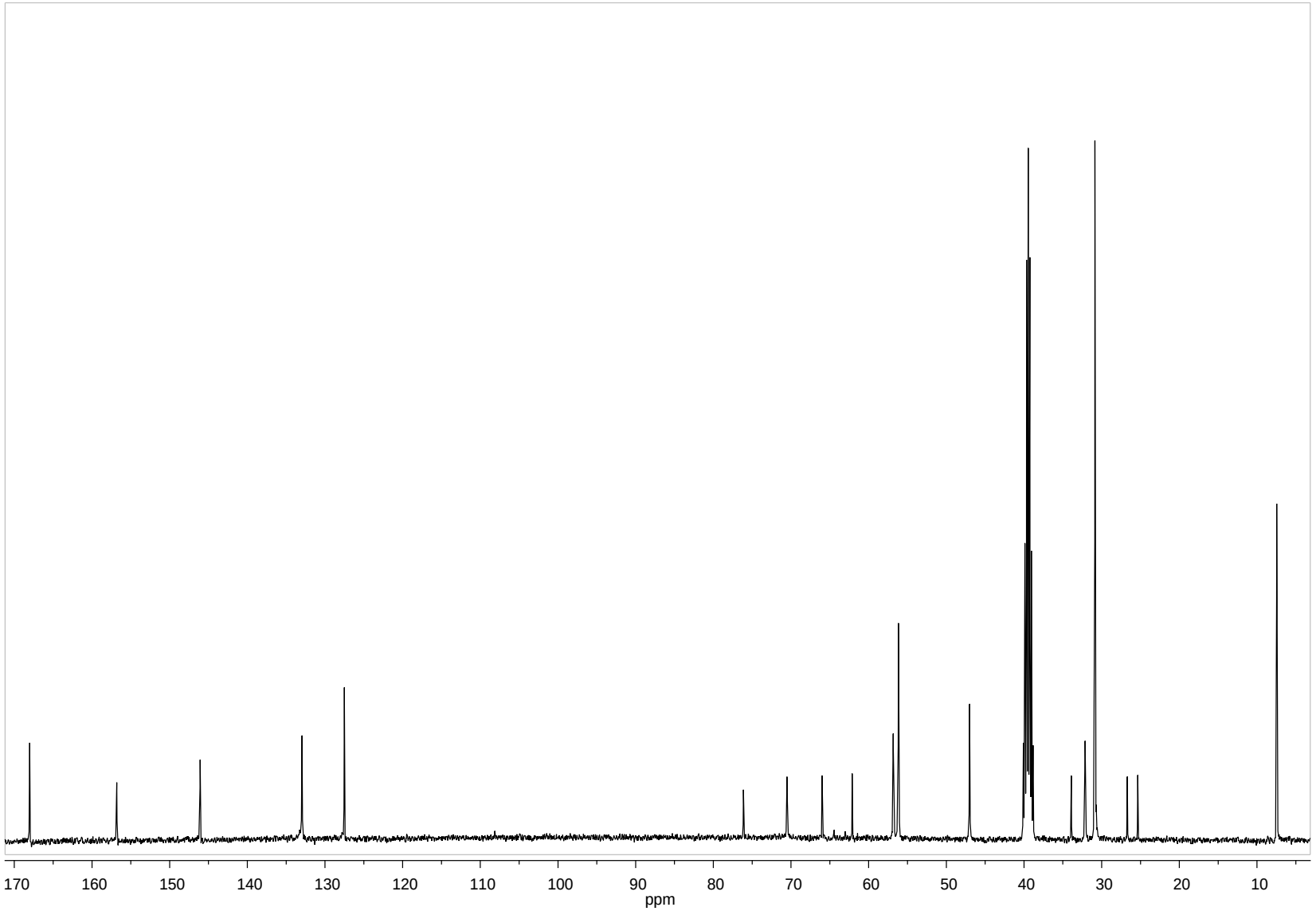

Fig. S63. ^{13}C NMR spectrum of 5,11,17,23-tetra-*tert*-butyl-25,26,27,28-tetrakis[(N-(2',2',2'-triethyl)ammoniumethyl)carbomoylmethoxy]-2,8,14,20-tetrathiacalix[4]arene tetraiodide (*1,3-alternate* **32**), **DMSO-d_6, 298 K, 100 MHz**

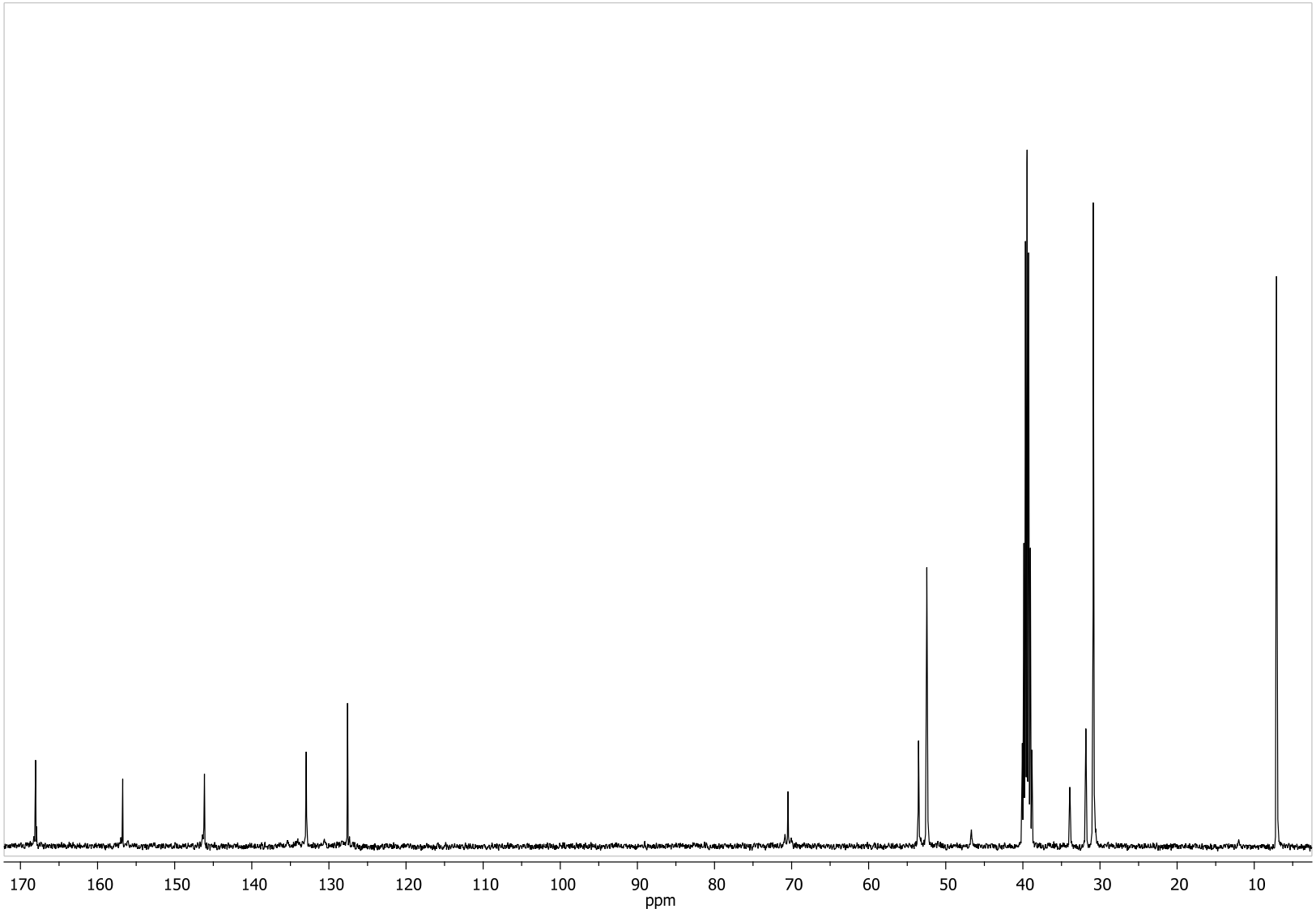

Fig. S64. ^{13}C NMR spectrum of 5,11,17,23-tetra-*tert*-butyl-25,26,27,28-tetrakis[(N-(2',2'-diethyl-2'-(benzyl)ammoniumpropyl)carbomoylmethoxy]-2,8,14,20-tetrathiacalix[4]arene tetrabromide (*1,3-alternate* **33**), **DMSO-d$_6$, 298 K, 100 MHz**

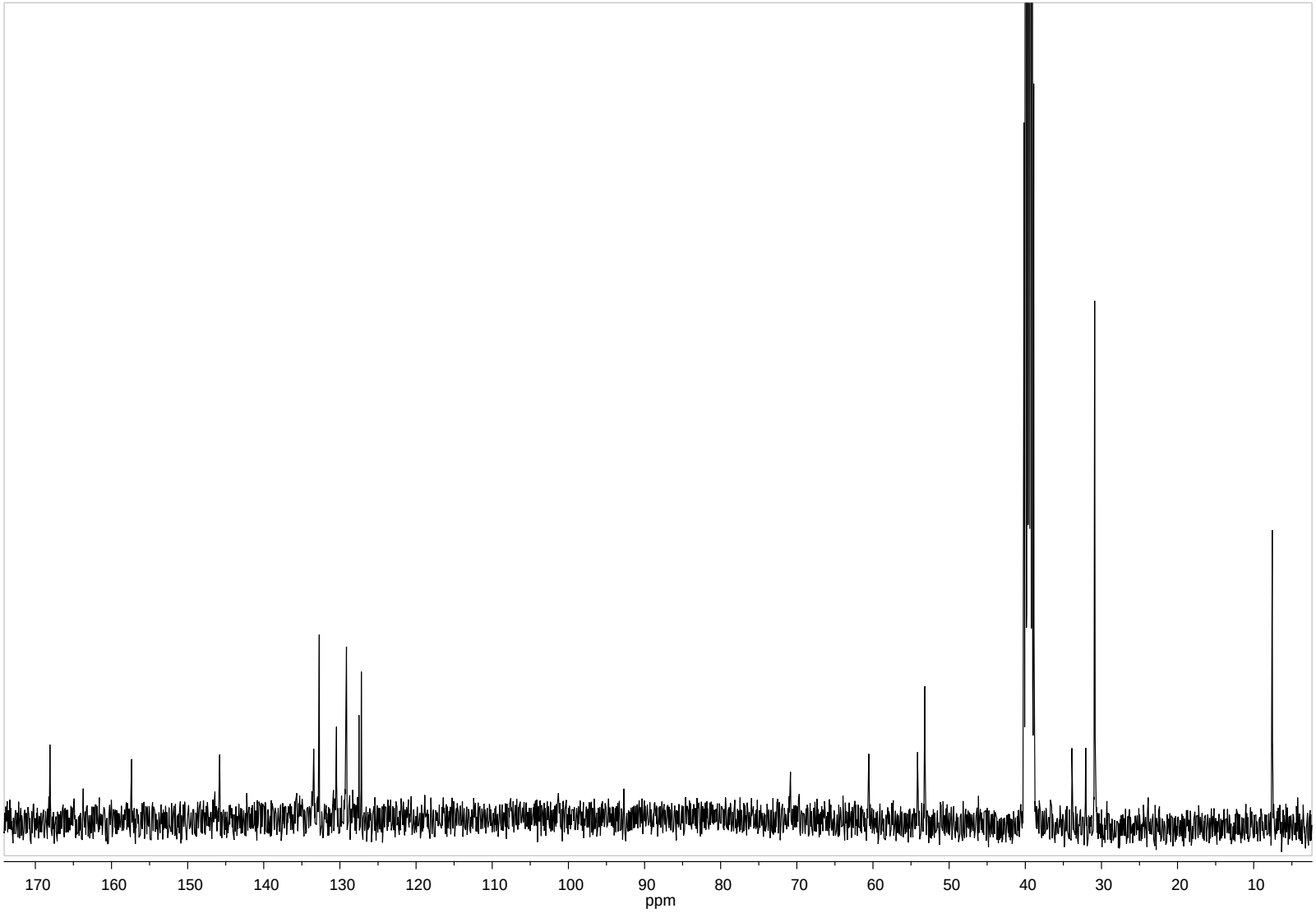

Fig. S65. ^{13}C NMR spectrum of 5,11,17,23-tetra-*tert*-butyl-25,26,27,28-tetrakis[(N-(2',2'-diethyl-2'-(ethoxycarbonylmethyl)-ammoniumethyl)carbomoylmethoxy]-2,8,14,20-tetrathiacalix[4]arene tetrabromide (*1,3-alternate* **34**), **DMSO-d$_6$, 298 K, 100 MHz**

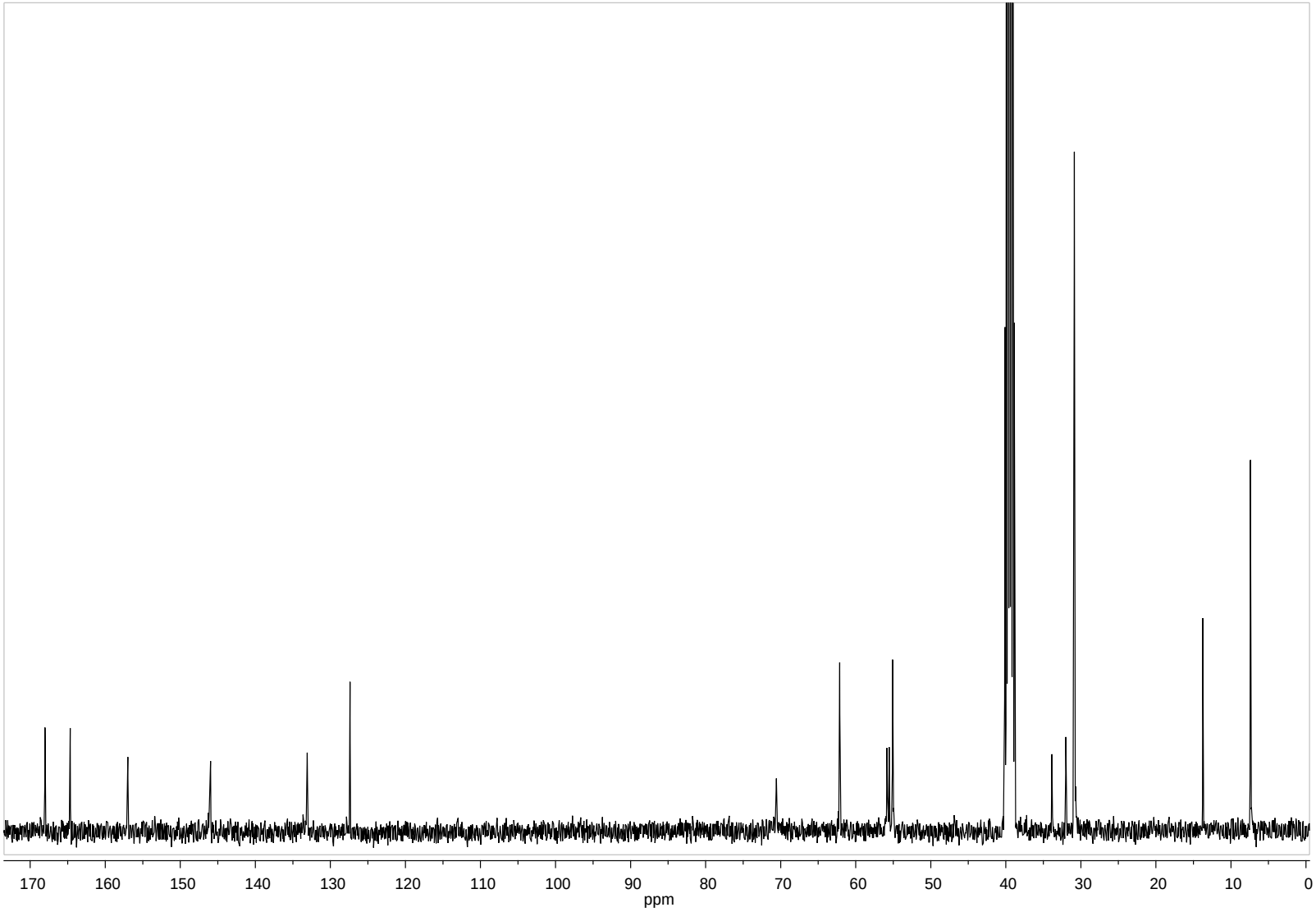

Fig. S66. ^{13}C NMR spectrum of 5,11,17,23-tetra-*tert*-butyl-25,26,27,28-tetrakis[(N-(2',2'-diethyl-2'-(pentoxycarbonylmethyl)-ammoniumethyl)carbomoylmethoxy]-2,8,14,20-tetrathiacalix[4]arene tetrabromide (*1,3-alternate* **35**), **DMSO-d_6, 298 K, 100 MHz**

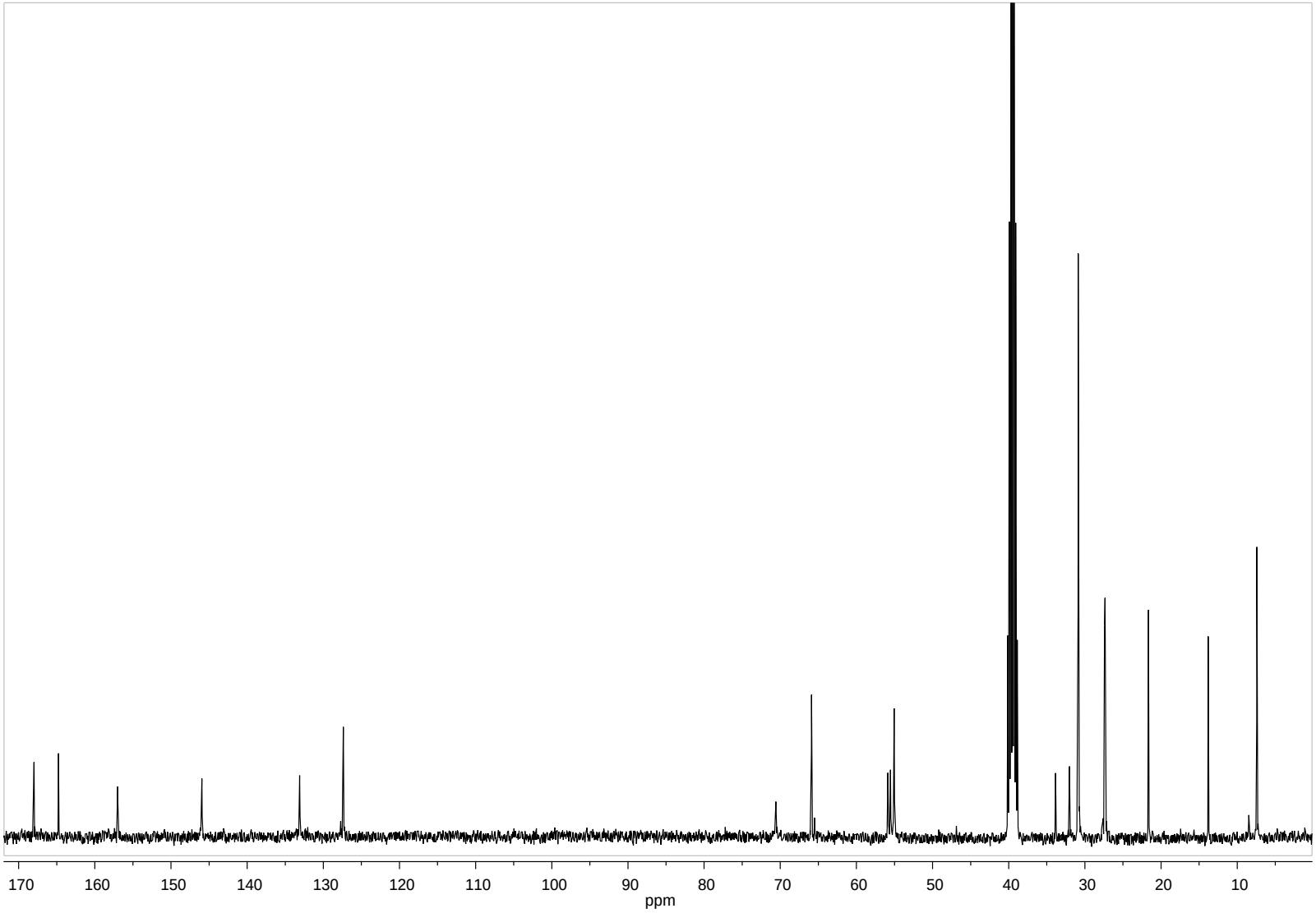

Fig. S67. ^{13}C NMR spectrum of 5,11,17,23-tetra-*tert*-butyl-25,26,27,28-tetrakis[(N-(3',3',3'-trimethyl)ammoniumpropyl)carbomoylmethoxy]-2,8,14,20-tetrathiacalix[4]arene tetra[bis(trifluoromethylsulfonyl)imide] (*cone* **39**), **DMSO-d$_6$, 298 K, 100 MHz**

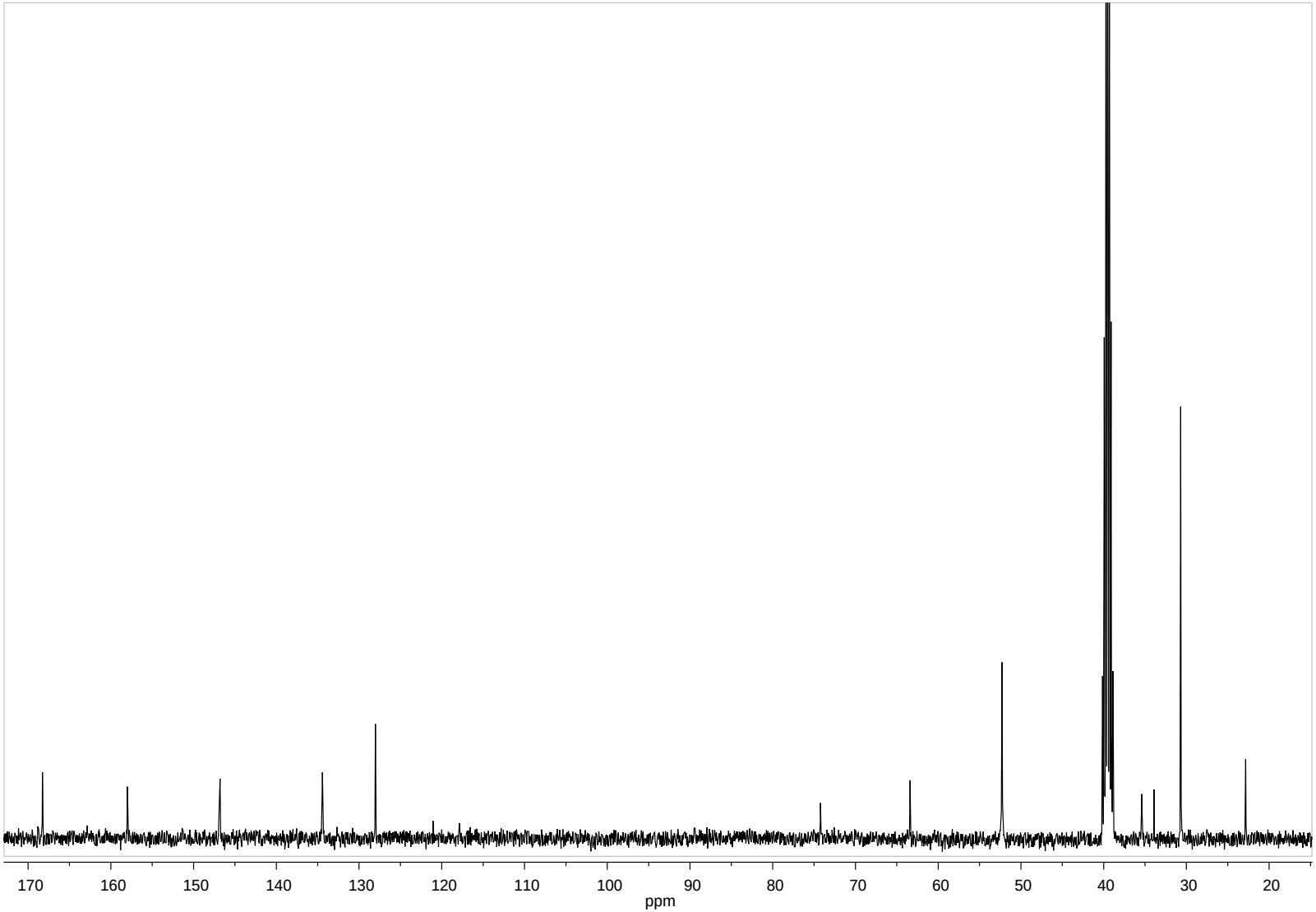

Fig. S68. ^{13}C NMR spectrum of 5,11,17,23-tetra-*tert*-butyl-25,26,27,28-tetrakis[(N-(3',3'-dimethyl-3'-ethyl)ammoniumpropyl)-carbomoylmethoxy]-2,8,14,20-tetrathiacalix[4]arene tetra[bis(trifluoromethylsulfonyl)imide] (*cone* **40**), **DMSO-d$_6$, 298 K, 100 MHz**

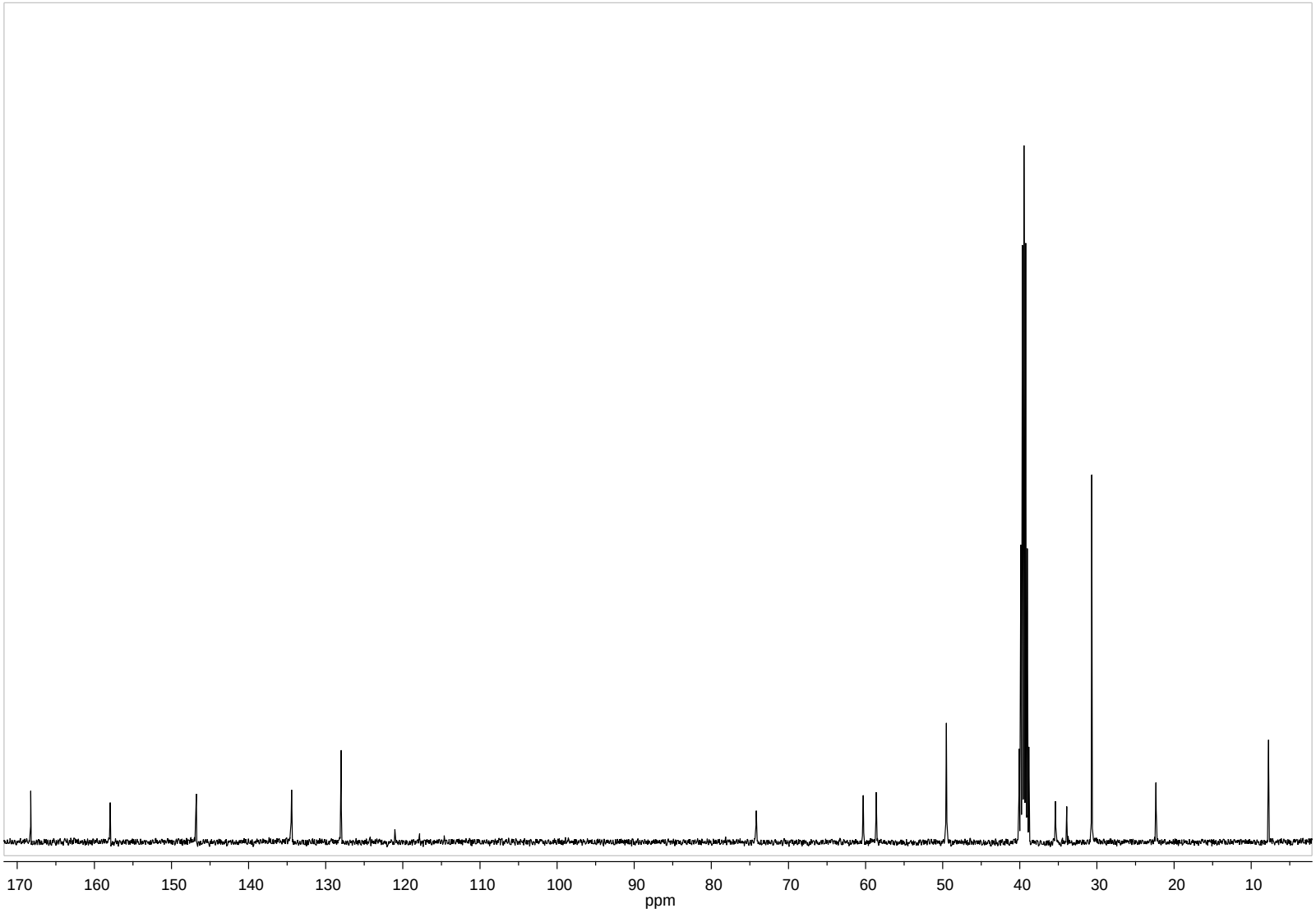

Fig. S69. ^{13}C NMR spectrum of 5,11,17,23-tetra-*tert*-butyl-25,26,27,28-tetrakis[(N-(3',3'-dimethyl-3'-benzyl)ammoniumpropyl)-carbomoylmethoxy]-2,8,14,20-tetrathiacalix[4]arene tetra[bis(trifluoromethylsulfonyl)imide] (*cone* **41**), **$CDCl_3$, 298 K, 100 MHz**

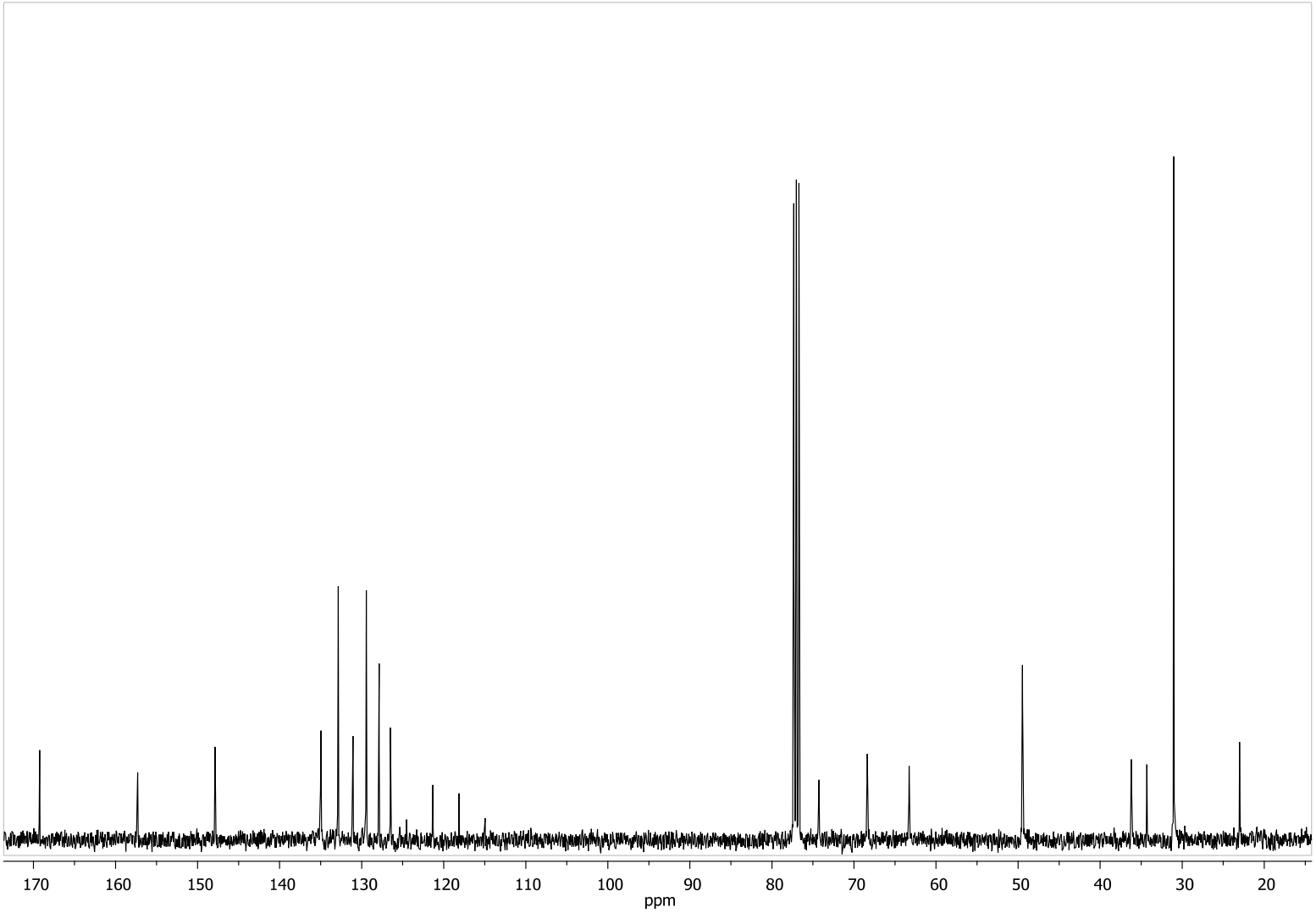

Fig. S70. ^{13}C NMR spectrum of 5,11,17,23-tetra-*tert*-butyl-25,26,27,28-tetrakis[(N-(3',3'-dimethyl-3'-(ethoxycarbonylmethyl)ammoniumpropyl)carbomoylmethoxy]-2,8,14,20-tetrathiacalix[4]arene tetra[bis(trifluoromethylsulfonyl)imide] (*cone* **42**), **$CDCl_3$, 298 K, 100 MHz**

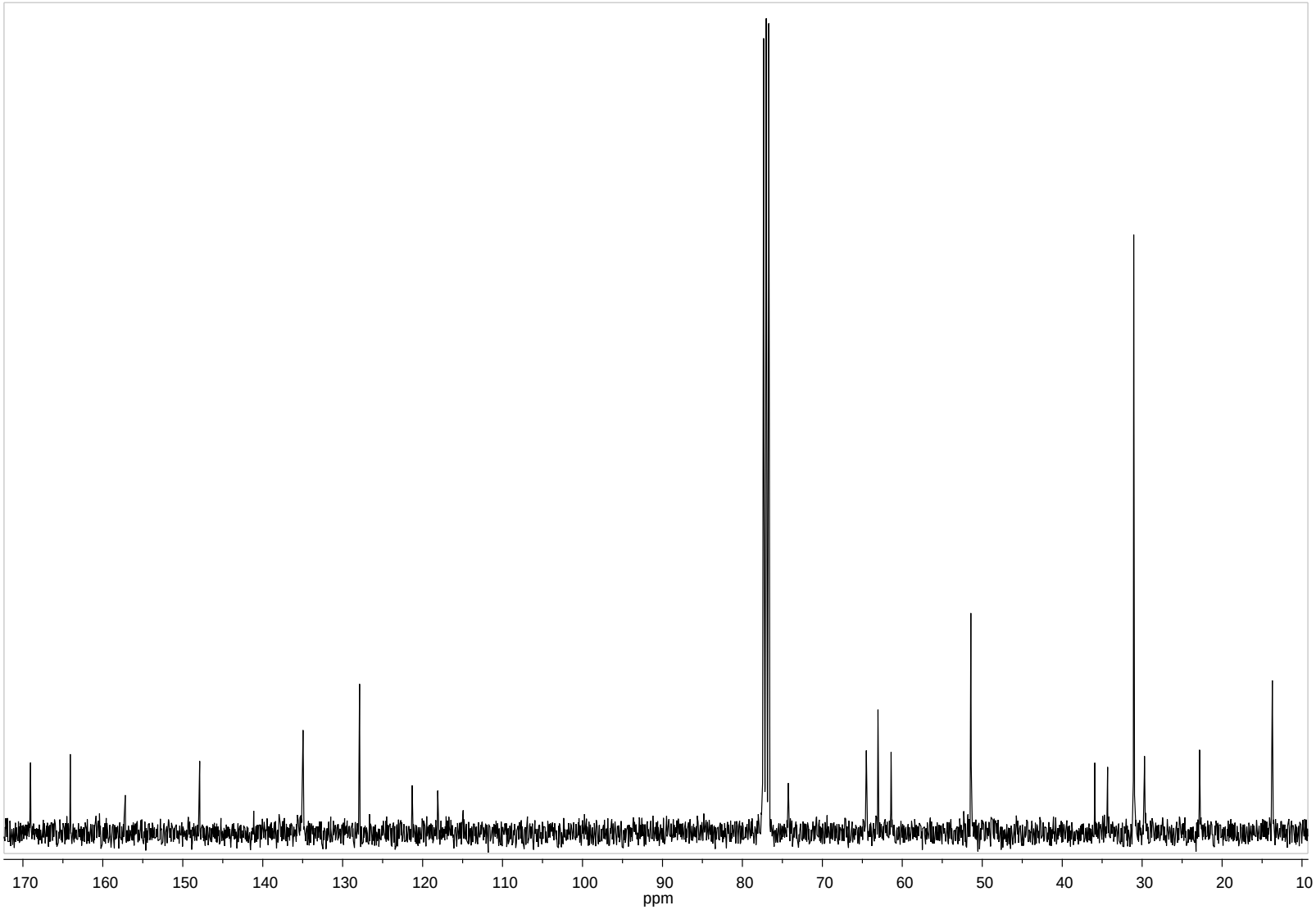

Fig. S71. ^{13}C NMR spectrum of 5,11,17,23-tetra-*tert*-butyl-25,26,27,28-tetrakis[(N-(3',3'-dimethyl-3'-(pentoxycarbonylmethyl)ammoniumpropyl)carbomoylmethoxy]-2,8,14,20-tetrathiacalix[4]arene tetra[bis(trifluoromethylsulfonyl)imide] (*cone* **43**), **DMSO-d_6, 298 K, 100 MHz**

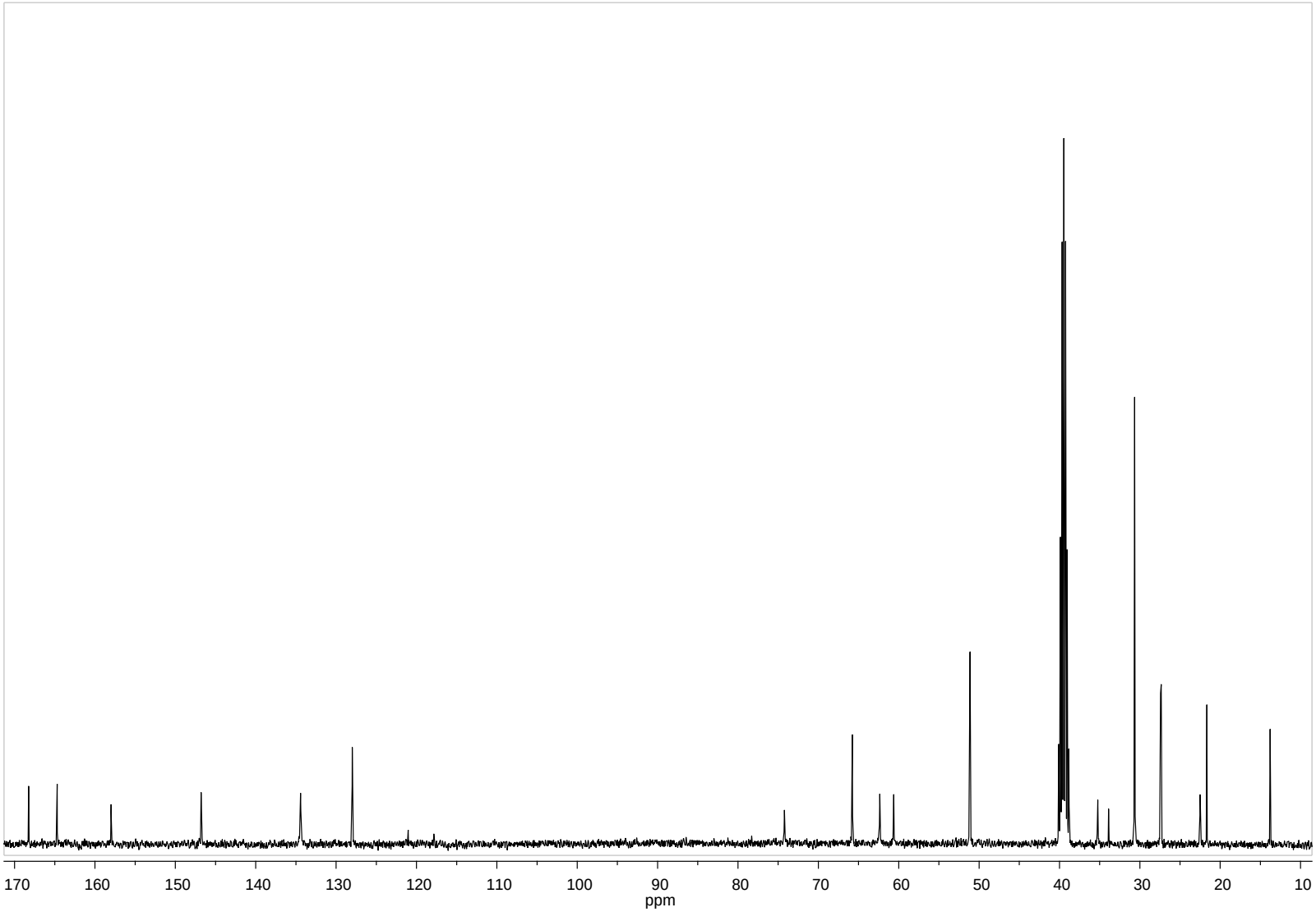

Fig. S72. ^{13}C NMR spectrum of 5,11,17,23-tetra-*tert*-butyl-25,26,27,28-tetrakis[(N-(3',3'-dimethyl-3'-{(ethoxycarbonylmethyl)amidocarbonylmethyl}-ammoniumpropyl)carbomoylmethoxy]-2,8,14,20-tetrathiacalix[4]arene tetra[bis(trifluoromethylsulfonyl)imide] (*cone* 44), $CDCl_3$, 298 K, 100 MHz

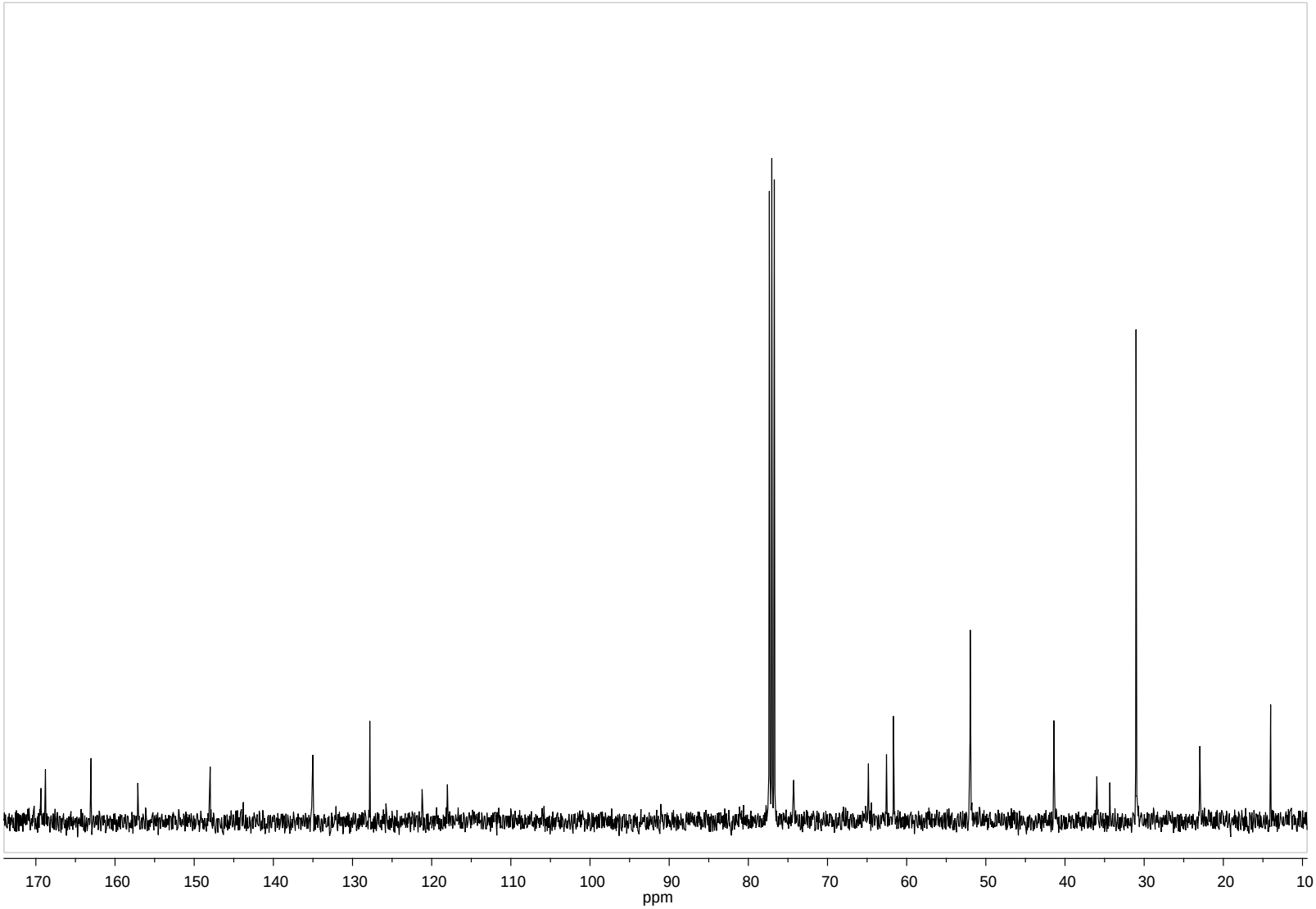

Fig. S73. ^{13}C NMR spectrum of 5,11,17,23-tetra-*tert*-butyl-25,26,27,28-tetrakis[(N-(3',3'-dimethyl-3'-{([ethoxycarbonylmethyl]-amidocarbonylmethyl)amidocarbonylmethyl}ammoniumpropyl)carbomoylmethoxy]-2,8,14,20-tetrathiacalix[4]arene tetra[bis(trifluoromethylsulfonyl)imide] (*cone* **45**), **DMSO-d$_6$, 298 K, 100 MHz**

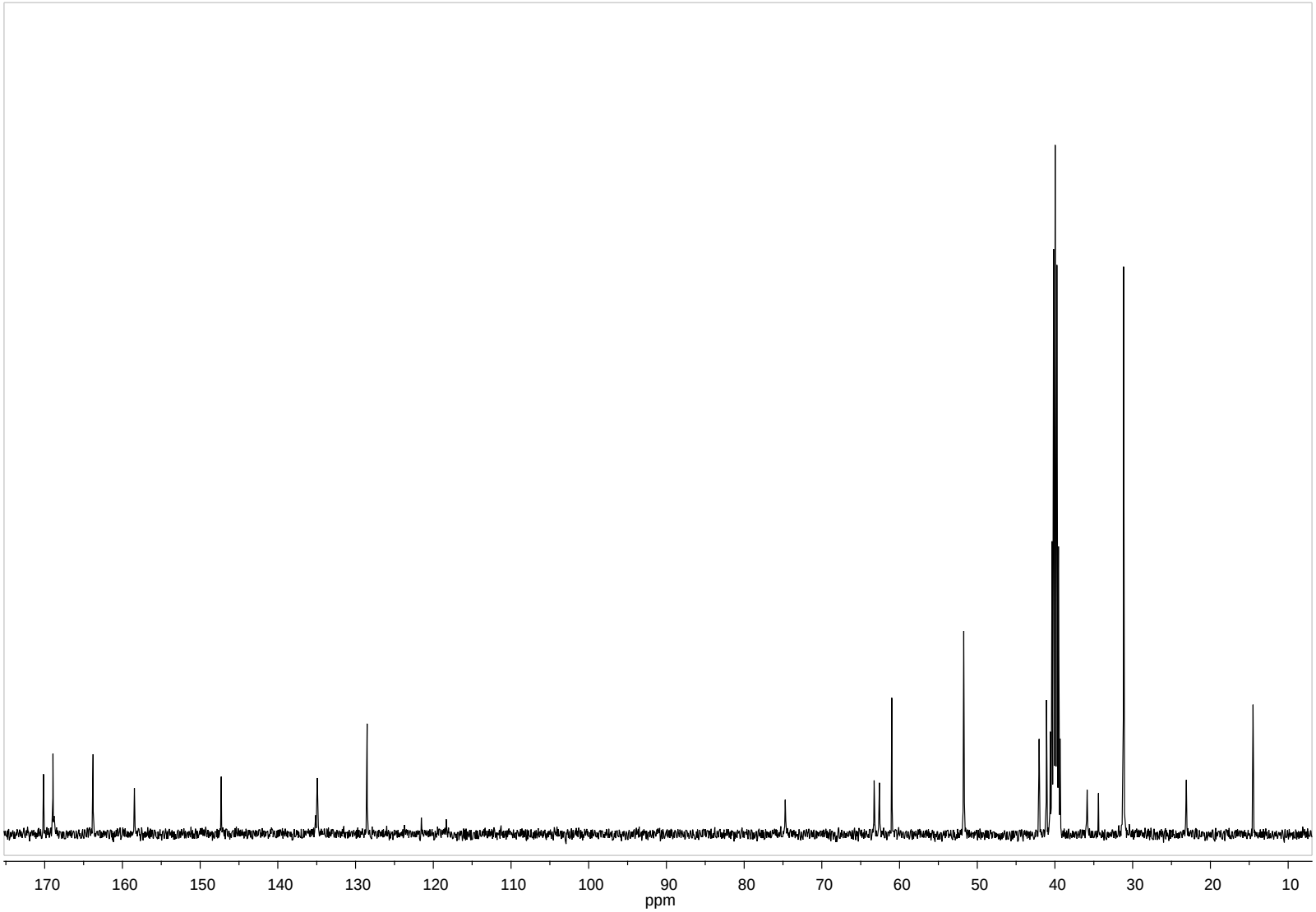

Fig. S74. ^{13}C NMR spectrum of 5,11,17,23-tetra-*tert*-butyl-25,26,27,28-tetrakis[(N-(3',3'-dimethyl-3'-{(ethoxycarbonyl[S-methyl]methyl)amidocarbonylmethyl}ammoniumpropyl)carbomoylmethoxy]-2,8,14,20-tetrathiacalix[4]arene tetra[bis(trifluoromethylsulfonyl)imide] (*cone* **46**), **DMSO-d_6, 298 K, 100 MHz**

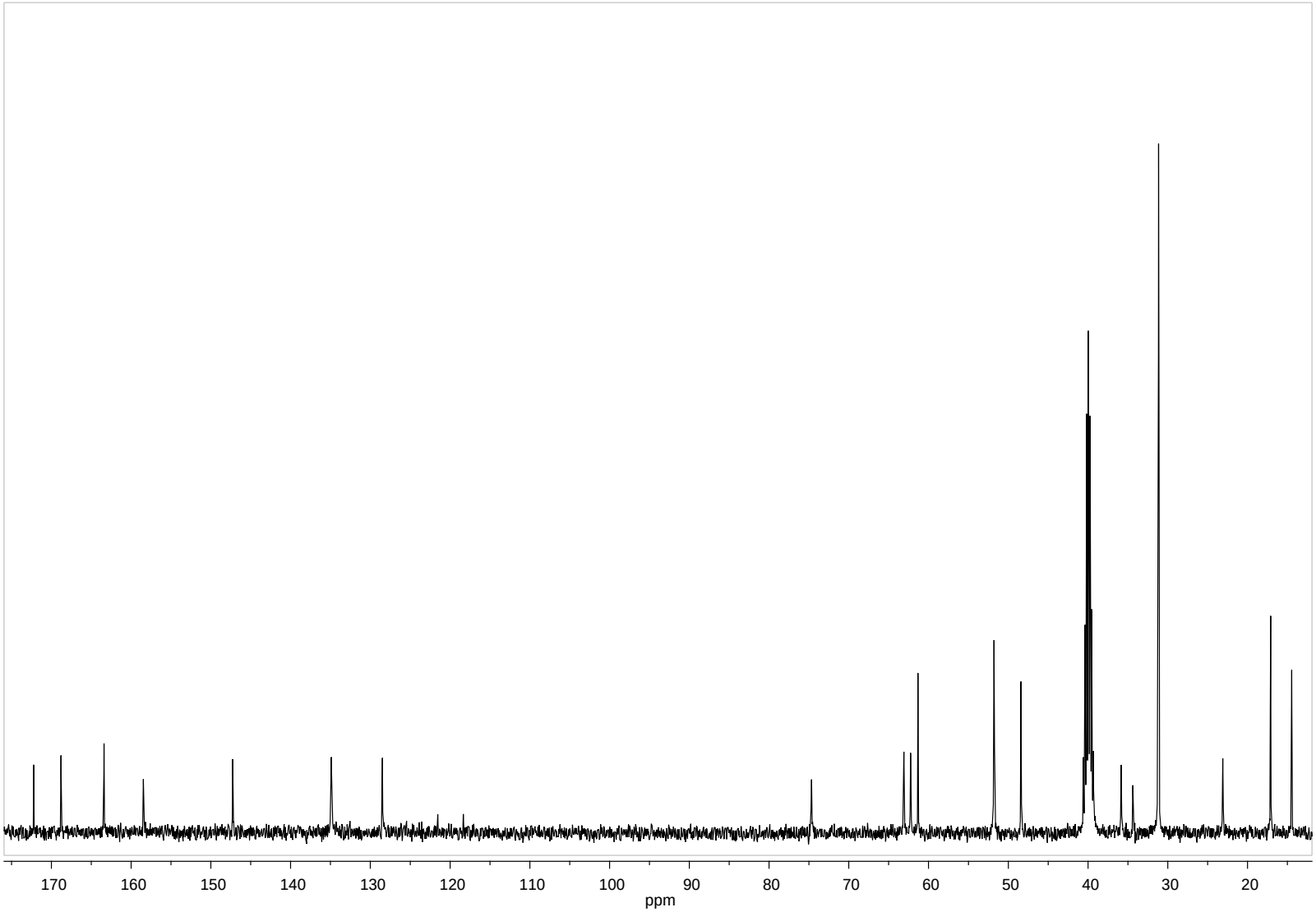

Fig. S75. ^{13}C NMR spectrum of 5,11,17,23-tetra-*tert*-butyl-25,26,27,28-tetrakis[(N-(3',3'-dimethyl-3'-{3''-propylphtalimide}ammoniumpropyl)carbomoylmethoxy]-2,8,14,20-tetrathiacalix[4]arene tetra[bis(trifluoromethylsulfonyl)imide] (*cone* **47**), **DMSO-d_6, 298 K, 100 MHz**

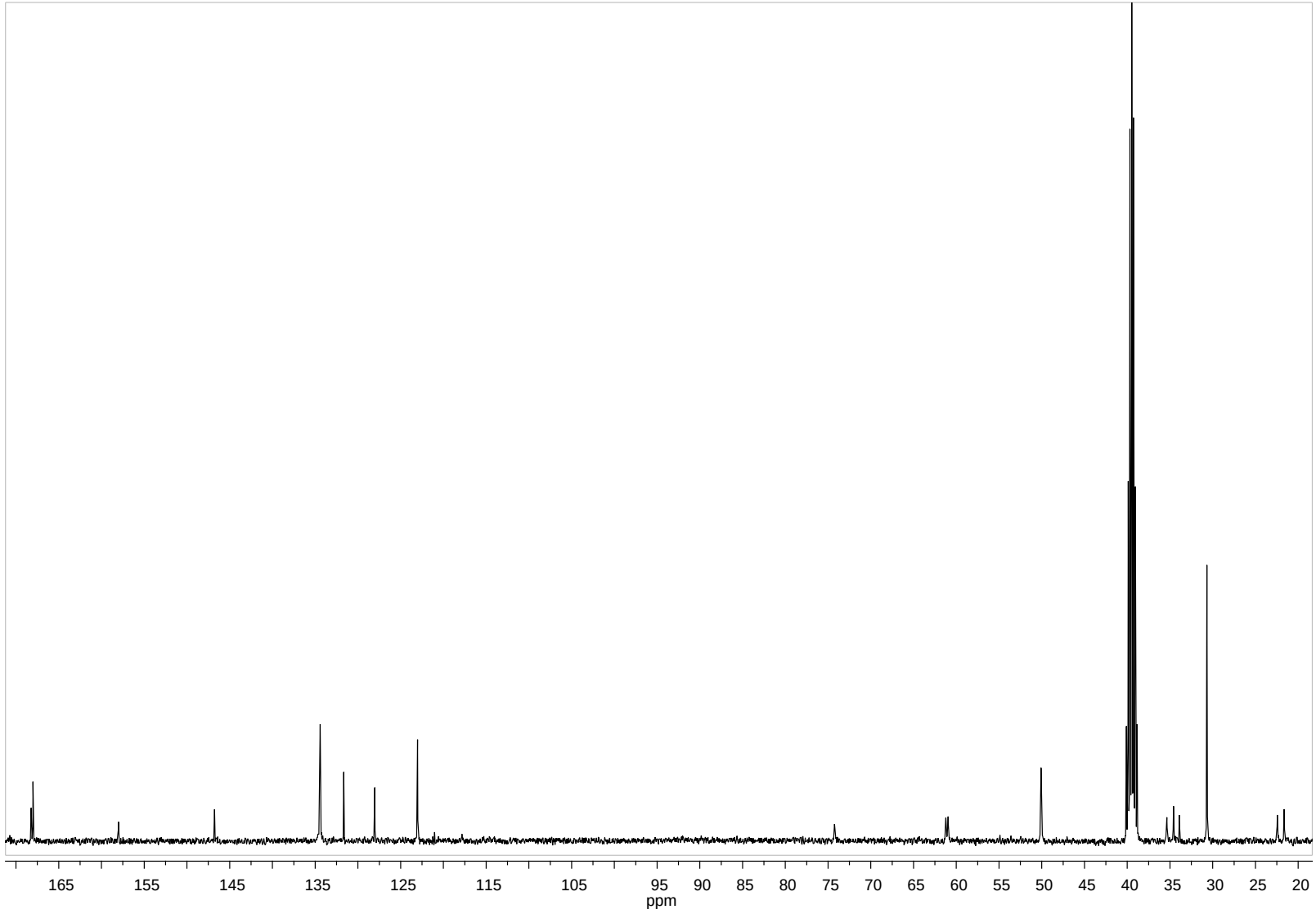

Fig. S76. ^{13}C NMR spectrum of 5,11,17,23-tetra-*tert*-butyl-25,26,27,28-tetrakis[(N-(2'-methyl-2',2'-diethyl)ammoniumethyl)-carbomoylmethoxy]-2,8,14,20-tetrathiacalix[4]arene tetra[bis(trifluoromethylsulfonyl)imide] (*cone* **48**), **$CDCl_3$, 298 K, 100 MHz**

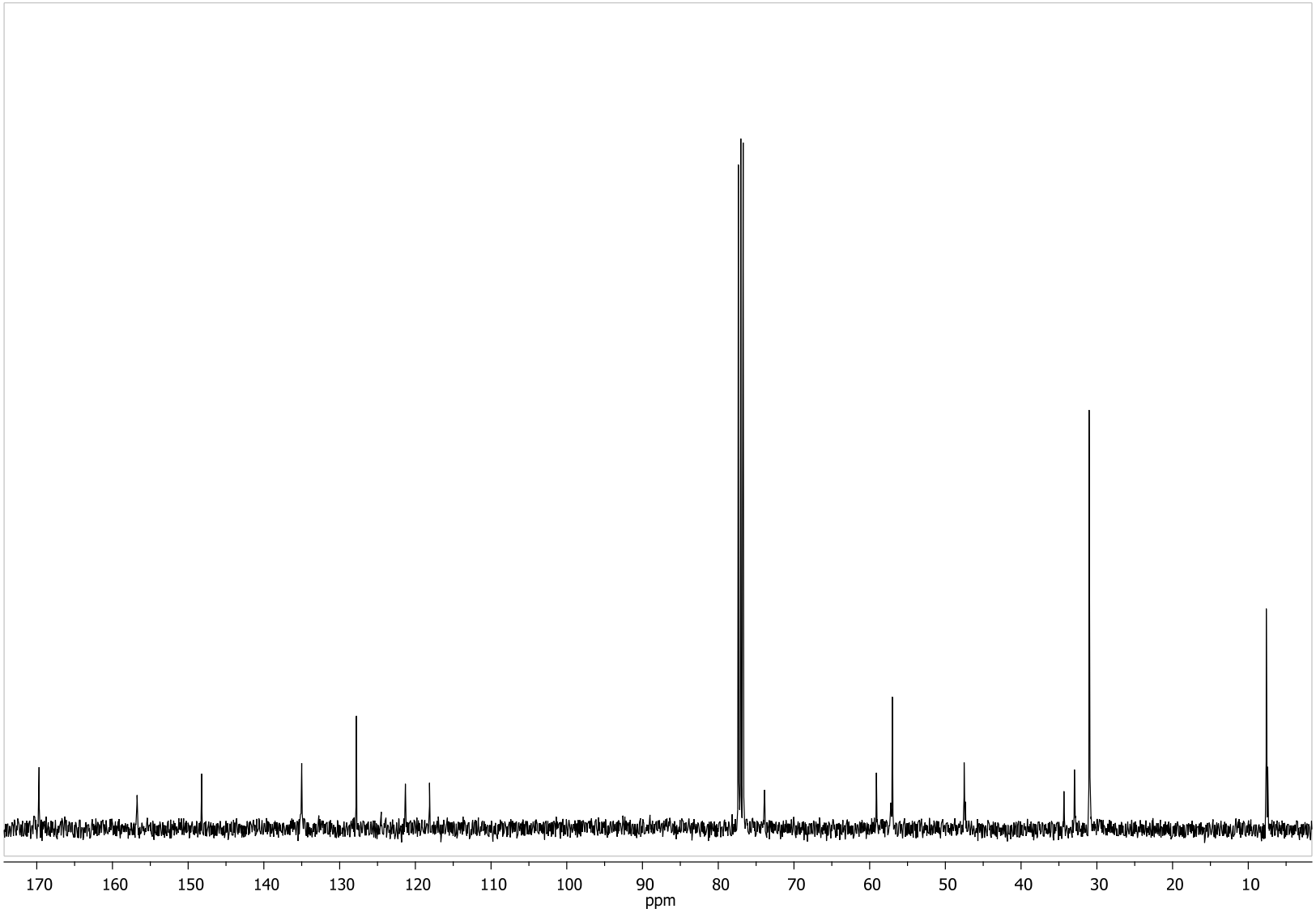

Fig. S77. ^{13}C NMR spectrum of 5,11,17,23-tetra-*tert*-butyl-25,26,27,28-tetrakis[(N-(2',2',2'-triethyl)ammoniumethyl)carbomoylmethoxy]-2,8,14,20-tetrathiacalix[4]arene tetra[bis(trifluoromethylsulfonyl)imide] (*cone* **49**), **$CDCl_3$, 298 K, 100 MHz**

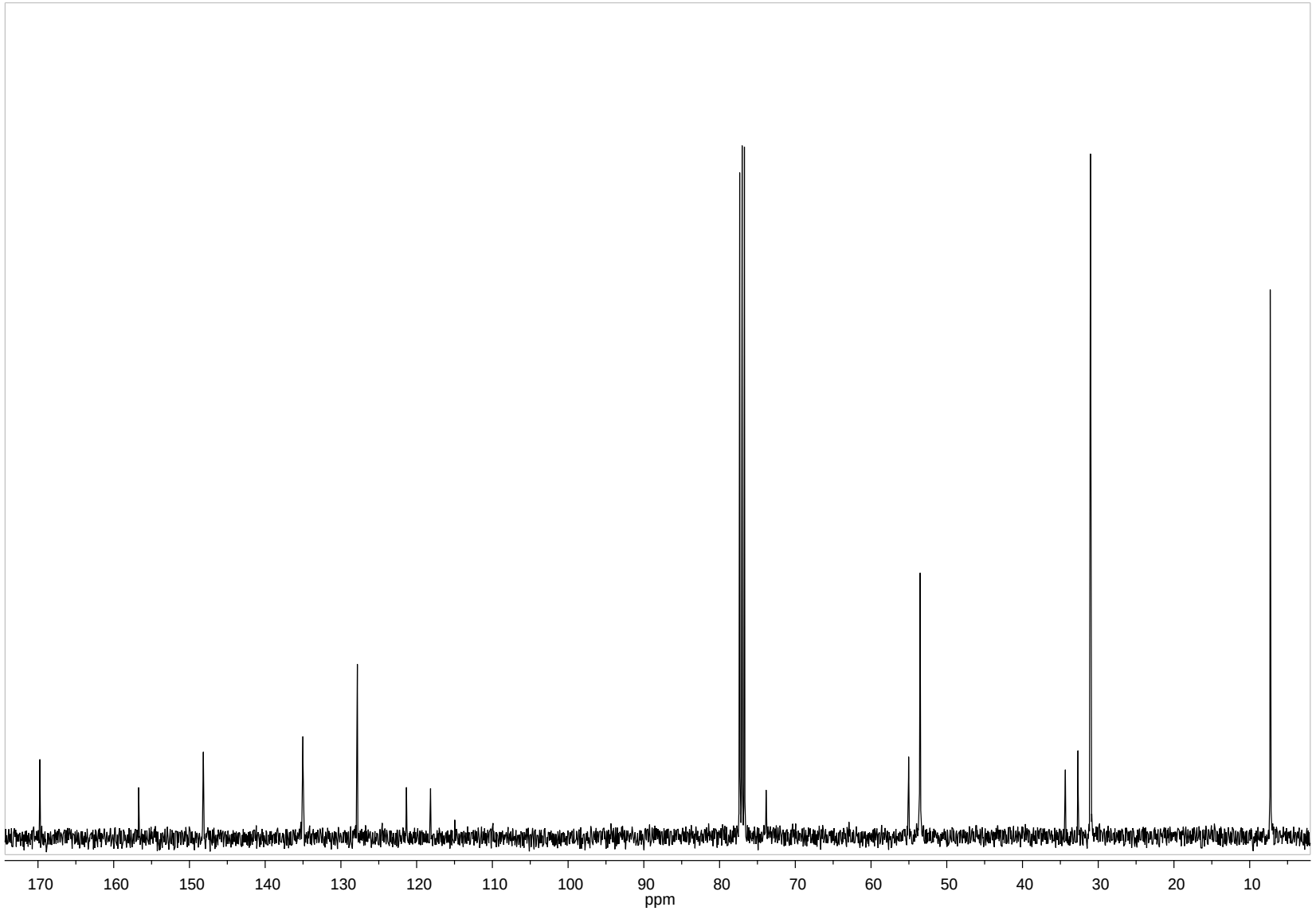

Fig. S78. ^{13}C NMR spectrum of 5,11,17,23-tetra-*tert*-butyl-25,26,27,28-tetrakis[(N-(2',2'-diethyl-2'–benzyl)ammoniumethyl)carbomoylmethoxy]-2,8,14,20-tetrathiacalix[4]arene tetra[bis(trifluoromethylsulfonyl)imide] (*cone* **50**), **$CDCl_3$, 298 K, 100 MHz**

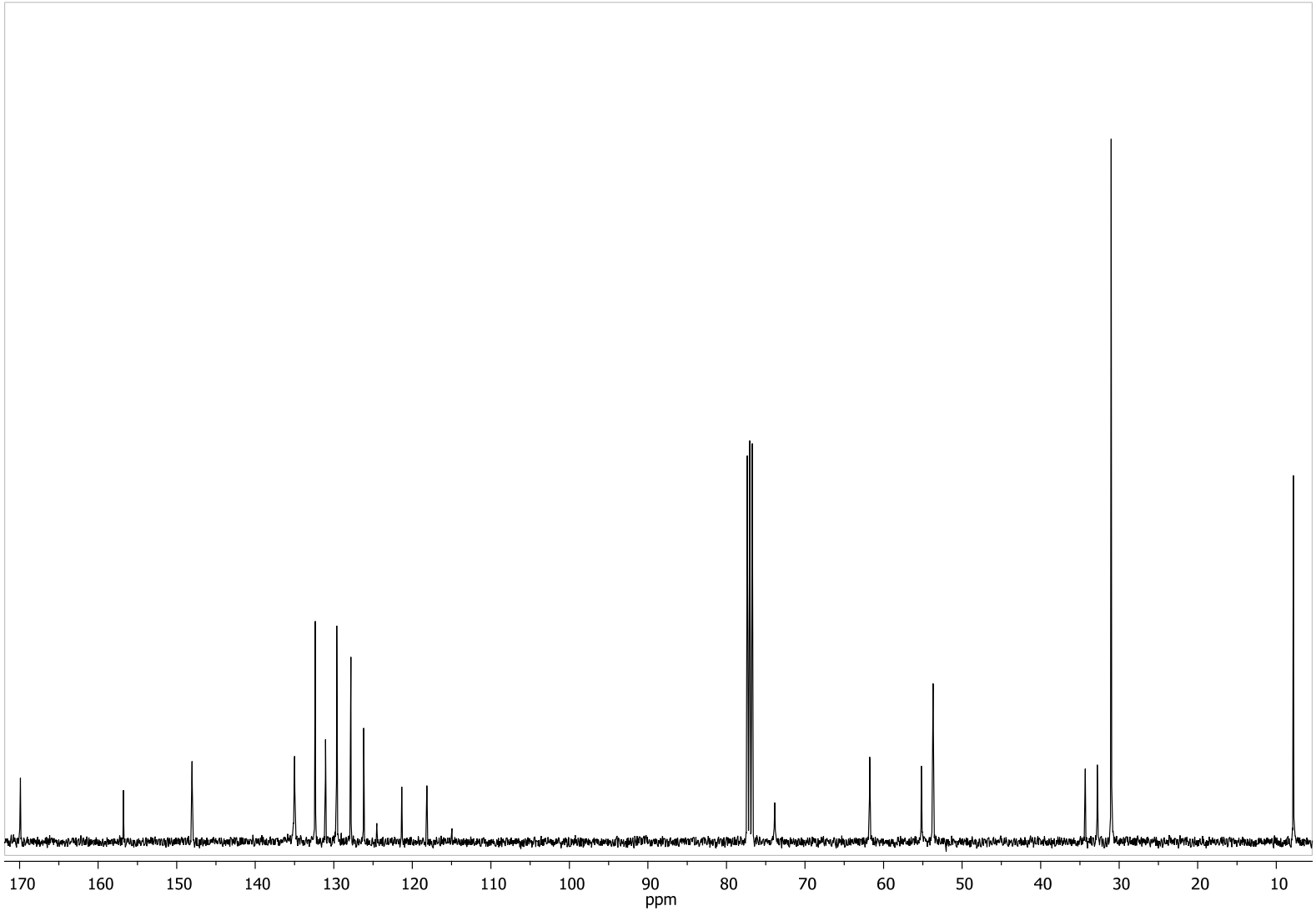

Fig. S79. ^{13}C NMR spectrum of 5,11,17,23-tetra-*tert*-butyl-25,26,27,28-tetrakis[(N-(2',2'-diethyl-2'-(ethoxycarbonylmethyl)ammoniumethyl)-carbomoylmethoxy]-2,8,14,20-tetrathiacalix[4]arene tetra[bis(trifluoromethylsulfonyl)imide] (*cone* **51**), **$CDCl_3$, 298 K, 100 MHz**

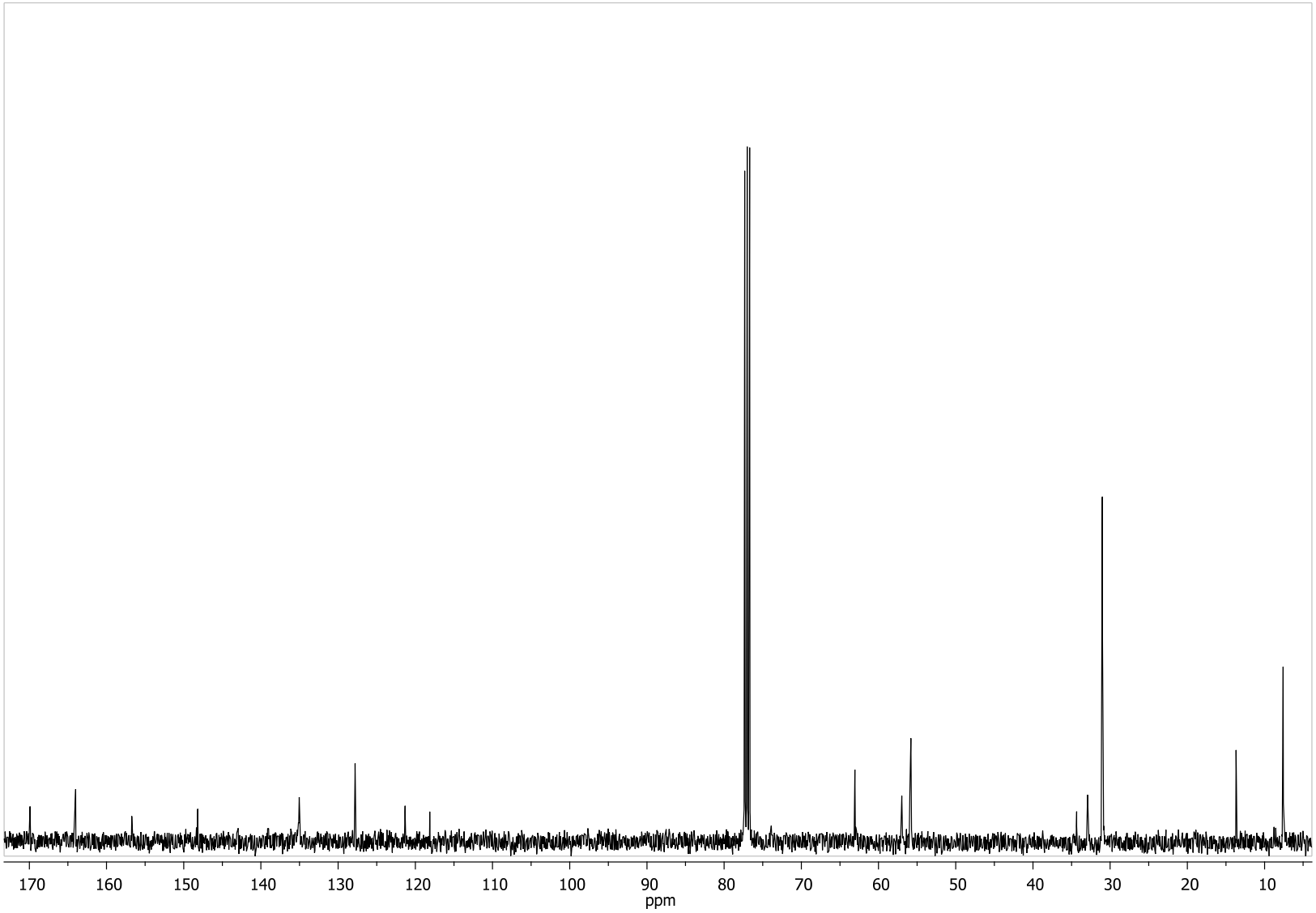

Fig. S80. ^{13}C NMR spectrum of 5,11,17,23-tetra-*tert*-butyl-25,26,27,28-tetrakis[(N-(2',2'-diethyl-2'-(pentoxycarbonylmethyl)ammoniumethyl)-carbomoylmethoxy]-2,8,14,20-tetrathiacalix[4]arene tetra[bis(trifluoromethylsulfonyl)imide] (*cone* **52**), **DMSO-d$_6$, 298 K, 100 MHz**

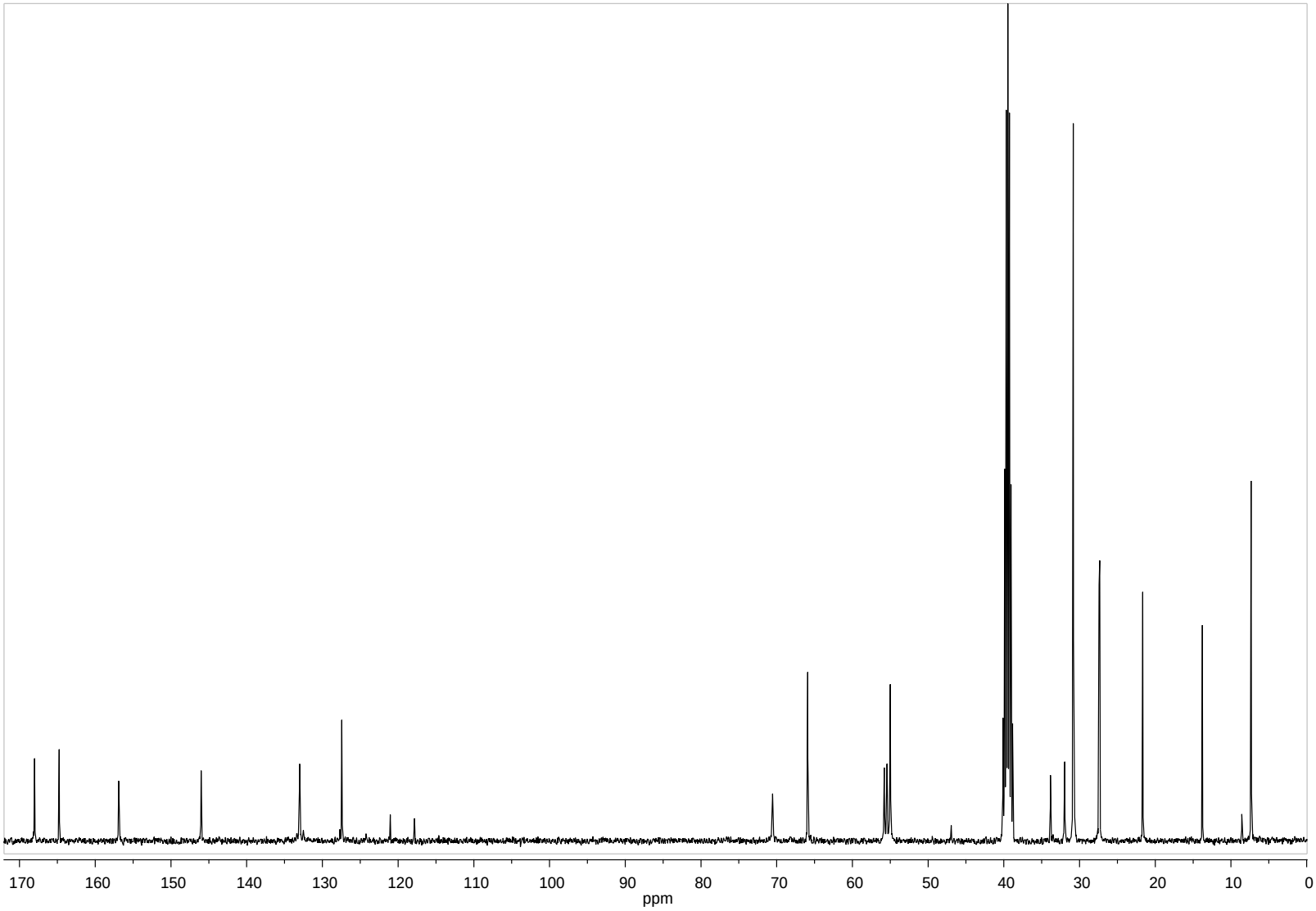

Fig. S81. ^{13}C NMR spectrum of 5,11,17,23-tetra-*tert*-butyl-25,26,27,28-tetrakis[(N-(2',2'-diethyl-2'-{(ethoxycarbonylmethyl)amidocarbonylmethyl})-ammoniumethyl)carbomoylmethoxy]-2,8,14,20-tetrathiacalix[4]arene tetra[bis(trifluoromethylsulfonyl)imide] (*cone* **53**), **DMSO-d_6, 298 K, 100 MHz**

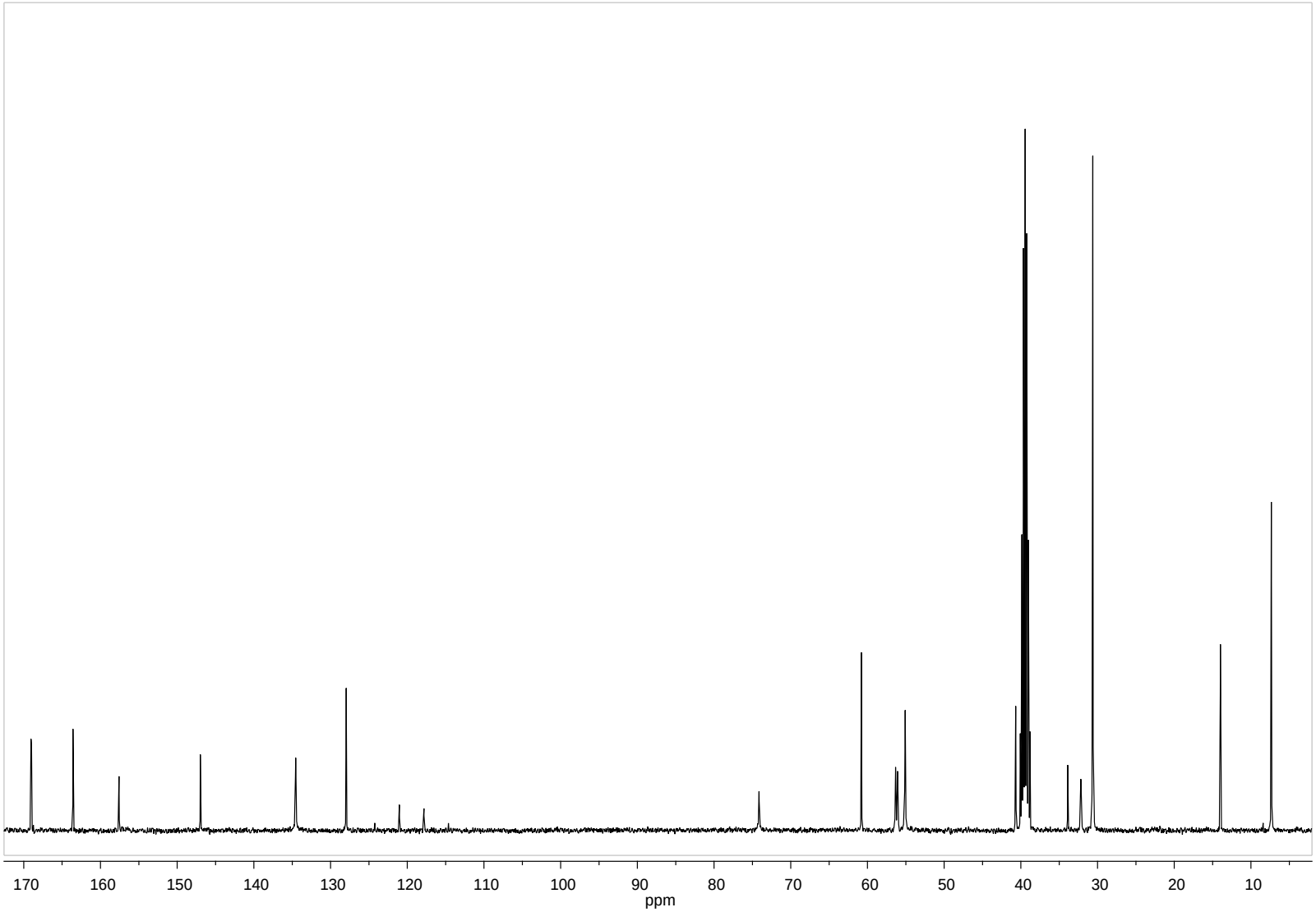

Fig. S82. ^{13}C NMR spectrum of 5,11,17,23-tetra-*tert*-butyl-25,26,27,28-tetrakis[(N-(2',2'-diethyl-2'-{([ethoxycarbonylmethyl]-amidocarbonylmethyl)amidocarbonylmethyl}ammoniumethyl)carbomoylmethoxy]-2,8,14,20-tetrathiacalix[4]arene tetra[bis(trifluoromethylsulfonyl)imide] (*cone* **54**), **DMSO-d$_6$, 298 K, 100 MHz**

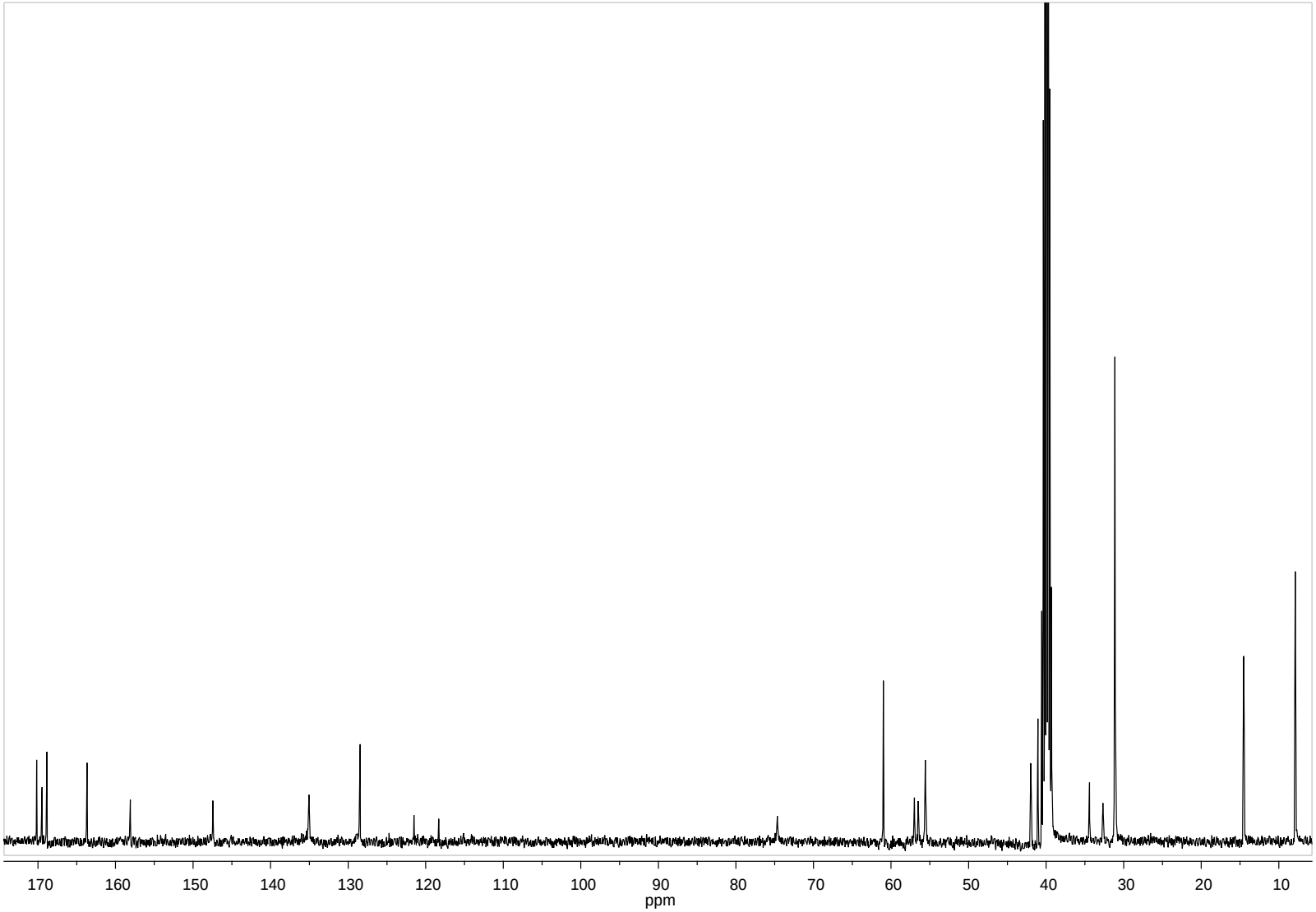

Fig. S83. ^{13}C NMR spectrum of 5,11,17,23-tetra-*tert*-butyl-25,26,27,28-tetrakis[(N-(2',2'-diethyl-2'-{(ethoxycarbonyl[S-methyl]methyl)amidocarbonylmethyl}ammoniumethyl)carbomoylmethoxy]-2,8,14,20-tetrathiacalix[4]arene tetra[bis(trifluoromethylsulfonyl)imide] (*cone* **55**), **DMSO-d_6, 298 K, 100 MHz**

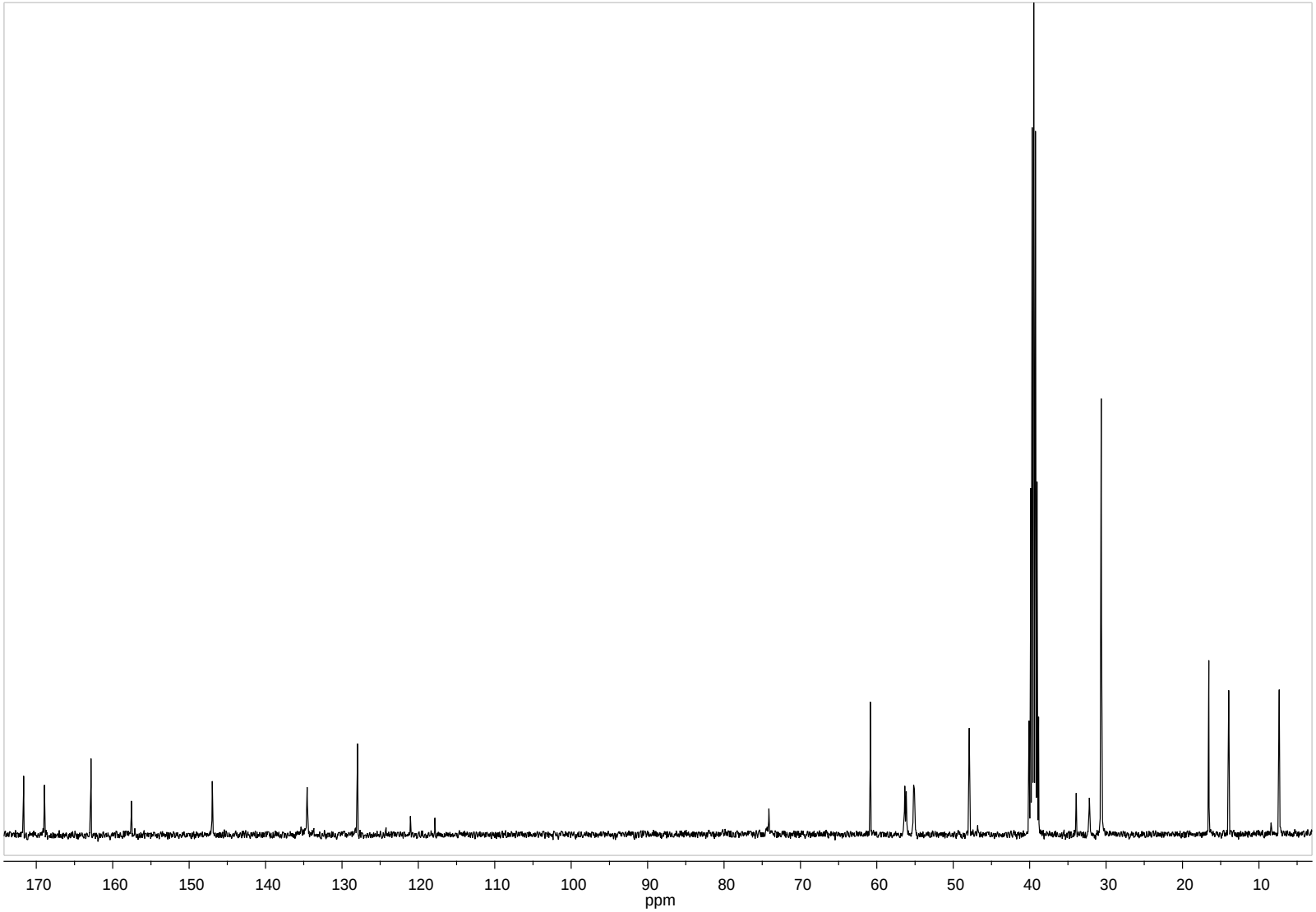

Fig. S84. ^{13}C NMR spectrum of 5,11,17,23-tetra-*tert*-butyl-25,26,27,28-tetrakis[(N-(3',3',3'-trimethyl)ammoniumpropyl)carbomoylmethoxy]-2,8,14,20-tetrathiacalix[4]arene tetra[bis(trifluoromethylsulfonyl)imide] (*1,3-alternate* **56**), **DMSO-d$_6$, 298 K, 100 MHz**

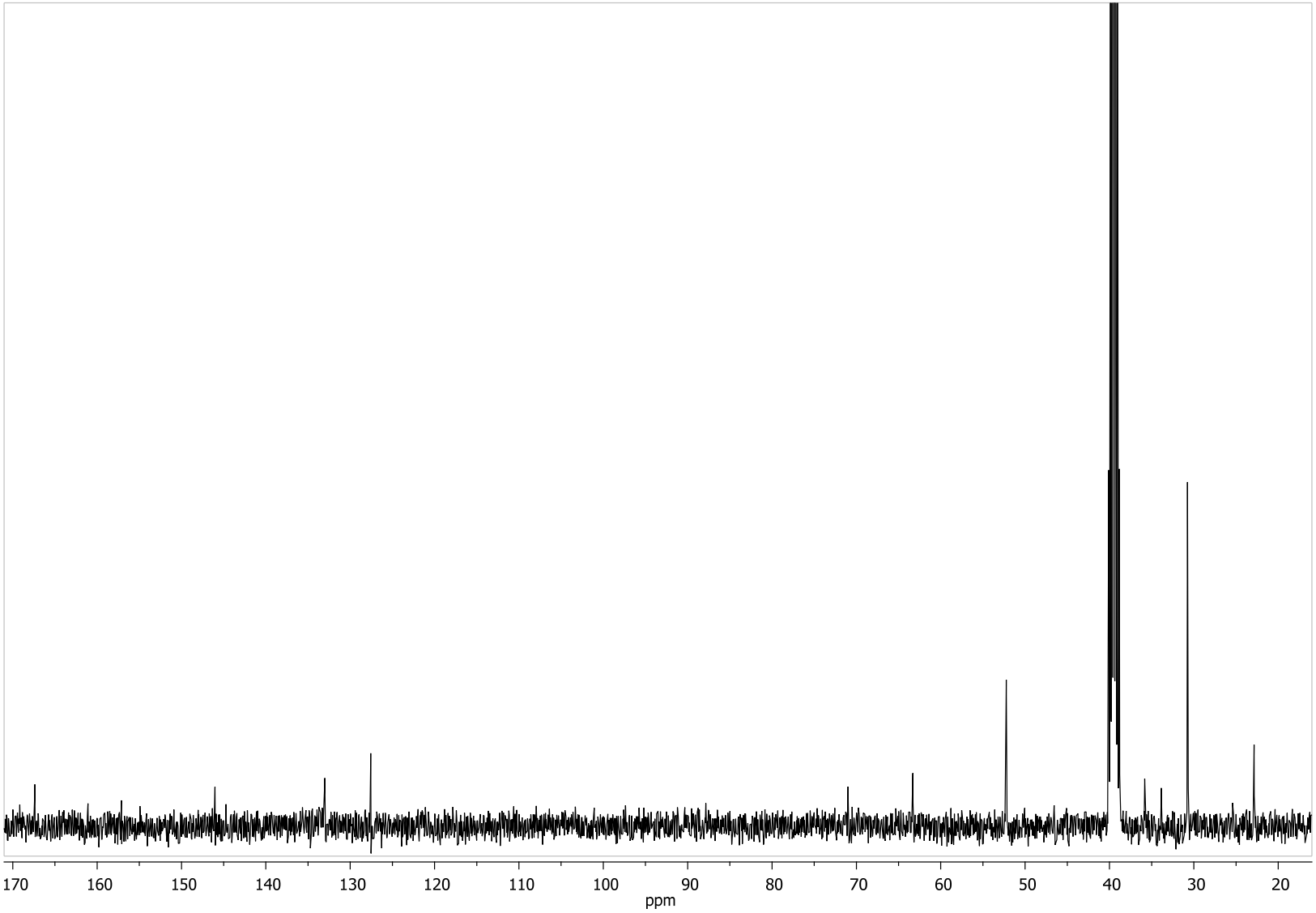

Fig. S85. ^{13}C NMR spectrum of 5,11,17,23-tetra-*tert*-butyl-25,26,27,28-tetrakis[(N-(3',3'-dimethyl-3'-ethyl)ammoniumpropyl)-carbomoylmethoxy]-2,8,14,20-tetrathiacalix[4]arene tetra[bis(trifluoromethylsulfonyl)imide] (*1,3-alternate* **57**), **DMSO-d_6, 298 K, 100 MHz**

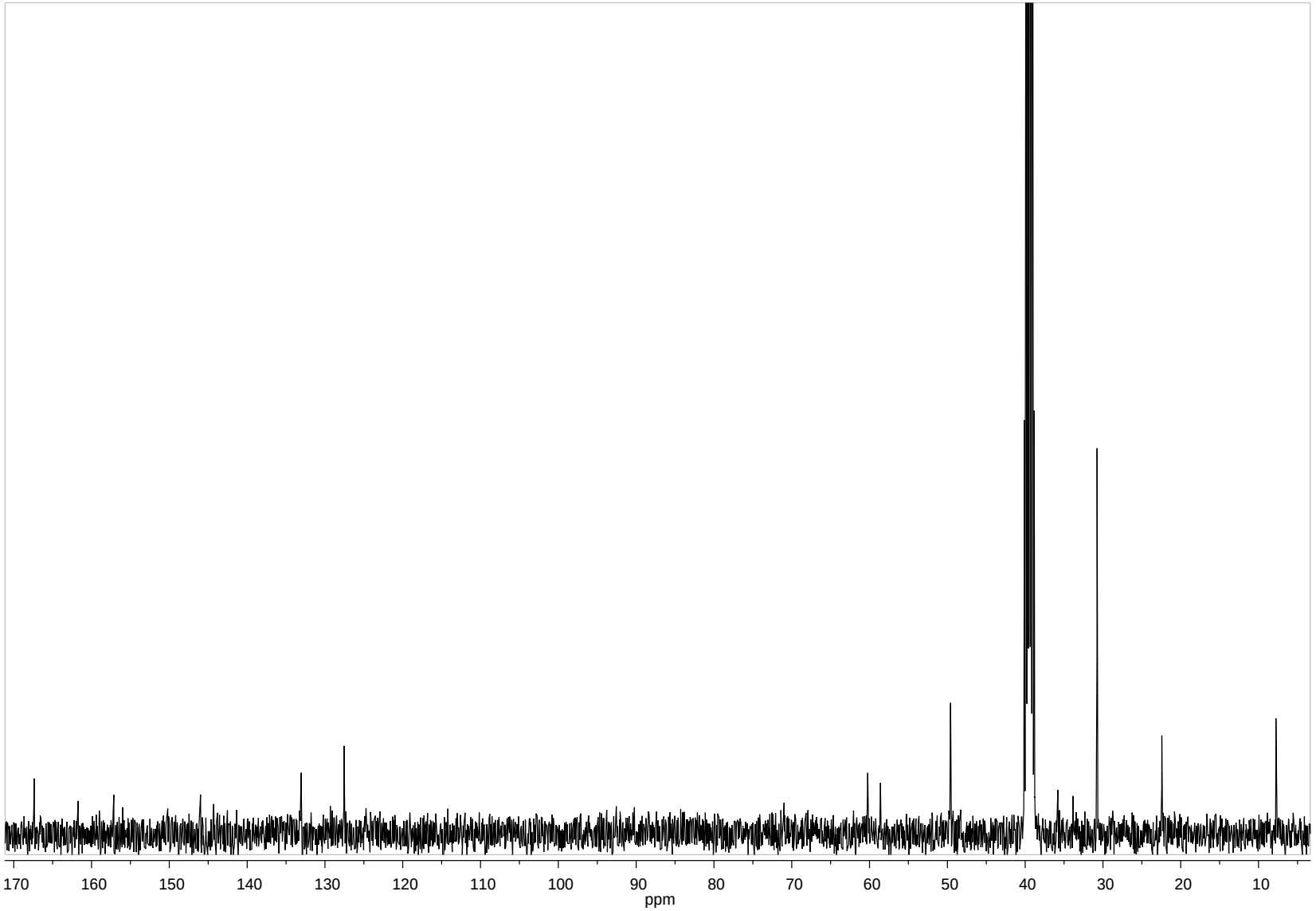

Fig. S86. ^{13}C NMR spectrum of 5,11,17,23-tetra-*tert*-butyl-25,26,27,28-tetrakis[(N-(3',3'-dimethyl-3'-benzyl)ammoniumpropyl)carbomoylmethoxy]-2,8,14,20-tetrathiacalix[4]arene tetra[bis(trifluoromethylsulfonyl)imide] (*1,3-alternate* **58**), **DMSO-d_6, 298 K, 100 MHz**

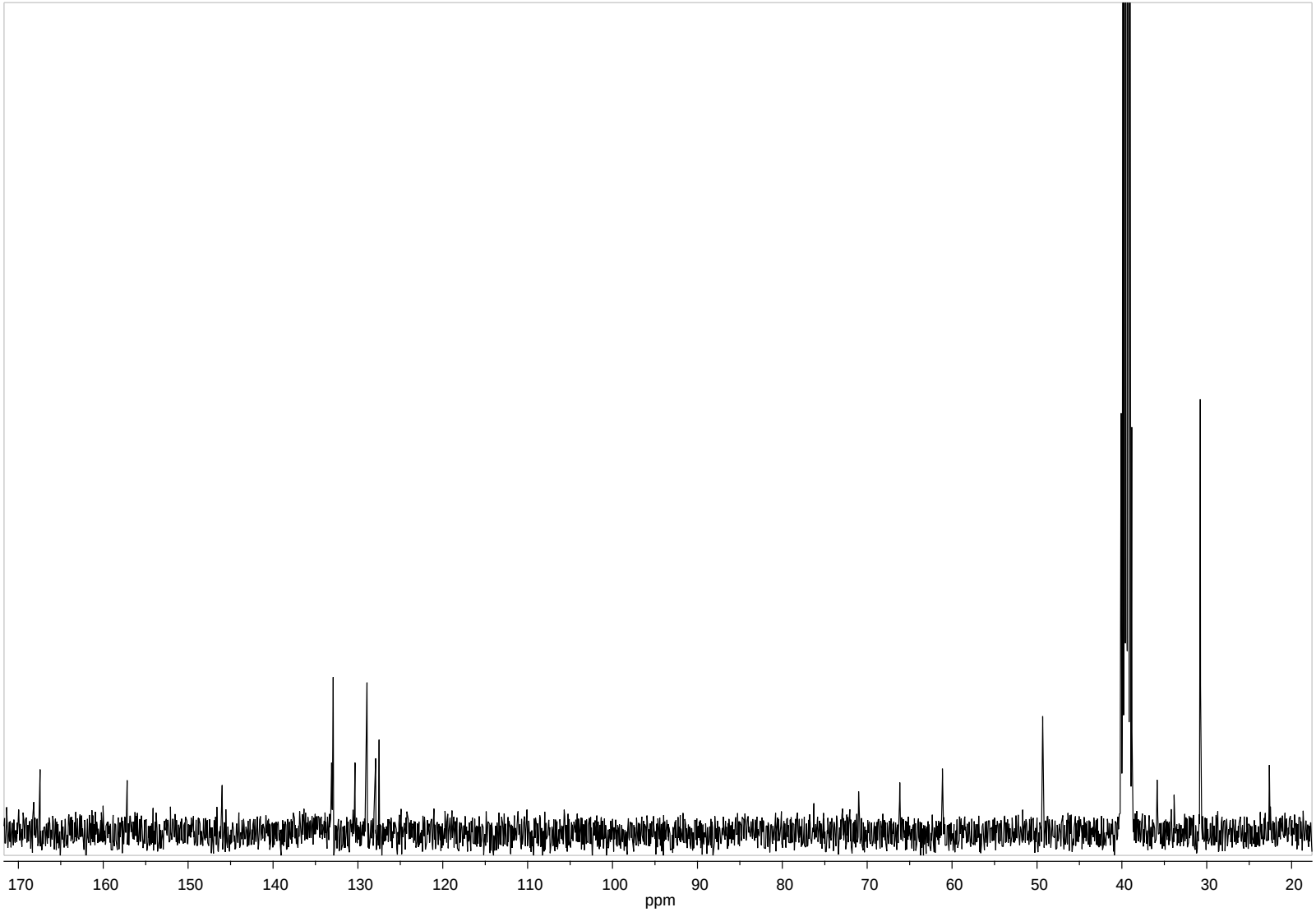

Fig. S87. ^{13}C NMR spectrum of 5,11,17,23-tetra-*tert*-butyl-25,26,27,28-tetrakis[(N-(3',3'-dimethyl-3'-(ethoxycarbonylmethyl)ammoniumpropyl)carbomoylmethoxy]-2,8,14,20-tetrathiacalix[4]arene tetra[bis(trifluoromethylsulfonyl)imide] (*1,3-alternate* **59**), **DMSO-d$_6$, 298 K, 100 MHz**

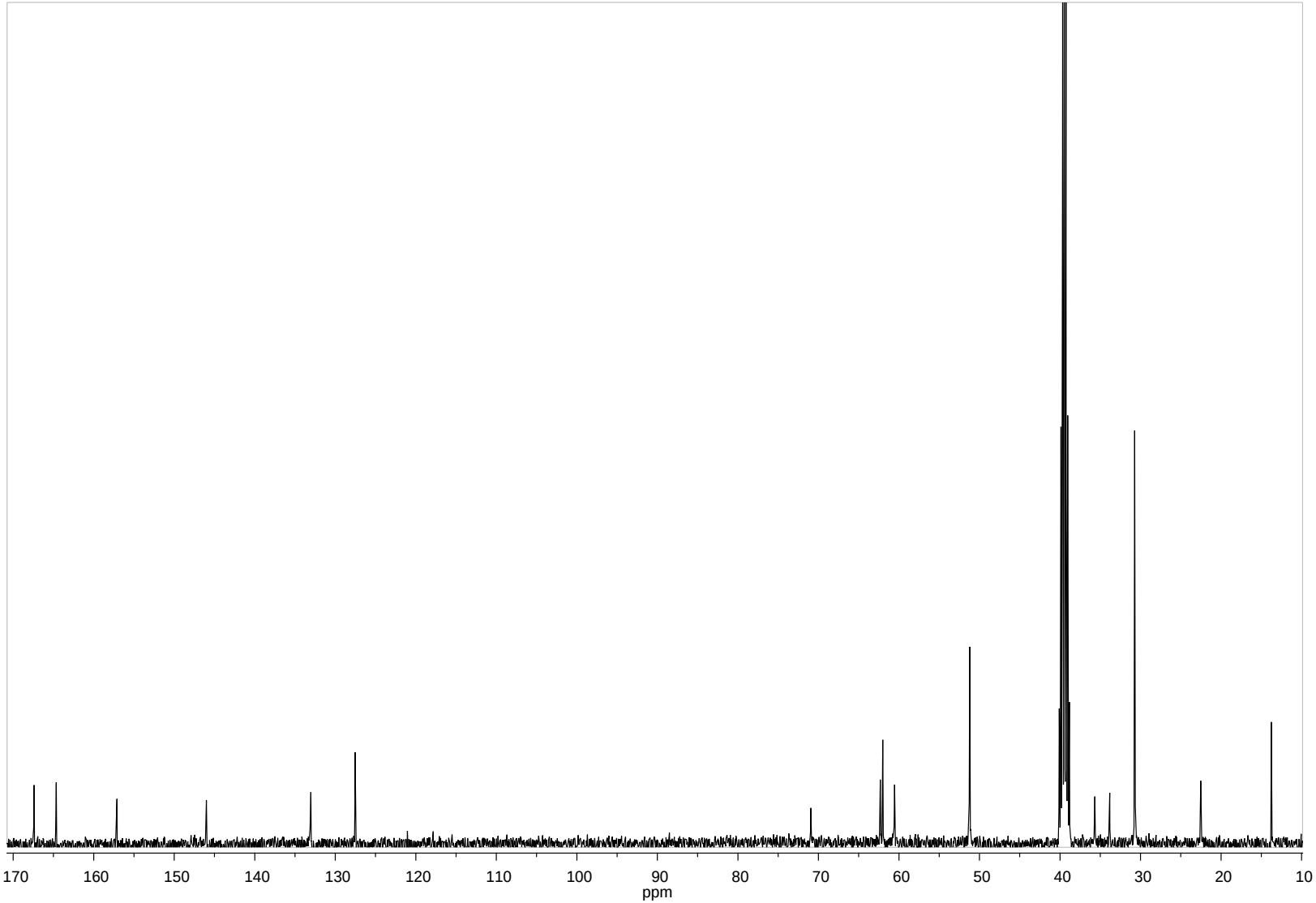

Fig. S88. ^{13}C NMR spectrum of 5,11,17,23-tetra-*tert*-butyl-25,26,27,28-tetrakis[(N-(3',3'-dimethyl-3'-(pentoxycarbonylmethyl)ammoniumpropyl)-carbomoylmethoxy]-2,8,14,20-tetrathiacalix[4]arene tetra[bis(trifluoromethylsulfonyl)imide] (*1,3-alternate* **60**), **DMSO-d_6, 298 K, 100 MHz**

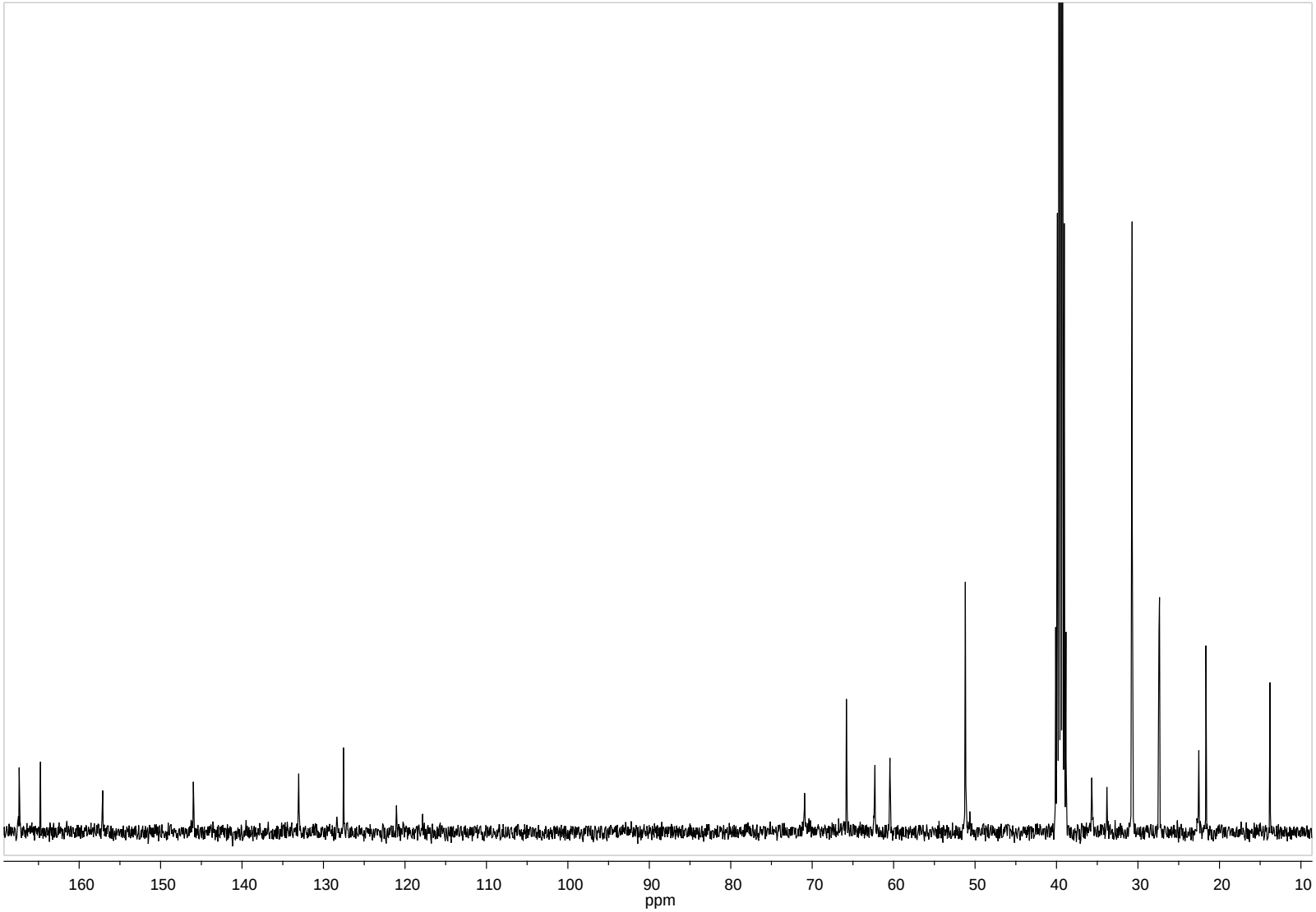

Fig. S89. ^{13}C NMR spectrum of 5,11,17,23-tetra-*tert*-butyl-25,26,27,28-tetrakis[(N-(3',3'-dimethyl-3'-{(ethoxycarbonylmethyl)amidocarbonylmethyl}-ammoniumpropyl)carbomoylmethoxy]-2,8,14,20-tetrathiacalix[4]arene tetra[bis(trifluoromethylsulfonyl)imide] (*1,3-alternate* **61**), **DMSO-d$_6$, 298 K, 100 MHz**

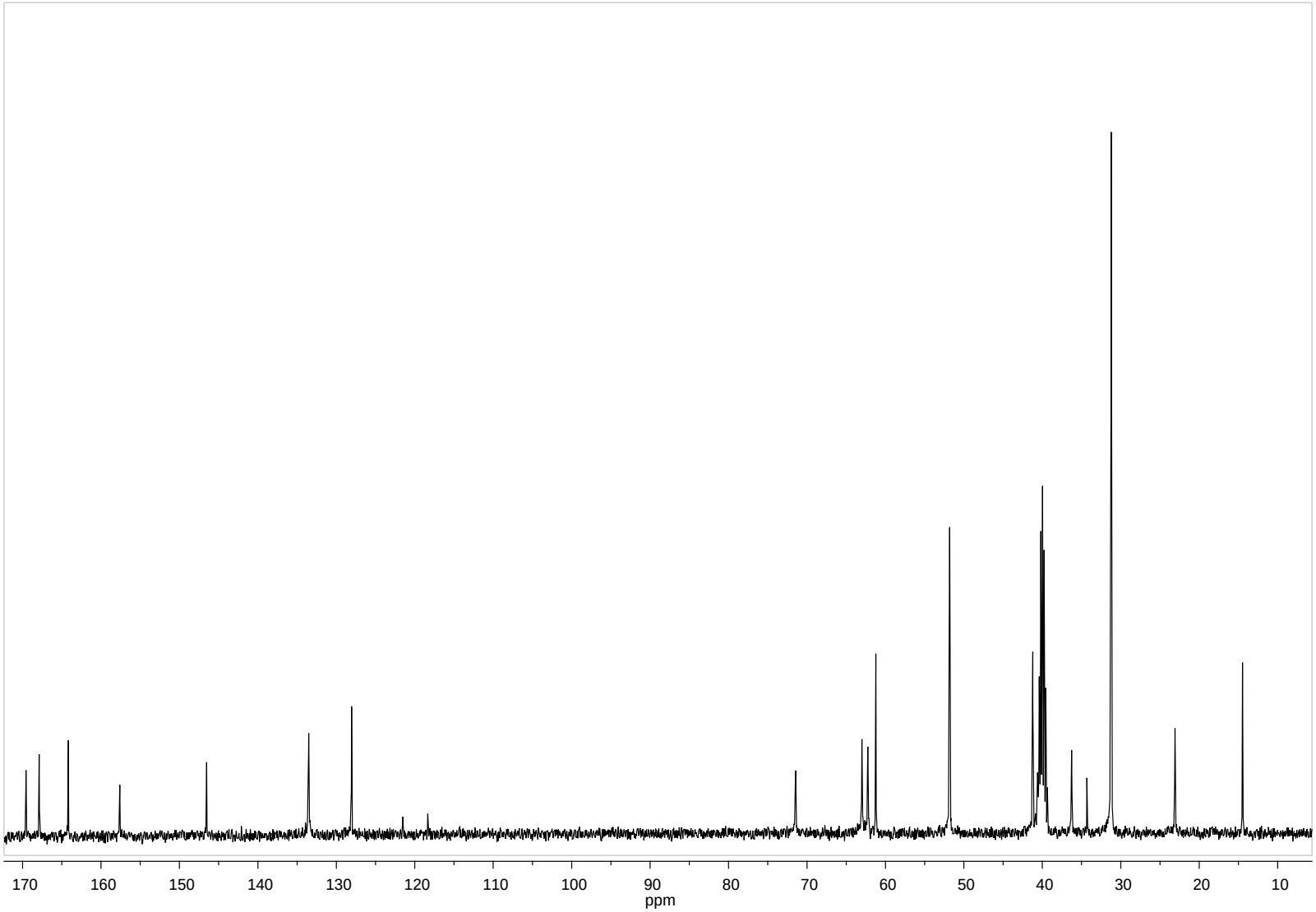

Fig. S90. ^{13}C NMR spectrum of 5,11,17,23-tetra-*tert*-butyl-25,26,27,28-tetrakis[(N-(3',3'-dimethyl-3'-{([ethoxycarbonylmethyl]amidocarbonylmethyl)amidocarbonylmethyl}ammoniumpropyl)carbomoylmethoxy]-2,8,14,20-tetrathiacalix[4]arene tetra[bis(trifluoromethylsulfonyl)imide] (*1,3-alternate* **62**), **DMSO-d_6, 298 K, 100 MHz**

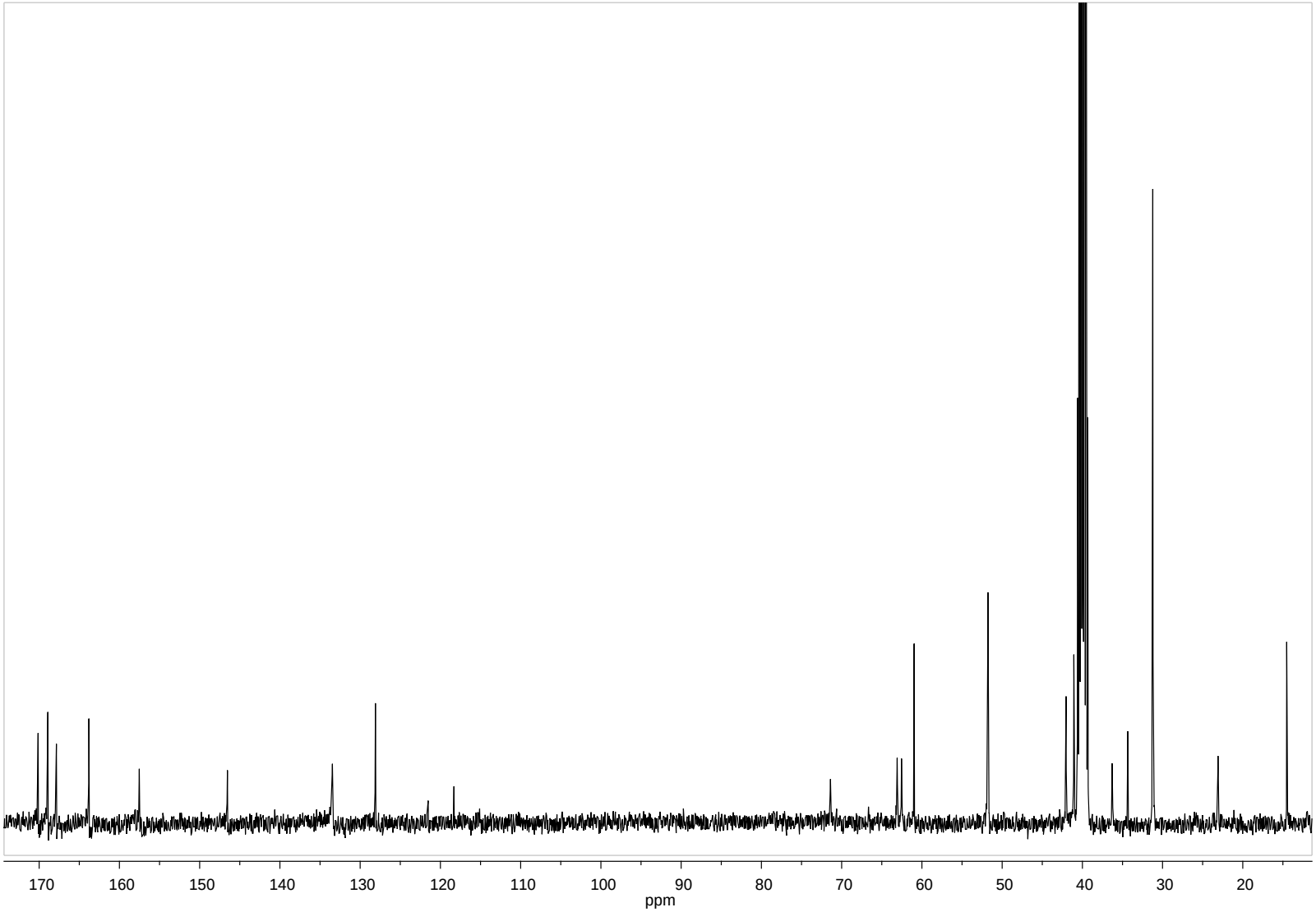

Fig. S91. ^{13}C NMR spectrum of 5,11,17,23-tetra-*tert*-butyl-25,26,27,28-tetrakis[(N-(3',3'-dimethyl-3'-{(ethoxycarbonyl[S-methyl]methyl)amidocarbonylmethyl}ammoniumpropyl)carbomoylmethoxy]-2,8,14,20-tetrathiacalix[4]arene tetra[bis(trifluoromethylsulfonyl)imide] (*1,3-alternate* **63**), **DMSO-d$_6$, 298 K, 100 MHz**

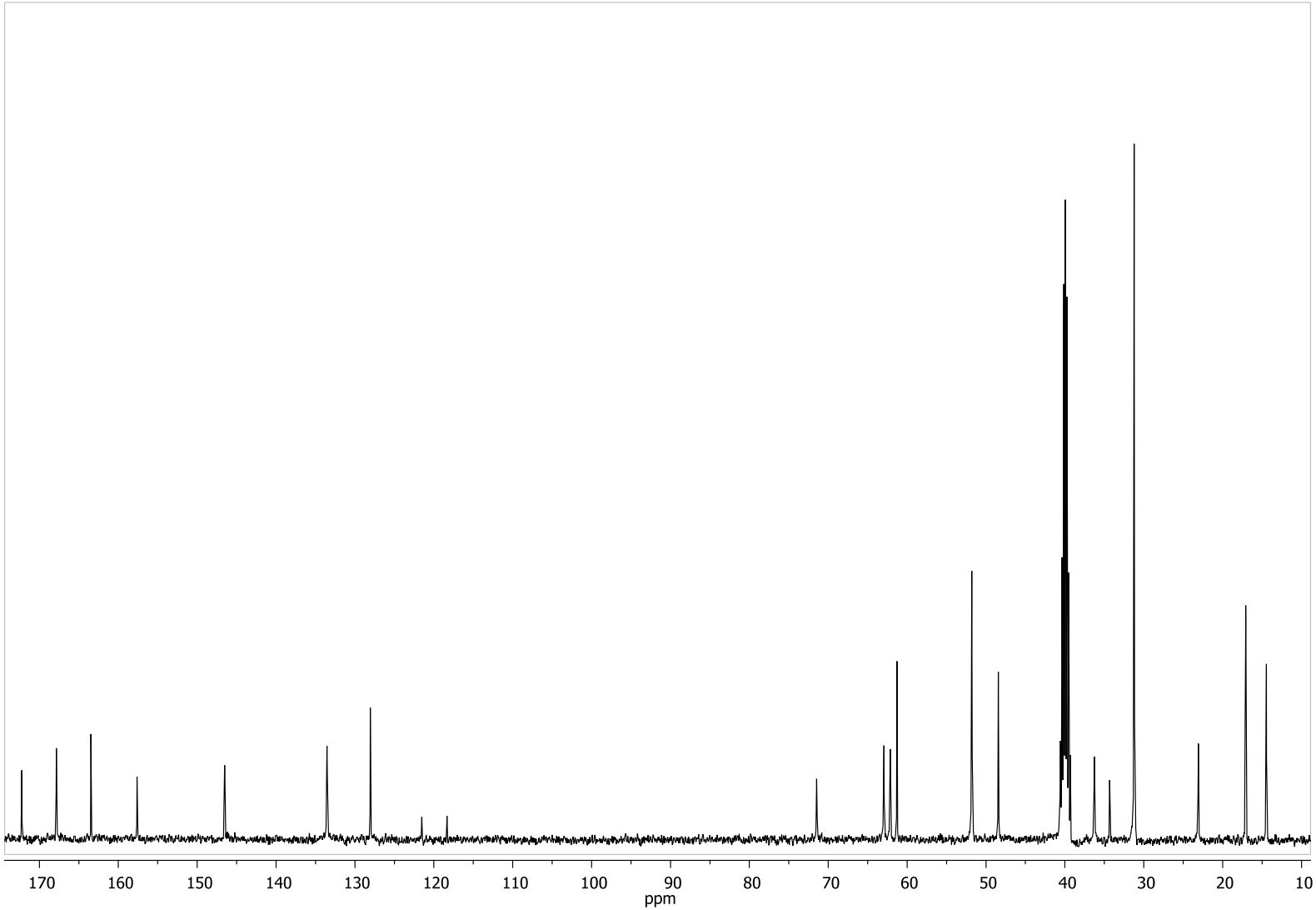

Fig. S92. ^{13}C NMR spectrum of 5,11,17,23-tetra-*tert*-butyl-25,26,27,28-tetrakis[(N-(3',3'-dimethyl-3'-{3''-propylphtalimide}ammoniumpropyl)-carbomoylmethoxy]-2,8,14,20-tetrathiacalix[4]arene tetra[bis(trifluoromethylsulfonyl)imide] (*1,3-alternate* **64**), **DMSO-d$_6$, 298 K, 100 MHz**

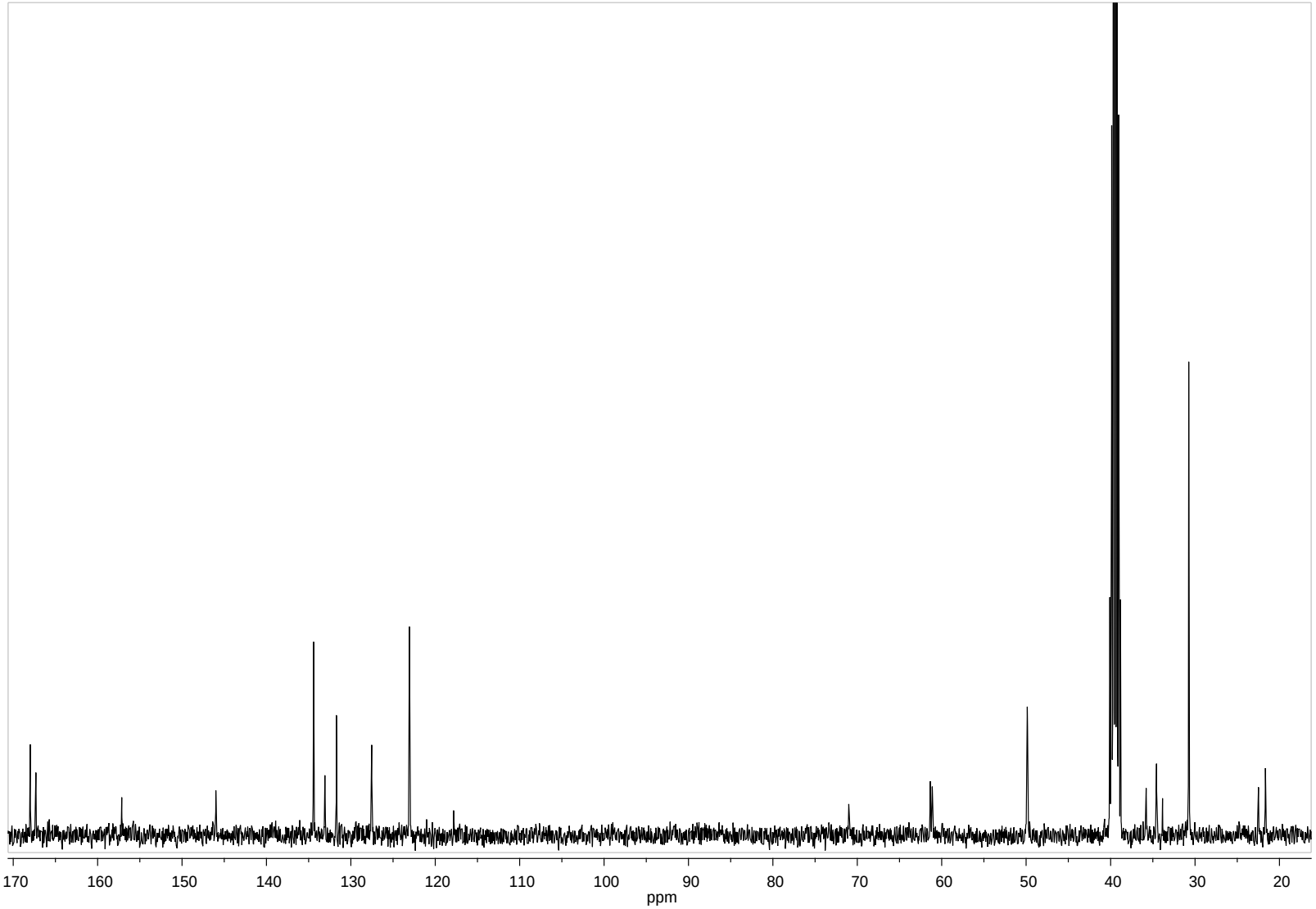

Fig. S93. ^{13}C NMR spectrum of 5,11,17,23-tetra-*tert*-butyl-25,26,27,28-tetrakis[(N-(2'-methyl-2',2'-diethyl)ammoniumethyl)carbomoylmethoxy]-2,8,14,20-tetrathiacalix[4]arene tetra[bis(trifluoromethylsulfonyl)imide] (*1,3-alternate* **65**), **DMSO-d_6, 298 K, 100 MHz**

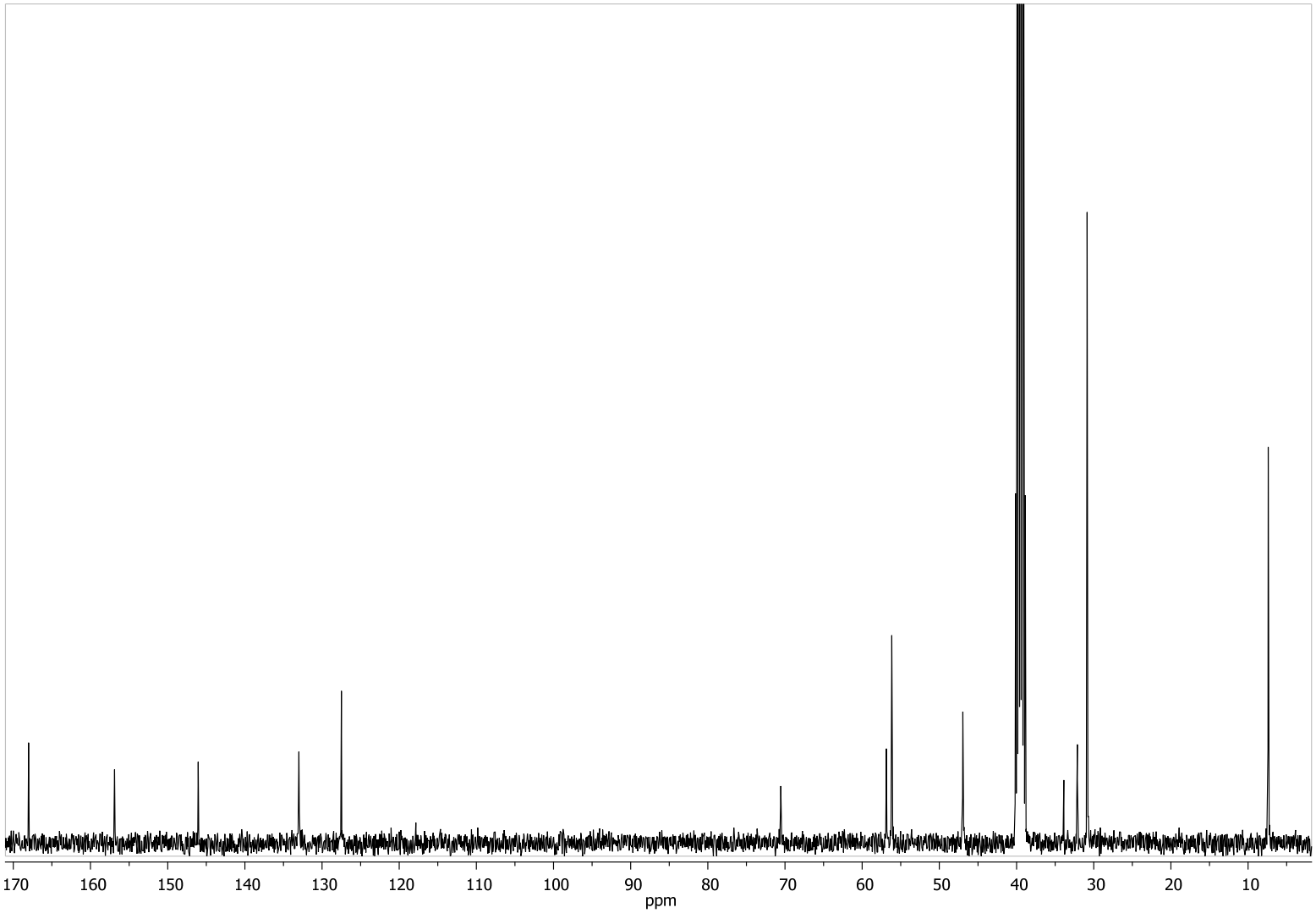

Fig. S94. ^{13}C NMR spectrum of 5,11,17,23-tetra-*tert*-butyl-25,26,27,28-tetrakis[(N-(2',2',2'-triethyl)ammoniumethyl)carbomoylmethoxy]-2,8,14,20-tetrathiacalix[4]arene tetra[bis(trifluoromethylsulfonyl)imide] (*1,3-alternate* **66**), **DMSO-d$_6$, 298 K, 100 MHz**

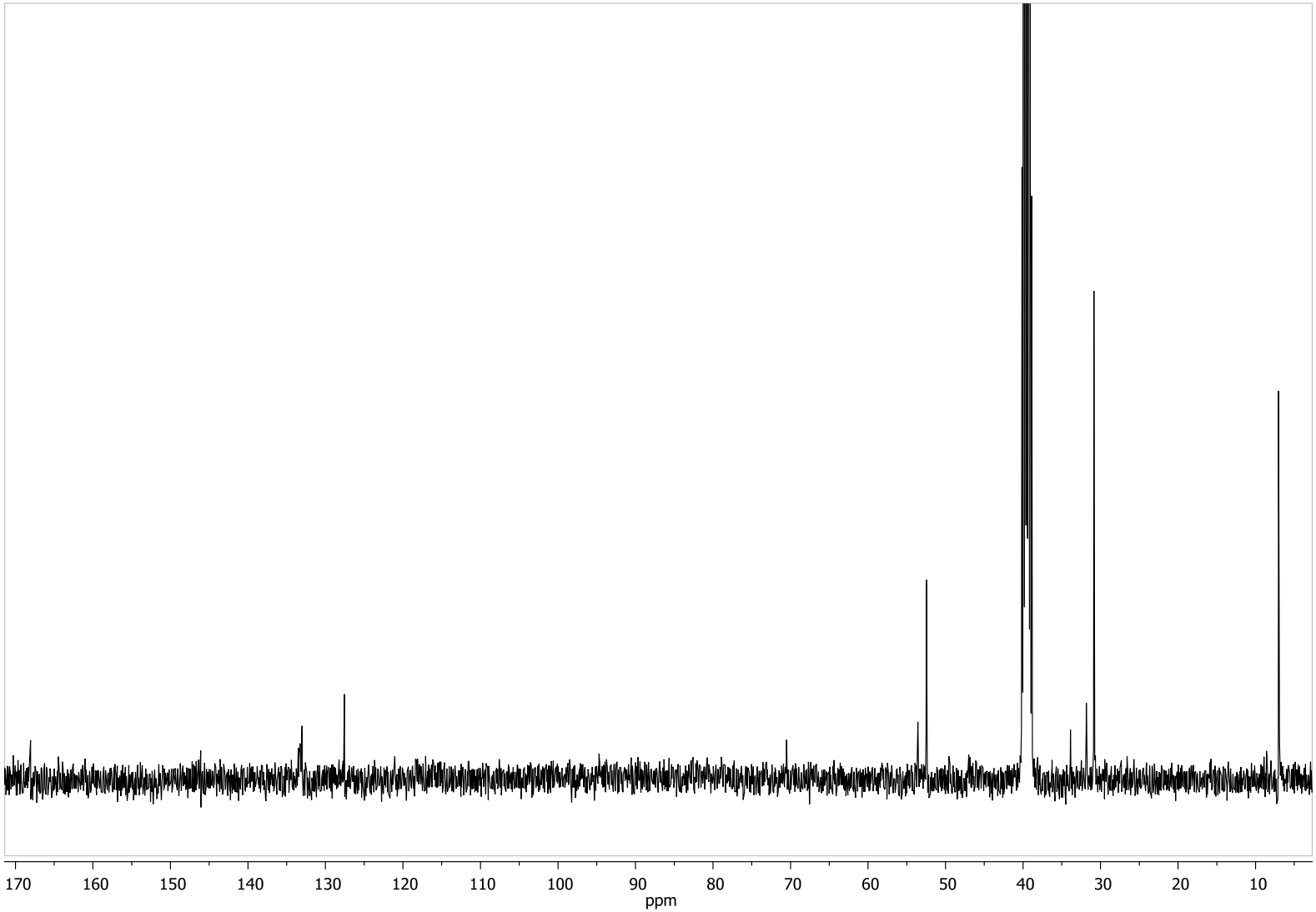

Fig. S95. ^{13}C NMR spectrum of 5,11,17,23-tetra-*tert*-butyl-25,26,27,28-tetrakis[(N-(2',2'-diethyl-2'-benzyl)ammoniumethyl)carbomoylmethoxy]-2,8,14,20-tetrathiacalix[4]arene tetra[bis(trifluoromethylsulfonyl)imide] (*1,3-alternate* **67**), **DMSO-d$_6$, 298 K, 100 MHz**

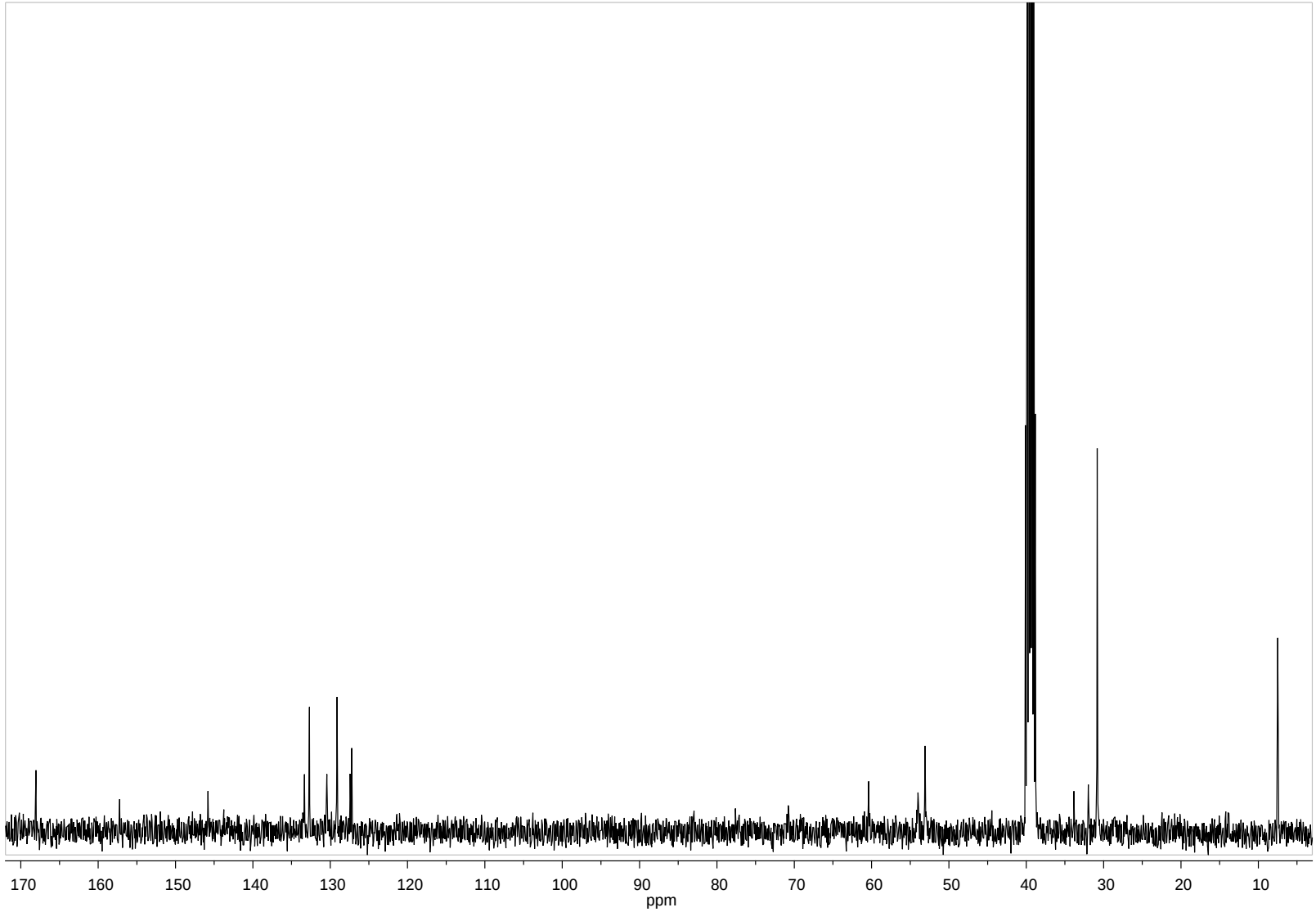

Fig. S96. ^{13}C NMR spectrum of 5,11,17,23-tetra-*tert*-butyl-25,26,27,28-tetrakis[(N-(2',2'-diethyl-2'-(ethoxycarbonylmethyl)ammoniumethyl)-carbomoylmethoxy]-2,8,14,20-tetrathiacalix[4]arene tetra[bis(trifluoromethylsulfonyl)imide] (*1,3-alternate* **68**), **DMSO-d_6, 298 K, 100 MHz**

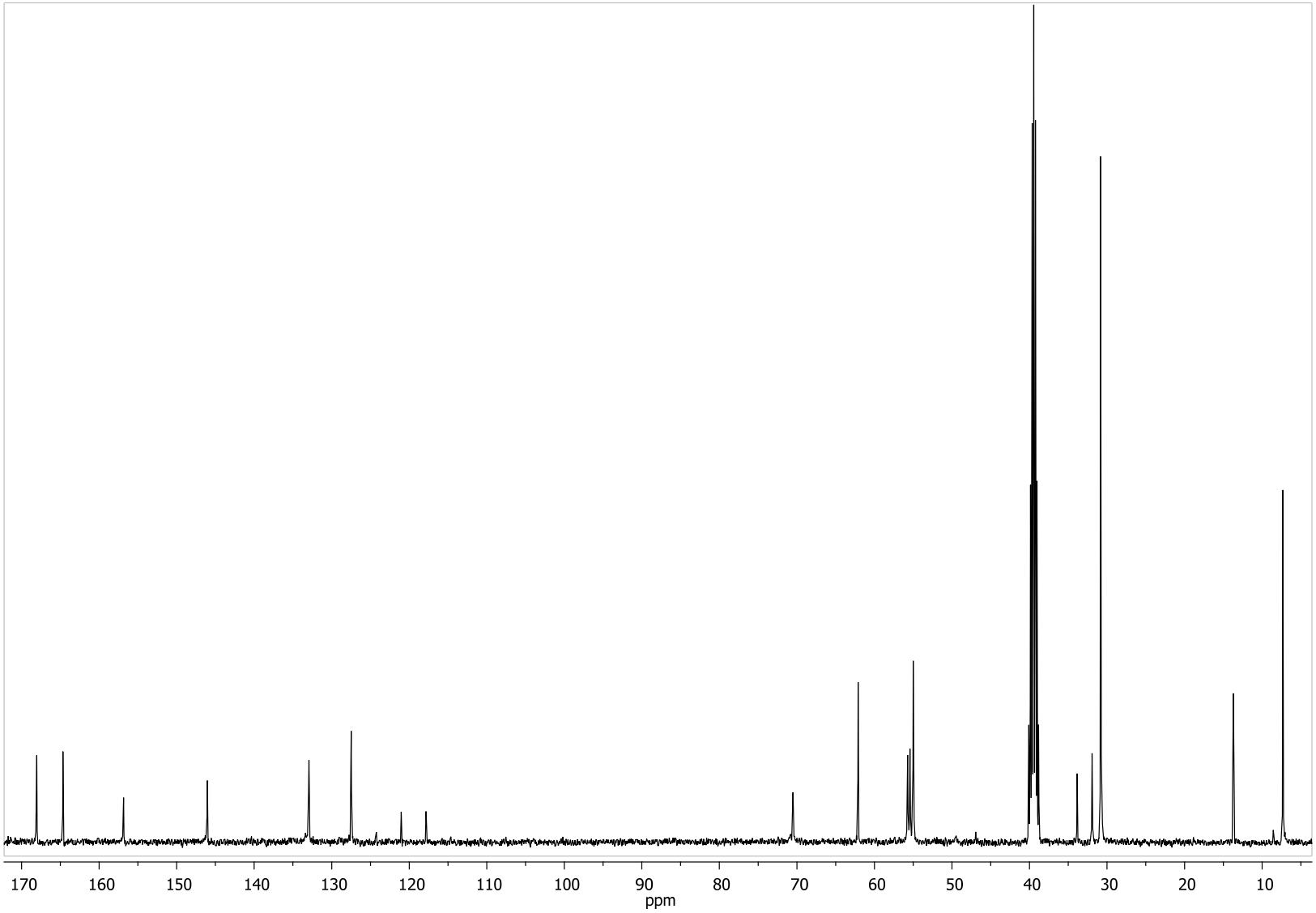

Fig. S97. ^{13}C NMR spectrum of 5,11,17,23-tetra-*tert*-butyl-25,26,27,28-tetrakis[(N-(2',2'-diethyl-2'-(pentoxycarbonylmethyl)ammoniumethyl)-carbomoylmethoxy]-2,8,14,20-tetrathiacalix[4]arene tetra[bis(trifluoromethylsulfonyl)imide] (*1,3-alternate* **69**), **DMSO-d$_6$, 298 K, 100 MHz**

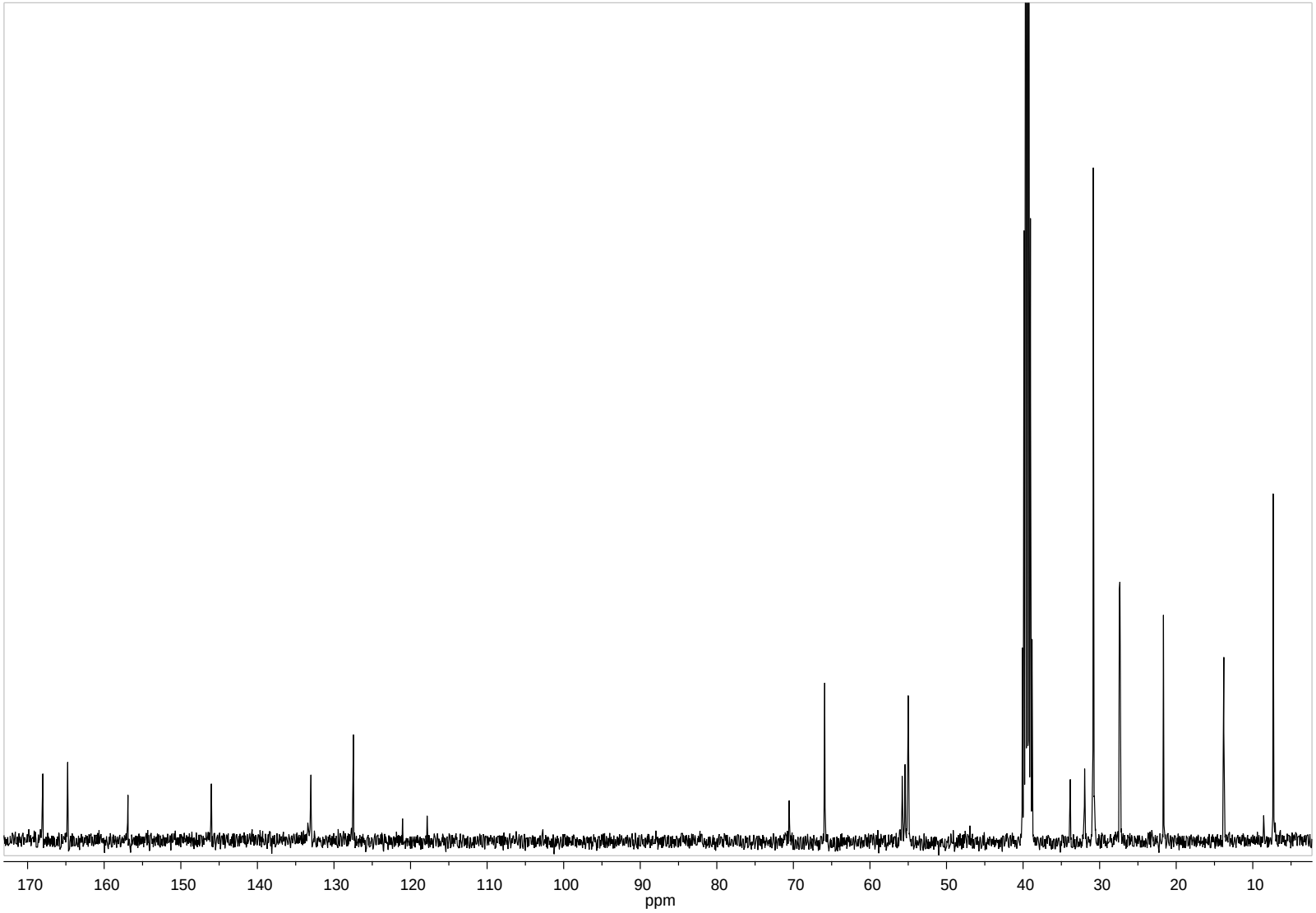

Fig. S98. ^{13}C NMR spectrum of 5,11,17,23-tetra-*tert*-butyl-25,26,27,28-tetrakis[(N-(2',2'-diethyl-2'-{(ethoxycarbonylmethyl)amidocarbonylmethyl})-ammoniumethyl)carbomoylmethoxy]-2,8,14,20-tetrathiacalix[4]arene tetra[bis(trifluoromethylsulfonyl)imide] (*1,3-alternate* **70**), **DMSO-d$_6$, 298 K, 100 MHz**

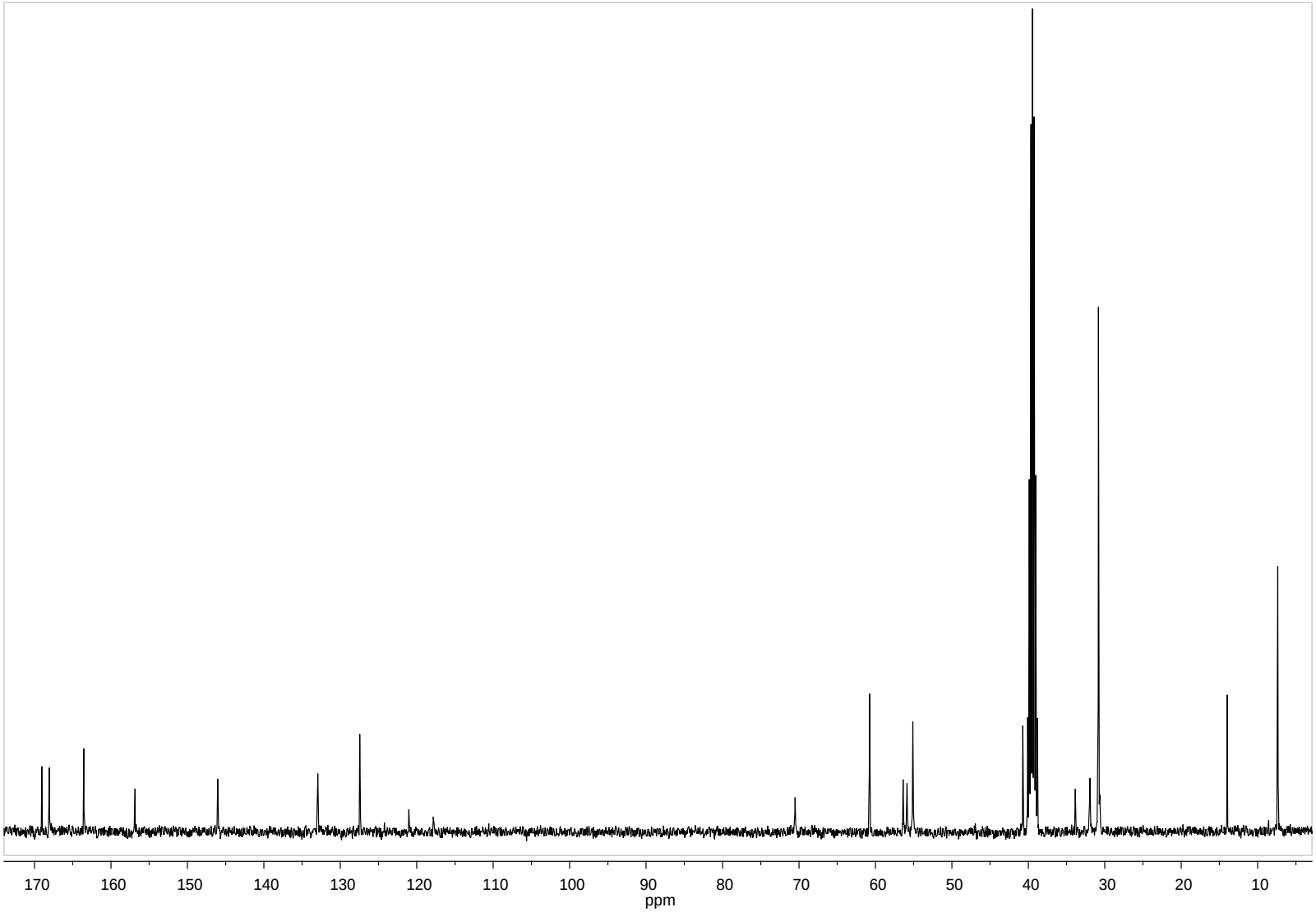

Fig. S99. ^{13}C NMR spectrum of 5,11,17,23-tetra-*tert*-butyl-25,26,27,28-tetrakis[(N-(2',2'-diethyl-2'-{([ethoxycarbonylmethyl]amidocarbonylmethyl)amidocarbonylmethyl}ammoniumethyl)carbomoylmethoxy]-2,8,14,20-tetrathiacalix[4]arene tetra[bis(trifluoromethylsulfonyl)imide] (*1,3-alternate* **71**), **DMSO-d$_6$, 298 K, 100 MHz**

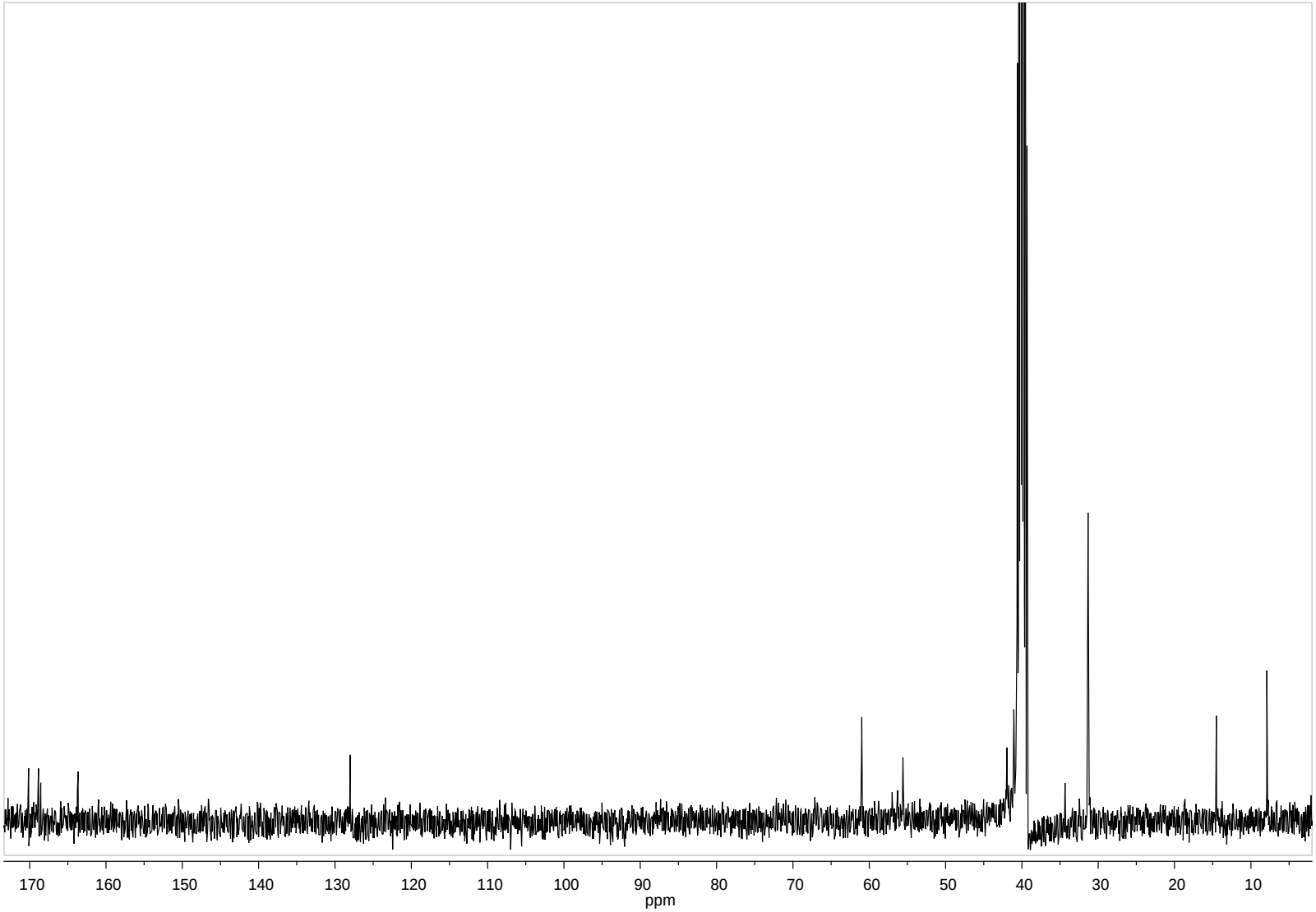

Fig. S100. ^{13}C NMR spectrum of 5,11,17,23-tetra-*tert*-butyl-25,26,27,28-tetrakis[(N-(2',2'-diethyl-2'-{(ethoxycarbonyl[S-methyl]methyl)amidocarbonylmethyl}ammoniumethyl)carbomoylmethoxy]-2,8,14,20-tetrathiacalix[4]arene tetra[bis(trifluoromethylsulfonyl)imide] (*1,3-alternate* **72**), **DMSO-d$_6$, 298 K, 100 MHz**

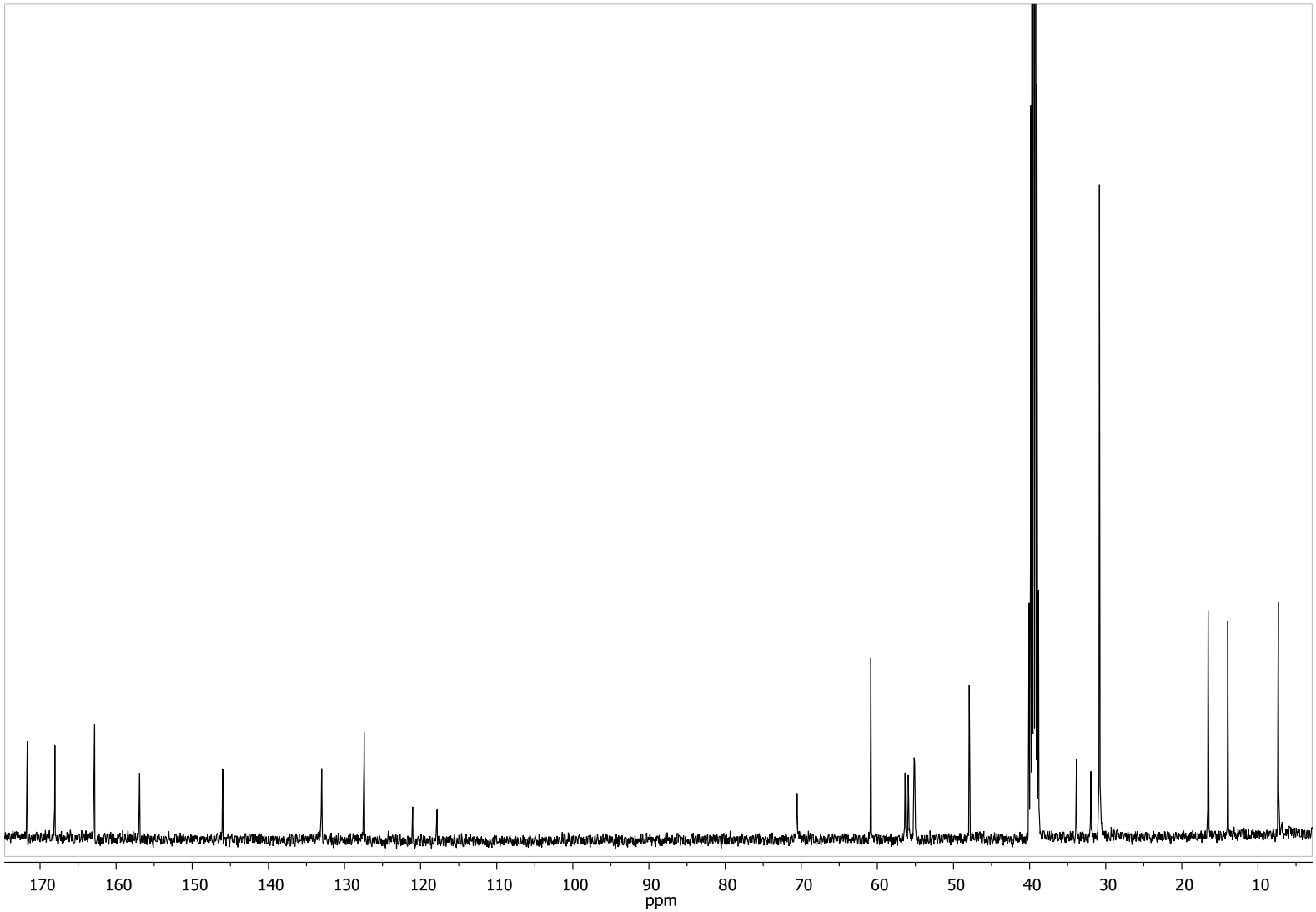

Fig. S101. Mass spectrum (ESI) of 5,11,17,23-tetra-*tert*-butyl-25,26,27,28-tetrakis[(N-(3',3'-dimethyl-3'-(pentoxycarbonylmethyl)-ammoniumpropyl)carbomoylmethoxy]-2,8,14,20-tetrathiacalix[4]arene tetrabromide (*cone* **9**)

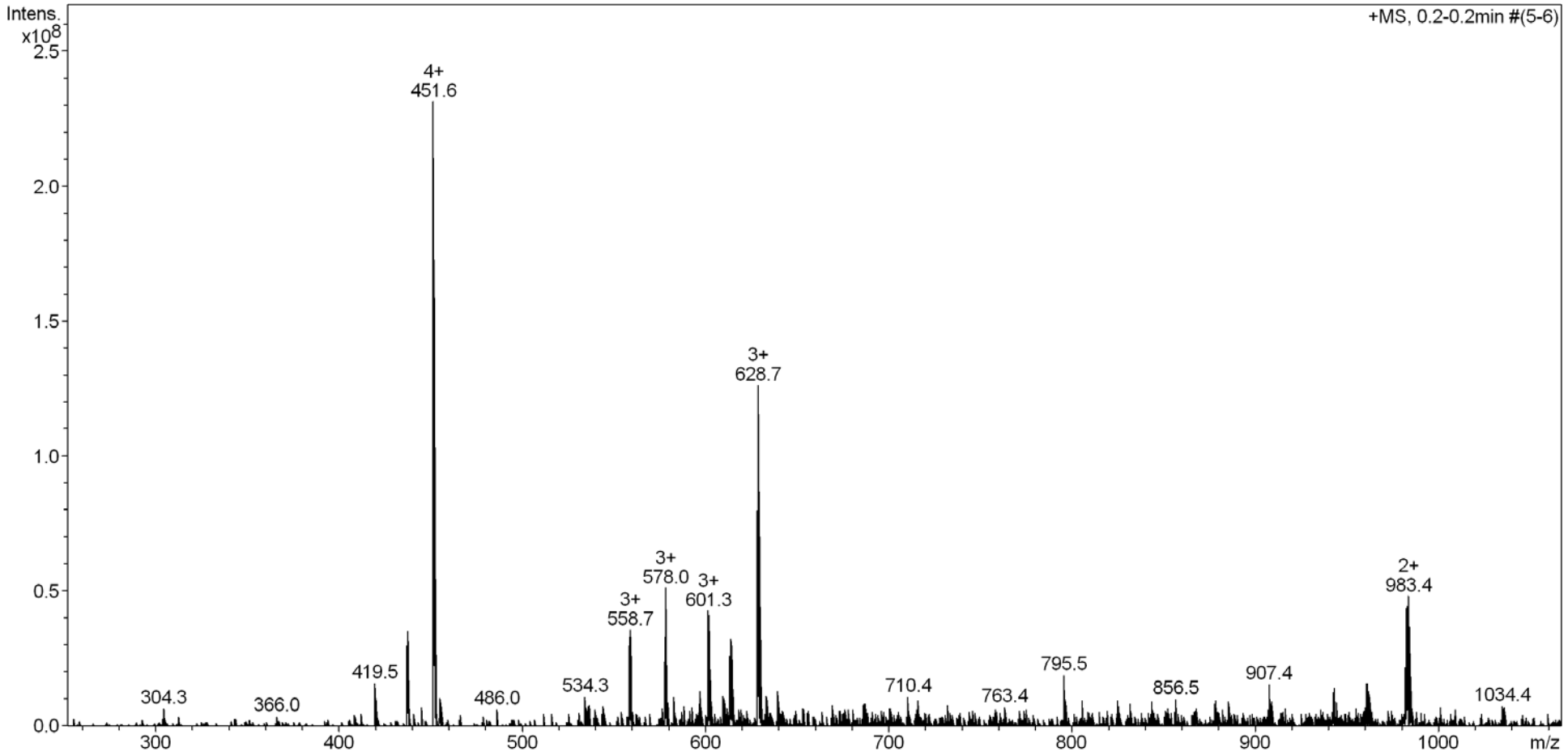

Fig. S102. Mass spectrum (ESI) of 5,11,17,23-tetra-*tert*-butyl-25,26,27,28-tetrakis[(N-(2',2',2'-triethyl)ammoniumethyl)carbomoylmethoxy]-2,8,14,20-tetrathiacalix[4]arene tetraiodide (*cone* **15**)

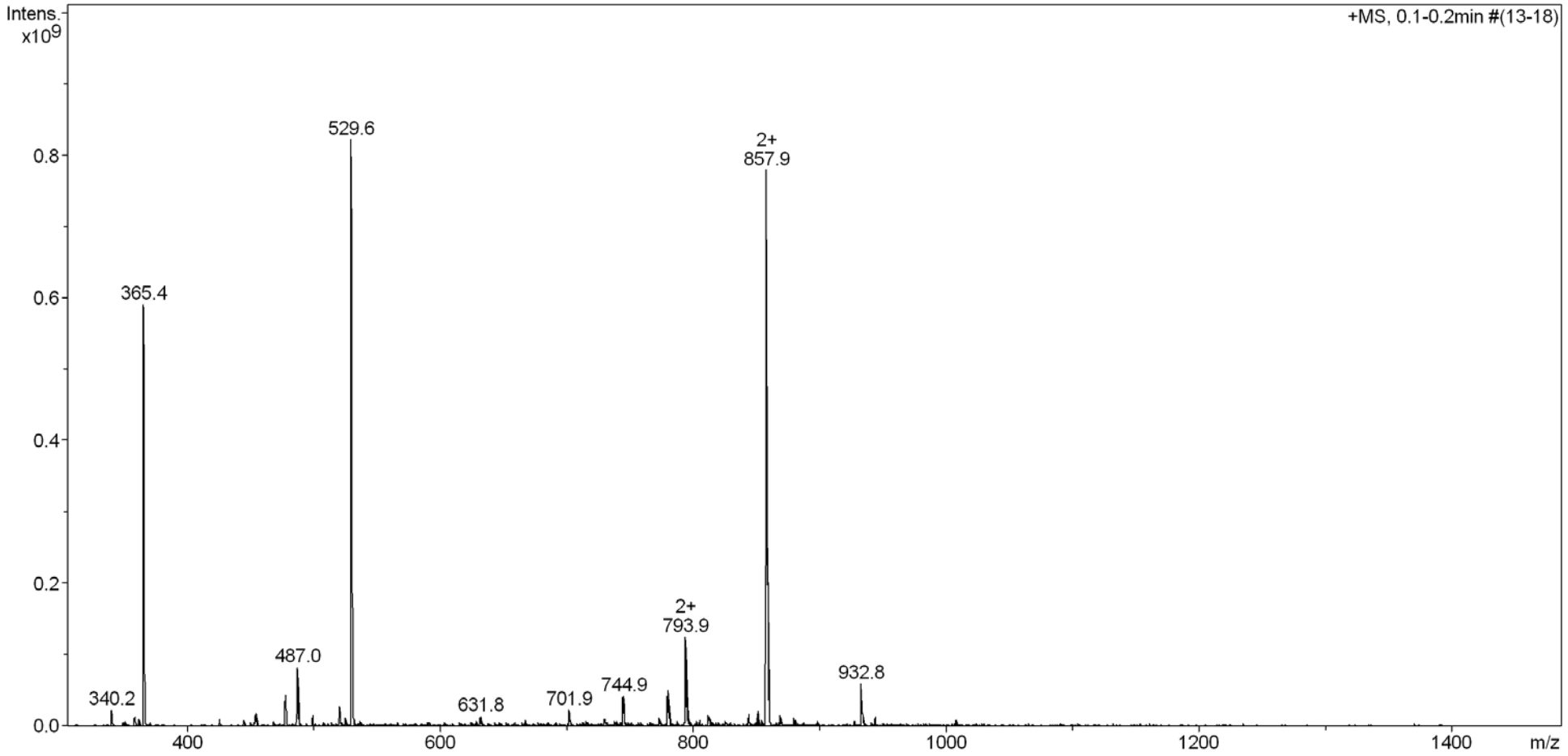

Fig. S103. Mass spectrum (ESI) of 5,11,17,23-tetra-*tert*-butyl-25,26,27,28-tetrakis[(N-(2',2'-diethyl-2'-benzyl)ammoniumethyl)carbomoylmethoxy]-2,8,14,20-tetrathiacalix[4]arene tetrabromide (*cone* **16**)

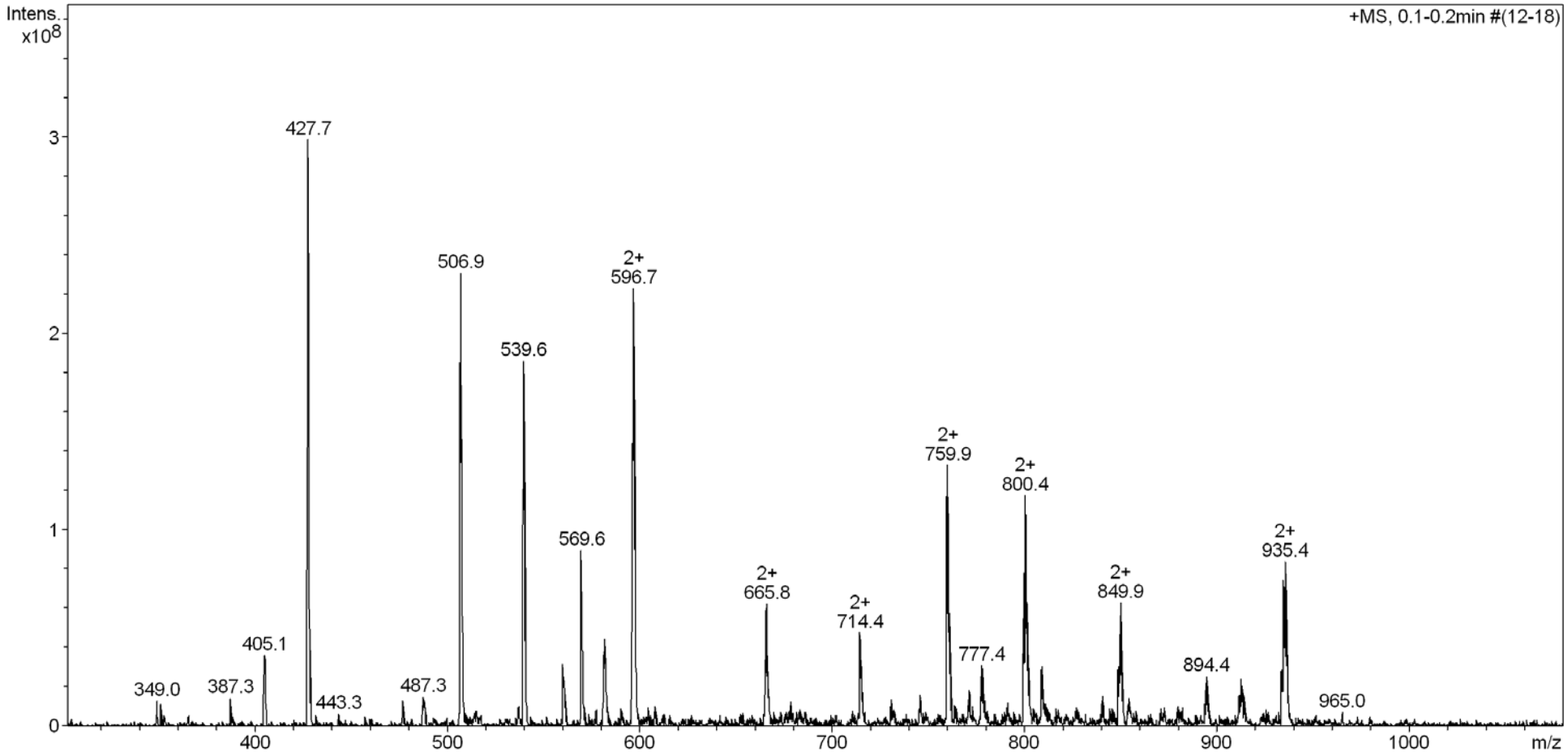

Fig. S104. Mass spectrum (ESI) of 5,11,17,23-tetra-*tert*-butyl-25,26,27,28-tetrakis[(N-(2',2'-diethyl-2'-(ethoxycarbonylmethyl)-ammoniumethyl)carbomoylmethoxy]-2,8,14,20-tetrathiacalix[4]arene tetrabromide (*cone* **17**)

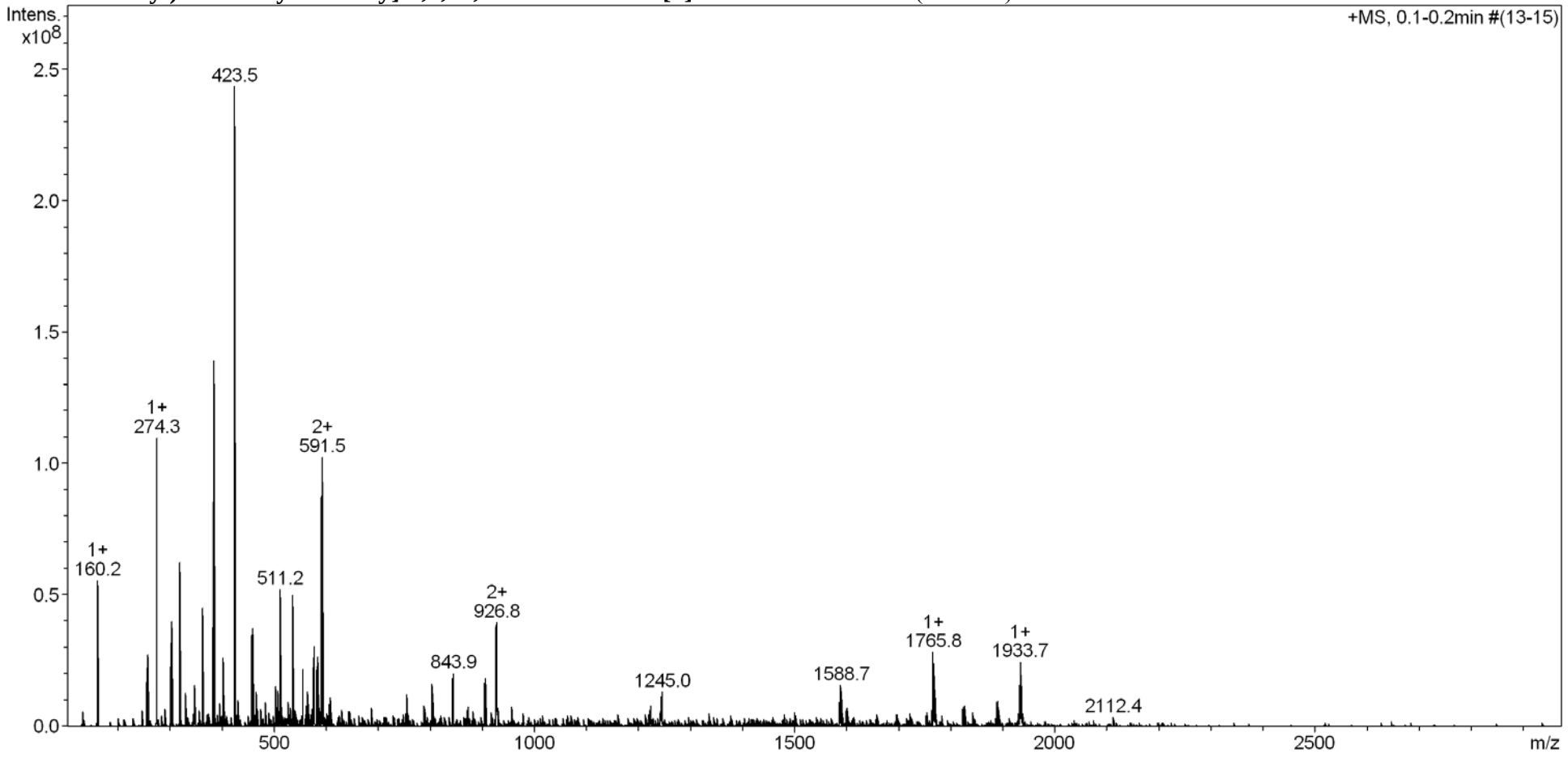

Fig. S105. Mass spectrum (ESI) of 5,11,17,23-tetra-*tert*-butyl-25,26,27,28-tetrakis[(N-(2',2'-diethyl-2'-(pentoxycarbonylmethyl)-ammoniumethyl)carbomoylmethoxy]-2,8,14,20-tetrathiacalix[4]arene tetrabromide (*cone* **18**)

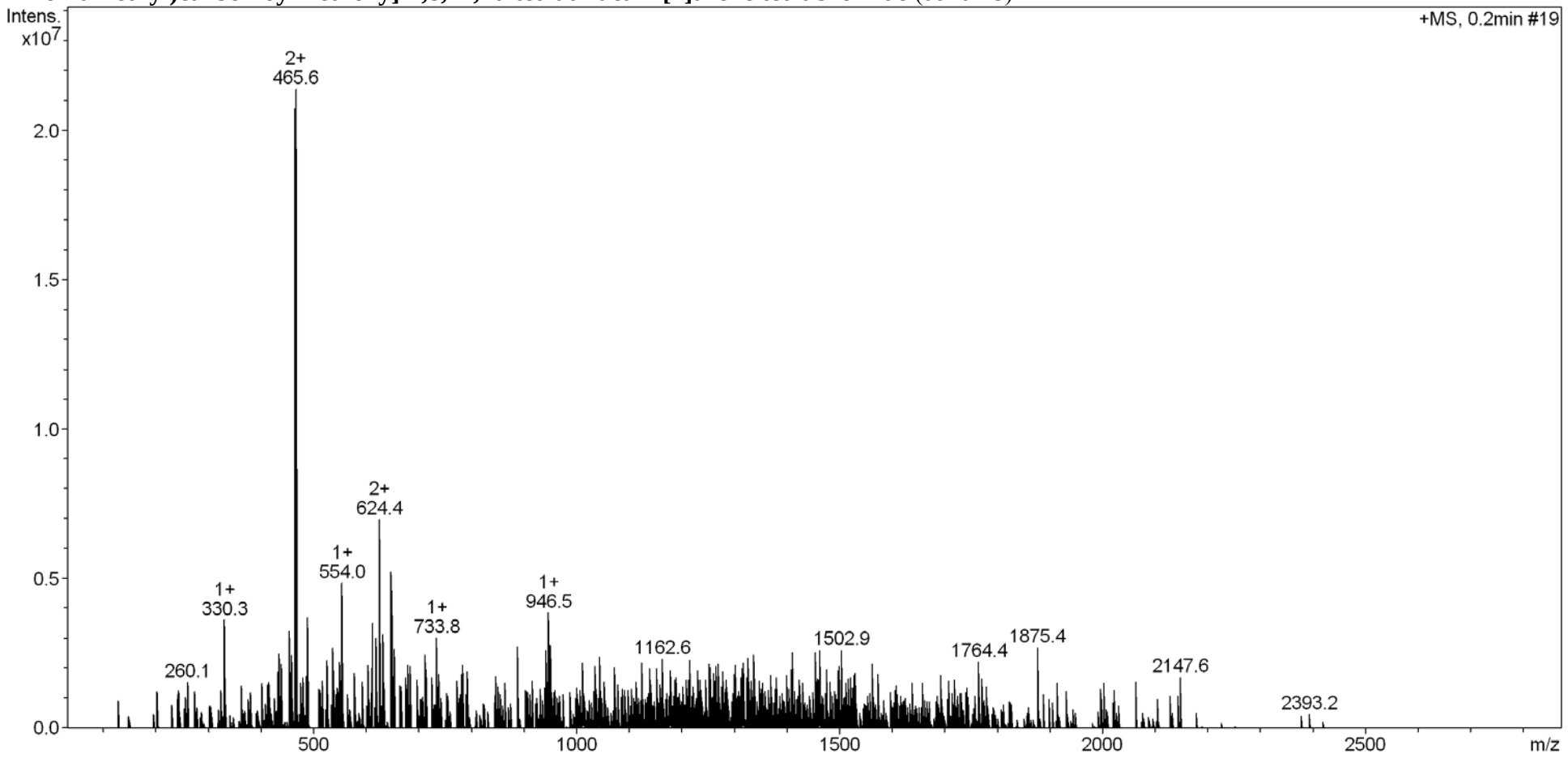

Fig. S106. Mass spectrum (MALDI-TOF, 4-nitroaniline matrix) of 5,11,17,23-tetra-*tert*-butyl-25,26,27,28-tetrakis[(N-(3',3',3'-trimethyl)ammoniumpropyl)carbomoylmethoxy]-2,8,14,20-tetrathiacalix[4]arene tetraiodide (*1,3-alternate* **22**)

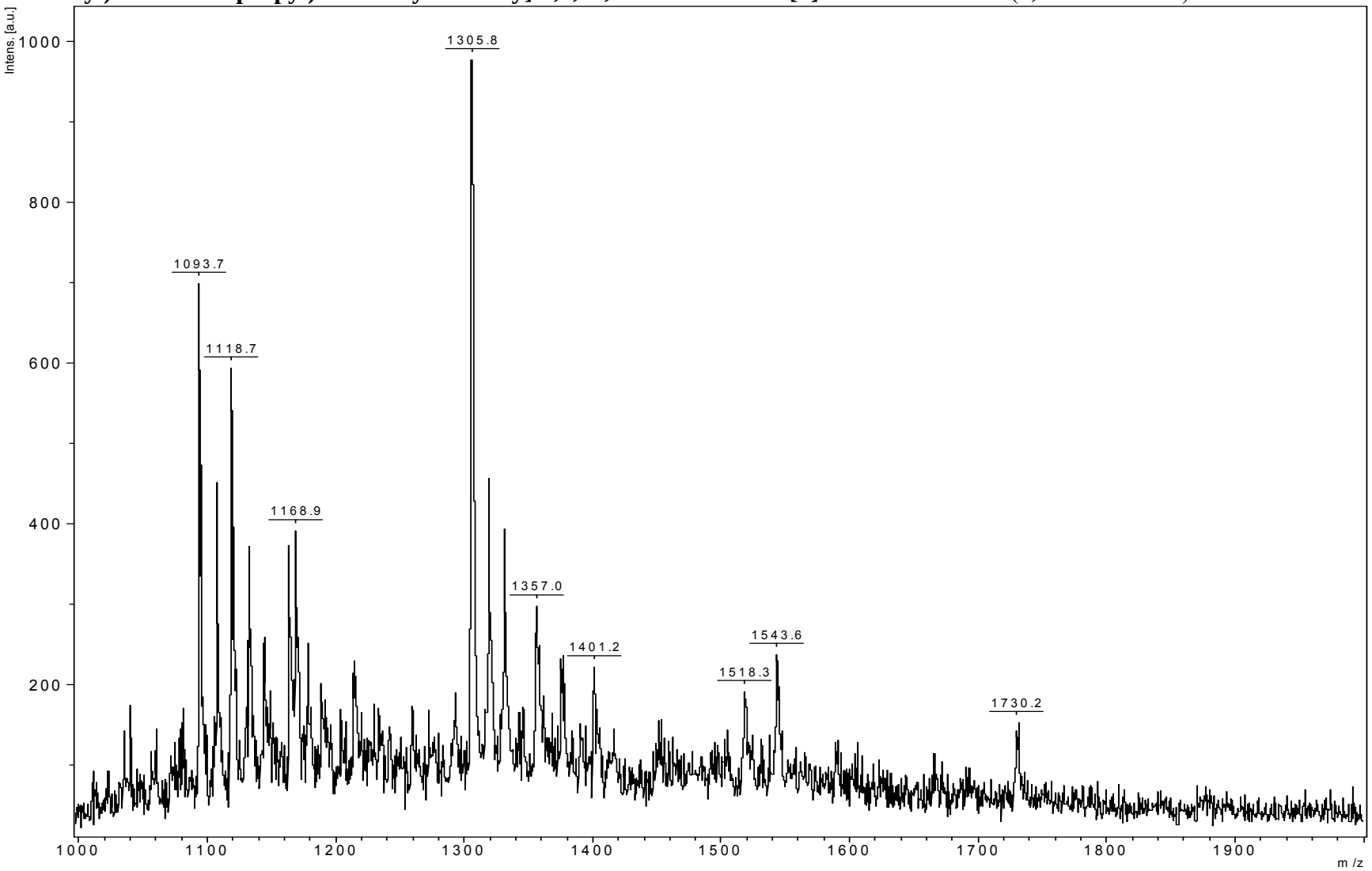

Fig. S107. Mass spectrum (MALDI-TOF, 4-nitroaniline matrix) of 5,11,17,23-tetra-*tert*-butyl-25,26,27,28-tetrakis[(N-(3',3'-dimethyl-3'-ethyl)ammoniumpropyl)carbomoylmethoxy]-2,8,14,20-tetrathiacalix[4]arene tetraiodide (*1,3-alternate* **23**)

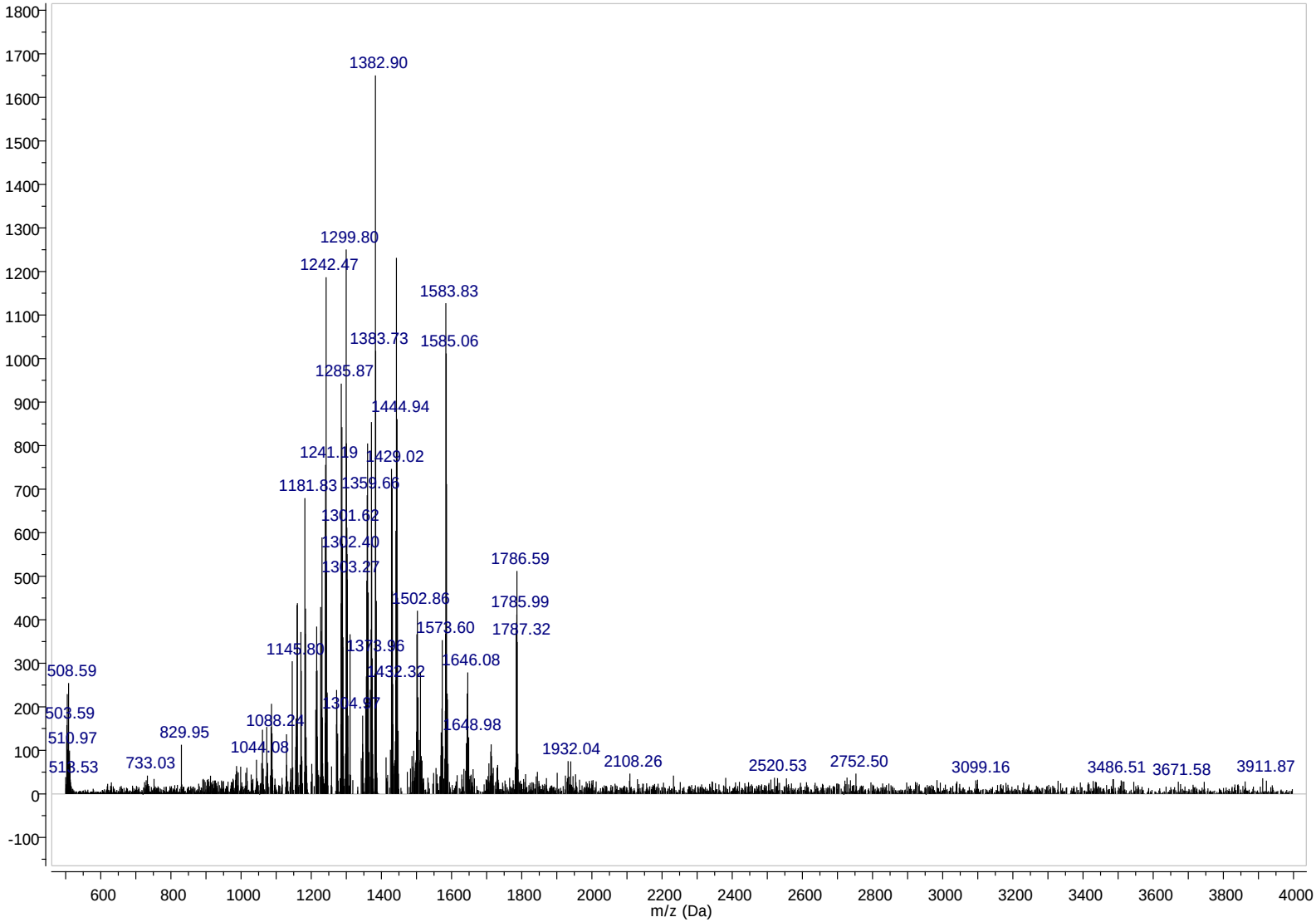

Fig. S108. Mass spectrum (MALDI-TOF, 4-nitroaniline matrix) of 5,11,17,23-tetra-*tert*-butyl-25,26,27,28-tetrakis[(N-(3',3'-dimethyl-3'-benzyl)ammoniumpropyl)carbomoylmethoxy]-2,8,14,20-tetrathiacalix[4]arene tetrabromide (*1,3-alternate* **24**)

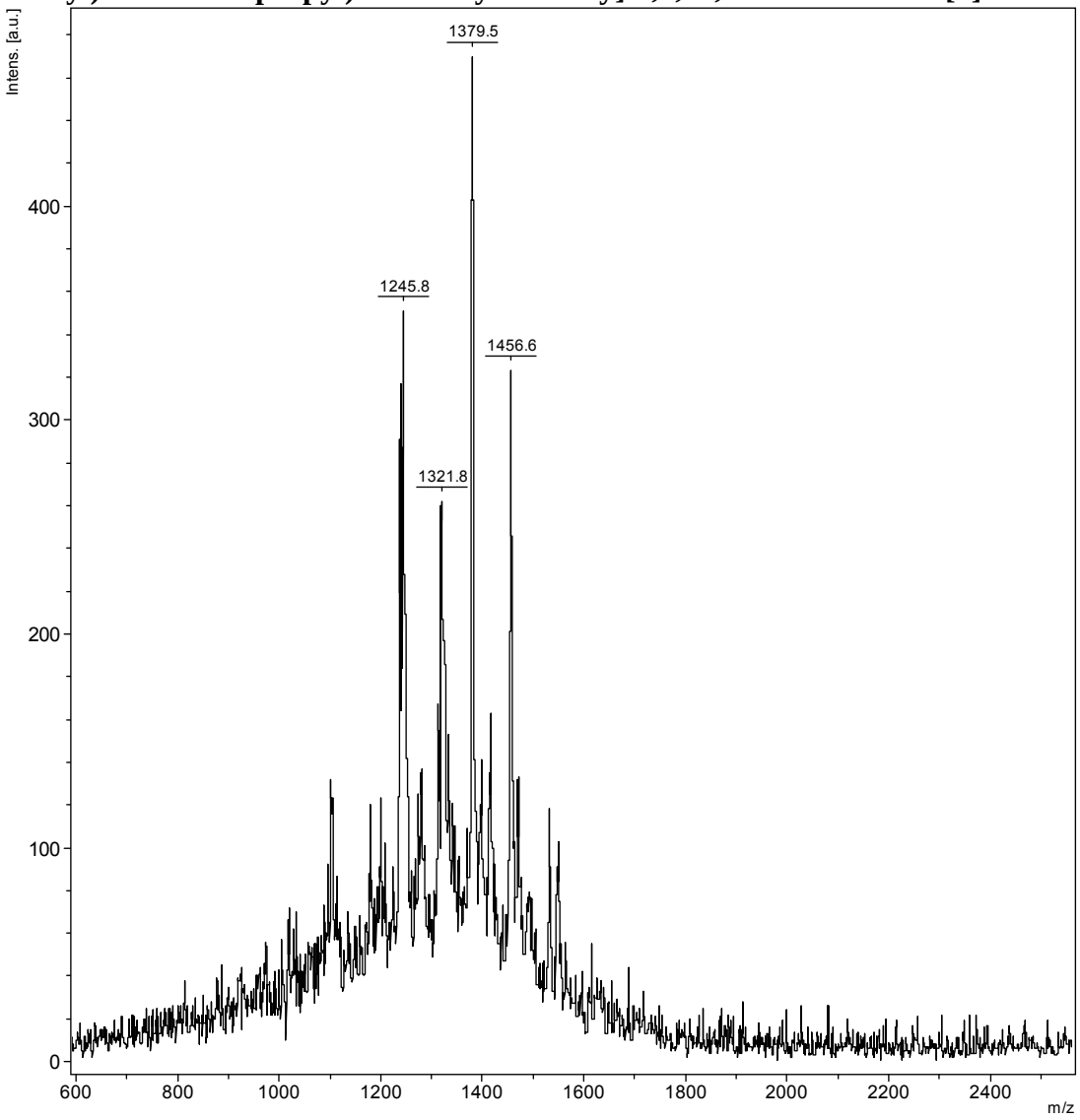

Fig. S109. Mass spectrum (ESI) of 5,11,17,23-tetra-*tert*-butyl-25,26,27,28-tetrakis[(N-(3',3'-dimethyl-3'-(ethoxycarbonylmethyl)-ammoniumpropyl)carbomoylmethoxy]-2,8,14,20-tetrathiacalix[4]arene tetrabromide (*1,3-alternate* **25**)

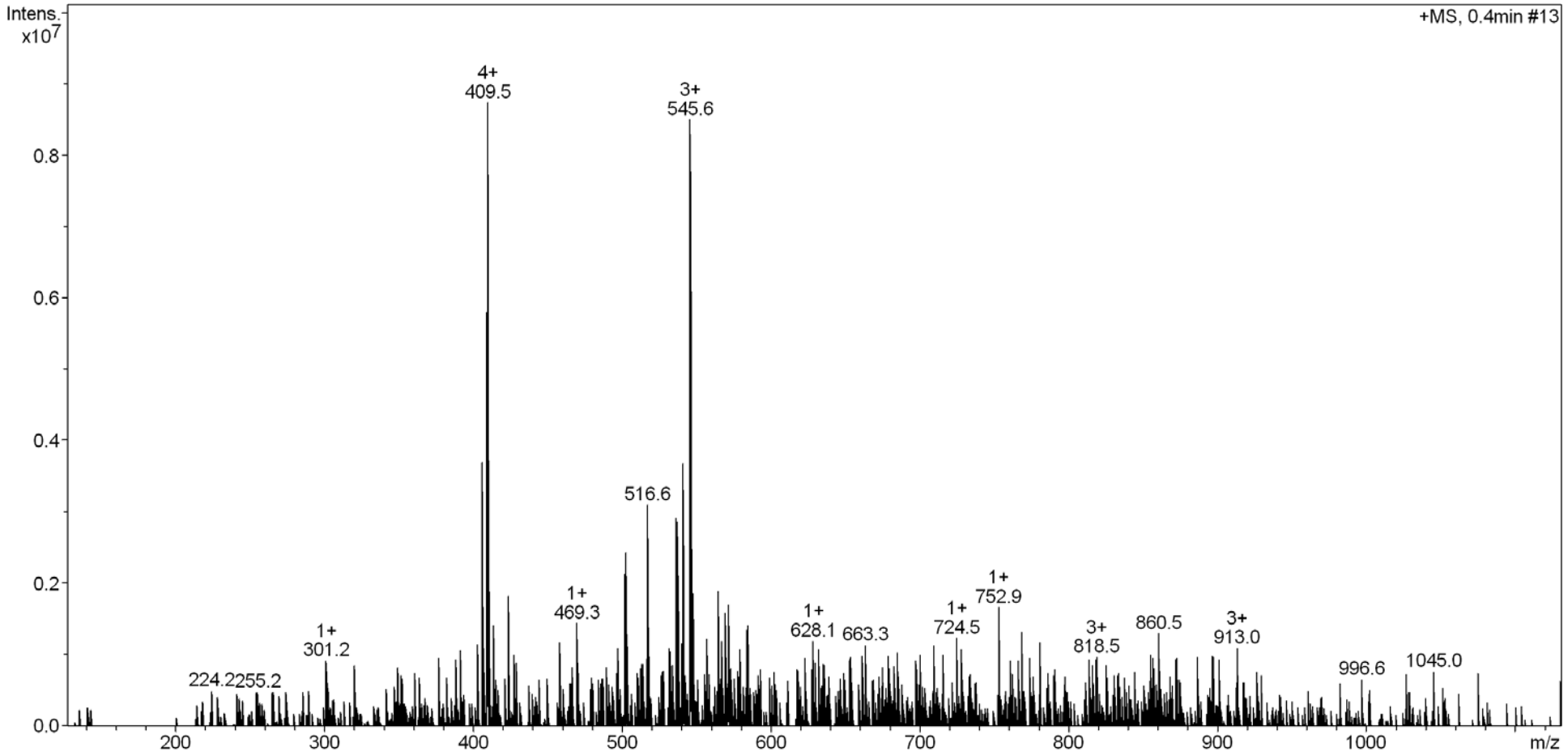

Fig. S110. Mass spectrum (ESI) of 5,11,17,23-tetra-*tert*-butyl-25,26,27,28-tetrakis[(N-(3',3'-dimethyl-3'-(pentoxycarbonylmethyl)-ammoniumpropyl)carbomoylmethoxy]-2,8,14,20-tetrathiacalix[4]arene tetrabromide (*1,3-alternate* **26**)

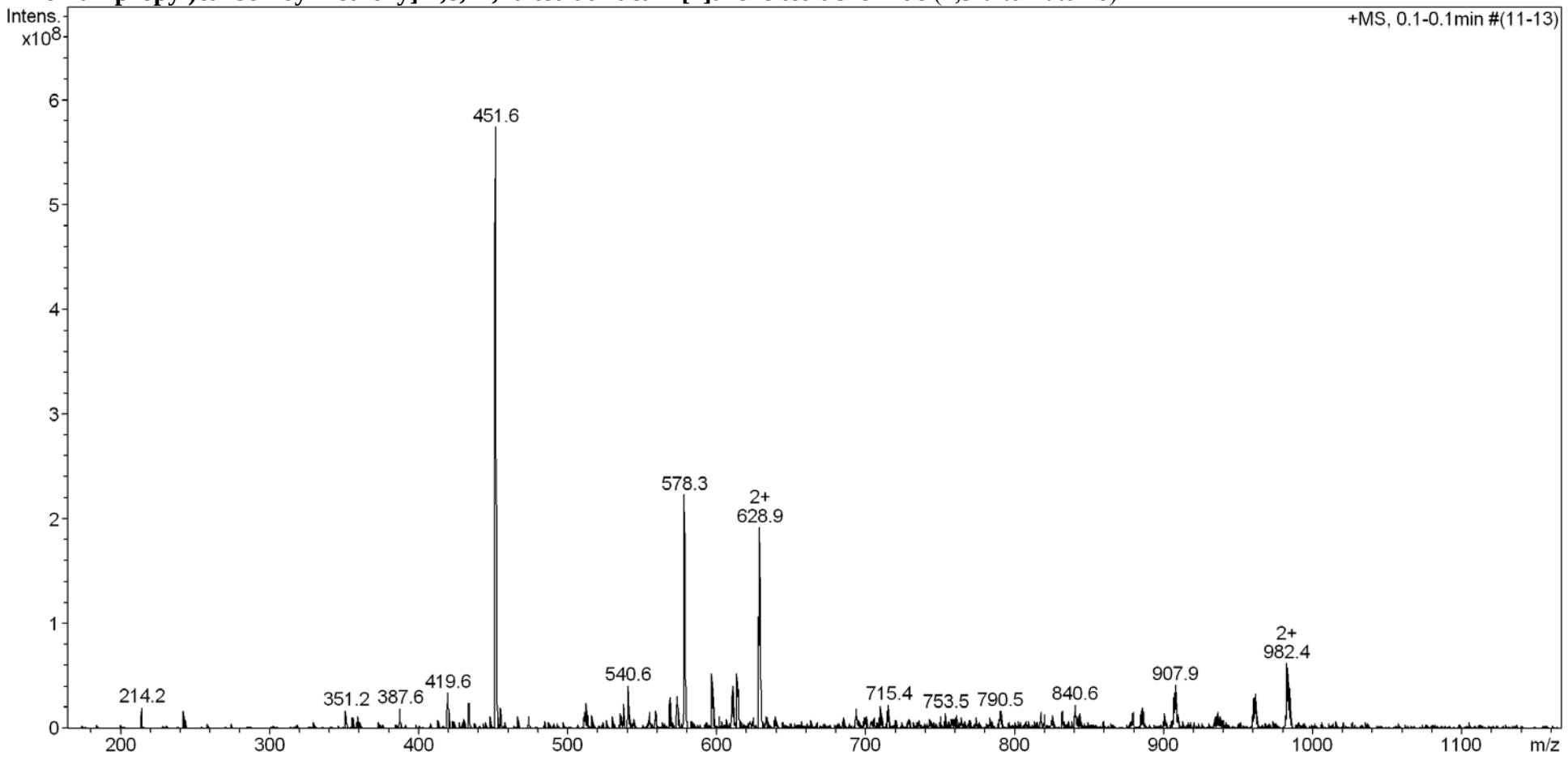

Fig. S111. Mass spectrum (ESI) of 5,11,17,23-tetra-*tert*-butyl-25,26,27,28-tetrakis[(N-(3',3'-dimethyl-3'-{3''-propylphtalimide}-ammoniumpropyl)carbomoylmethoxy]-2,8,14,20-tetrathiacalix[4]arene tetrabromide (*1,3-alternate* **30**)

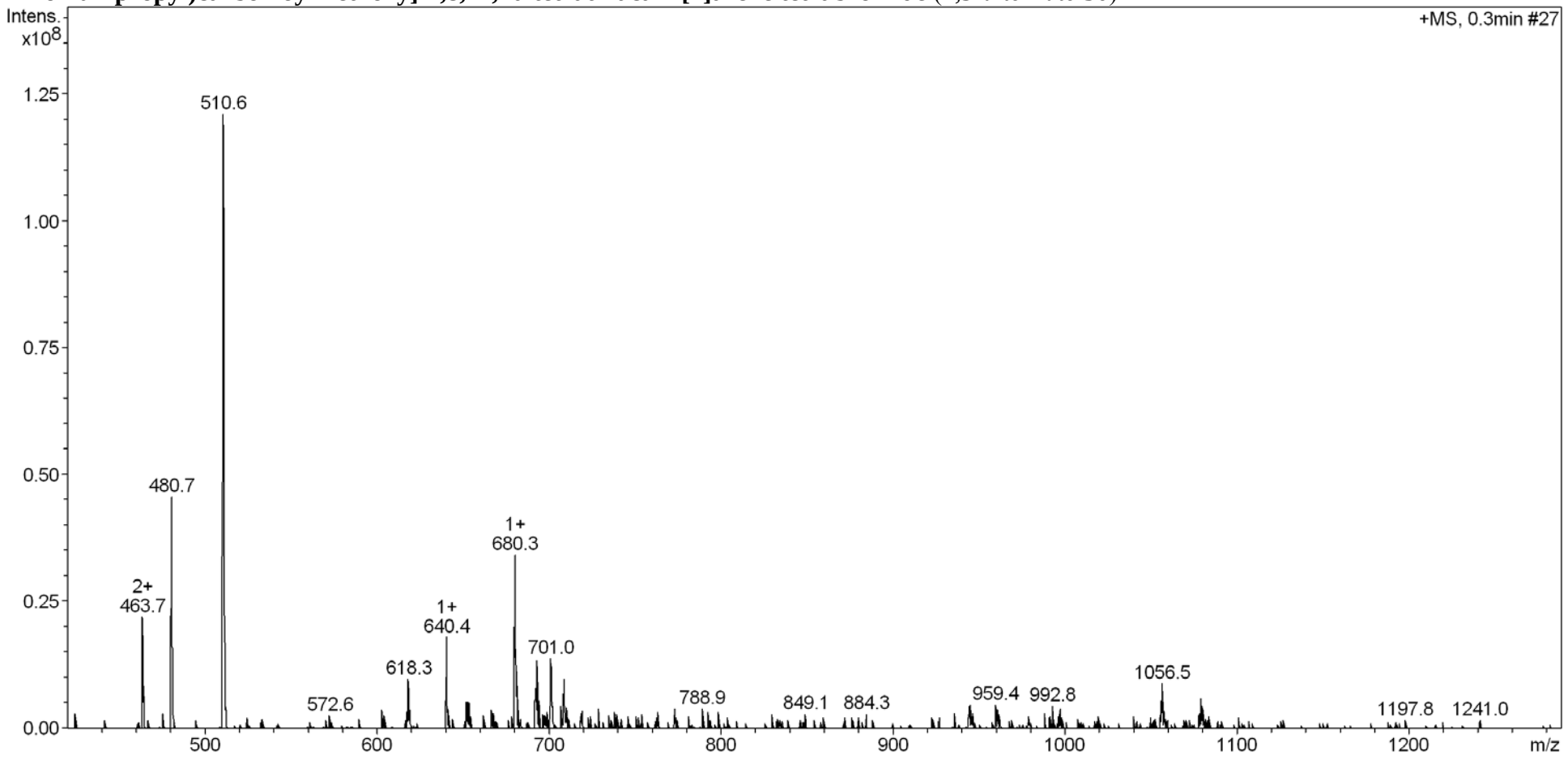

Fig. S112. Mass spectrum (ESI) of 5,11,17,23-tetra-*tert*-butyl-25,26,27,28-tetrakis[(N-(2'-methyl-2',2'-diethyl)ammoniumethyl)carbomoylmethoxy]-2,8,14,20-tetrathiacalix[4]arene tetraiodide (*1,3-alternate* **31**)

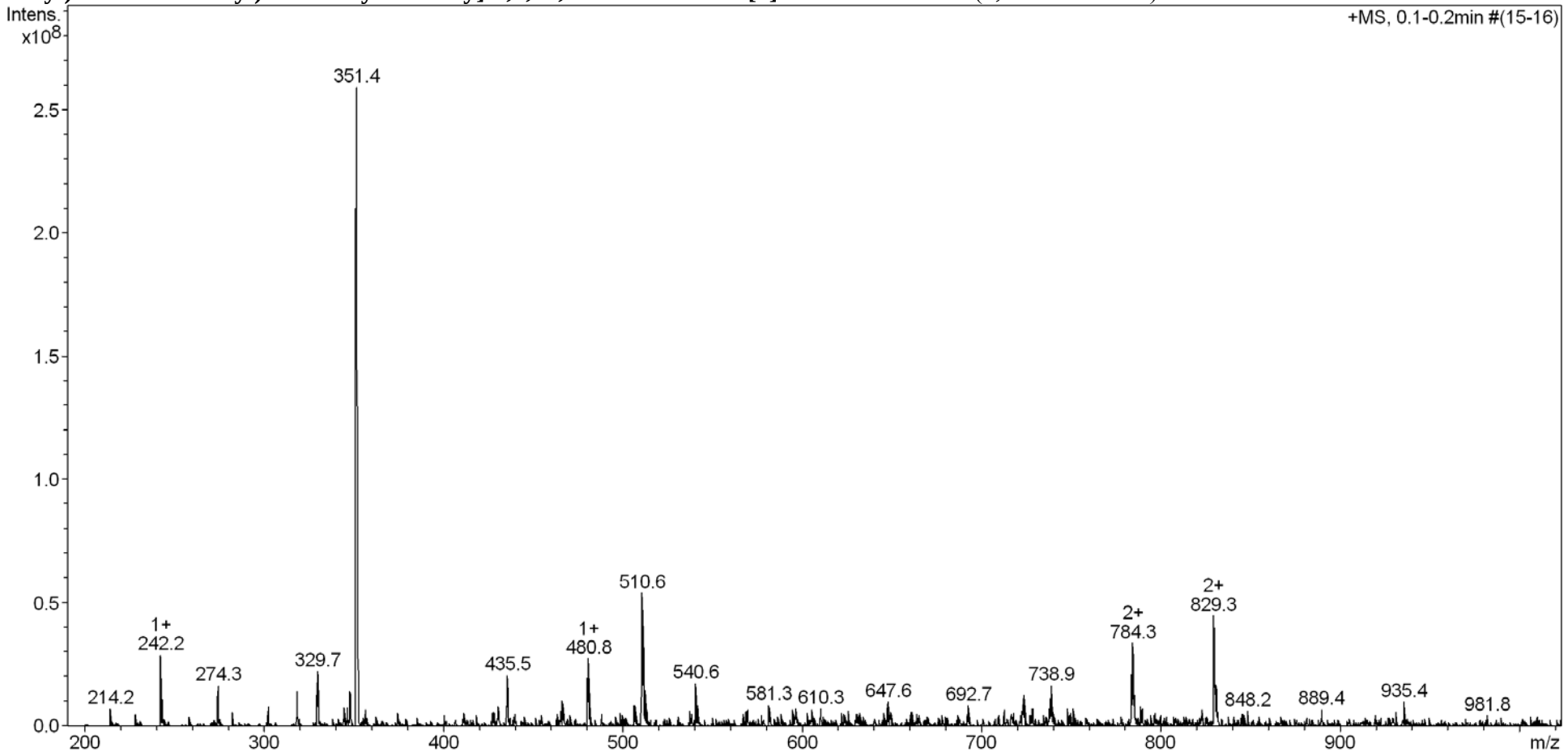

Fig. S113. Mass spectrum (ESI) of 5,11,17,23-tetra-*tert*-butyl-25,26,27,28-tetrakis[(N-(2',2',2'-triethyl)ammoniumethyl)carbomoylmethoxy]-2,8,14,20-tetrathiacalix[4]arene tetraiodide (*1,3-alternate* **32**)

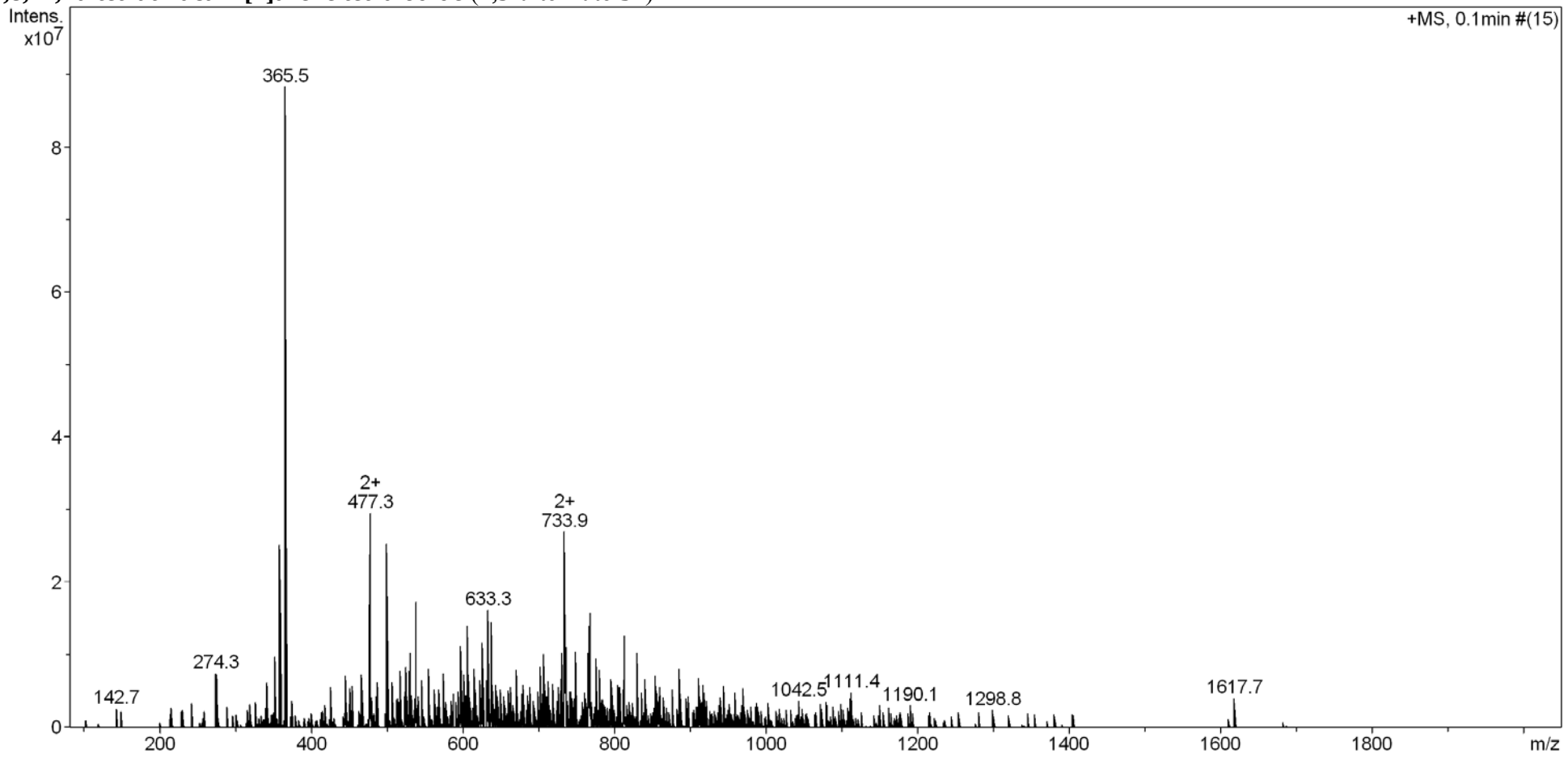

Fig. S114. Mass spectrum (ESI) of 5,11,17,23-tetra-*tert*-butyl-25,26,27,28-tetrakis[(N-(2',2'-diethyl-2'-(benzyl)ammoniumpropyl)carbomoylmethoxy]-2,8,14,20-tetrathiacalix[4]arene tetrabromide (*1,3-alternate* **33**)

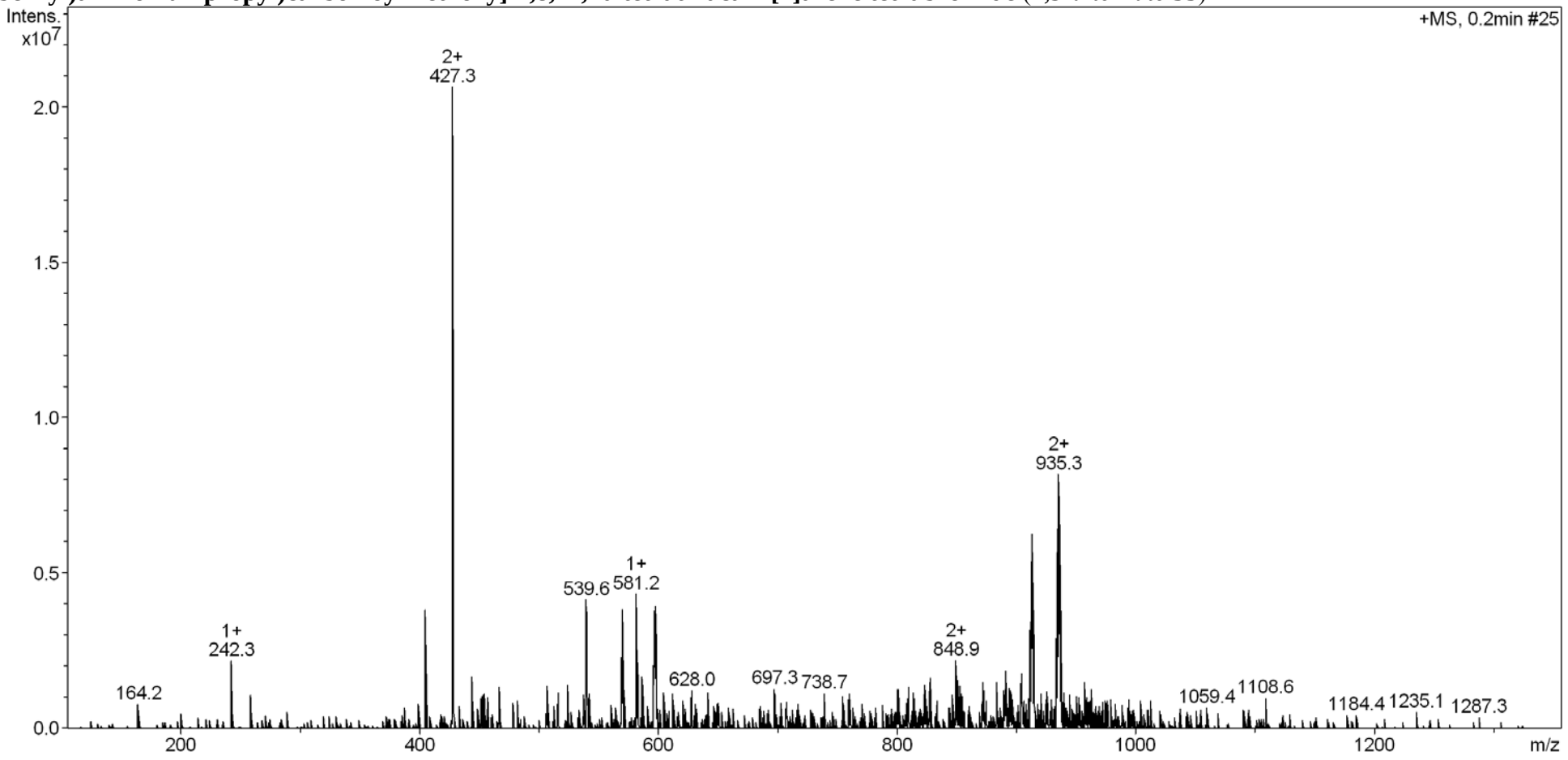

Fig. S115. Mass spectrum (ESI) of 5,11,17,23-tetra-*tert*-butyl-25,26,27,28-tetrakis[(N-(2',2'-diethyl-2'-(ethoxycarbonylmethyl)-ammoniumethyl)carbomoylmethoxy]-2,8,14,20-tetrathiacalix[4]arene tetrabromide (*1,3-alternate* **34**)

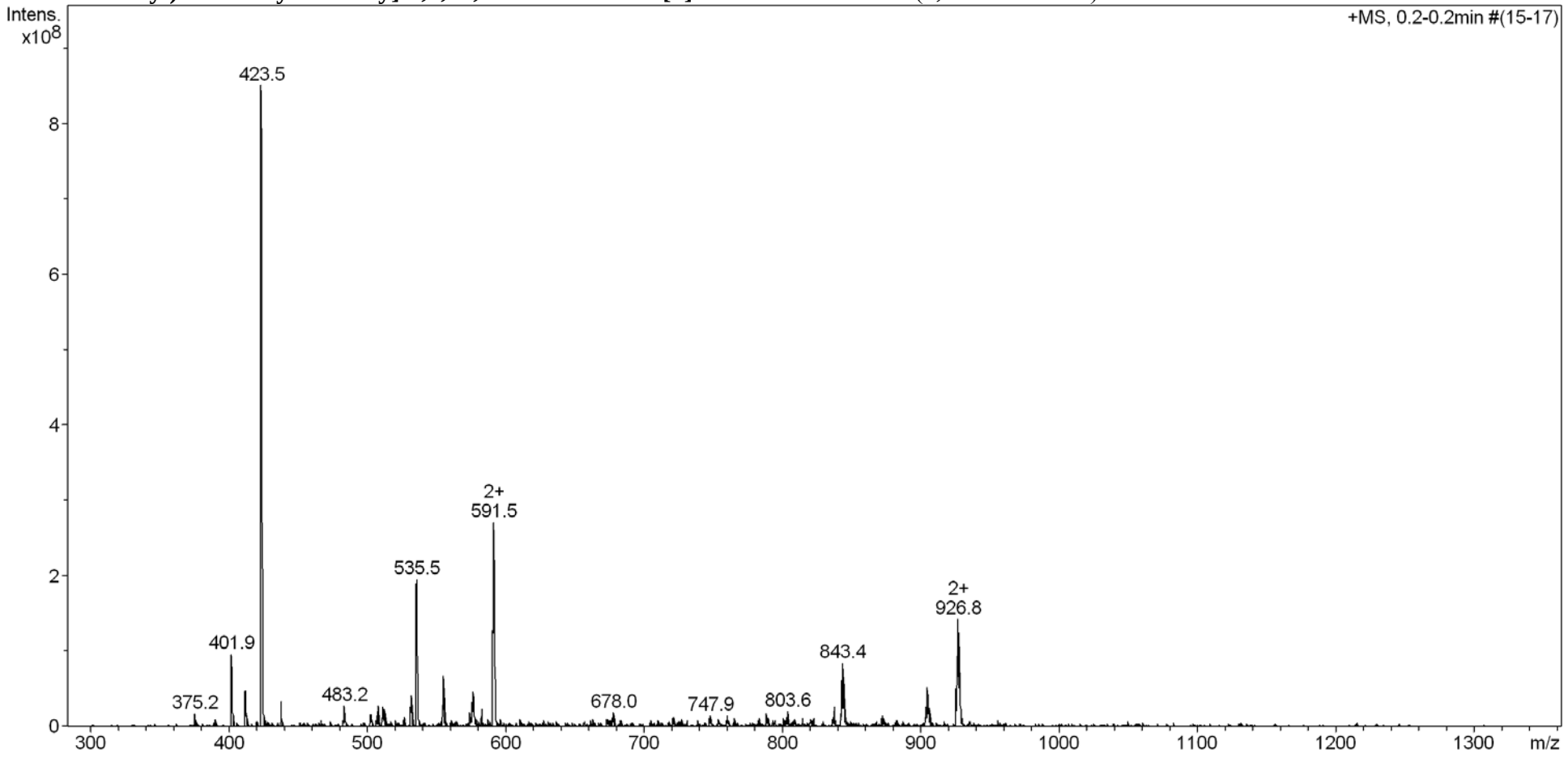

Fig. S116. Mass spectrum (ESI) of 5,11,17,23-tetra-*tert*-butyl-25,26,27,28-tetrakis[(N-(2',2'-diethyl-2'-(pentoxycarbonylmethyl)-ammoniumethyl)carbomoylmethoxy]-2,8,14,20-tetrathiacalix[4]arene tetrabromide (*1,3-alternate* **35**)

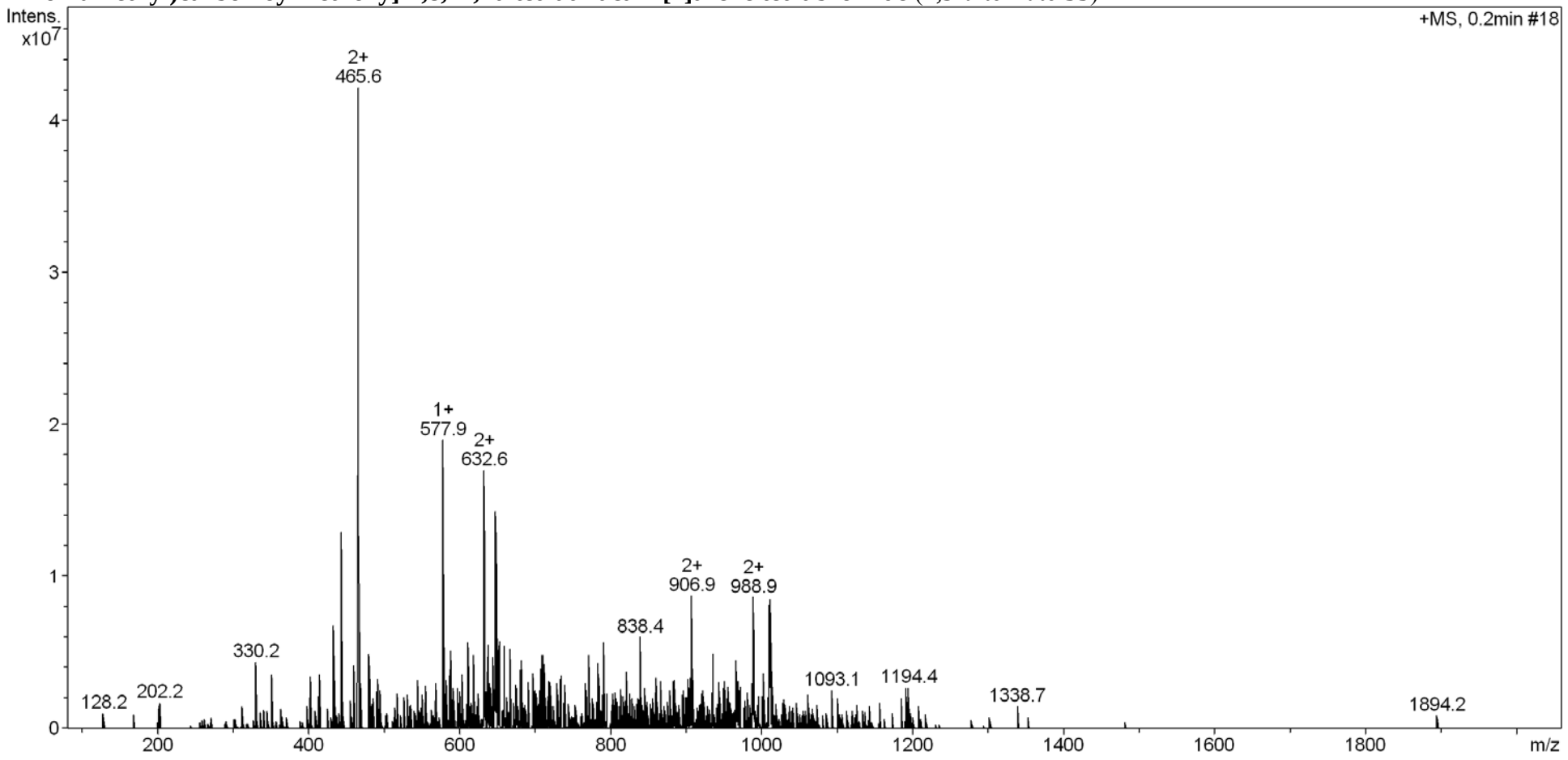

Fig. S117. Mass spectrum (MALDI-TOF, 4-nitroaniline matrix) of 5,11,17,23-tetra-*tert*-butyl-25,26,27,28-tetrakis[(N-(3',3',3'-trimethyl)ammoniumpropyl)carbomoylmethoxy]-2,8,14,20-tetrathiacalix[4]arene tetra[bis(trifluoromethylsulfonyl)imide] (*cone* **39**)

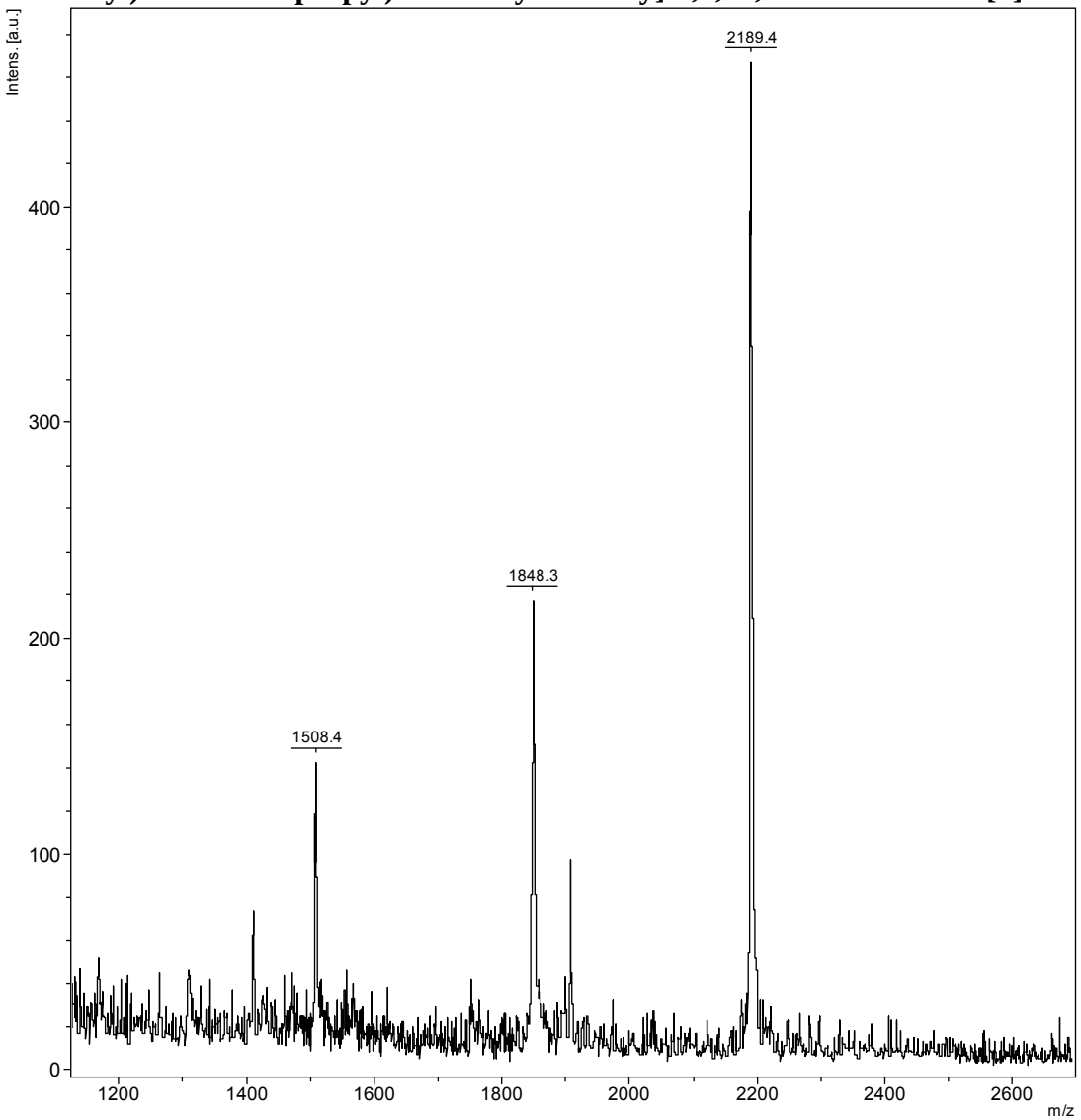

Fig. S118. Mass spectrum (MALDI-TOF, 4-nitroaniline matrix) of 5,11,17,23-tetra-*tert*-butyl-25,26,27,28-tetrakis[(N-(3',3'-dimethyl-3'-ethyl)ammoniumpropyl)carbomoylmethoxy]-2,8,14,20-tetrathiacalix[4]arene tetra[bis(trifluoromethylsulfonyl)imide] (*cone* **40**)

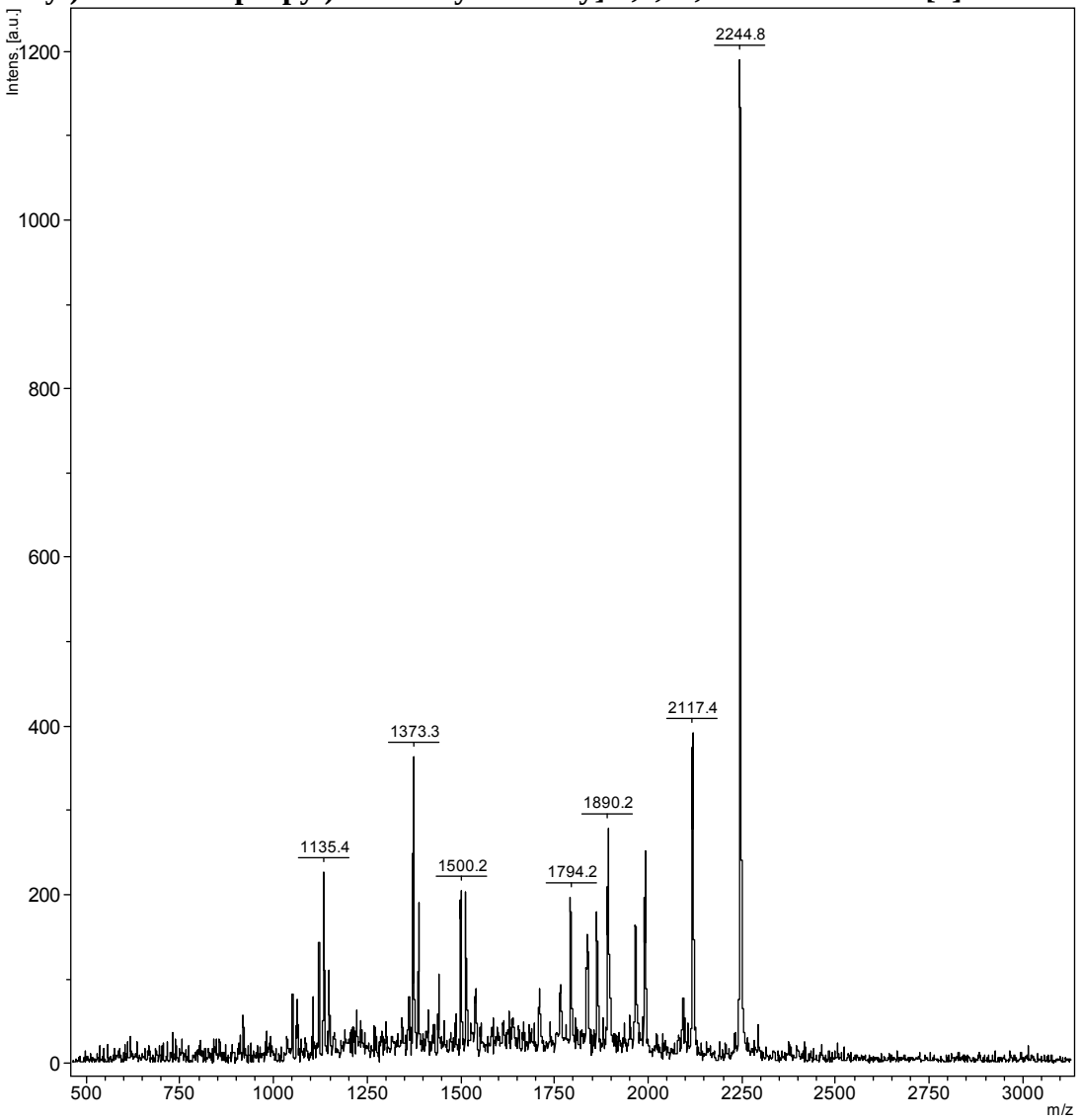

Fig. S119. Mass spectrum (MALDI-TOF, 4-nitroaniline matrix) of 5,11,17,23-tetra-*tert*-butyl-25,26,27,28-tetrakis[(N-(3',3'-dimethyl-3'-benzyl)ammoniumpropyl)carbomoylmethoxy]-2,8,14,20-tetrathiacalix[4]arene tetra[bis(trifluoromethylsulfonyl)imide] (*cone* **41**)

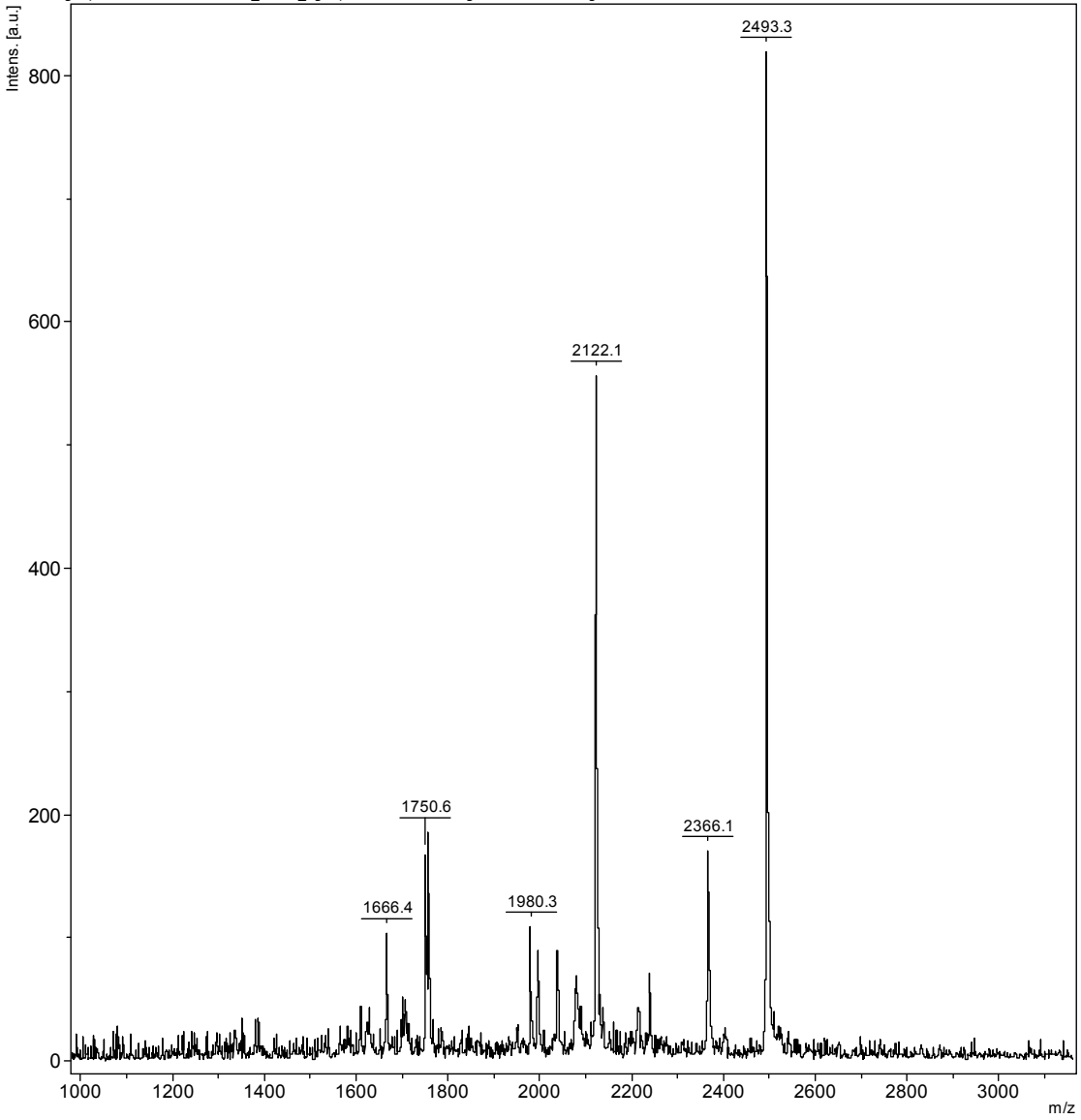

Fig. S120. Mass spectrum (MALDI-TOF, 4-nitroaniline matrix) of 5,11,17,23-tetra-*tert*-butyl-25,26,27,28-tetrakis[(N-(3',3'-dimethyl-3'-(ethoxycarbonylmethyl)ammoniumpropyl)-carbomoylmethoxy]-2,8,14,20-tetrathiacalix[4]arene tetra[bis(trifluoromethylsulfonyl)imide] (*cone* **42**)

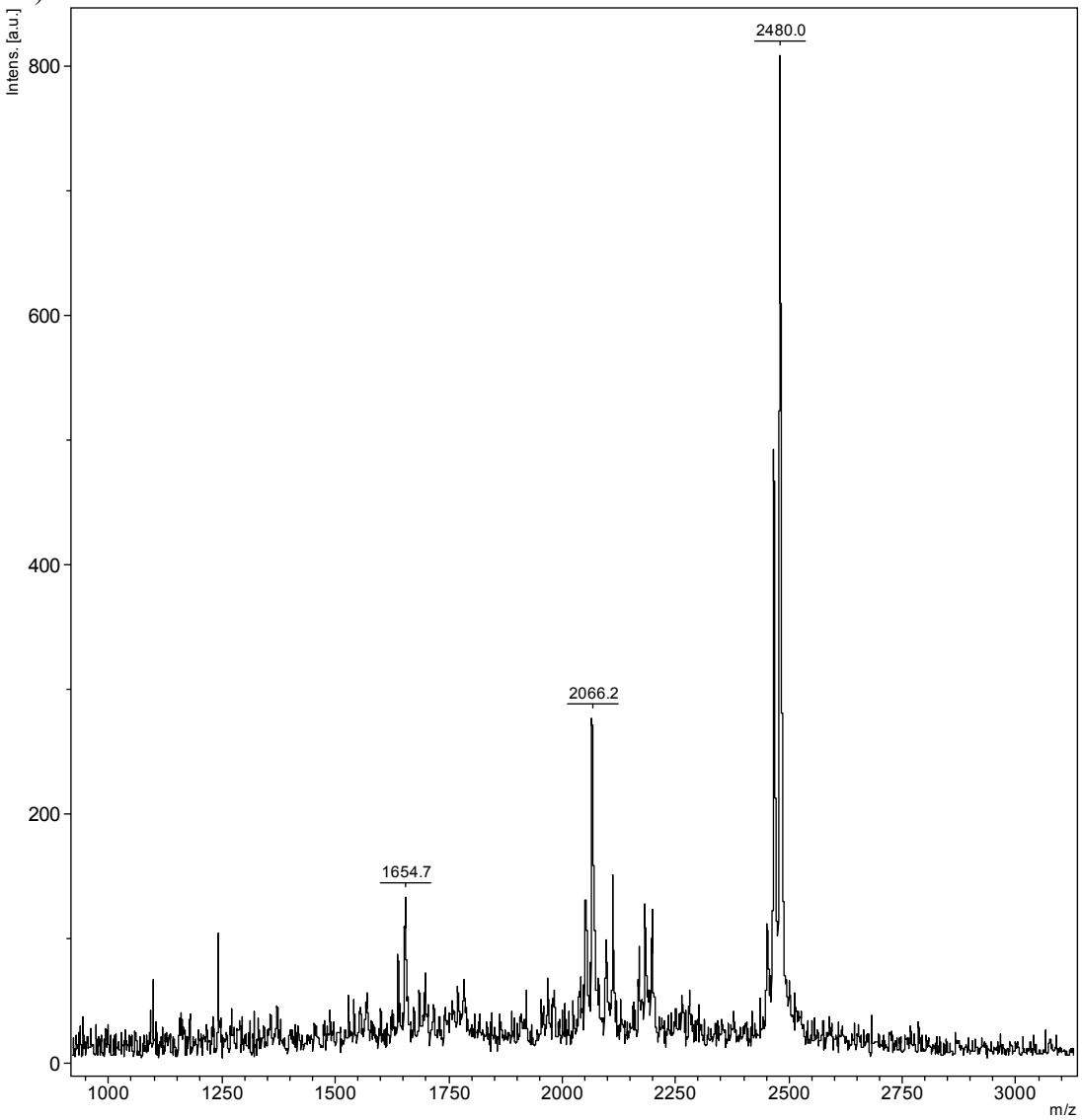

Fig. S121. Mass spectrum (ESI) of 5,11,17,23-tetra-*tert*-butyl-25,26,27,28-tetrakis[(N-(3',3'-dimethyl-3'-(pentoxycarbonylmethyl)-ammoniumpropyl)carbomoylmethoxy]-2,8,14,20-tetrathiacalix[4]arene tetra[bis(trifluoromethylsulfonyl)imide] (*cone* **43**)

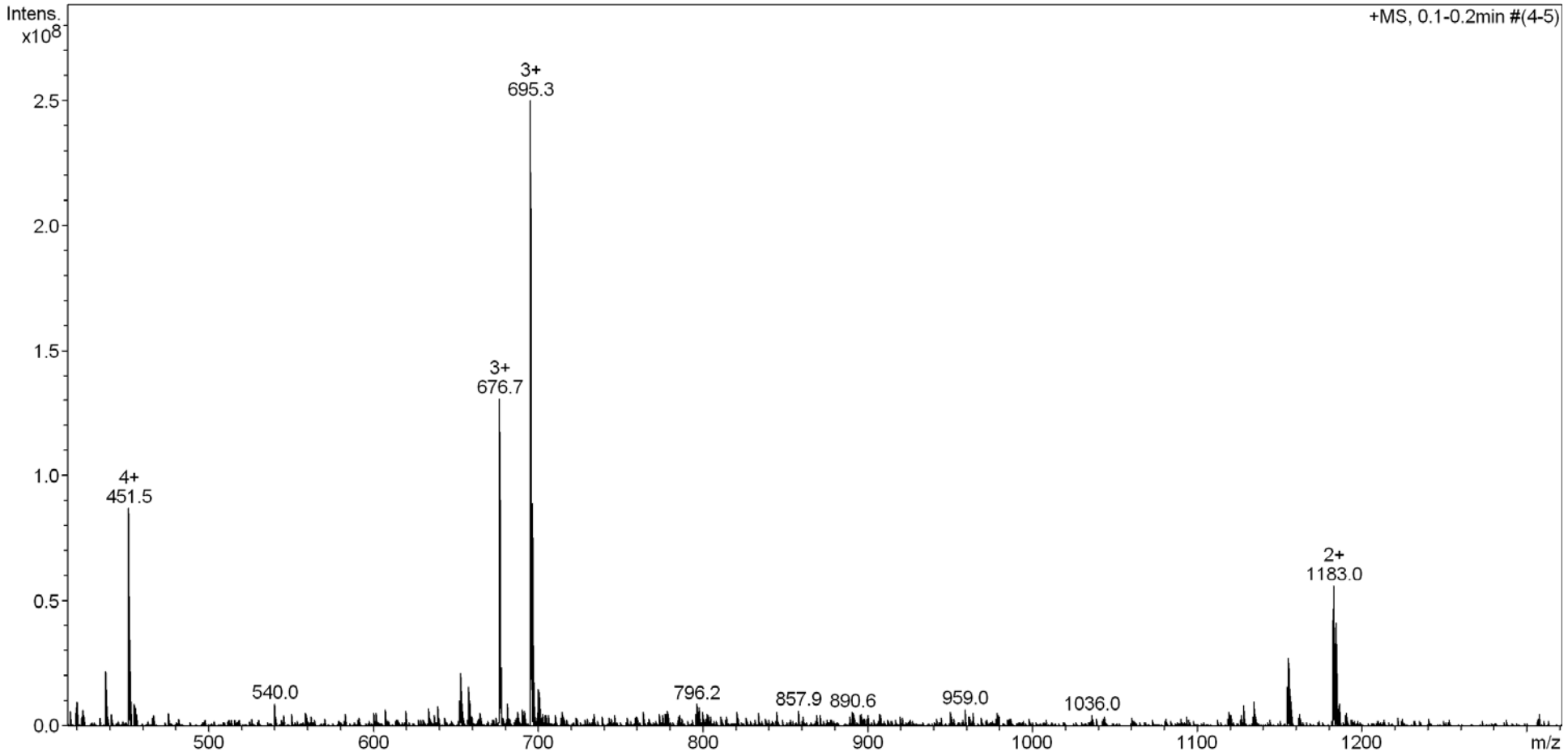

Fig. S122. Mass spectrum (ESI) of 5,11,17,23-tetra-*tert*-butyl-25,26,27,28-tetrakis[(N-(3',3'-dimethyl-3'-{(ethoxycarbonylmethyl)amidocarbonylmethyl}ammoniumpropyl)carbomoylmethoxy]-2,8,14,20-tetrathiacalix[4]arene tetra[bis(trifluoromethylsulfonyl)imide] (*cone* 44)

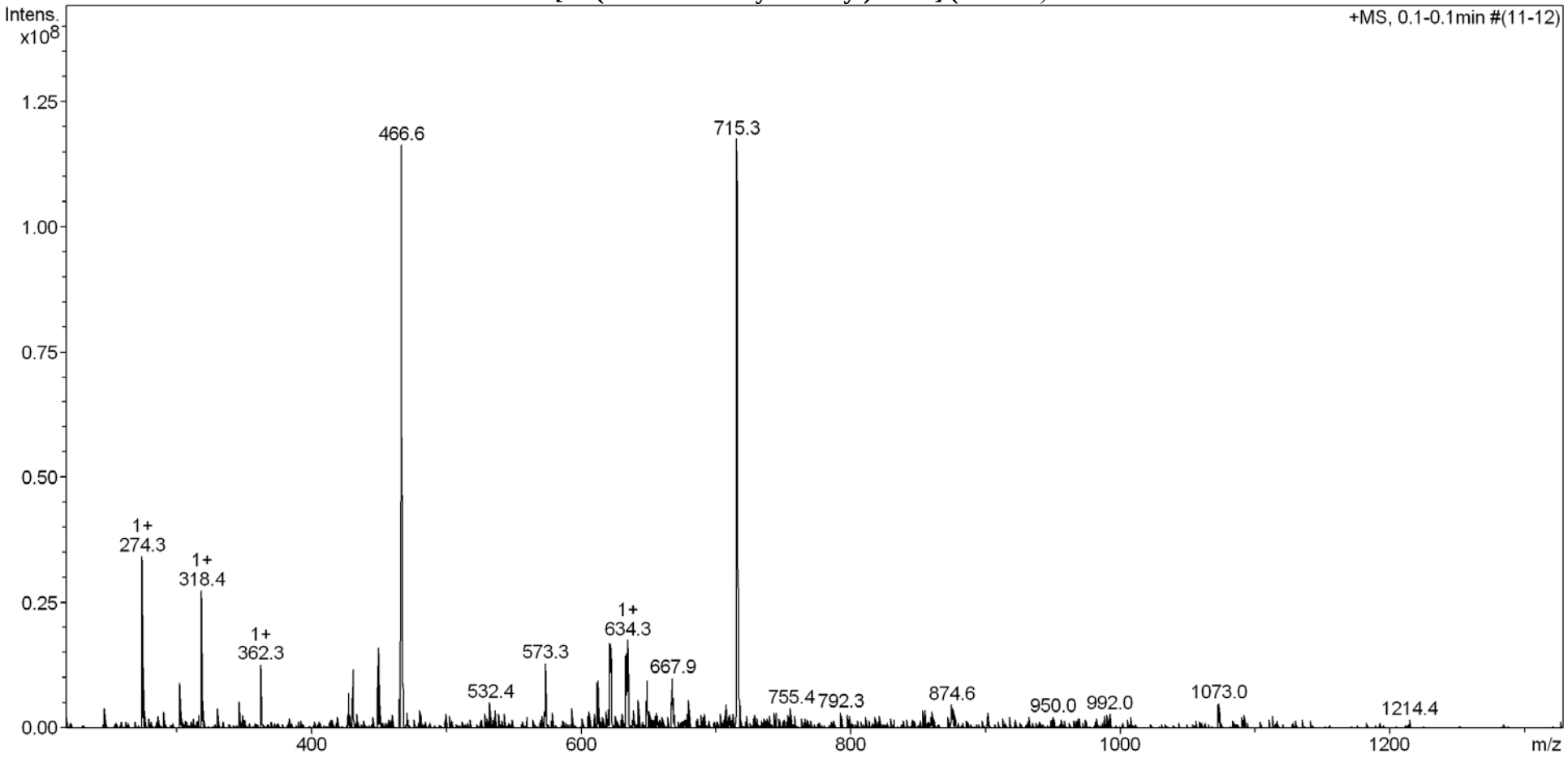

Fig. S123. Mass spectrum (ESI) of 5,11,17,23-tetra-*tert*-butyl-25,26,27,28-tetrakis[(N-(3',3'-dimethyl-3'-{([ethoxycarbonylmethyl]-amidocarbonylmethyl)amidocarbonylmethyl}ammoniumpropyl)carbomoylmethoxy]-2,8,14,20-tetrathiacalix[4]arene tetra[bis(trifluoromethylsulfonyl)imide] (*cone* **45**)

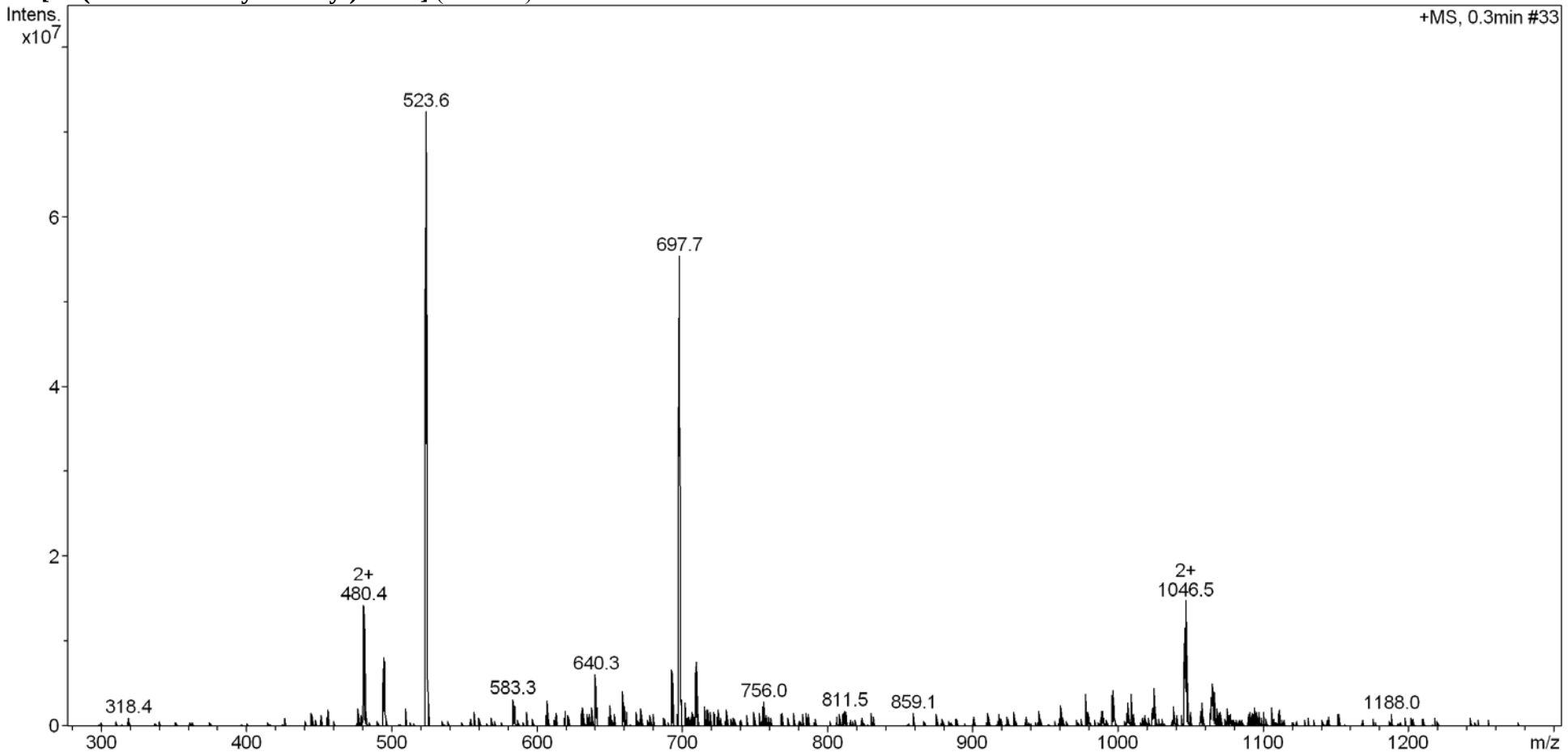

Fig. S124. Mass spectrum (ESI) of 5,11,17,23-tetra-*tert*-butyl-25,26,27,28-tetrakis[(N-(3',3'-dimethyl-3'-{(ethoxycarbonyl[S-methyl]methyl)amidocarbonylmethyl}ammoniumpropyl)carbomoylmethoxy]-2,8,14,20-tetrathiacalix[4]arene tetra[bis(trifluoromethylsulfonyl)imide] (*cone* **46**)

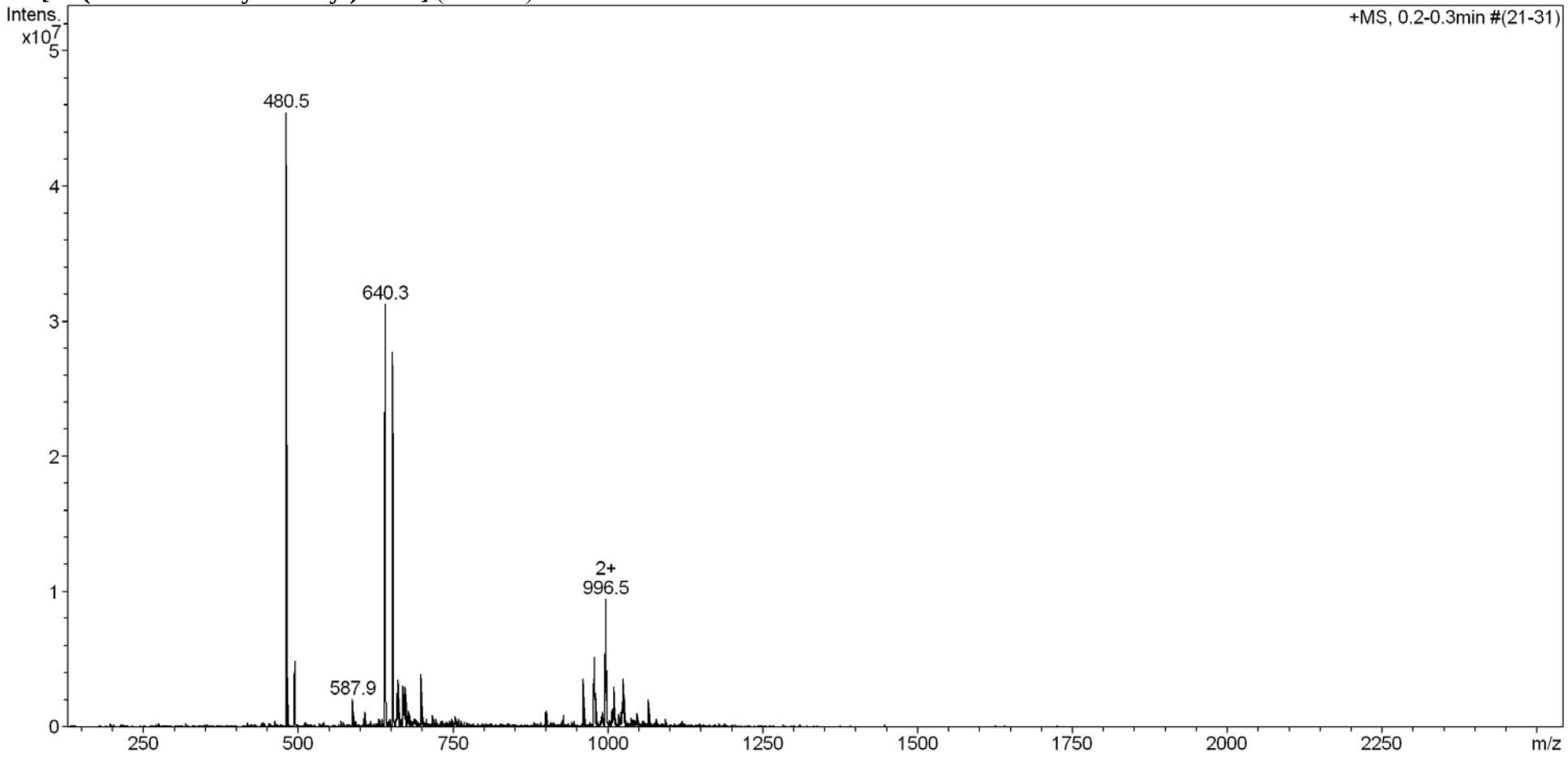

Fig. S125. Mass spectrum (ESI) of 5,11,17,23-tetra-*tert*-butyl-25,26,27,28-tetrakis[(N-(3',3'-dimethyl-3'-{3''-propylphtalimide}ammoniumpropyl)-carbomoylmethoxy]-2,8,14,20-tetrathiacalix[4]arene tetra[bis(trifluoromethylsulfonyl)imide] (*cone* **47**)

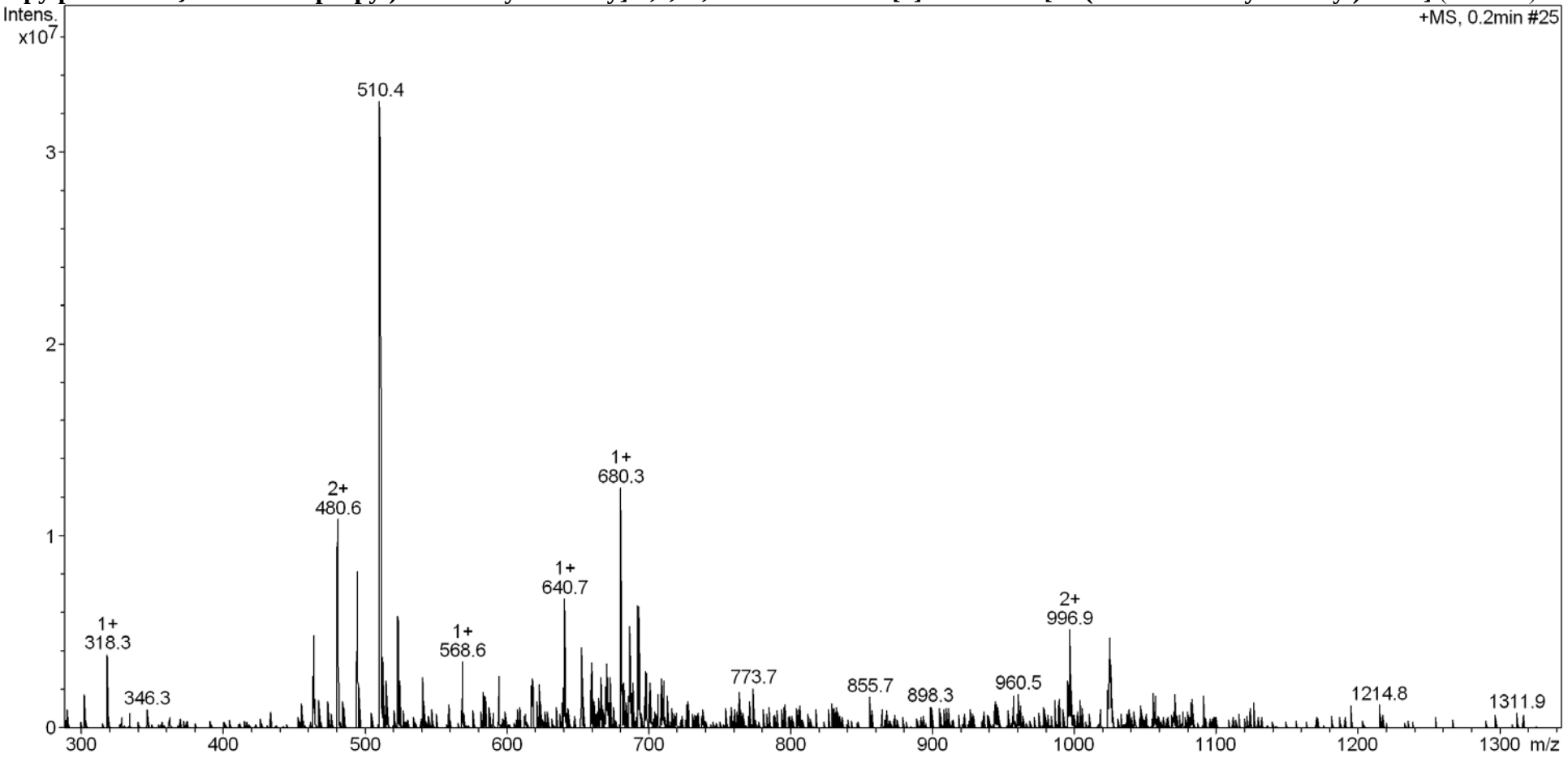

Fig. S126. Mass spectrum (ESI) of 5,11,17,23-tetra-*tert*-butyl-25,26,27,28-tetrakis[(N-(2'-methyl-2',2'-diethyl)ammoniumethyl)carbomoylmethoxy]-2,8,14,20-tetrathiacalix[4]arene tetra[bis(trifluoromethylsulfonyl)imide] (*cone* **48**)

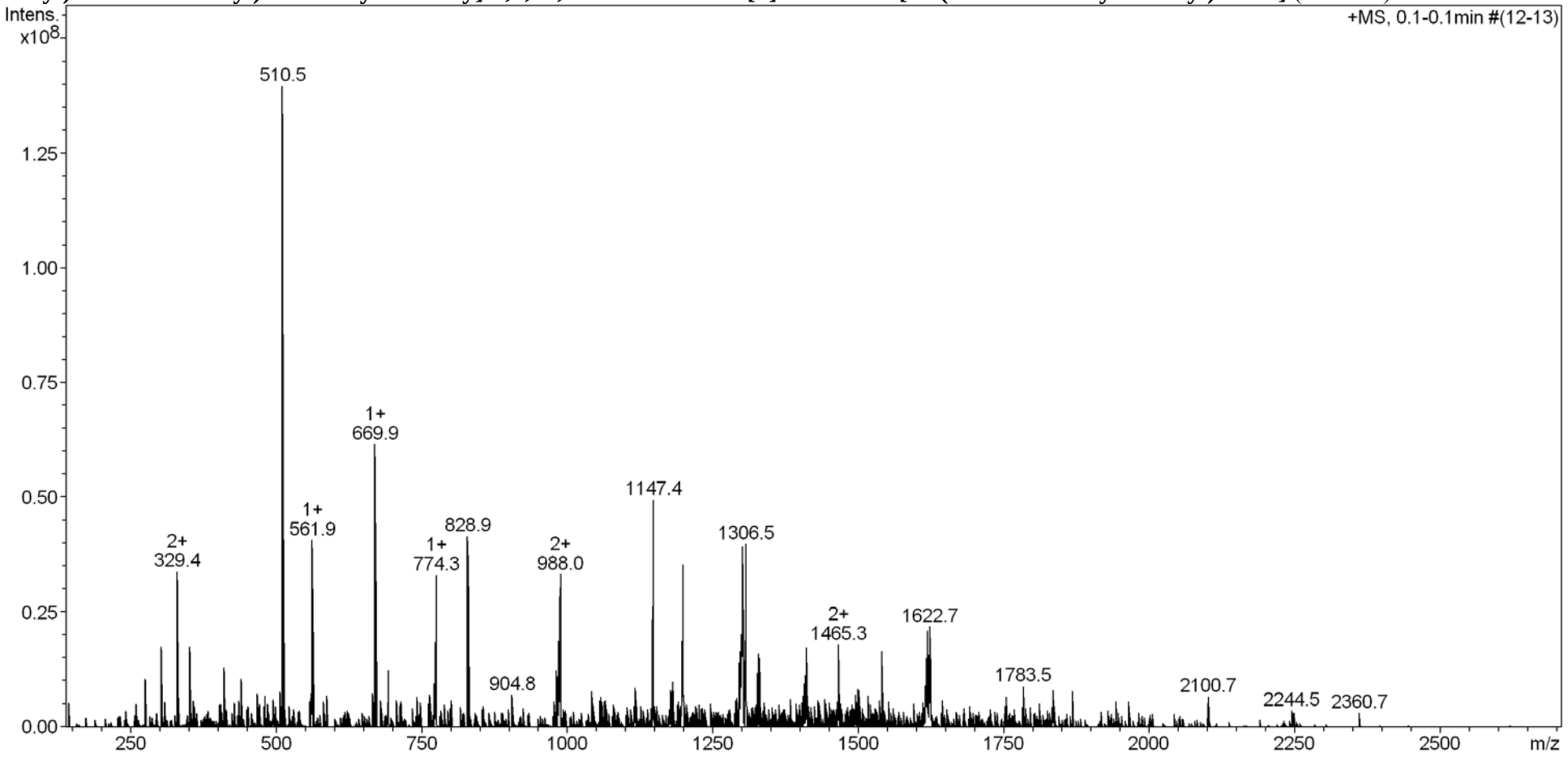

Fig. S127. Mass spectrum (ESI) of 5,11,17,23-tetra-*tert*-butyl-25,26,27,28-tetrakis[(N-(2',2',2'-triethyl)ammoniumethyl)carbomoylmethoxy]-2,8,14,20-tetrathiacalix[4]arene tetra[bis(trifluoromethylsulfonyl)imide] (*cone* **49**)

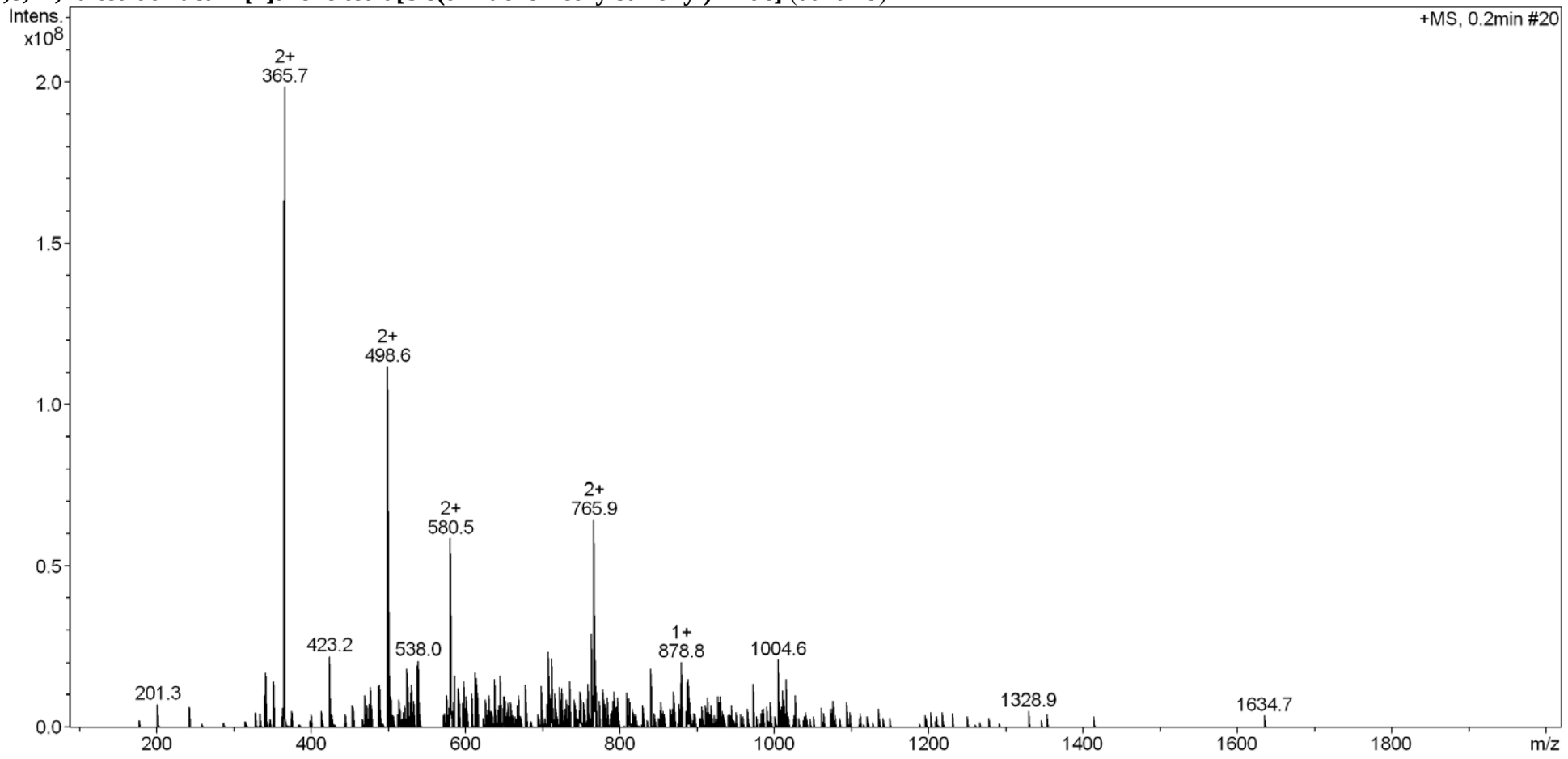

Fig. S128. Mass spectrum (ESI) of 5,11,17,23-tetra-*tert*-butyl-25,26,27,28-tetrakis[(N-(2',2'-diethyl-2'–benzyl)ammoniumethyl)carbomoylmethoxy]-2,8,14,20-tetrathiacalix[4]arene tetra[bis(trifluoromethylsulfonyl)imide] (*cone* **50**)

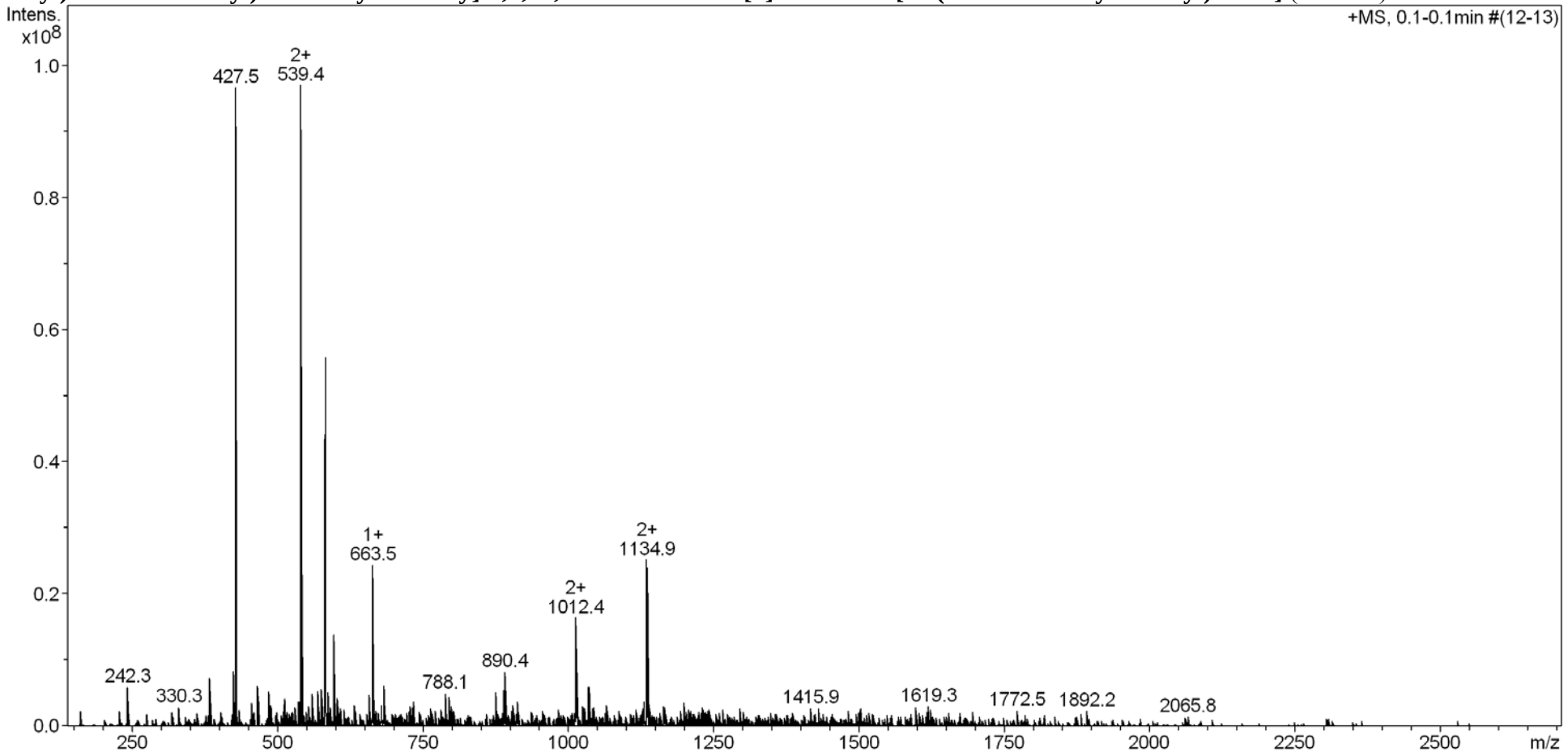

Fig. S129. Mass spectrum (ESI) of 5,11,17,23-tetra-*tert*-butyl-25,26,27,28-tetrakis[(N-(2',2'-diethyl-2'-(ethoxycarbonylmethyl)ammoniumethyl)-carbomoylmethoxy]-2,8,14,20-tetrathiacalix[4]arene tetra[bis(trifluoromethylsulfonyl)imide] (*cone* **51**)

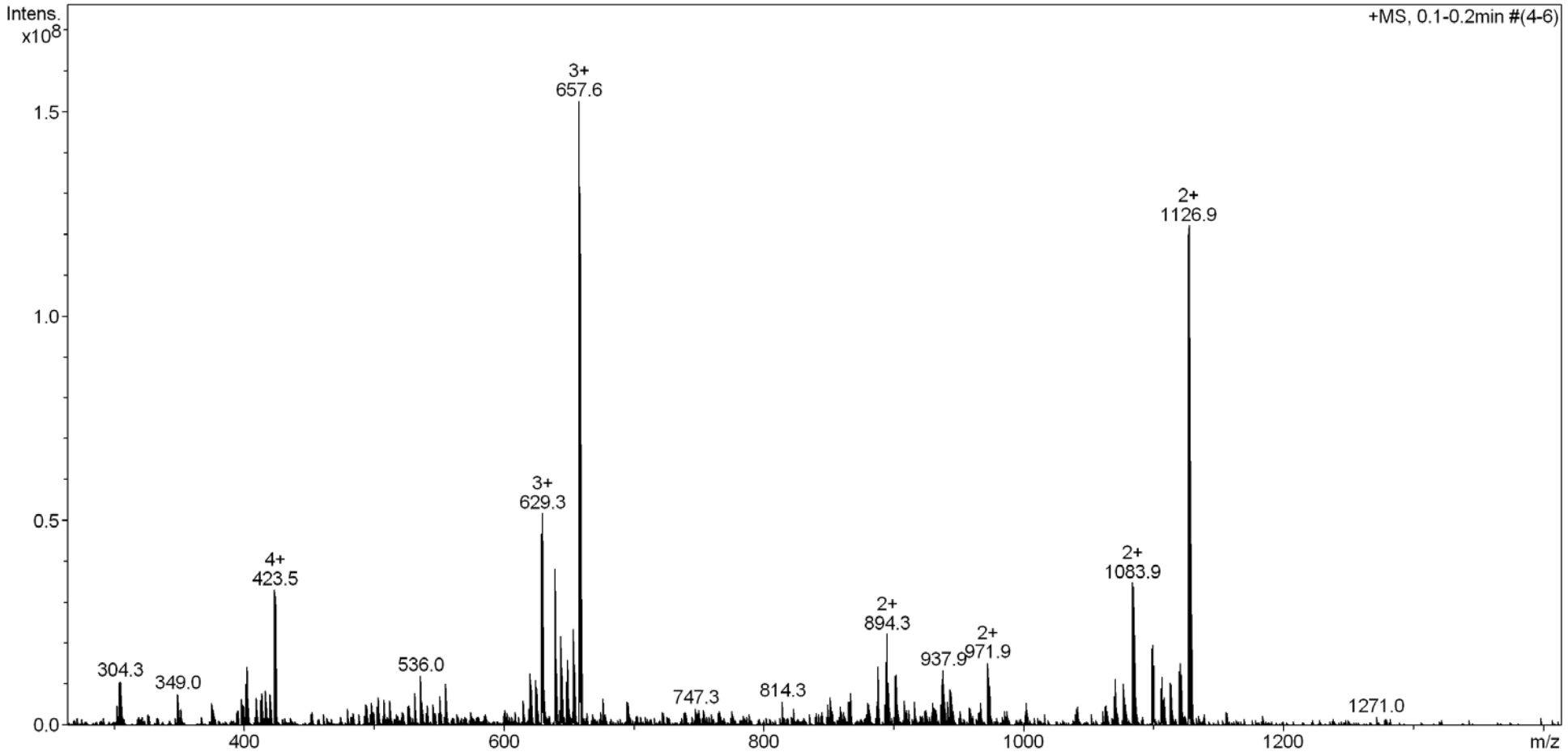

Fig. S130. Mass spectrum (ESI) of 5,11,17,23-tetra-*tert*-butyl-25,26,27,28-tetrakis[(N-(2',2'-diethyl-2'-(pentoxycarbonylmethyl)-ammoniumethyl) carbomoylmethoxy]-2,8,14,20-tetrathiacalix[4]arene tetra[bis(trifluoromethylsulfonyl)imide] (*cone* **52**)

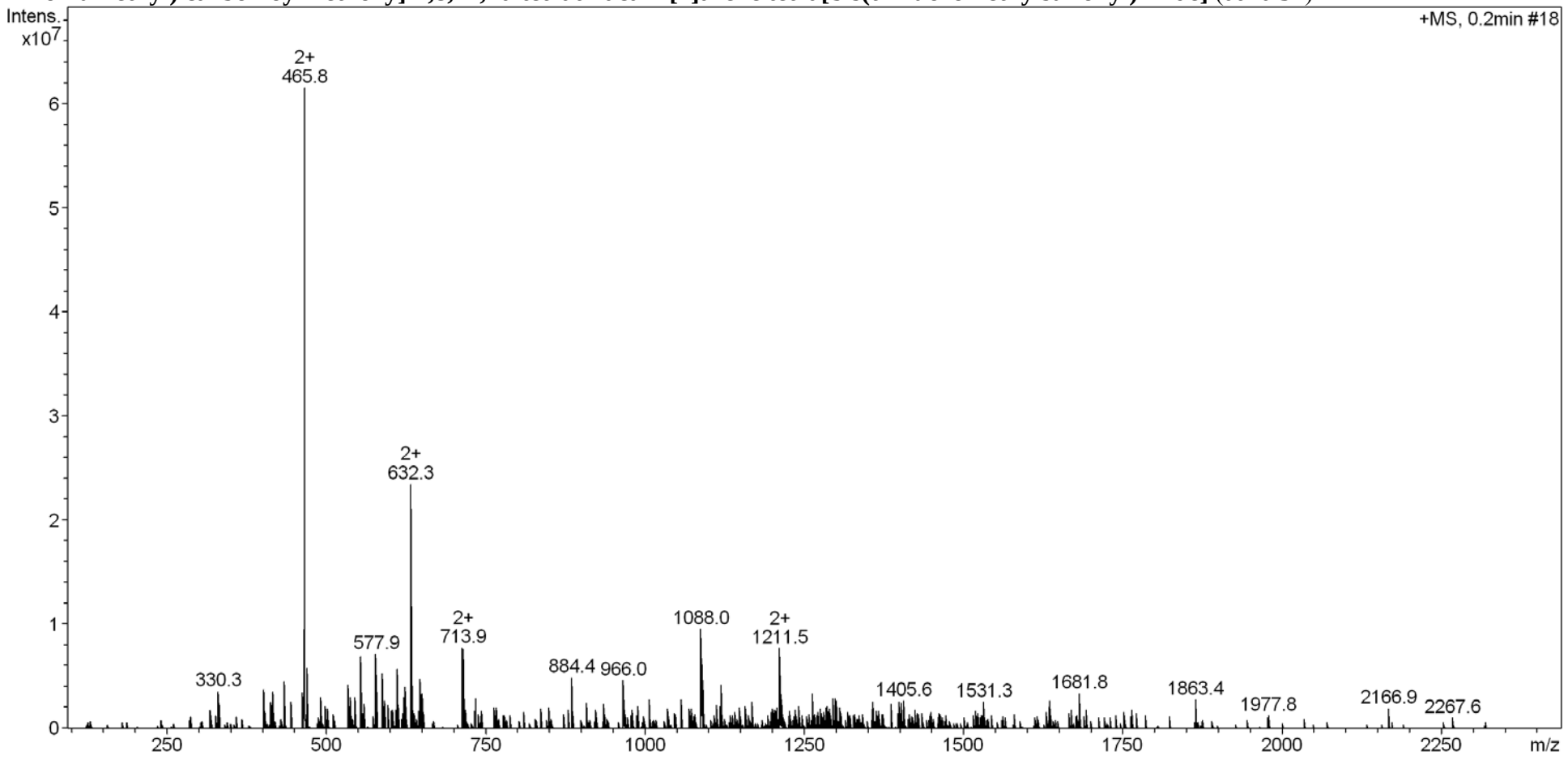

Fig. S131. Mass spectrum (ESI) of 5,11,17,23-tetra-*tert*-butyl-25,26,27,28-tetrakis[(N-(2',2'-diethyl-2'-{(ethoxycarbonylmethyl)amidocarbonylmethyl})-ammoniumethyl)carbomoylmethoxy]-2,8,14,20-tetrathiacalix[4]arene tetra[bis(trifluoromethylsulfonyl)imide] (*cone* **53**)

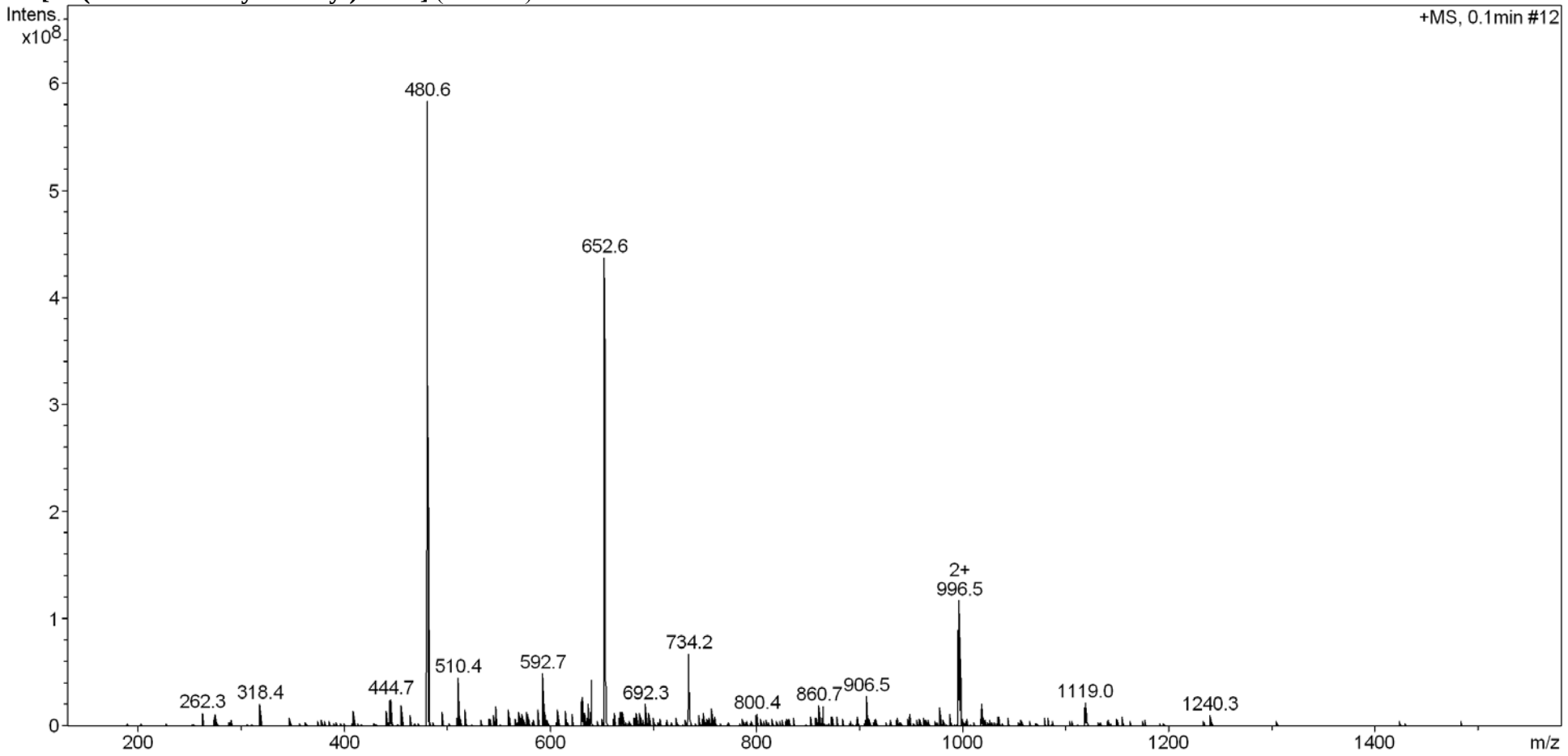

Fig. S132. Mass spectrum (ESI) of 5,11,17,23-tetra-*tert*-butyl-25,26,27,28-tetrakis[(N-(2',2'-diethyl-2'-{([ethoxycarbonylmethyl]-amidocarbonylmethyl)amidocarbonylmethyl}ammoniumethyl)carbomoylmethoxy]-2,8,14,20-tetrathiacalix[4]arene tetra[bis(trifluoromethylsulfonyl)imide] (*cone* **54**)

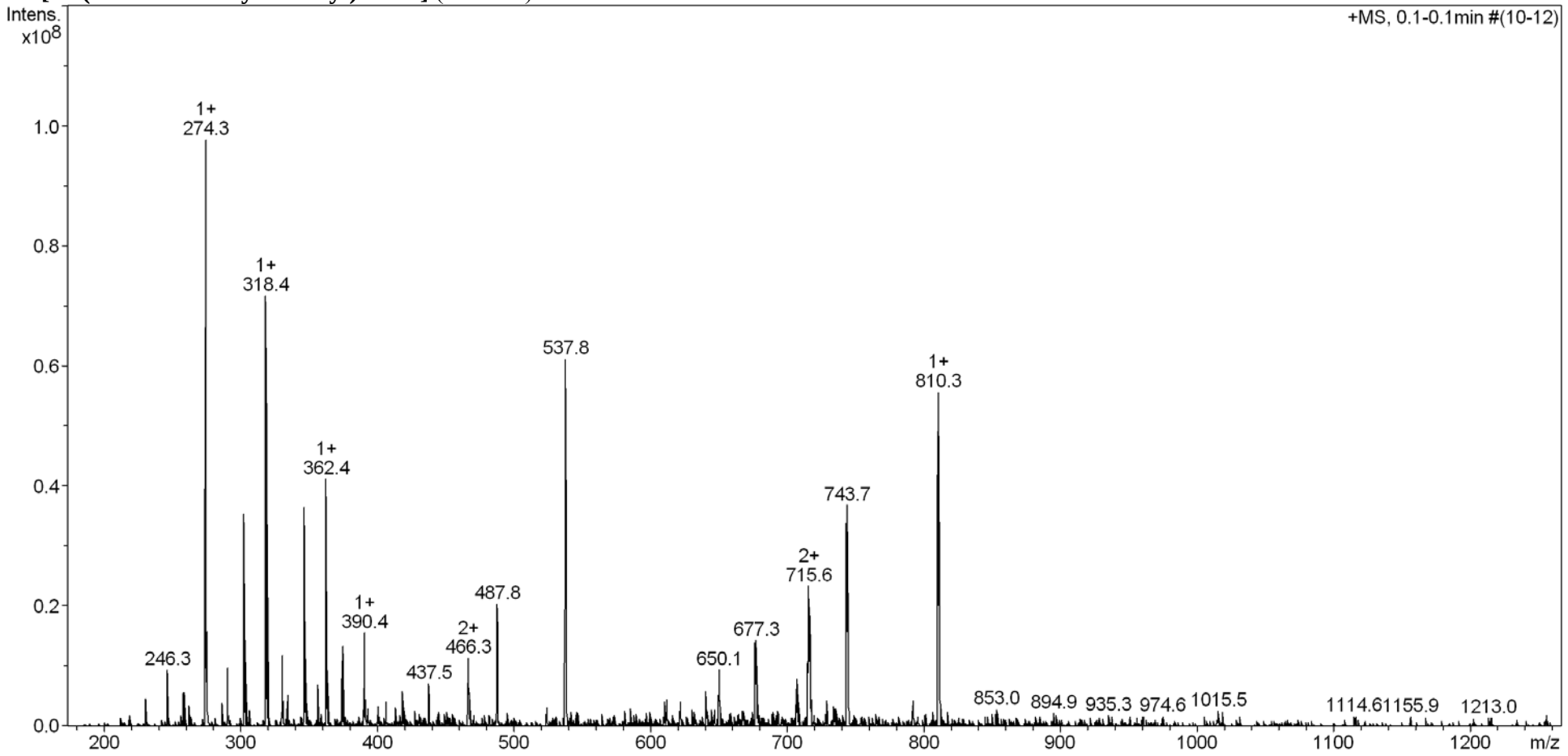

Fig. S133. Mass spectrum (ESI) of 5,11,17,23-tetra-*tert*-butyl-25,26,27,28-tetrakis[(N-(2',2'-diethyl-2'-{(ethoxycarbonyl[S-methyl]methyl)amidocarbonylmethyl}ammoniumethyl)carbomoylmethoxy]-2,8,14,20-tetrathiacalix[4]arene tetra[bis(trifluoromethylsulfonyl)imide] (*cone* **55**)

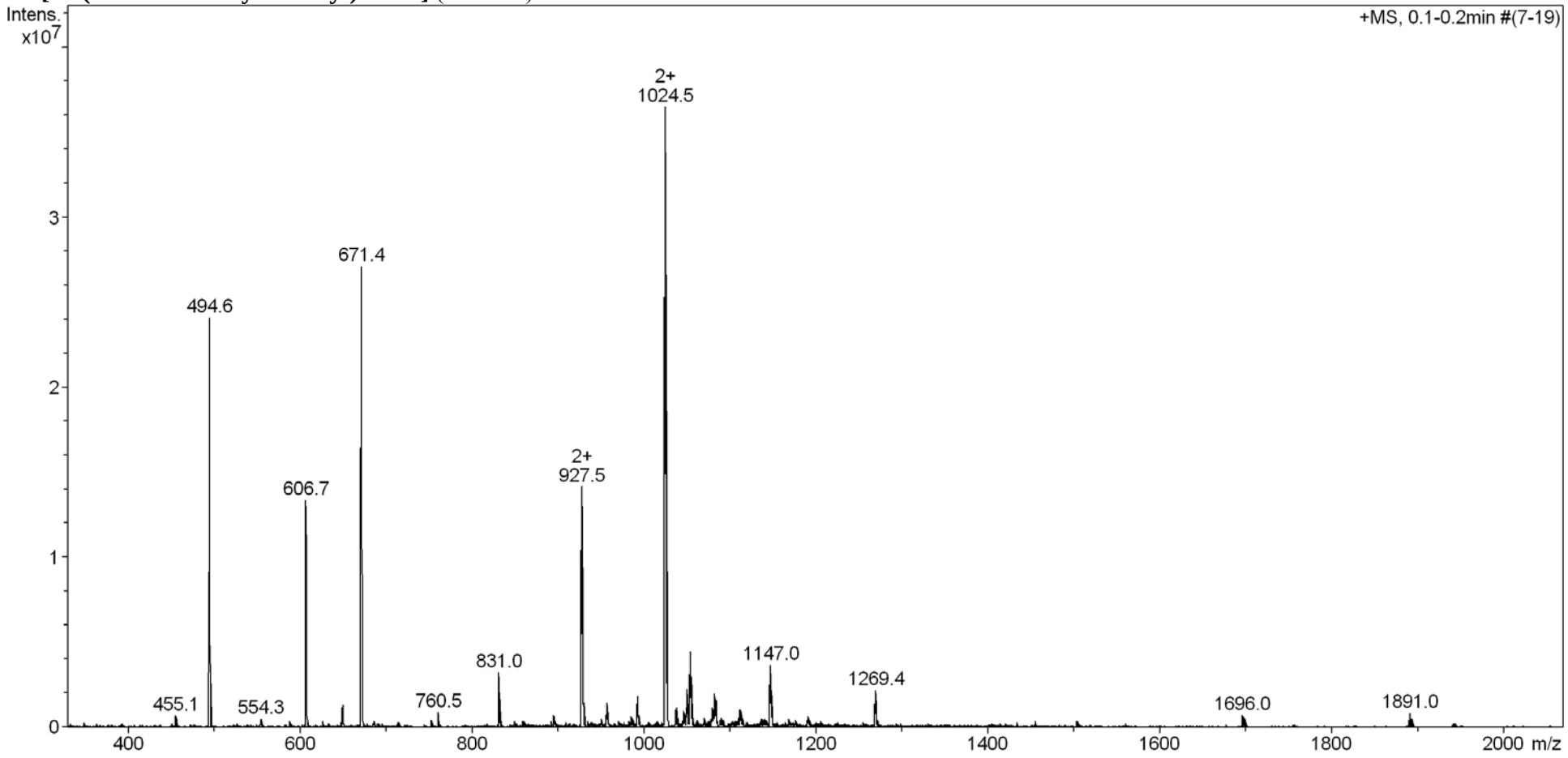

Fig. S134. Mass spectrum (MALDI-TOF, 4-nitroaniline matrix) of 5,11,17,23-tetra-*tert*-butyl-25,26,27,28-tetrakis[(N-(3',3',3'-trimethyl)ammoniumpropyl)carbomoylmethoxy]-2,8,14,20-tetrathiacalix[4]arene tetra[bis(trifluoromethylsulfonyl)imide] (*1,3-alternate* **56**)

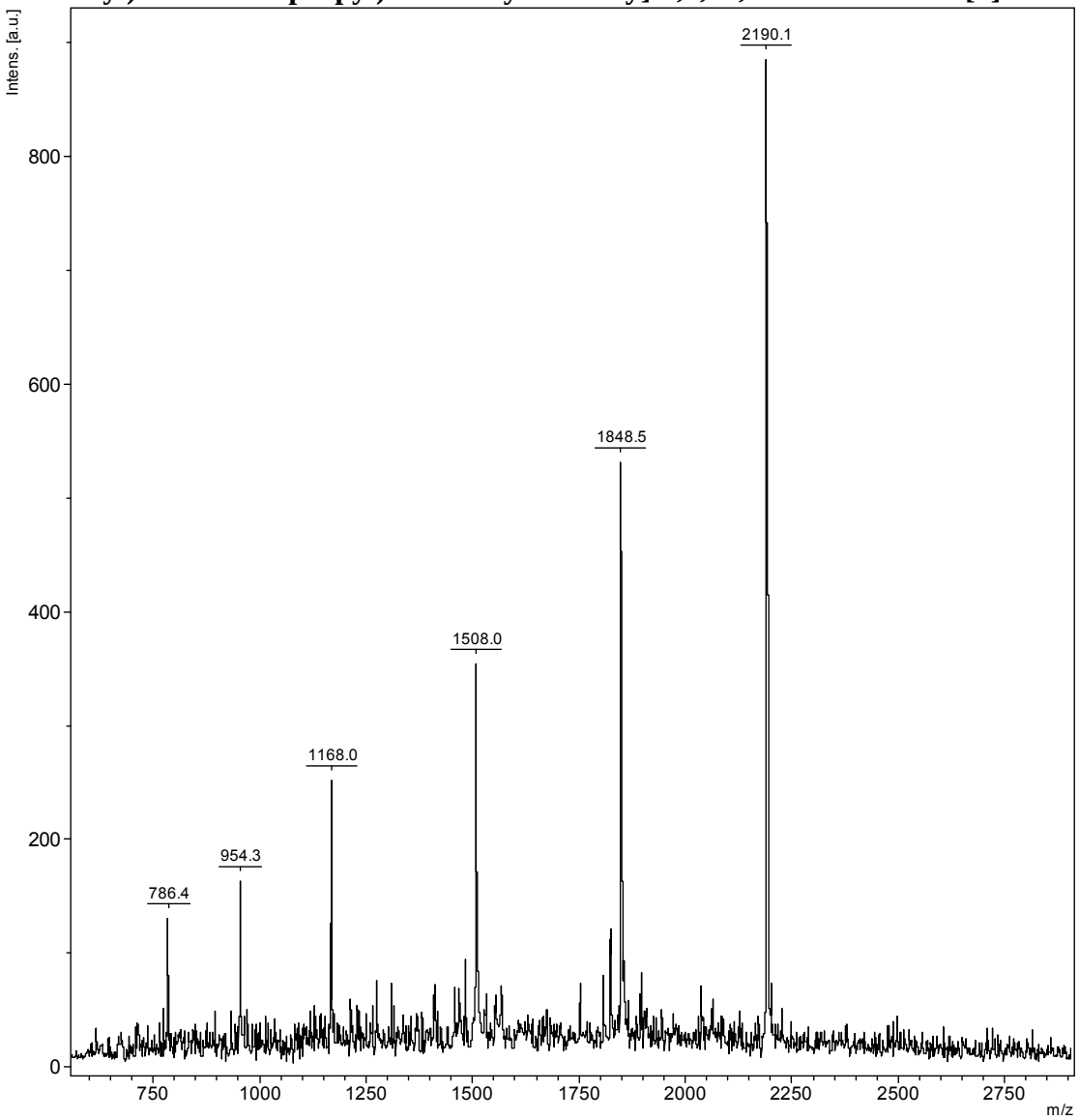

Fig. S135. Mass spectrum (MALDI-TOF, 4-nitroaniline matrix) of 5,11,17,23-tetra-*tert*-butyl-25,26,27,28-tetrakis[(N-(3',3'-dimethyl-3'-ethyl)ammoniumpropyl)carbomoylmethoxy]-2,8,14,20-tetrathiacalix[4]arene tetra[bis(trifluoromethylsulfonyl)imide] (*1,3-alternate* **57**)

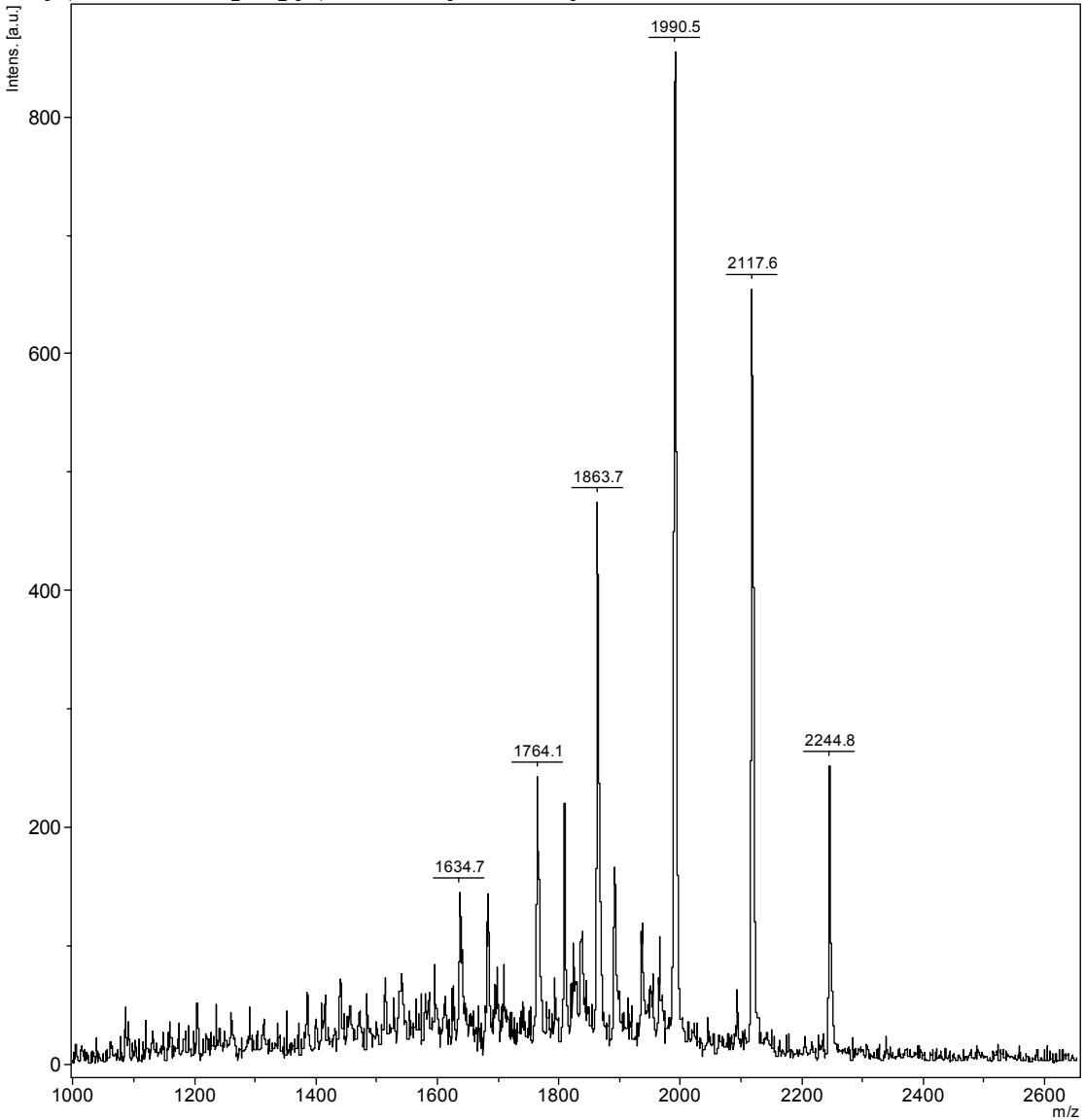

Fig. S136. Mass spectrum (MALDI-TOF, 4-nitroaniline matrix) of 5,11,17,23-tetra-*tert*-butyl-25,26,27,28-tetrakis[(N-(3',3'-dimethyl-3'-benzyl)ammoniumpropyl)carbomoylmethoxy]-2,8,14,20-tetrathiacalix[4]arene tetra[bis(trifluoromethylsulfonyl)imide] (*1,3-alternate* **58**)

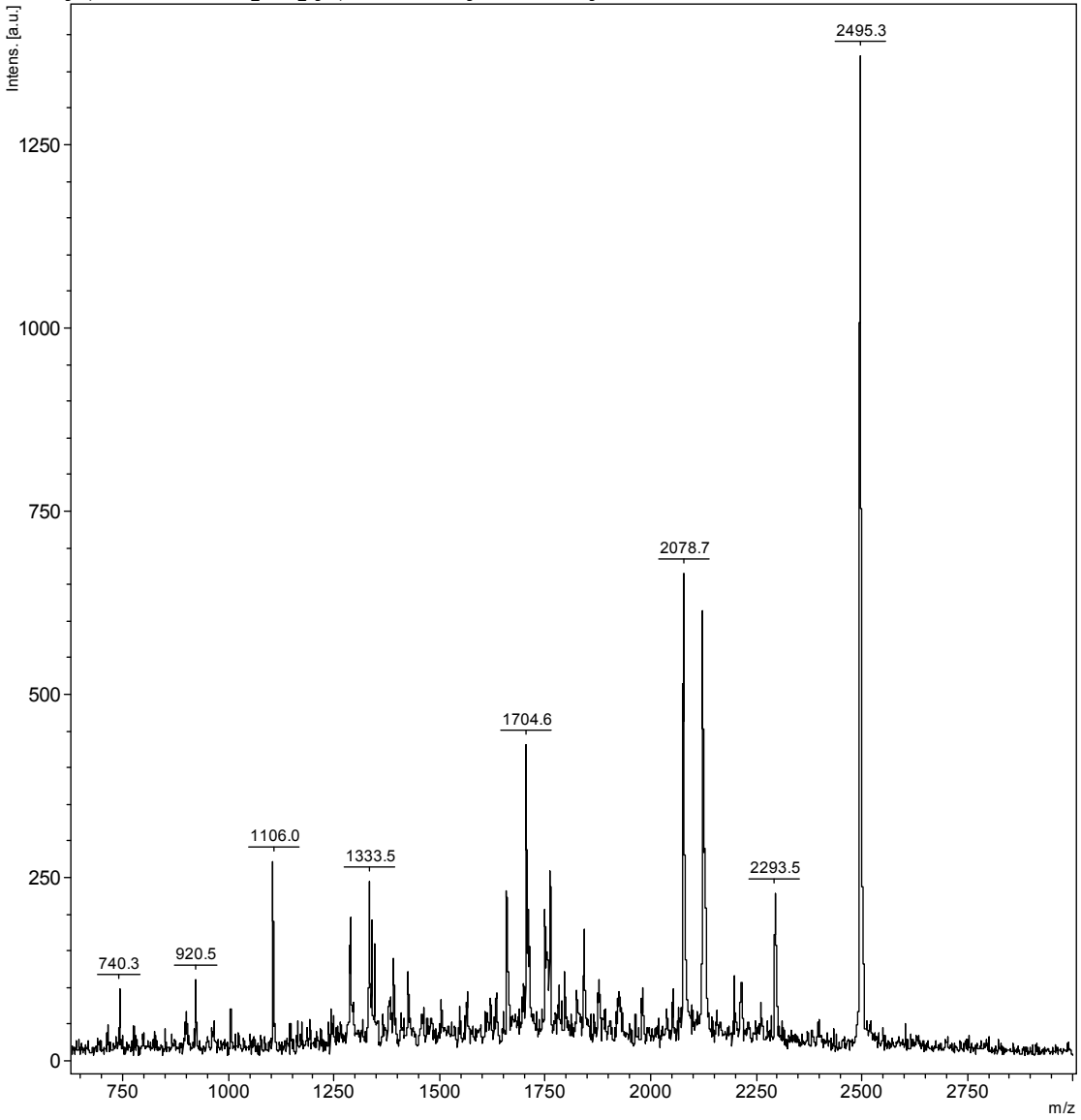

Fig. S137. Mass spectrum (MALDI-TOF, 4-nitroaniline matrix) of 5,11,17,23-tetra-*tert*-butyl-25,26,27,28-tetrakis[(N-(3',3'-dimethyl-3'-(ethoxycarbonylmethyl)ammoniumpropyl)-carbomoylmethoxy]-2,8,14,20-tetrathiacalix[4]arene tetra[bis(trifluoromethylsulfonyl)imide] (*1,3-alternate* **59**)

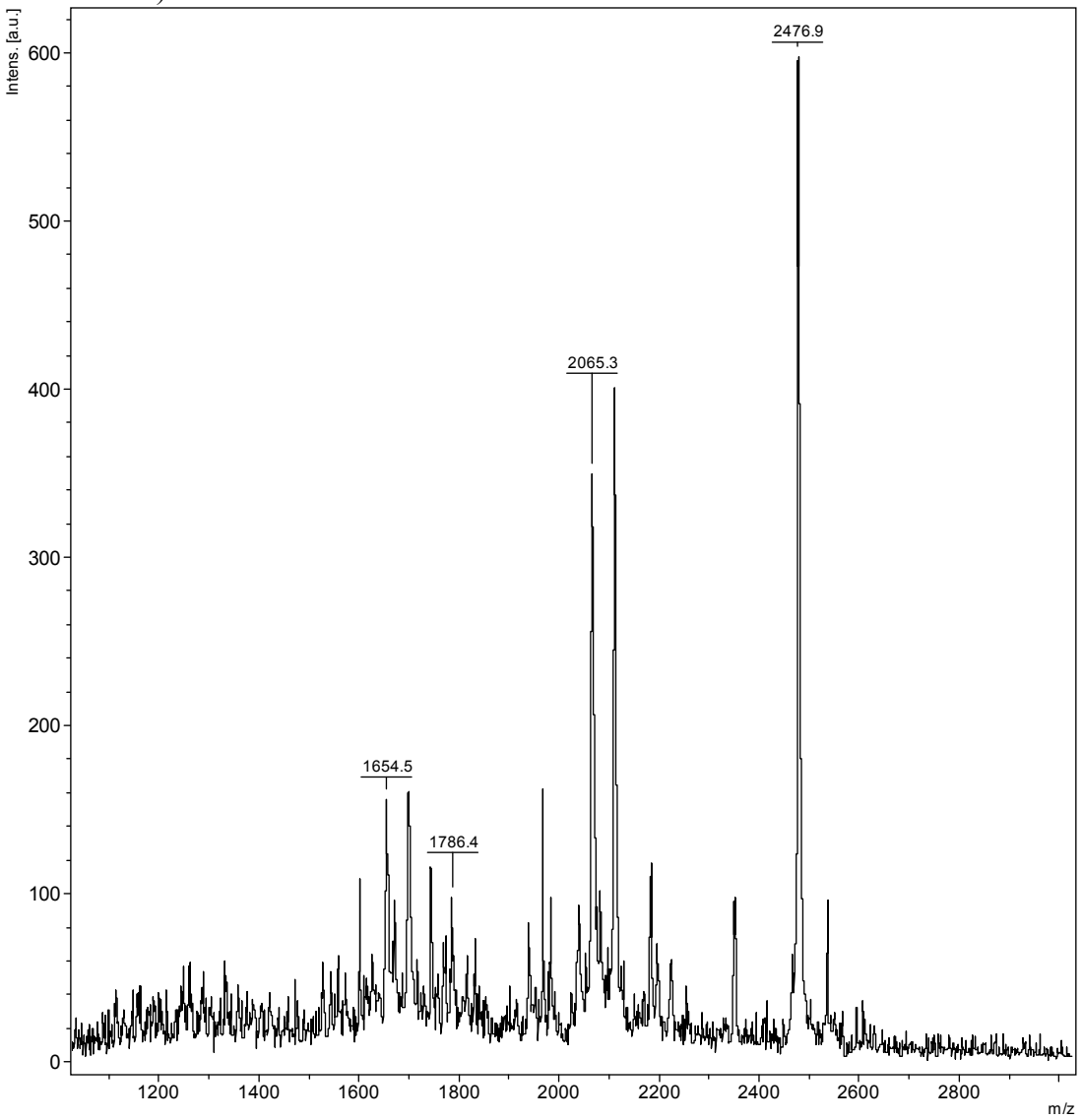

Fig. S138. Mass spectrum (ESI) of 5,11,17,23-tetra-*tert*-butyl-25,26,27,28-tetrakis[(N-(3',3'-dimethyl-3'-(pentoxycarbonylmethyl)-ammoniumpropyl)carbomoylmethoxy]-2,8,14,20-tetrathiacalix[4]arene tetra[bis(trifluoromethylsulfonyl)imide] (*1,3-alternate* **60**)

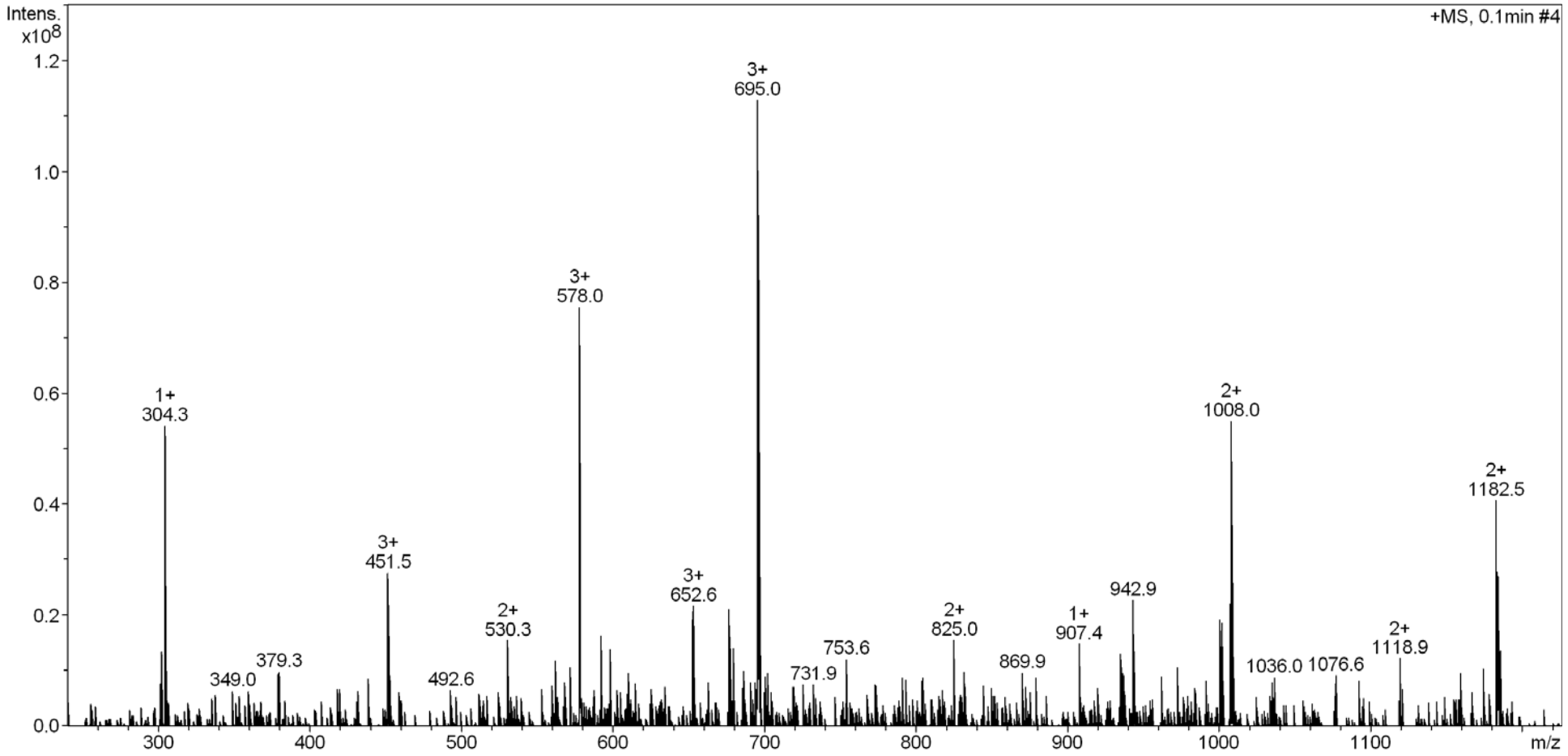

Fig. S139. Mass spectrum (ESI) of 5,11,17,23-tetra-*tert*-butyl-25,26,27,28-tetrakis[(N-(3',3'-dimethyl-3'-{(ethoxycarbonylmethyl)amidocarbonylmethyl}ammoniumpropyl)carbomoylmethoxy]-2,8,14,20-tetrathiacalix[4]arene tetra[bis(trifluoromethylsulfonyl)imide] (*1,3-alternate* **61**)

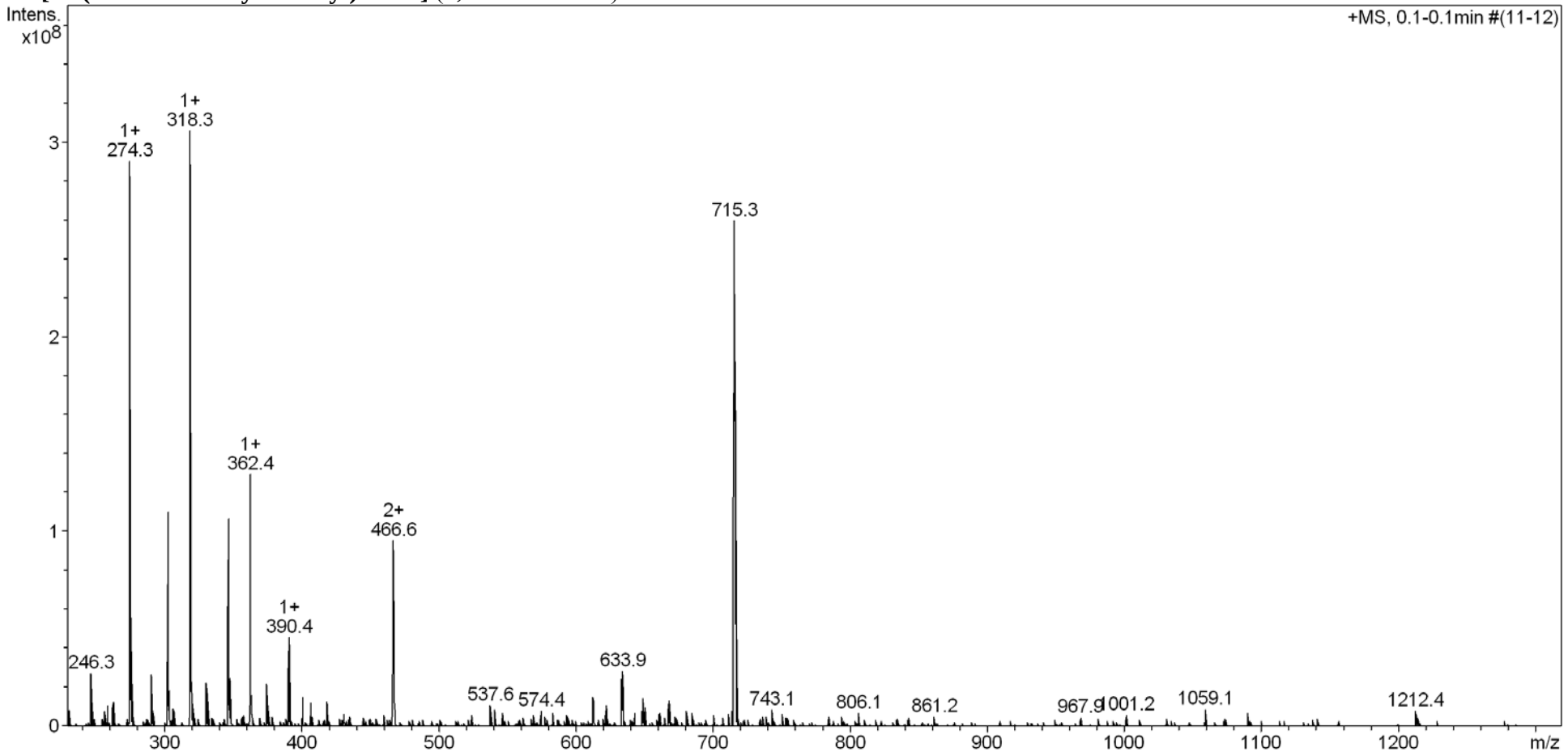

Fig. S140. Mass spectrum (ESI) of 5,11,17,23-tetra-*tert*-butyl-25,26,27,28-tetrakis[(N-(3',3'-dimethyl-3'-{([ethoxycarbonylmethyl]amidocarbonylmethyl)amidocarbonylmethyl}ammoniumpropyl)carbomoylmethoxy]-2,8,14,20-tetrathiacalix[4]arene tetra[bis(trifluoromethylsulfonyl)imide] (*1,3-alternate* **62**)

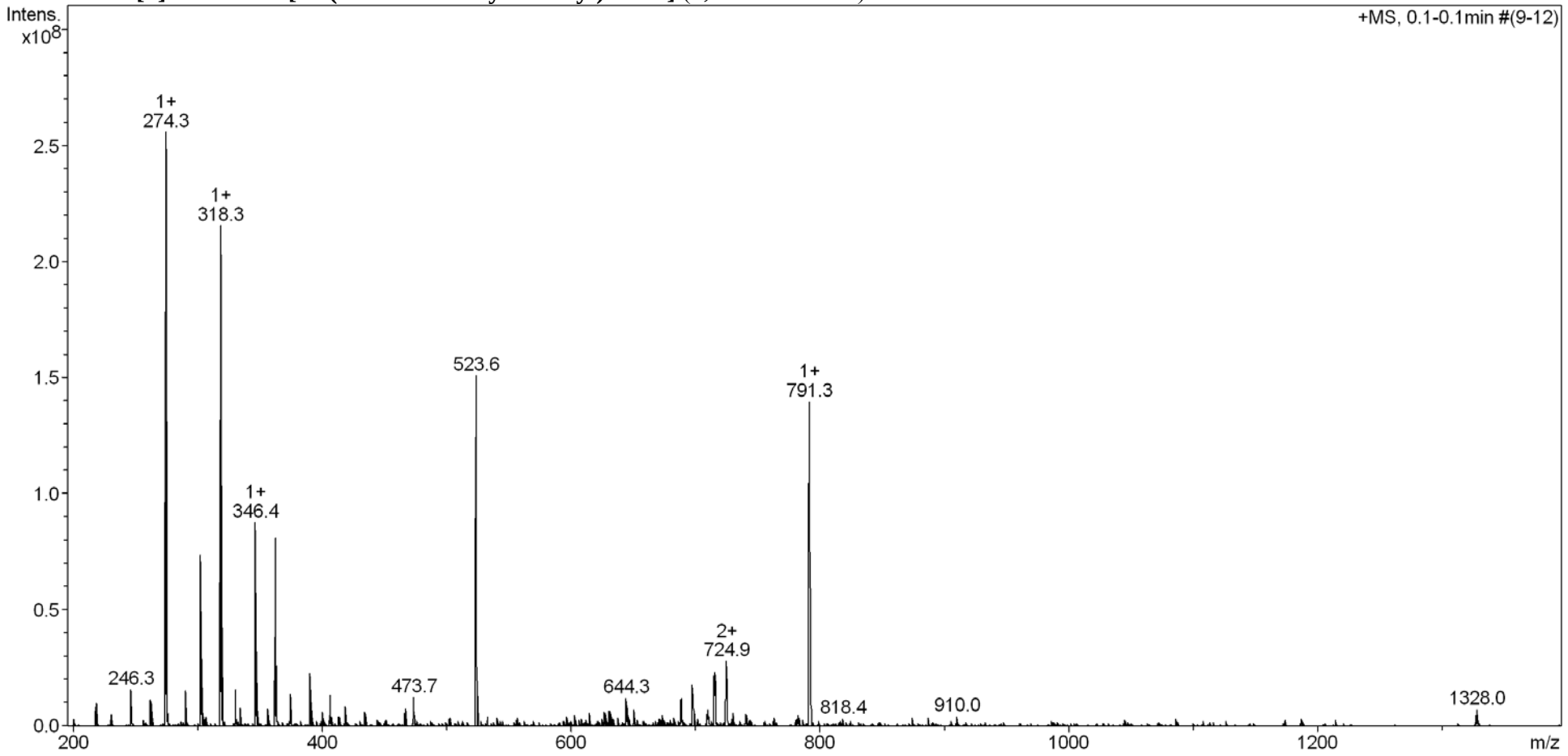

Fig. S141. Mass spectrum (ESI) of 5,11,17,23-tetra-*tert*-butyl-25,26,27,28-tetrakis[(N-(3',3'-dimethyl-3'-{(ethoxycarbonyl[S-methyl]methyl)amidocarbonylmethyl}ammoniumpropyl)carbomoylmethoxy]-2,8,14,20-tetrathiacalix[4]arene tetra[bis(trifluoromethylsulfonyl)imide] (*1,3-alternate* **63**)

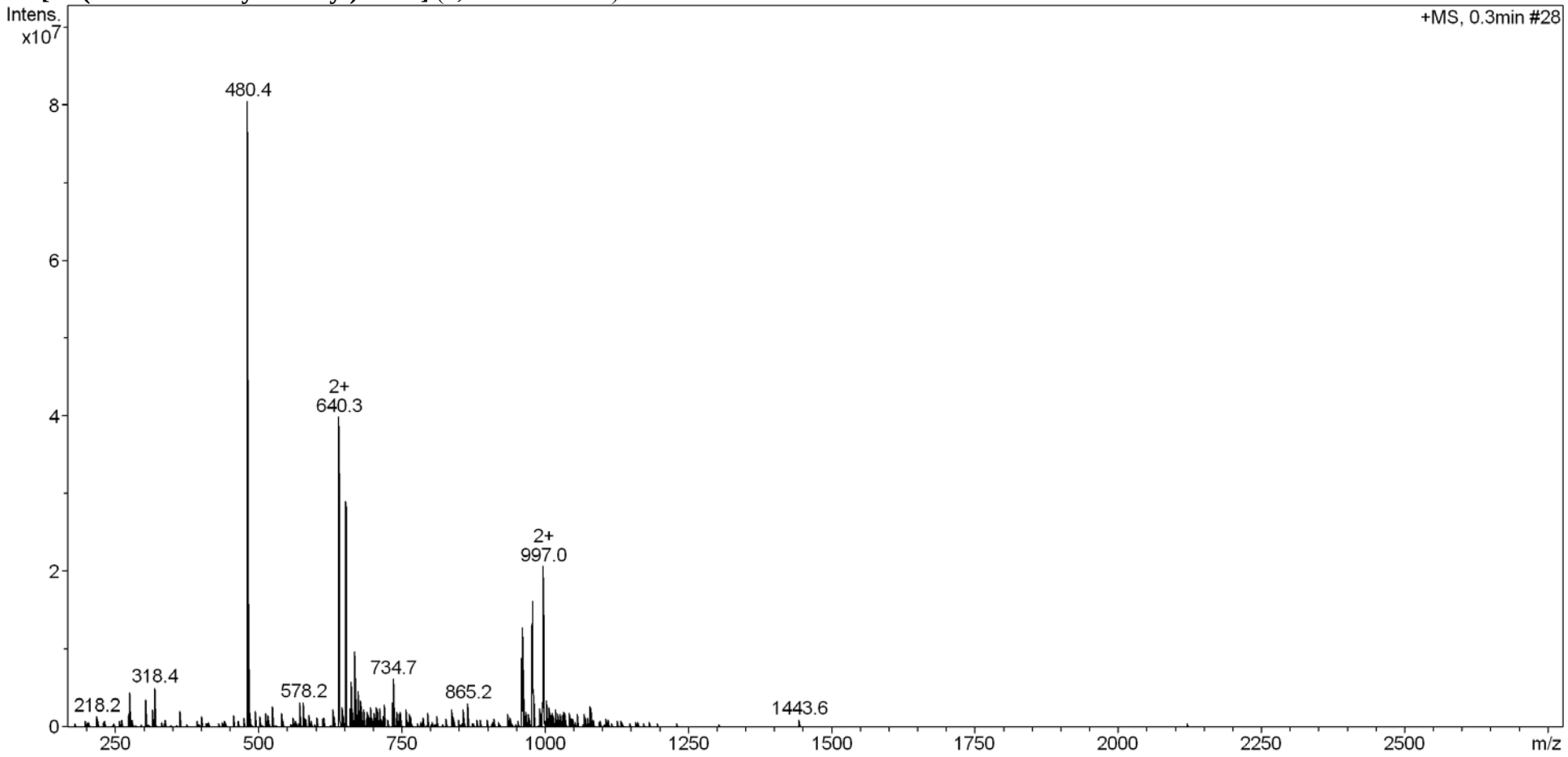

Fig. S142. Mass spectrum (ESI) of 5,11,17,23-tetra-*tert*-butyl-25,26,27,28-tetrakis[(N-(3',3'-dimethyl-3'-{3''-propylphtalimide}ammoniumpropyl)-carbomoylmethoxy]-2,8,14,20-tetrathiacalix[4]arene tetra[bis(trifluoromethylsulfonyl)imide] (*1,3-alternate* **64**)

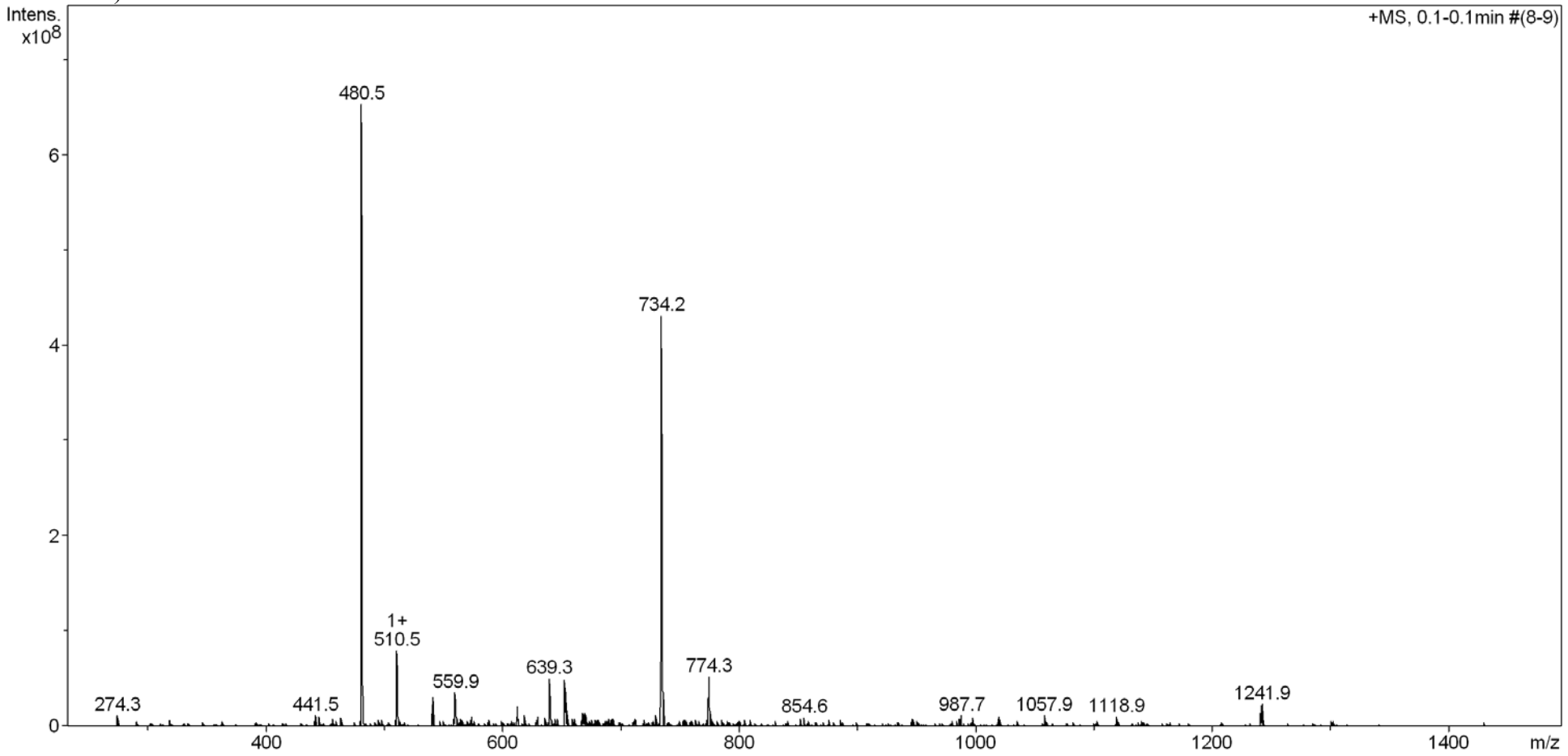

Fig. S143. Mass spectrum (ESI) of 5,11,17,23-tetra-*tert*-butyl-25,26,27,28-tetrakis[(N-(2'-methyl-2',2'-diethyl)ammoniumethyl)carbomoylmethoxy]-2,8,14,20-tetrathiacalix[4]arene tetra[bis(trifluoromethylsulfonyl)imide] (*1,3-alternate* **65**)

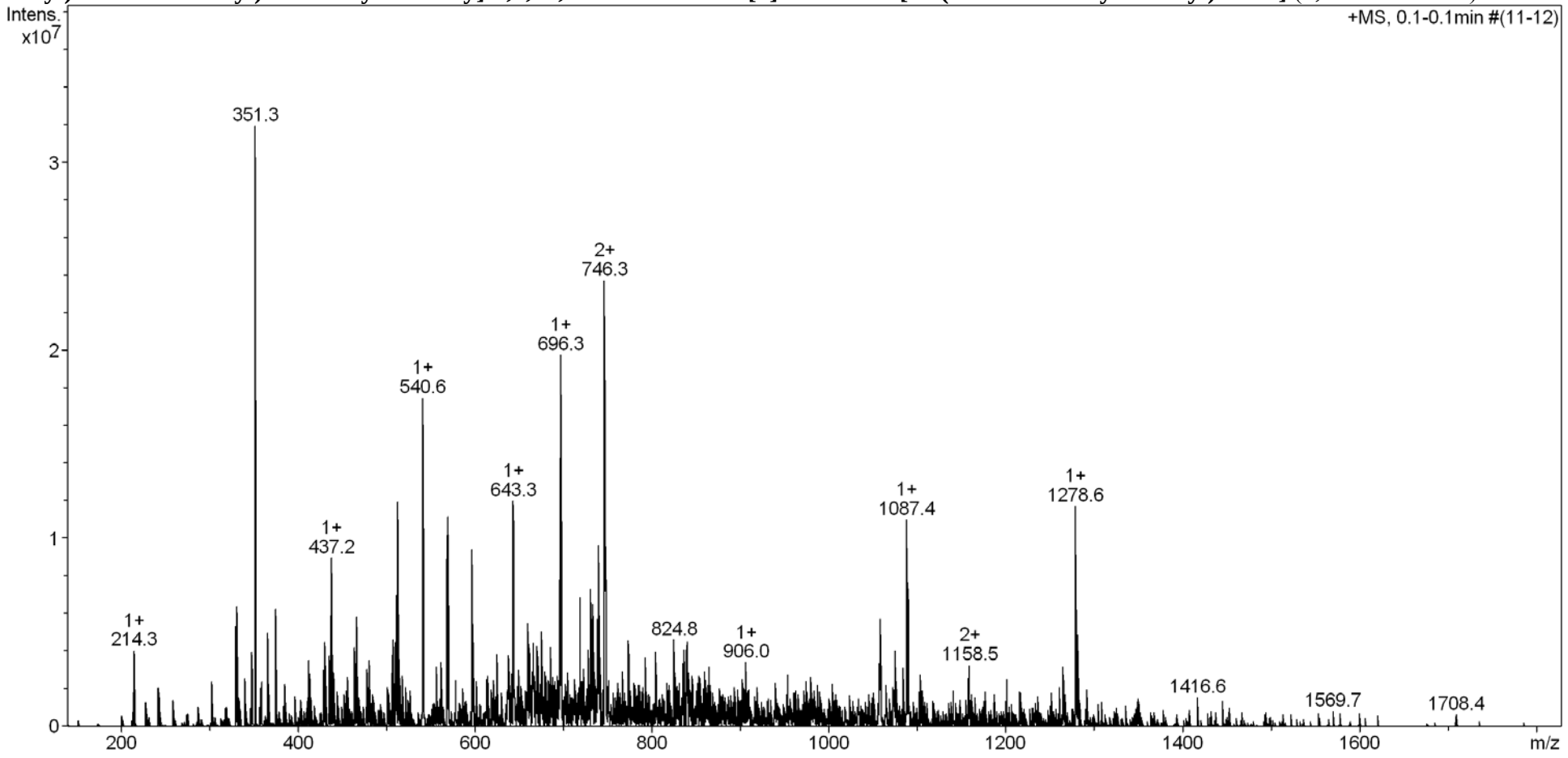

Fig. S144. Mass spectrum (ESI) of 5,11,17,23-tetra-*tert*-butyl-25,26,27,28-tetrakis[(N-(2',2',2'-triethyl)ammoniumethyl)carbomoylmethoxy]-2,8,14,20-tetrathiacalix[4]arene tetra[bis(trifluoromethylsulfonyl)imide] (*1,3-alternate* **66**)

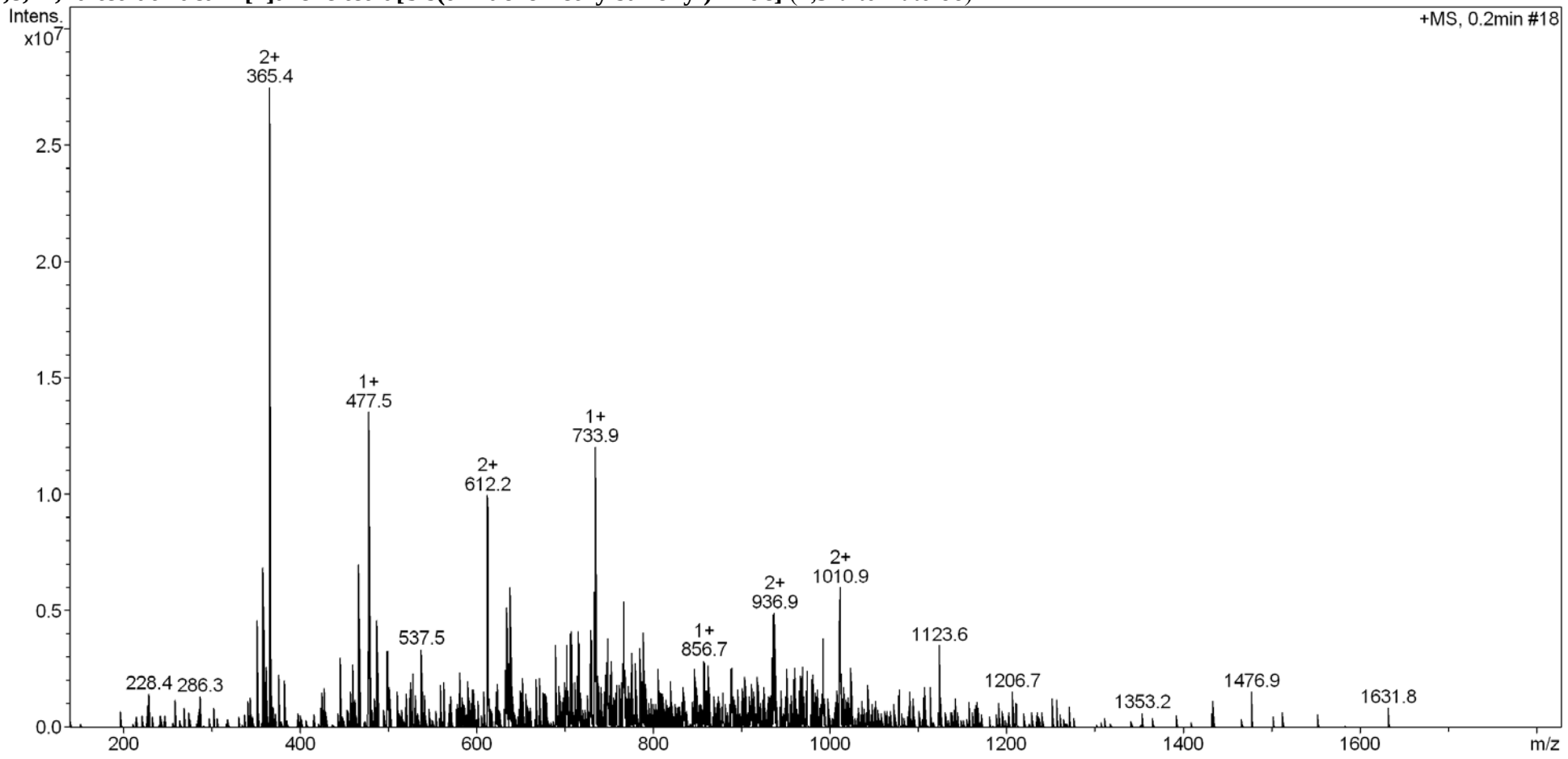

Fig. S145. Mass spectrum (ESI) of 5,11,17,23-tetra-*tert*-butyl-25,26,27,28-tetrakis[(N-(2',2'-diethyl-2'-benzyl)ammoniumethyl)carbomoylmethoxy]-2,8,14,20-tetrathiacalix[4]arene tetra[bis(trifluoromethylsulfonyl)imide] (*1,3-alternate* **67**)

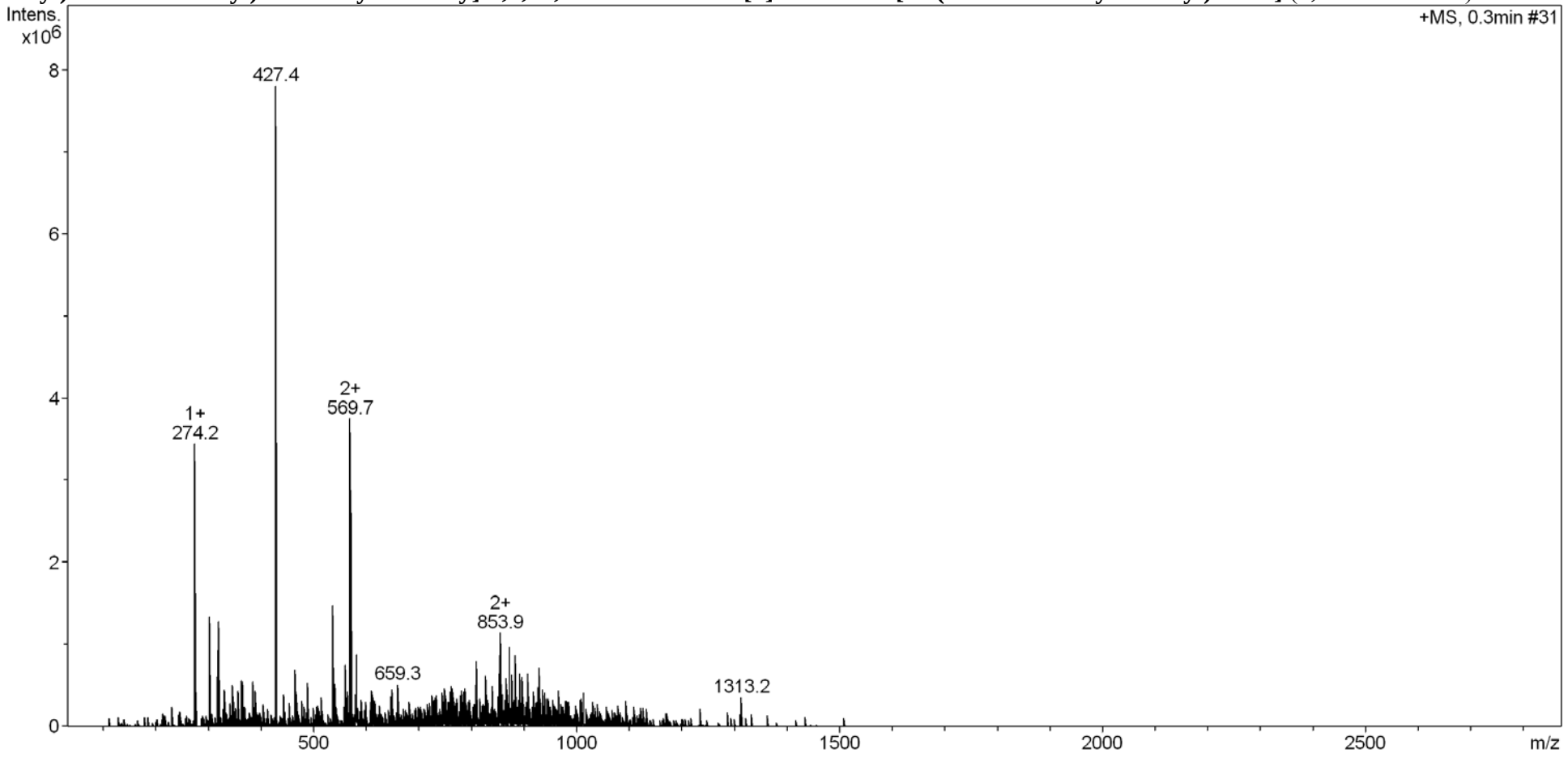

Fig. S146. Mass spectrum (ESI) of 5,11,17,23-tetra-*tert*-butyl-25,26,27,28-tetrakis[(N-(2',2'-diethyl-2'-(ethoxycarbonylmethyl)-ammoniumethyl)carbomoylmethoxy]-2,8,14,20-tetrathiacalix[4]arene tetra[bis(trifluoromethylsulfonyl)imide] (*1,3-alternate* **68**)

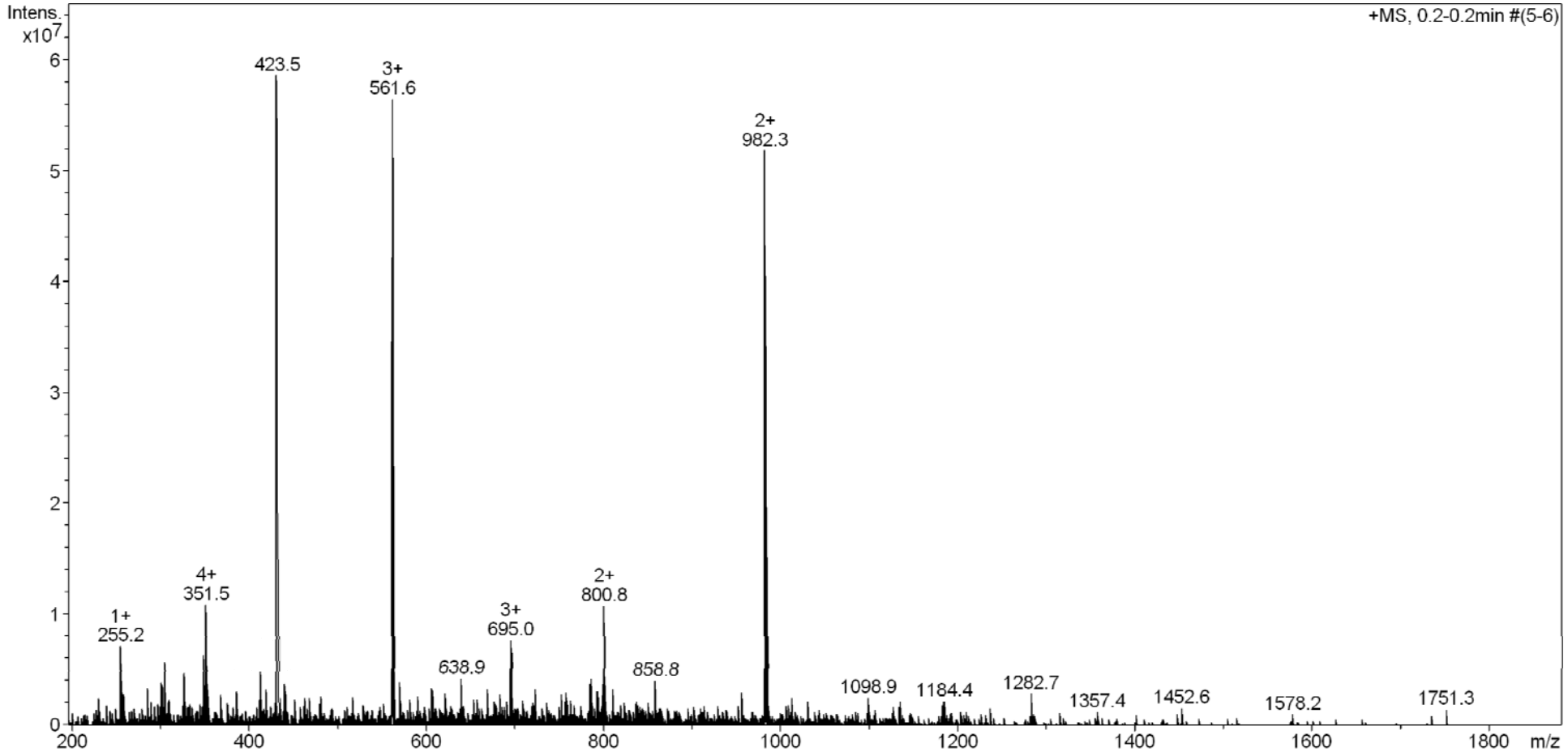

Fig. S147. Mass spectrum (ESI) of 5,11,17,23-tetra-*tert*-butyl-25,26,27,28-tetrakis[(N-(2',2'-diethyl-2'-(pentoxycarbonylmethyl)-ammoniumethyl)carbomoylmethoxy]-2,8,14,20-tetrathiacalix[4]arene tetra[bis(trifluoromethylsulfonyl)imide] (*1,3-alternate* **69**)

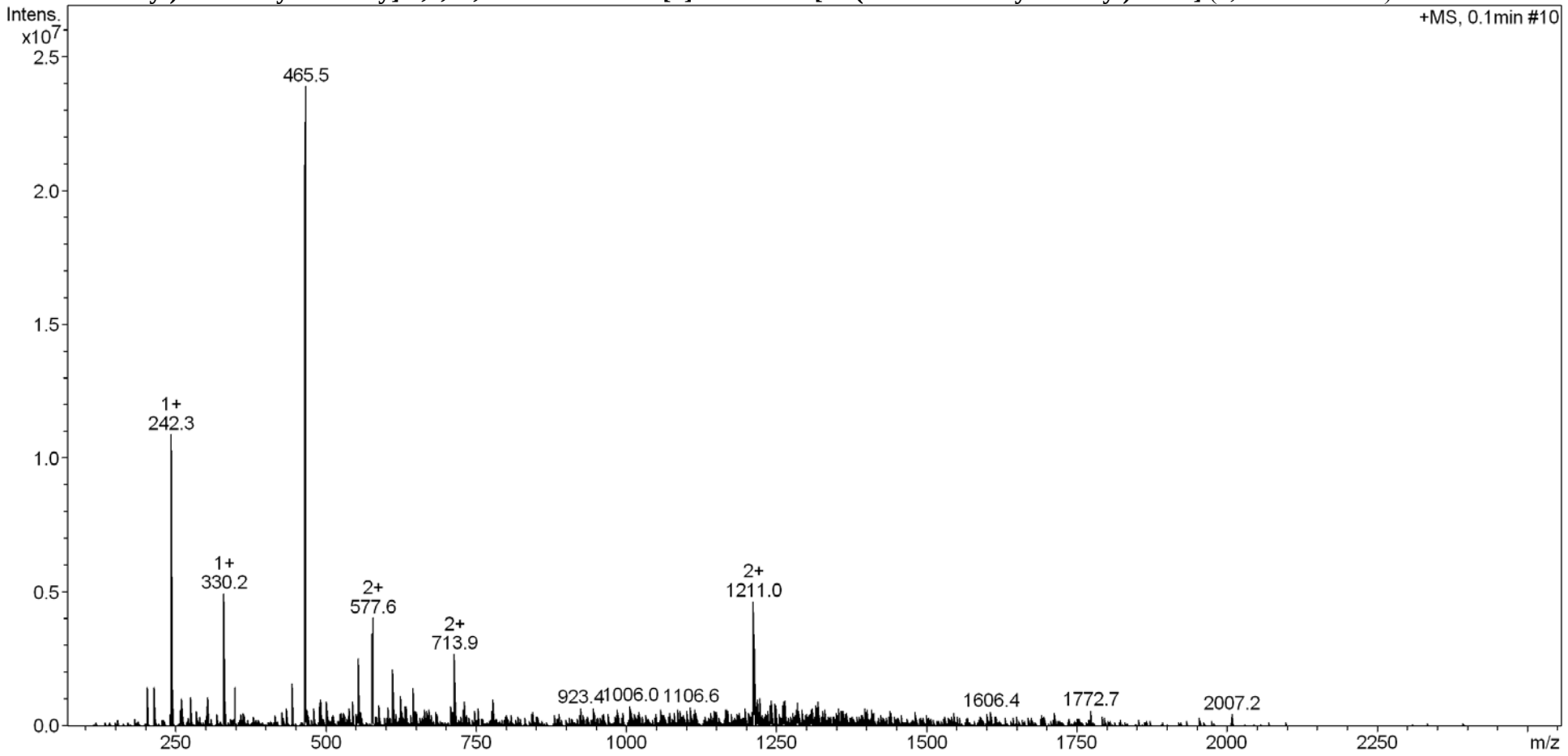

Fig. S148. Mass spectrum (ESI) of 5,11,17,23-tetra-*tert*-butyl-25,26,27,28-tetrakis[(N-(2',2'-diethyl-2'-{(ethoxycarbonylmethyl)amidocarbonylmethyl})-ammoniumethyl)carbomoylmethoxy]-2,8,14,20-tetrathiacalix[4]arene tetra[bis(trifluoromethylsulfonyl)imide] (*1,3-alternate* **70**)

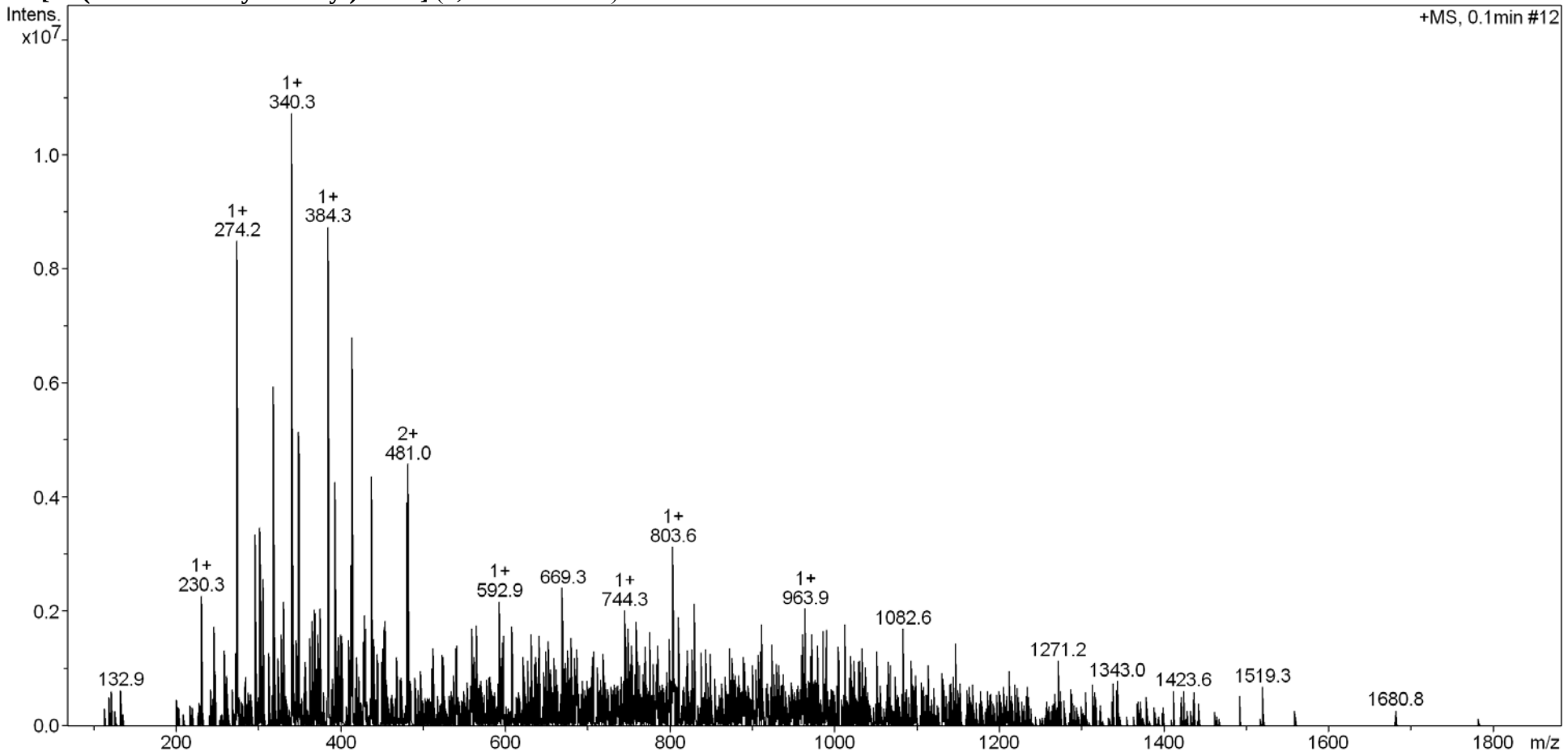

Fig. S149. Mass spectrum (ESI) of 5,11,17,23-tetra-*tert*-butyl-25,26,27,28-tetrakis[(N-(2',2'-diethyl-2'-{([ethoxycarbonylmethyl]amidocarbonylmethyl)-amidocarbonylmethyl}ammoniumethyl)carbomoylmethoxy]-2,8,14,20-tetrathiacalix[4]arene tetra[bis(trifluoromethylsulfonyl)imide] (*1,3-alternate* **71**)

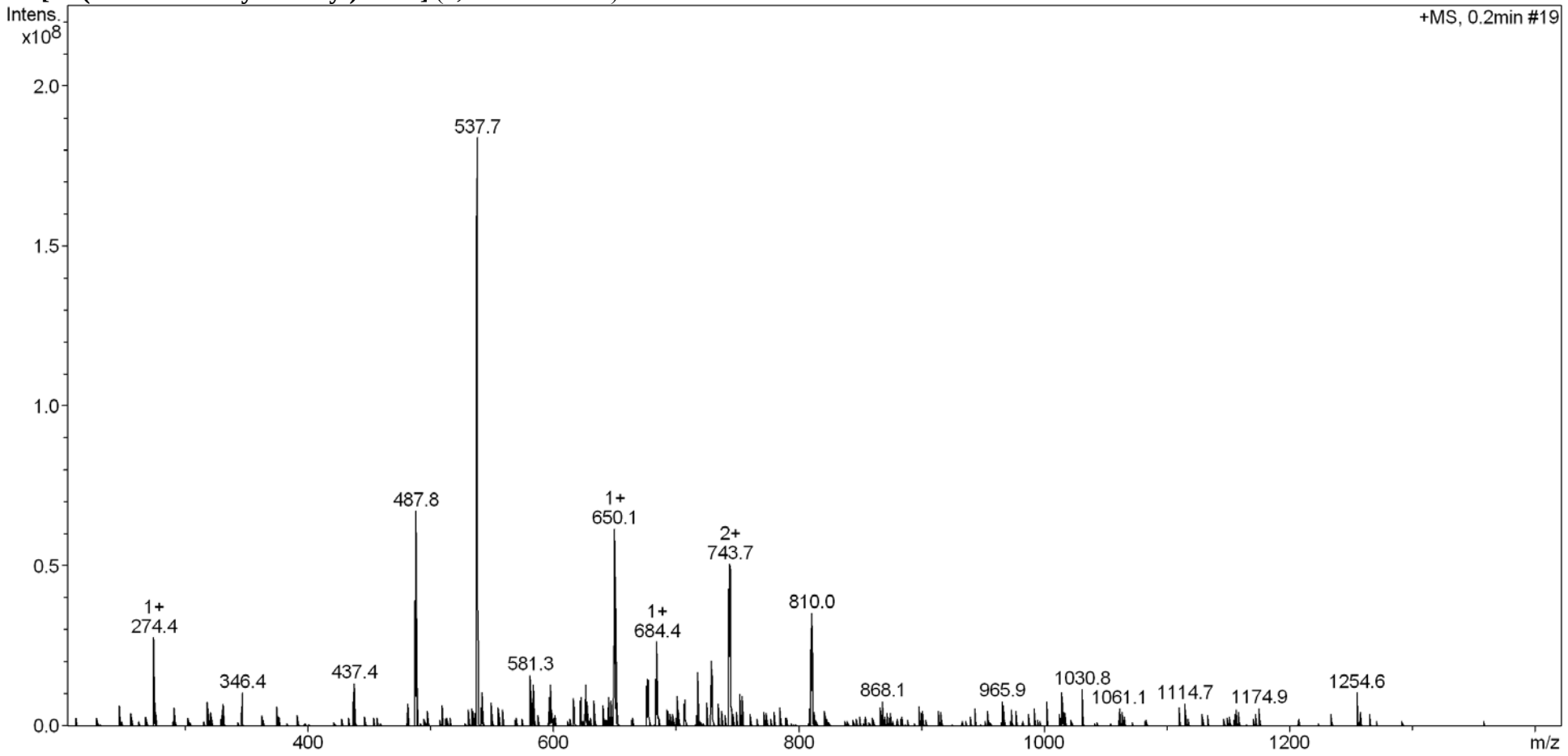

Fig. S150. Mass spectrum (ESI) of 5,11,17,23-tetra-*tert*-butyl-25,26,27,28-tetrakis[(N-(2',2'-diethyl-2'-{(ethoxycarbonyl[S-methyl]methyl)amidocarbonylmethyl}ammoniumethyl)carbomoylmethoxy]-2,8,14,20-tetrathiacalix[4]arene tetra[bis(trifluoromethylsulfonyl)imide] (*1,3-alternate* **72**)

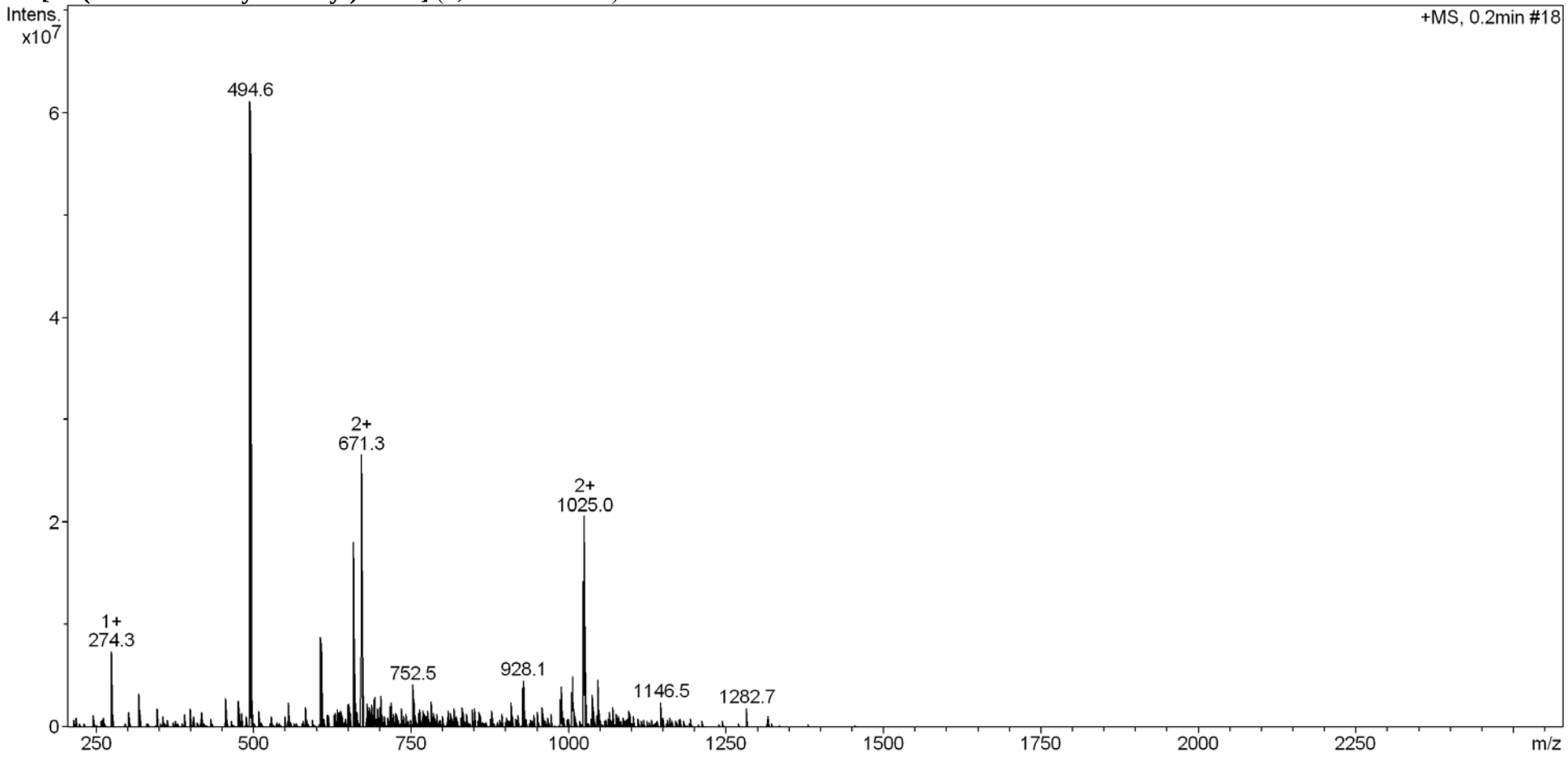

Fig. S151. IR spectrum of 5,11,17,23-tetra-*tert*-butyl-25,26,27,28-tetrakis[(N-(3',3'-dimethyl-3'-(pentoxycarbonylmethyl)-ammoniumpropyl)carbomoylmethoxy]-2,8,14,20-tetrathiacalix[4]arene tetrabromide (*cone* **9**)

Fig. S152. IR spectrum of 5,11,17,23-tetra-*tert*-butyl-25,26,27,28-tetrakis[(N-(2',2',2'-triethyl)ammoniumethyl)carbomoylmethoxy]-2,8,14,20-tetrathiacalix[4]arene tetraiodide (*cone* **15**)

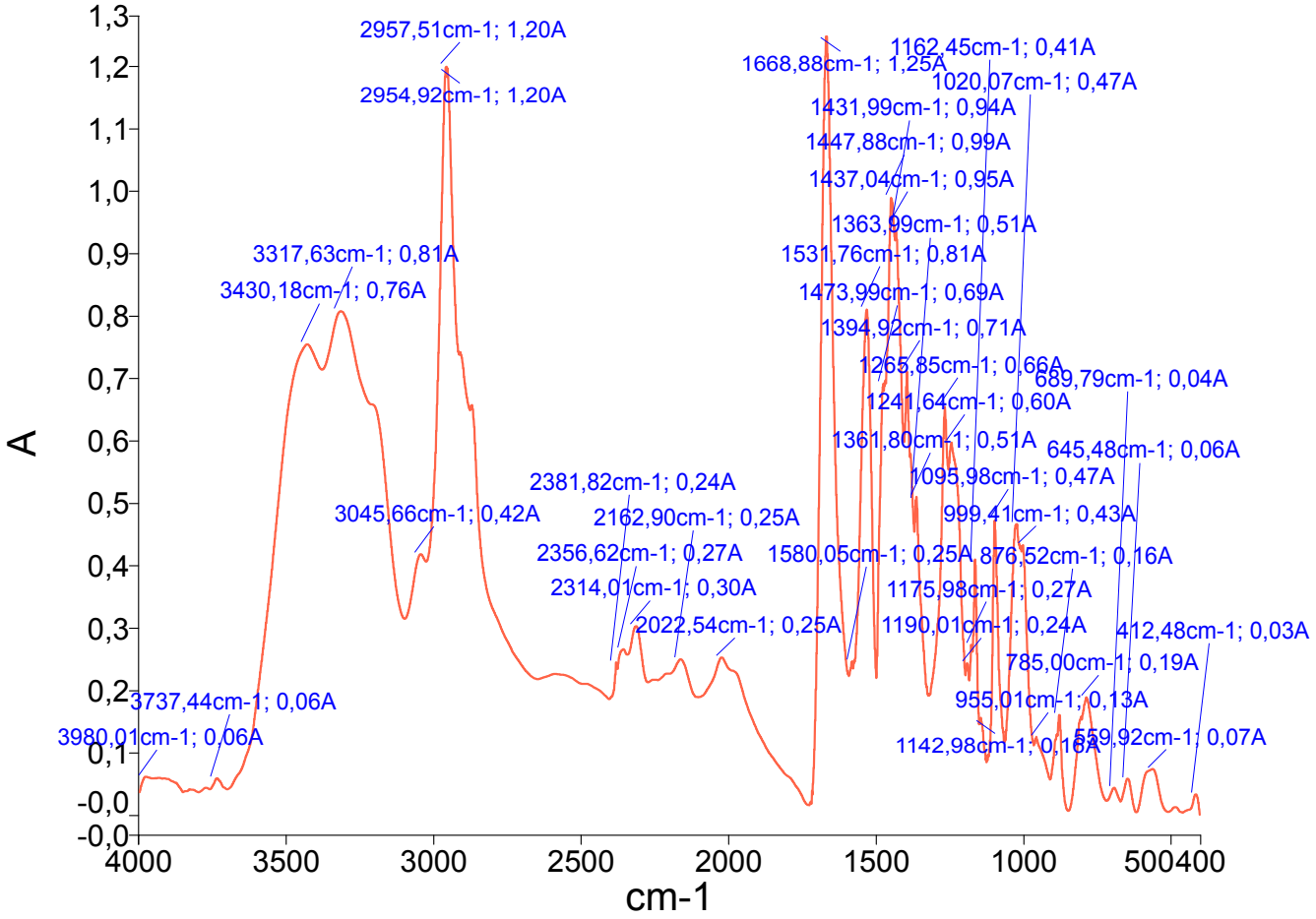

Fig. S153. IR spectrum of 5,11,17,23-tetra-*tert*-butyl-25,26,27,28-tetrakis[(N-(2',2'-diethyl-2'-benzyl)ammoniumethyl)carbomoylmethoxy]-2,8,14,20-tetrathiacalix[4]arene tetrabromide (*cone* **16**)

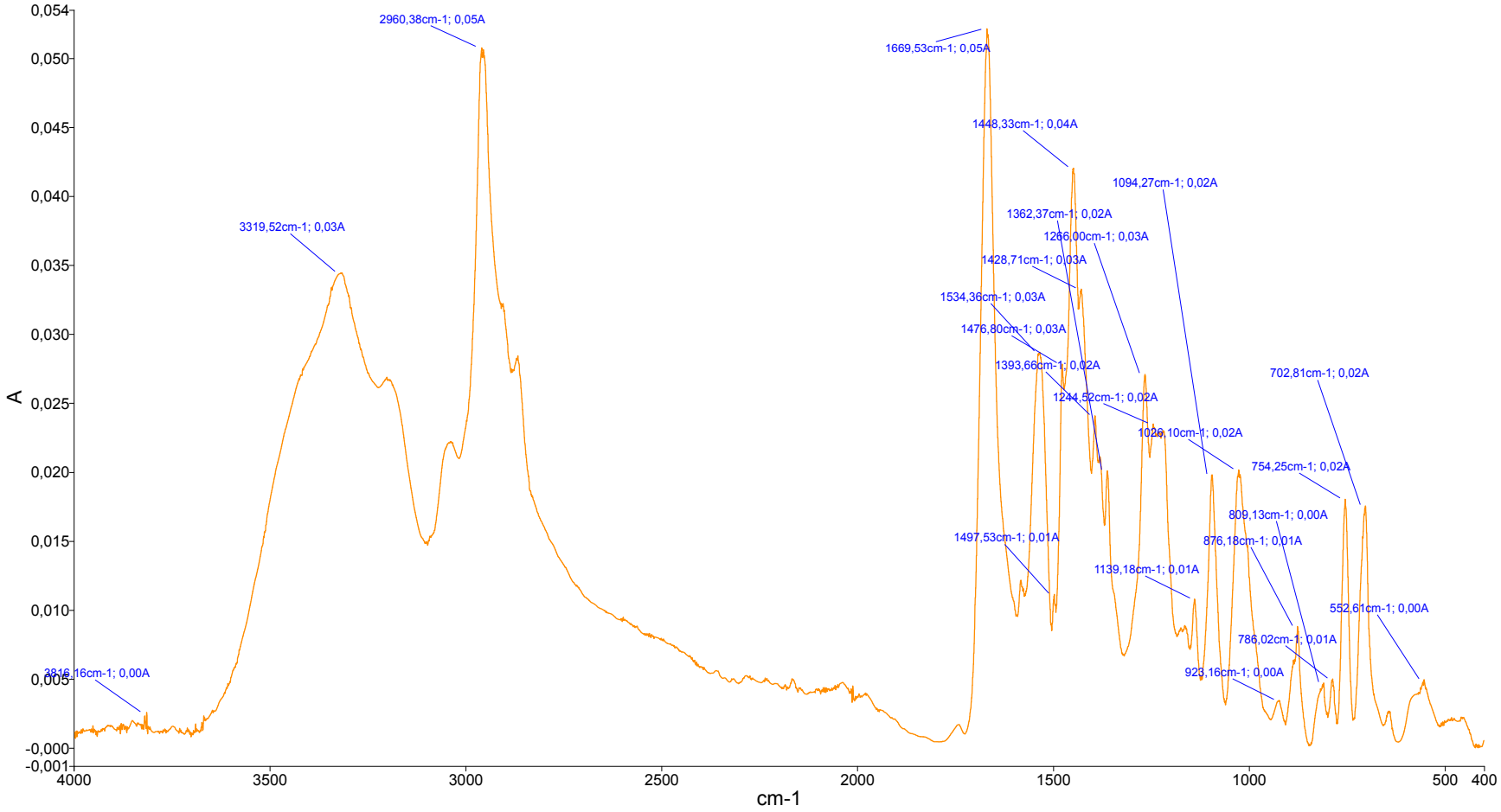

Fig. S154. IR spectrum of 5,11,17,23-tetra-*tert*-butyl-25,26,27,28-tetrakis[(N-(2',2'-diethyl-2'-(ethoxycarbonylmethyl)-ammoniumethyl)carbomoylmethoxy]-2,8,14,20-tetrathiacalix[4]arene tetrabromide (*cone* **17**)

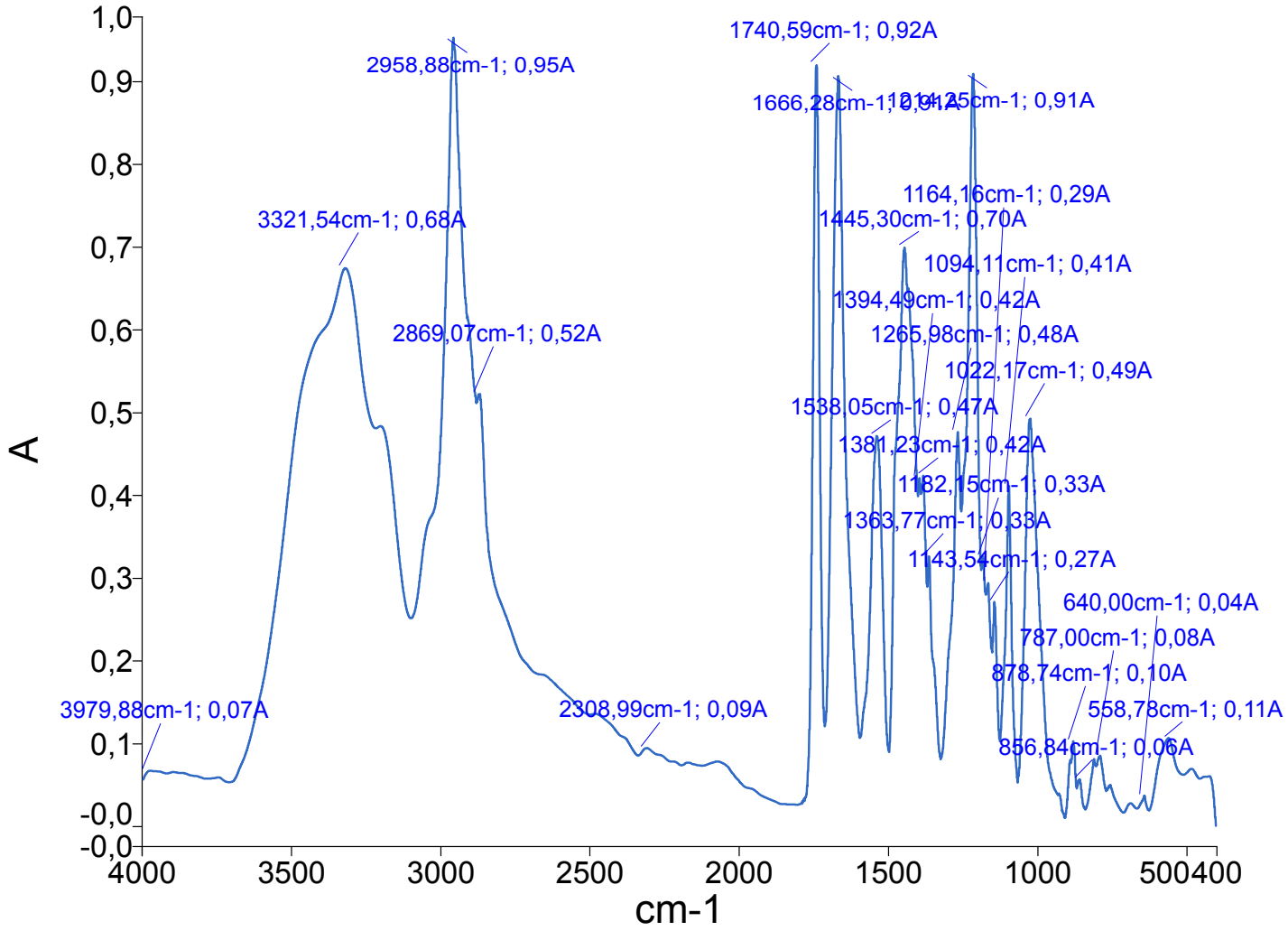

Fig. S155. IR spectrum of 5,11,17,23-tetra-*tert*-butyl-25,26,27,28-tetrakis[(N-(2',2'-diethyl-2'-(pentoxycarbonylmethyl)-ammoniumethyl)carbomoylmethoxy]-2,8,14,20-tetrathiacalix[4]arene tetrabromide (*cone* **18**)

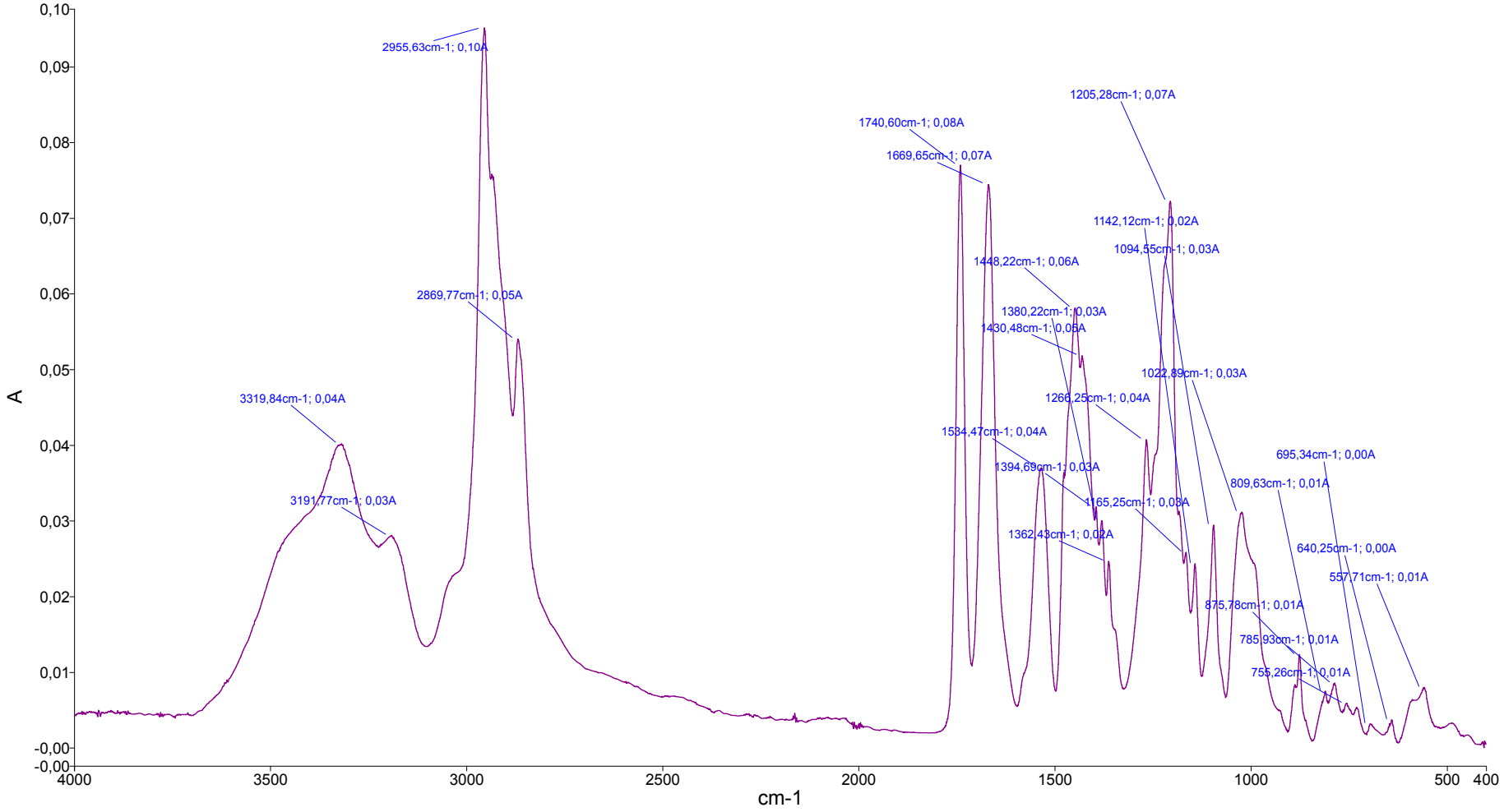

Fig. S156. IR spectrum of 5,11,17,23-tetra-*tert*-butyl-25,26,27,28-tetrakis[(N-(3',3',3'-trimethyl)ammoniumpropyl)carbomoylmethoxy]-2,8,14,20-tetrathiacalix[4]arene tetraiodide (*1,3-alternate* **22**)

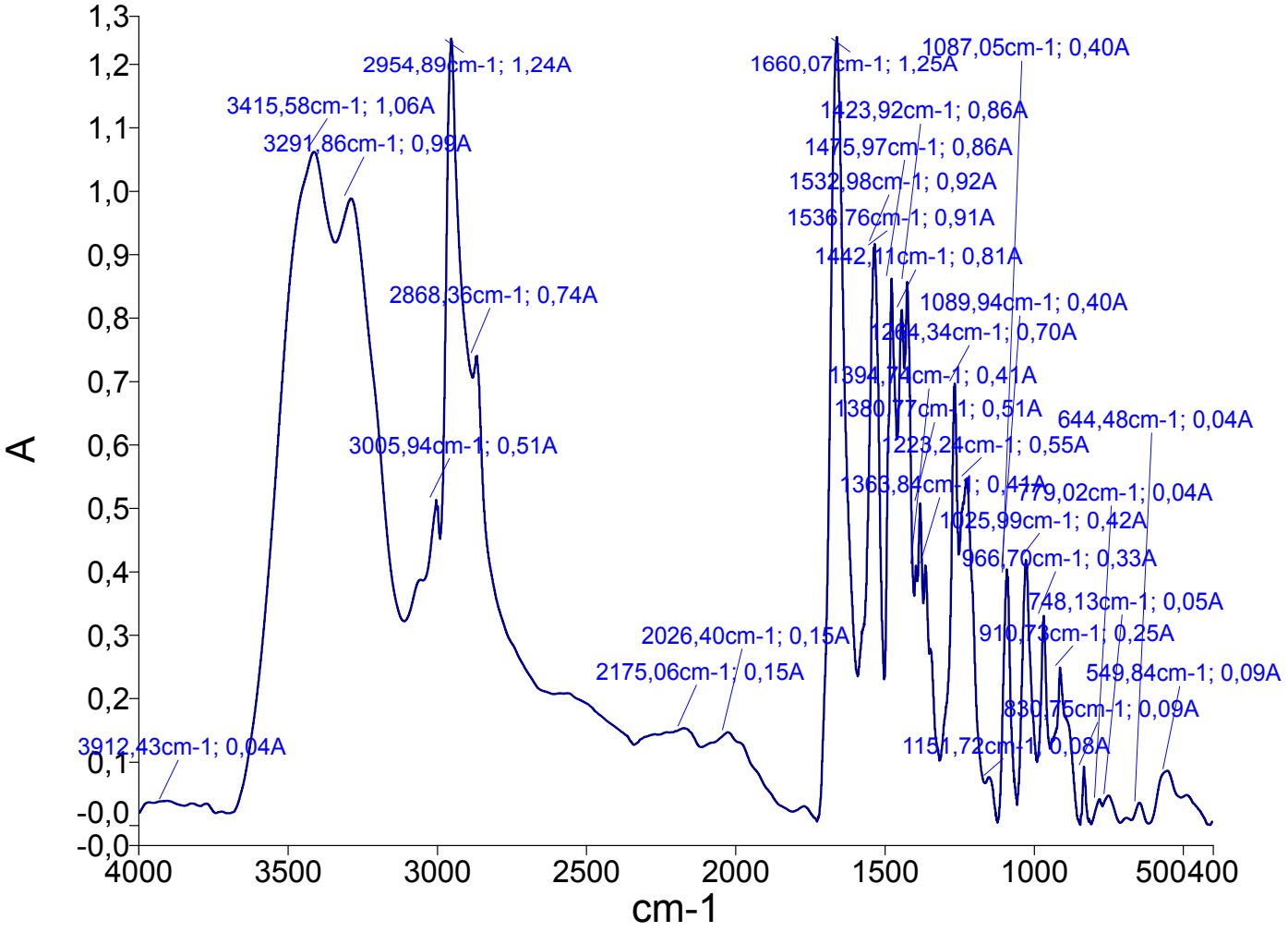

Fig. S157. IR spectrum of 5,11,17,23-tetra-*tert*-butyl-25,26,27,28-tetrakis[(N-(3',3'-dimethyl-3'-ethyl)ammoniumpropyl)carbomoylmethoxy]-2,8,14,20-tetrathiacalix[4]arene tetraiodide (*1,3-alternate* **23**)

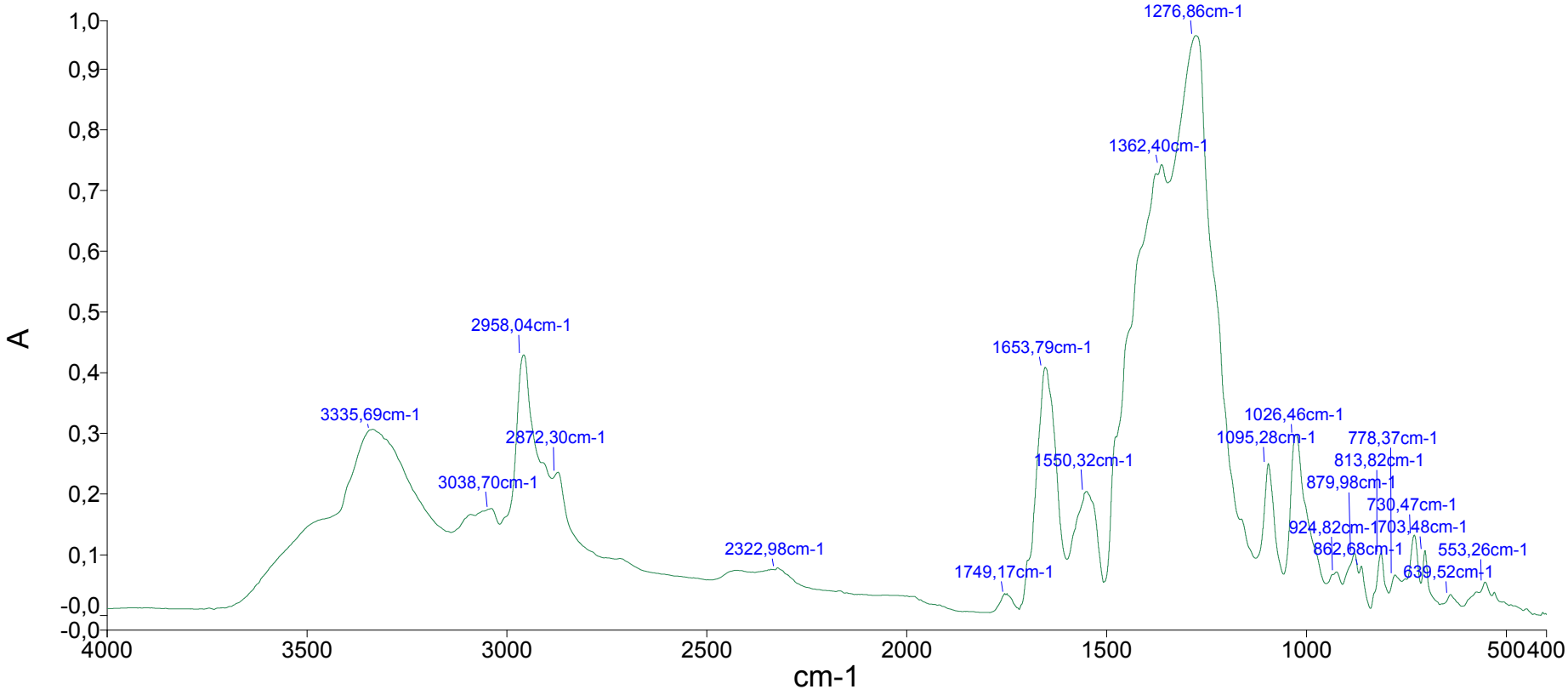

Fig. S158. IR spectrum of 5,11,17,23-tetra-*tert*-butyl-25,26,27,28-tetrakis[(N-(3',3'-dimethyl-3'-benzyl)ammoniumpropyl)carbomoylmethoxy]-2,8,14,20-tetrathiacalix[4]arene tetrabromide (*1,3-alternate* **24**)

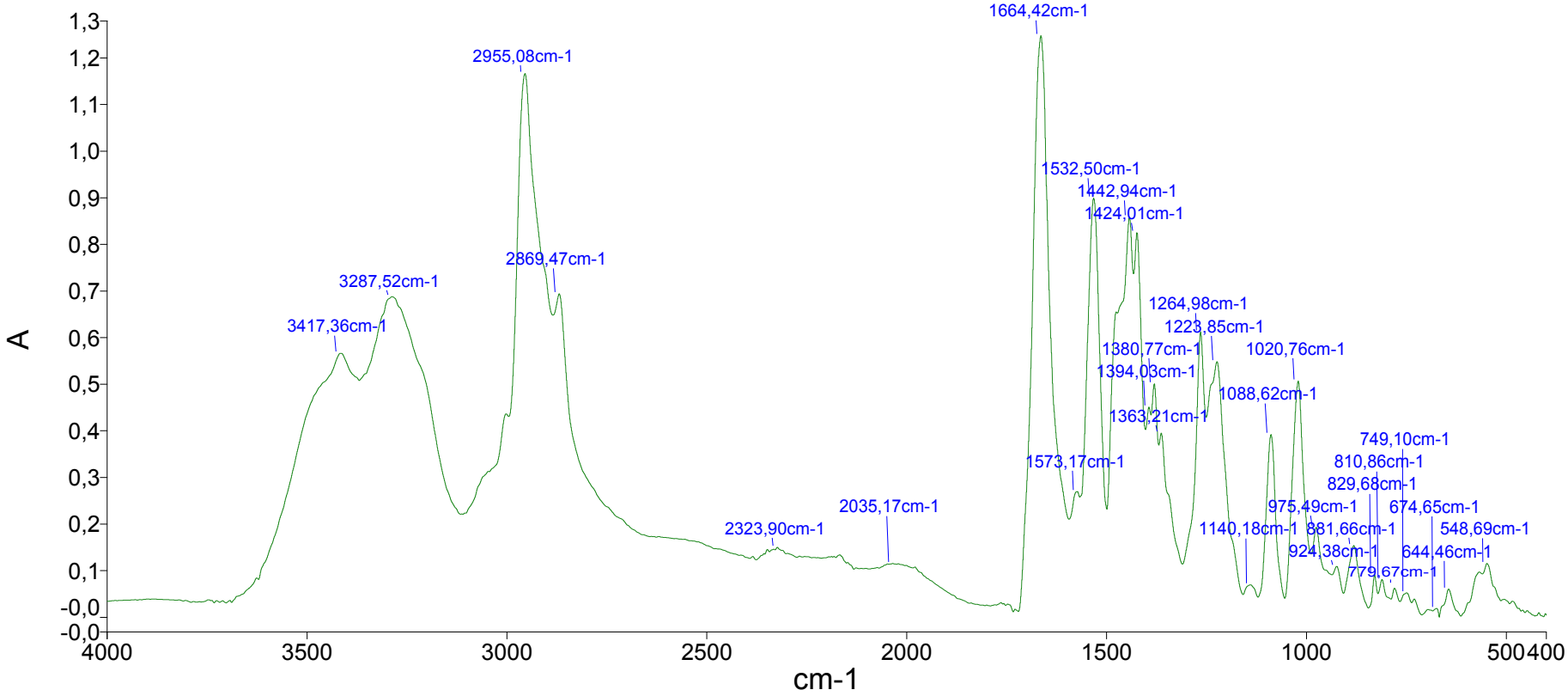

Fig. S159. IR spectrum of 5,11,17,23-tetra-*tert*-butyl-25,26,27,28-tetrakis[(N-(3',3'-dimethyl-3'-(ethoxycarbonylmethyl)-ammoniumpropyl)carbomoylmethoxy]-2,8,14,20-tetrathiacalix[4]arene tetrabromide (*1,3-alternate* **25**)

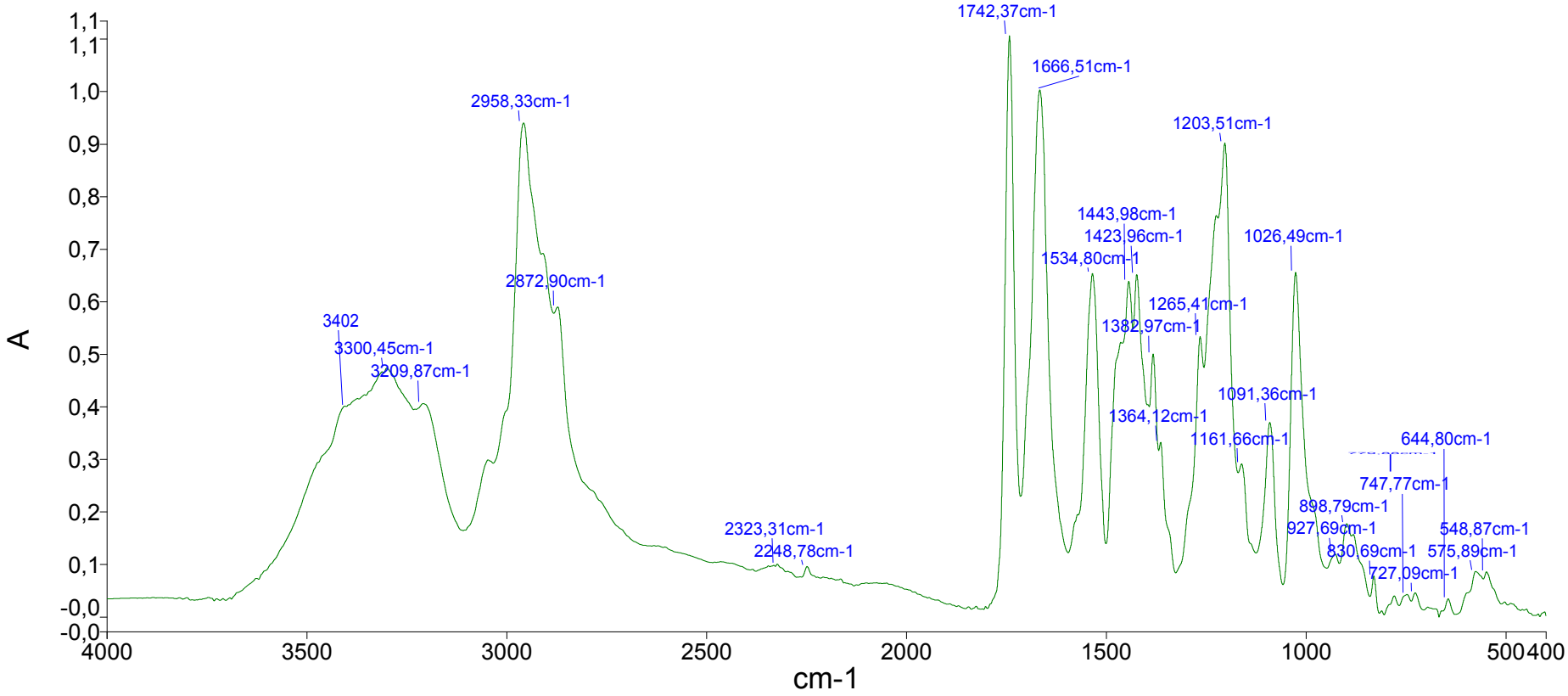

Fig. S160. IR spectrum of 5,11,17,23-tetra-*tert*-butyl-25,26,27,28-tetrakis[(N-(3',3'-dimethyl-3'-(pentoxycarbonylmethyl)-ammoniumpropyl)carbomoylmethoxy]-2,8,14,20-tetrathiacalix[4]arene tetrabromide (*1,3-alternate* **26**)

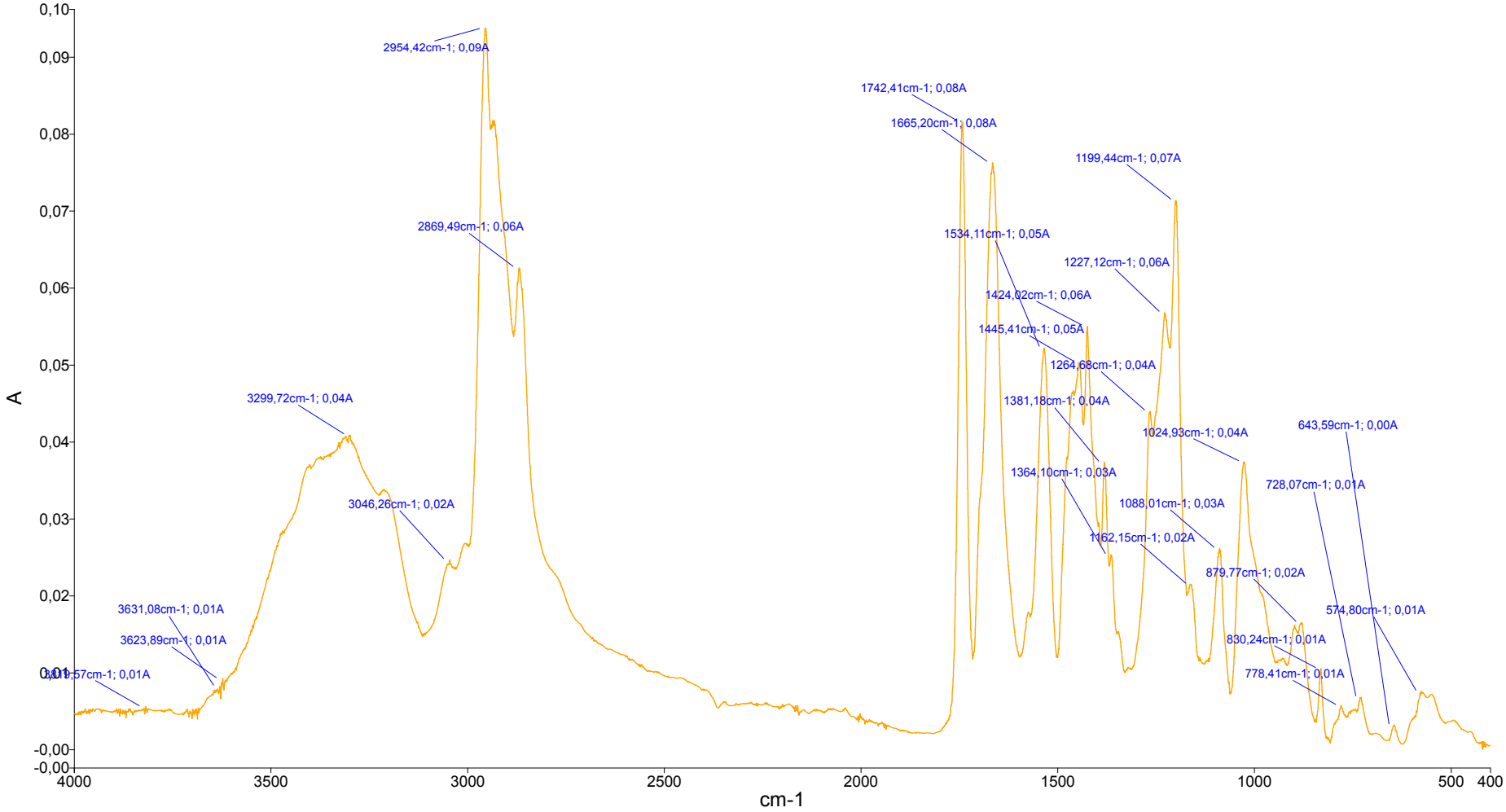

Fig. S161. IR spectrum of 5,11,17,23-tetra-*tert*-butyl-25,26,27,28-tetrakis[(N-(3',3'-dimethyl-3'-{3''-propylphtalimide}-ammoniumpropyl)carbomoylmethoxy]-2,8,14,20-tetrathiacalix[4]arene tetrabromide (*1,3-alternate* **30**)

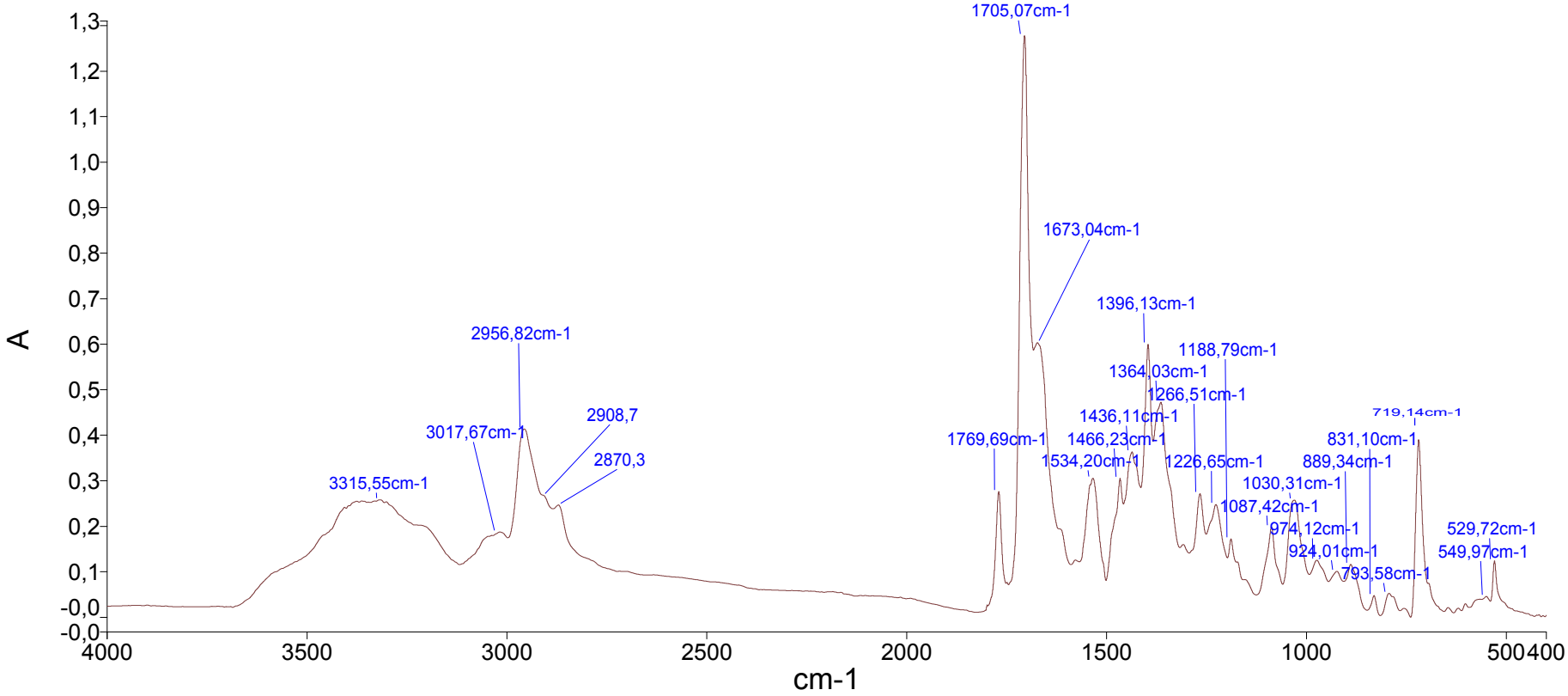

Fig. S162. IR spectrum of 5,11,17,23-tetra-*tert*-butyl-25,26,27,28-tetrakis[(N-(2'-methyl-2',2'-diethyl)ammoniumethyl)carbomoylmethoxy]-2,8,14,20-tetrathiacalix[4]arene tetraiodide (*1,3-alternate* **31**)

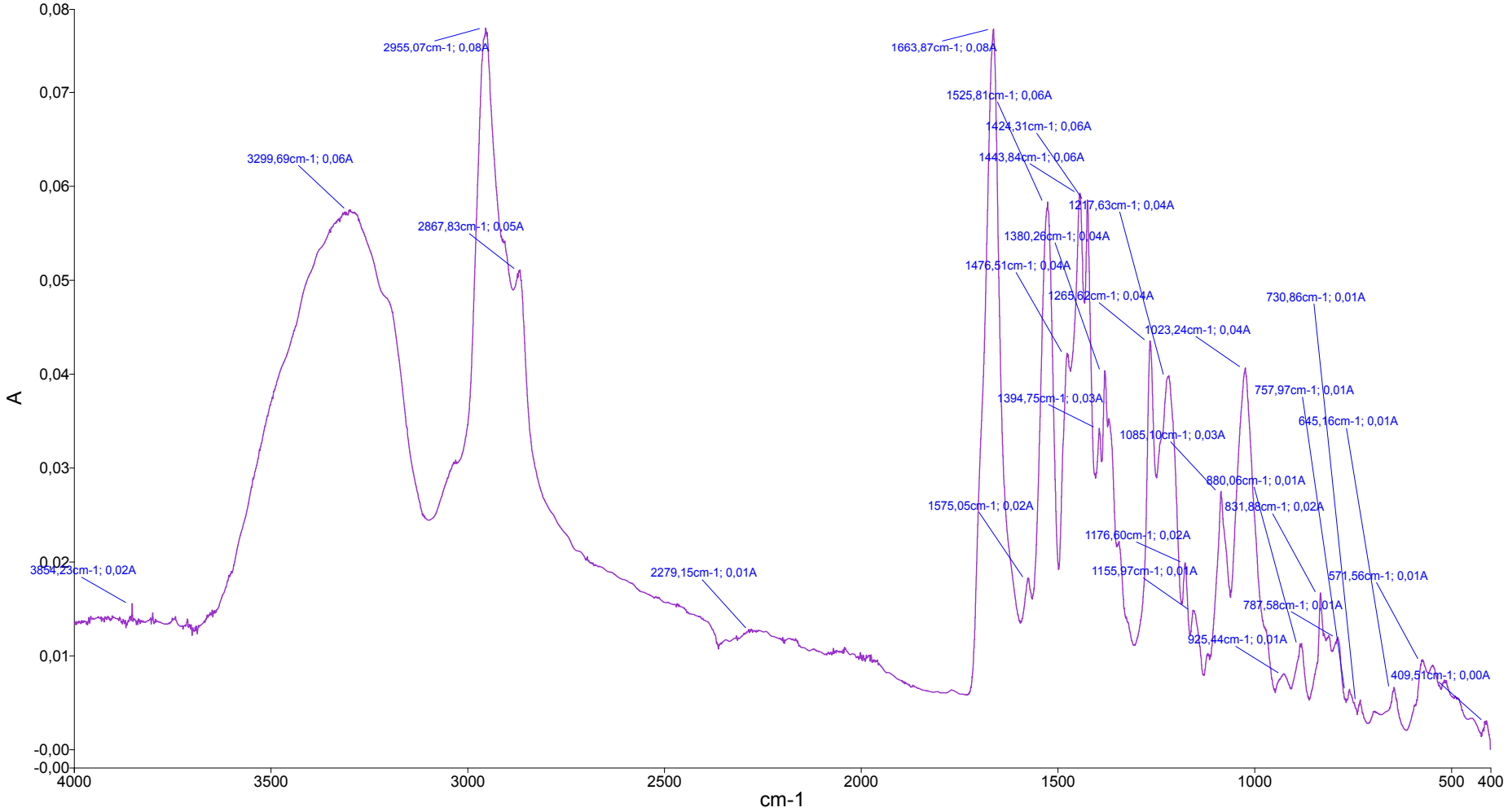

Fig. S163. IR spectrum of 5,11,17,23-tetra-*tert*-butyl-25,26,27,28-tetrakis[(N-(2',2',2'-triethyl)ammoniumethyl)carbomoylmethoxy]-2,8,14,20-tetrathiacalix[4]arene tetraiodide (*1,3-alternate* **32**)

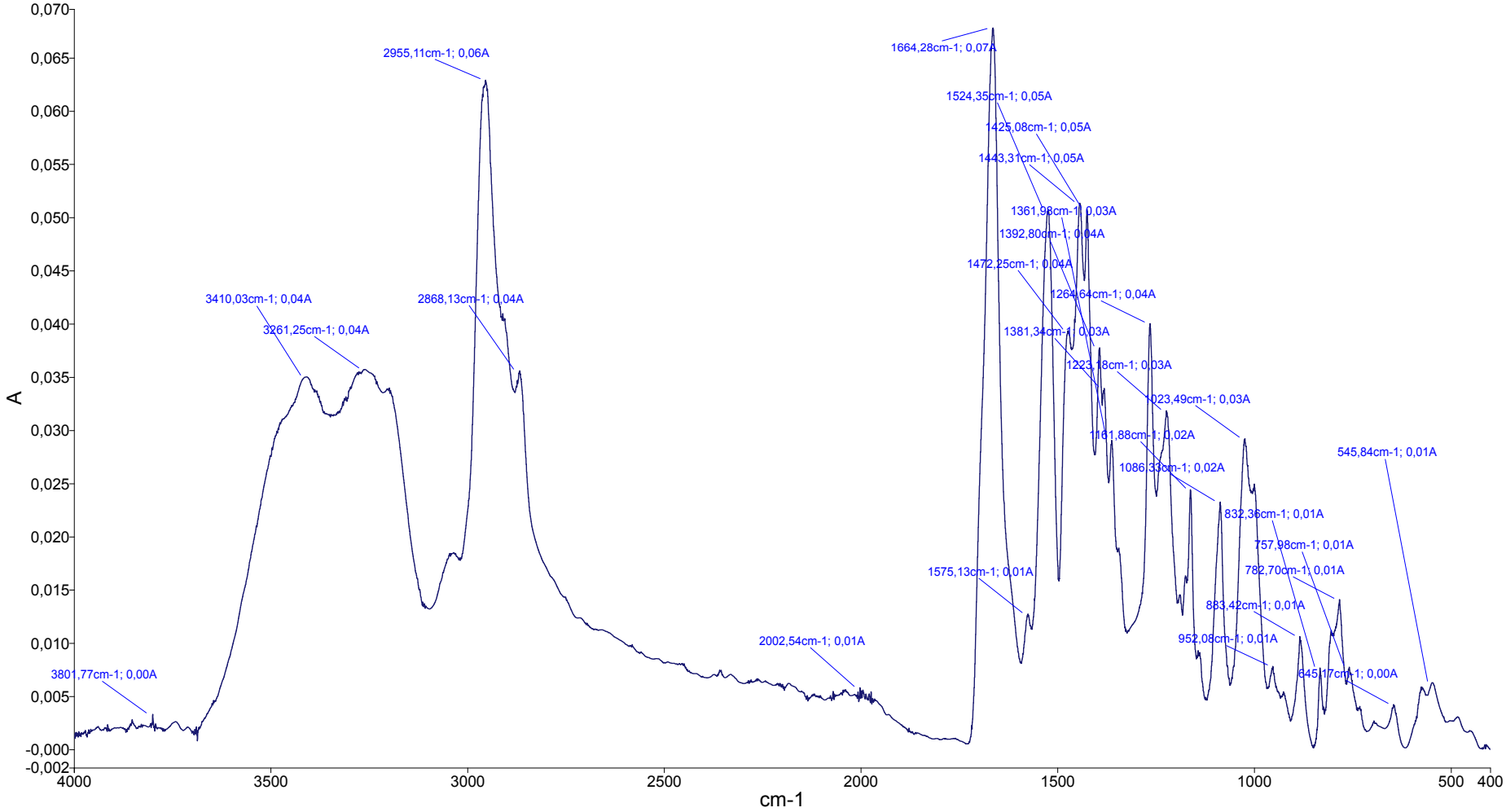

Fig. S164. IR spectrum of 5,11,17,23-tetra-*tert*-butyl-25,26,27,28-tetrakis[(N-(2',2'-diethyl-2'-(benzyl)ammoniumpropyl)carbomoylmethoxy]-2,8,14,20-tetrathiacalix[4]arene tetrabromide (*1,3-alternate* **33**)

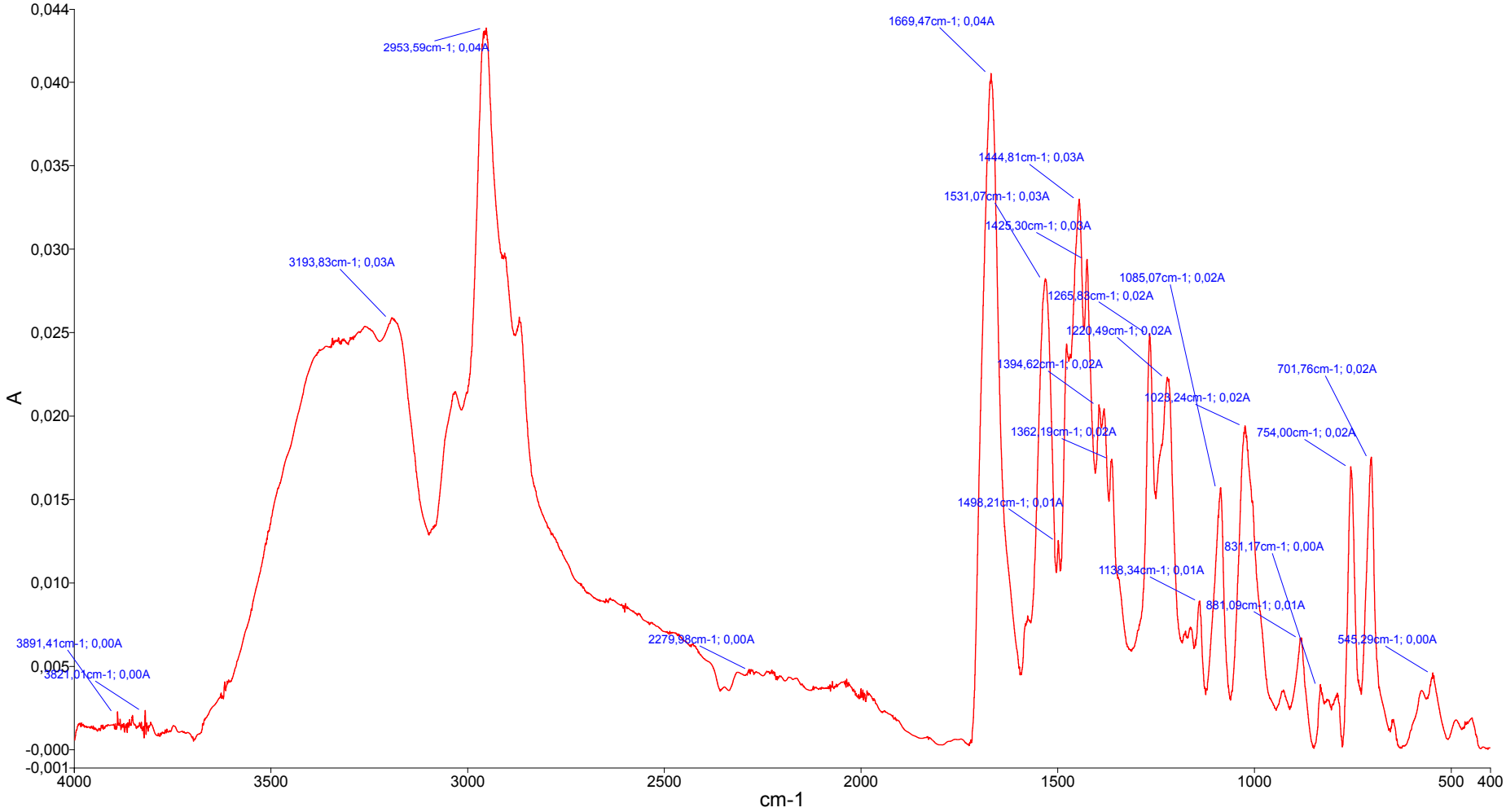

Fig. S165. IR spectrum of 5,11,17,23-tetra-*tert*-butyl-25,26,27,28-tetrakis[(N-(2',2'-diethyl-2'-(ethoxycarbonylmethyl)-ammoniumethyl)carbomoylmethoxy]-2,8,14,20-tetrathiacalix[4]arene tetrabromide (*1,3-alternate* **34**)

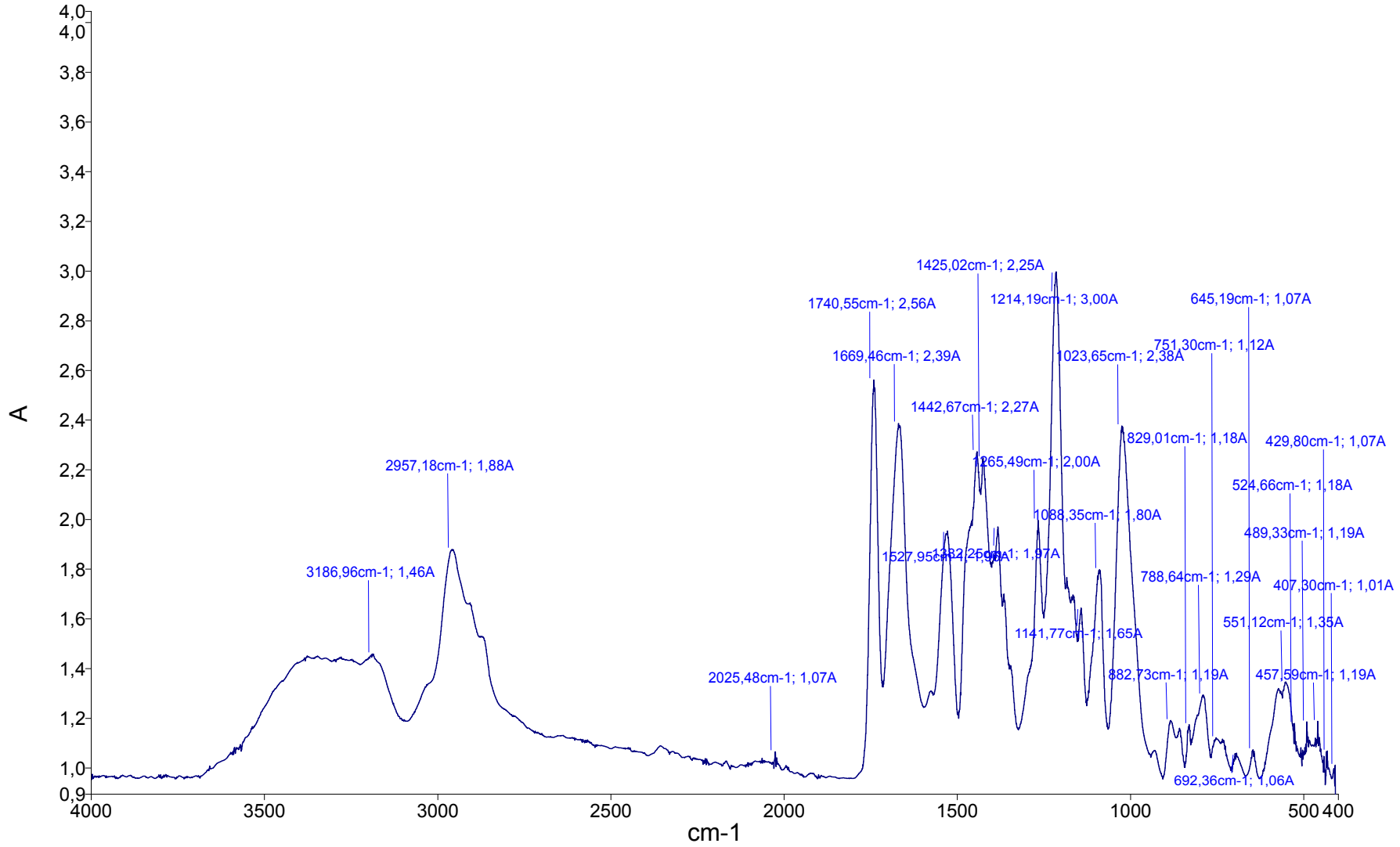

Fig. S166. IR spectrum of 5,11,17,23-tetra-*tert*-butyl-25,26,27,28-tetrakis[(N-(2',2'-diethyl-2'-(pentoxycarbonylmethyl)-ammoniumethyl)carbomoylmethoxy]-2,8,14,20-tetrathiacalix[4]arene tetrabromide (*1,3-alternate* **35**)

Fig. S167. IR spectrum of 5,11,17,23-tetra-*tert*-butyl-25,26,27,28-tetrakis[(N-(3',3',3'-trimethyl)ammoniumpropyl)carbomoylmethoxy]-2,8,14,20-tetrathiacalix[4]arene tetra[bis(trifluoromethylsulfonyl)imide] (*cone* **39**)

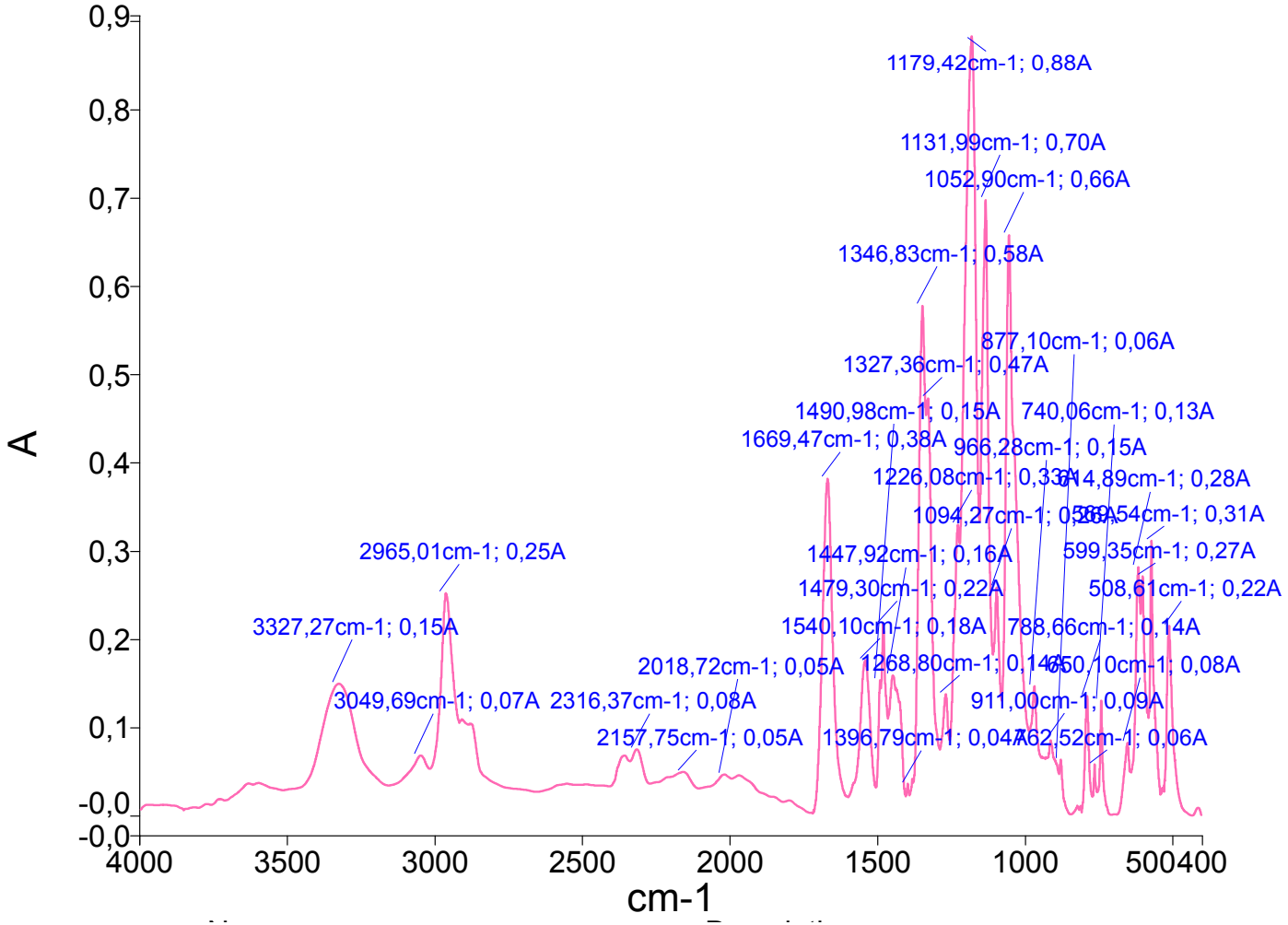

Fig. S168. IR spectrum of 5,11,17,23-tetra-*tert*-butyl-25,26,27,28-tetrakis[(N-(3',3'-dimethyl-3'-ethyl)ammoniumpropyl)carbomoylmethoxy]-2,8,14,20-tetrathiacalix[4]arene tetra[bis(trifluoromethylsulfonyl)imide] (*cone* **40**)

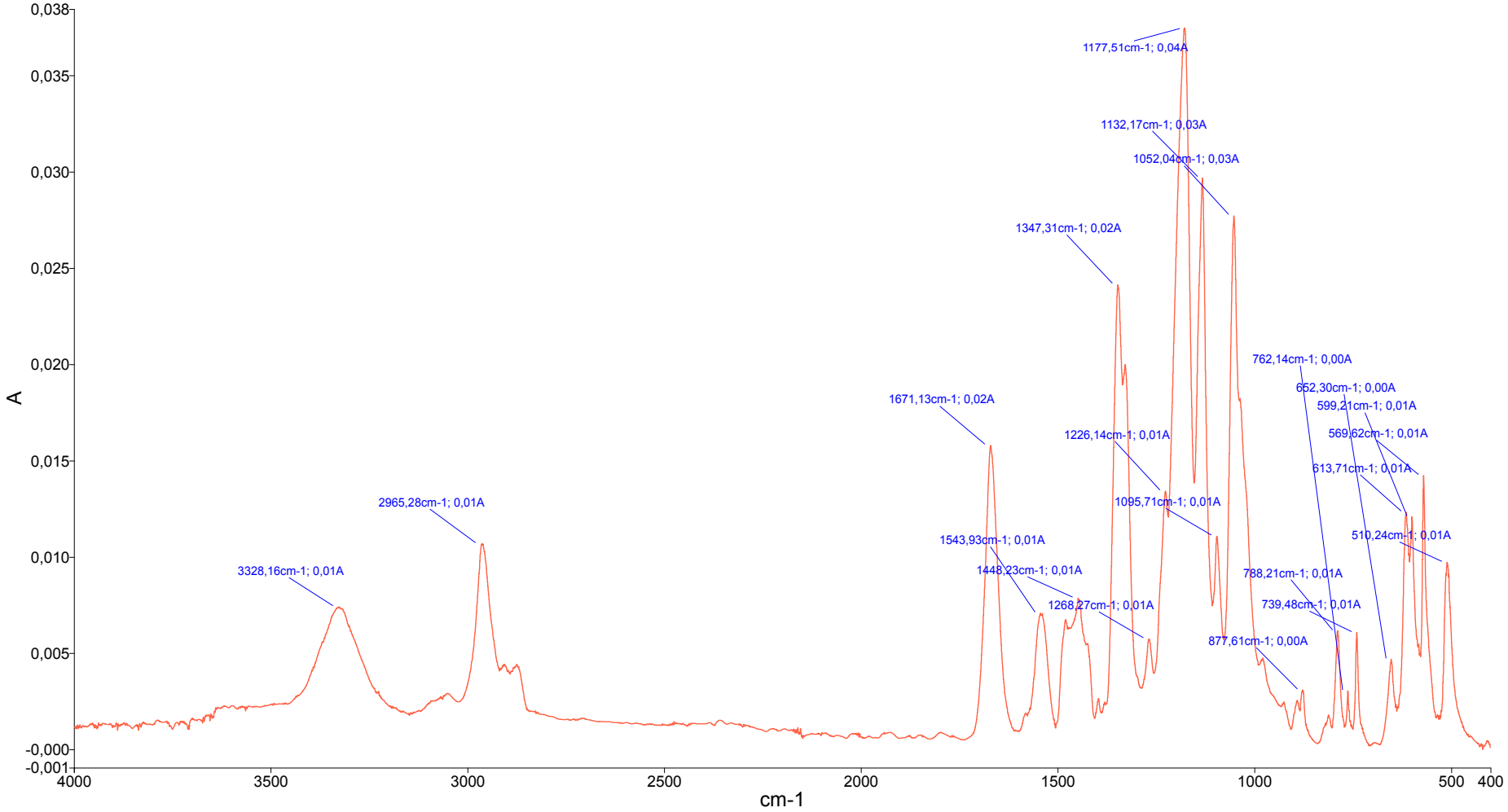

Fig. S169. IR spectrum of 5,11,17,23-tetra-*tert*-butyl-25,26,27,28-tetrakis[(N-(3',3'-dimethyl-3'-benzyl)ammoniumpropyl)carbomoylmethoxy]-2,8,14,20-tetrathiacalix[4]arene tetra[bis(trifluoromethylsulfonyl)imide] (*cone* **41**)

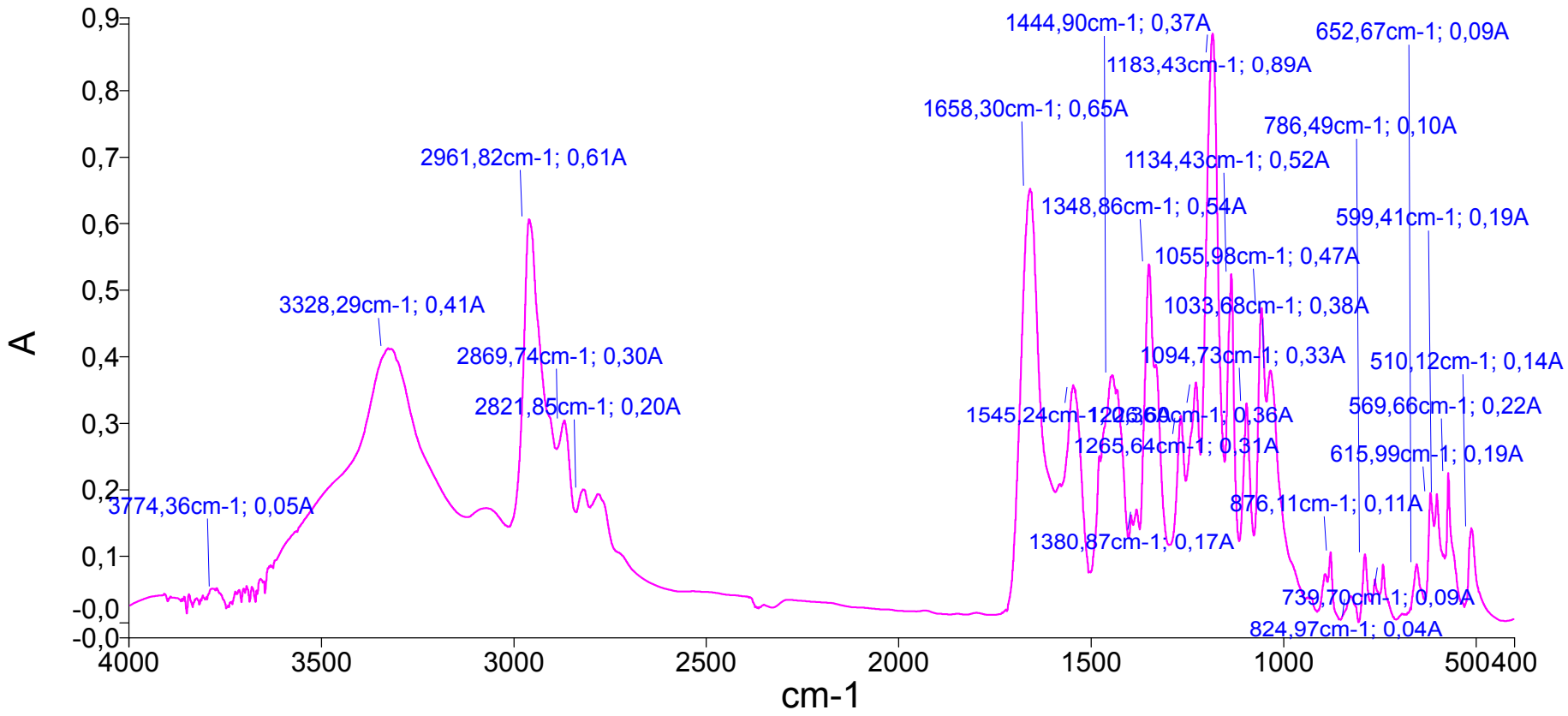

Fig. S170. IR spectrum of 5,11,17,23-tetra-*tert*-butyl-25,26,27,28-tetrakis[(N-(3',3'-dimethyl-3'-(ethoxycarbonylmethyl)ammoniumpropyl)-carbomoylmethoxy]-2,8,14,20-tetrathiacalix[4]arene tetra[bis(trifluoromethylsulfonyl)imide] (*cone* **42**)

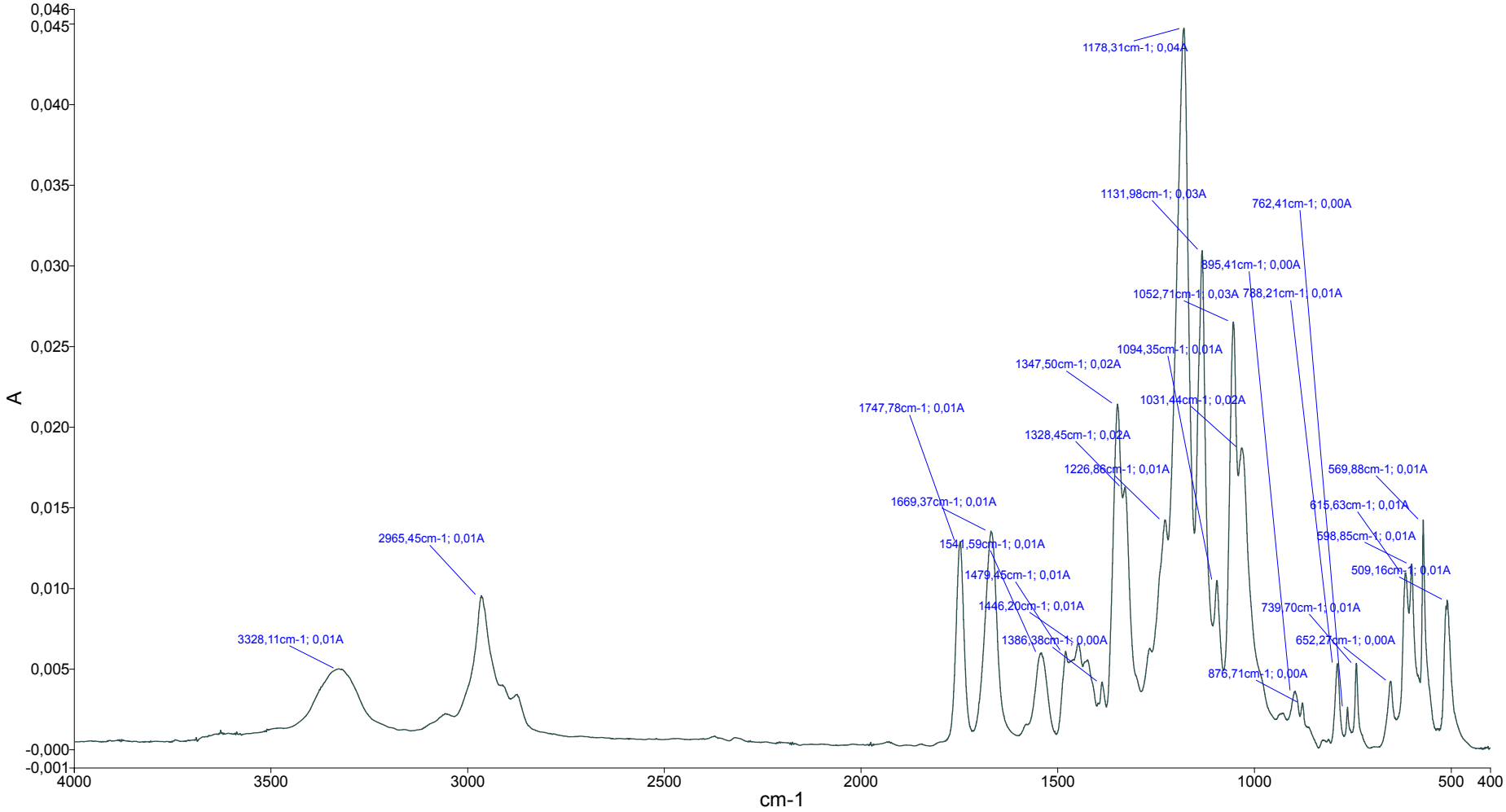

Fig. S171. IR spectrum of 5,11,17,23-tetra-*tert*-butyl-25,26,27,28-tetrakis[(N-(3',3'-dimethyl-3'-(pentoxycarbonylmethyl)ammoniumpropyl)-carbomoylmethoxy]-2,8,14,20-tetrathiacalix[4]arene tetra[bis(trifluoromethylsulfonyl)imide] (*cone* **43**)

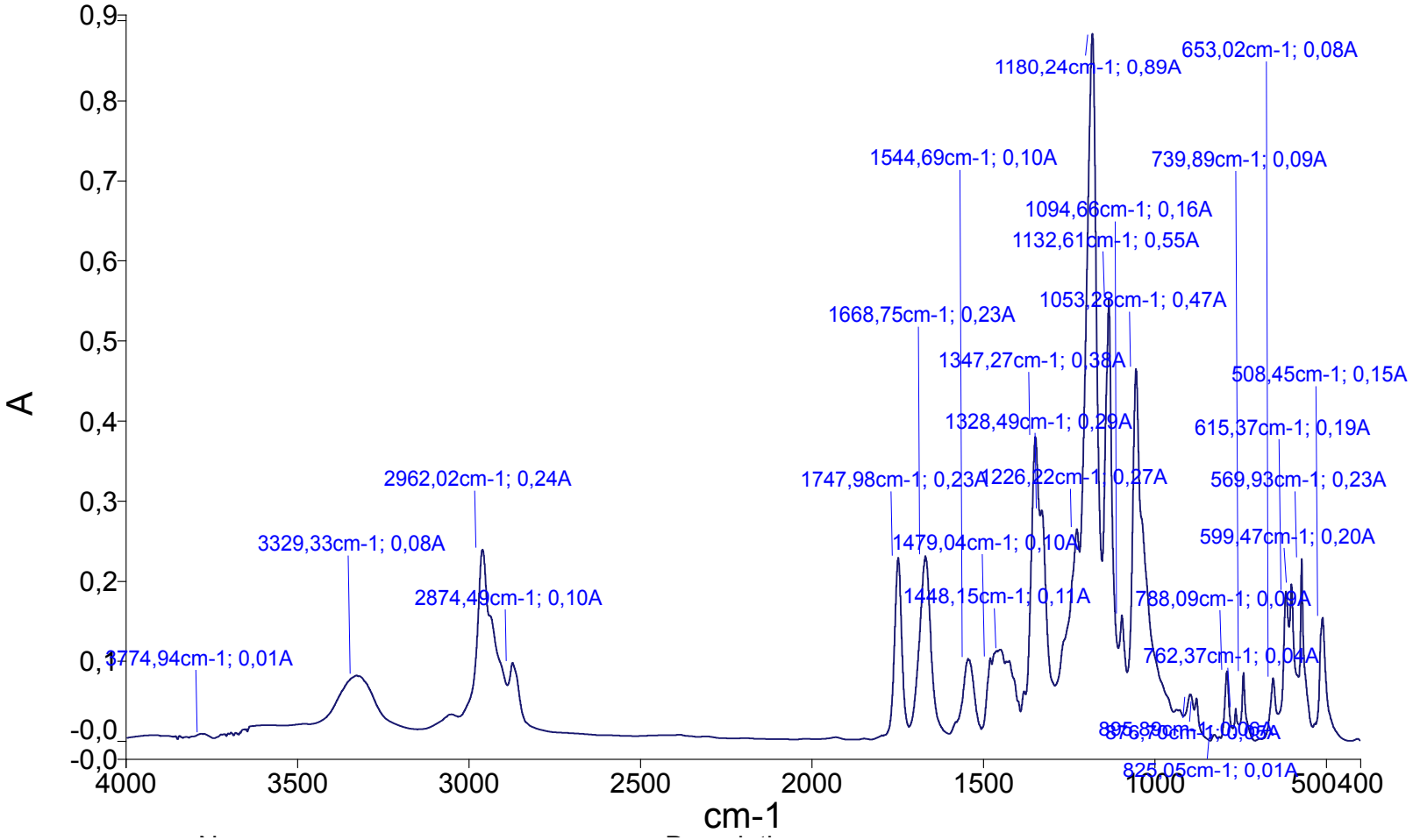

Fig. S172. IR spectrum of 5,11,17,23-tetra-*tert*-butyl-25,26,27,28-tetrakis[(N-(3',3'-dimethyl-3'-{(ethoxycarbonylmethyl)amidocarbonylmethyl}-ammoniumpropyl)carbomoylmethoxy]-2,8,14,20-tetrathiacalix[4]arene tetra[bis(trifluoromethylsulfonyl)imide] (*cone* 44)

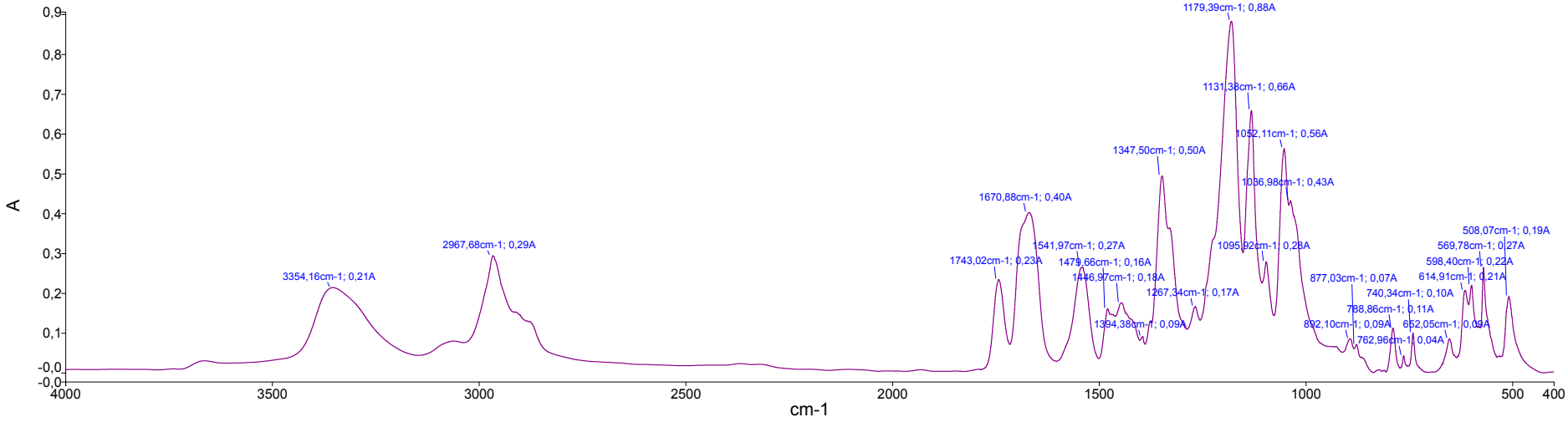

Fig. S173. IR spectrum of 5,11,17,23-tetra-*tert*-butyl-25,26,27,28-tetrakis[(N-(3',3'-dimethyl-3'-{([ethoxycarbonylmethyl]-amidocarbonylmethyl)amidocarbonylmethyl}ammoniumpropyl)carbomoylmethoxy]-2,8,14,20-tetrathiacalix[4]arene tetra[bis(trifluoromethylsulfonyl)imide] (*cone* **45**)

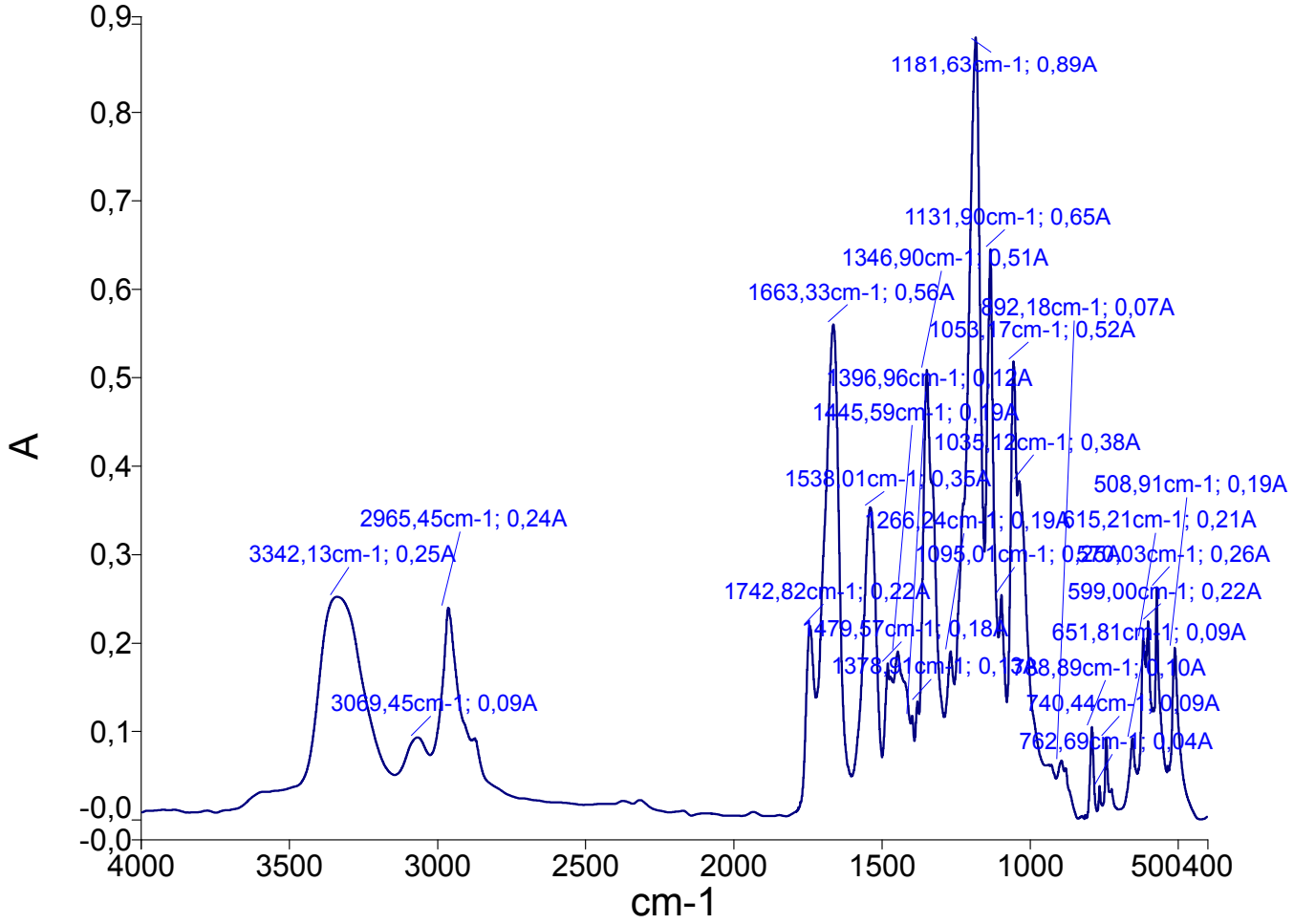

Fig. S174. IR spectrum of 5,11,17,23-tetra-*tert*-butyl-25,26,27,28-tetrakis[(N-(3',3'-dimethyl-3'-{(ethoxycarbonyl[S-methyl]methyl)amidocarbonylmethyl}ammoniumpropyl)carbomoylmethoxy]-2,8,14,20-tetrathiacalix[4]arene tetra[bis(trifluoromethylsulfonyl)imide] (*cone* **46**)

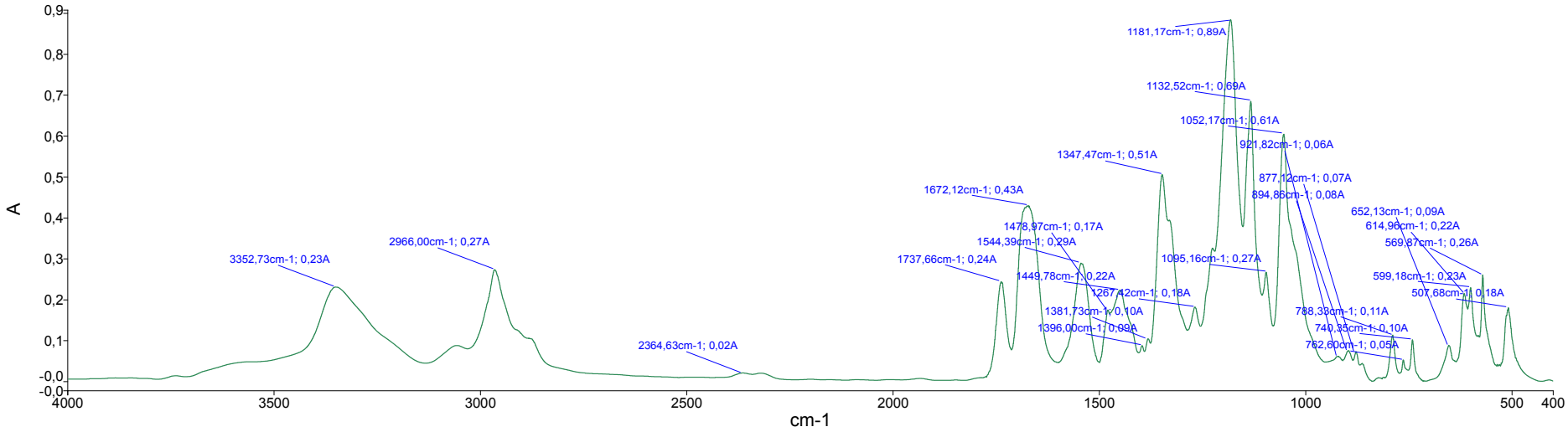

Fig. S175. IR spectrum of 5,11,17,23-tetra-*tert*-butyl-25,26,27,28-tetrakis[(N-(3',3'-dimethyl-3'-{3''-propylphtalimide}ammoniumpropyl)-carbomoylmethoxy]-2,8,14,20-tetrathiacalix[4]arene tetra[bis(trifluoromethylsulfonyl)imide] (*cone* **47**)

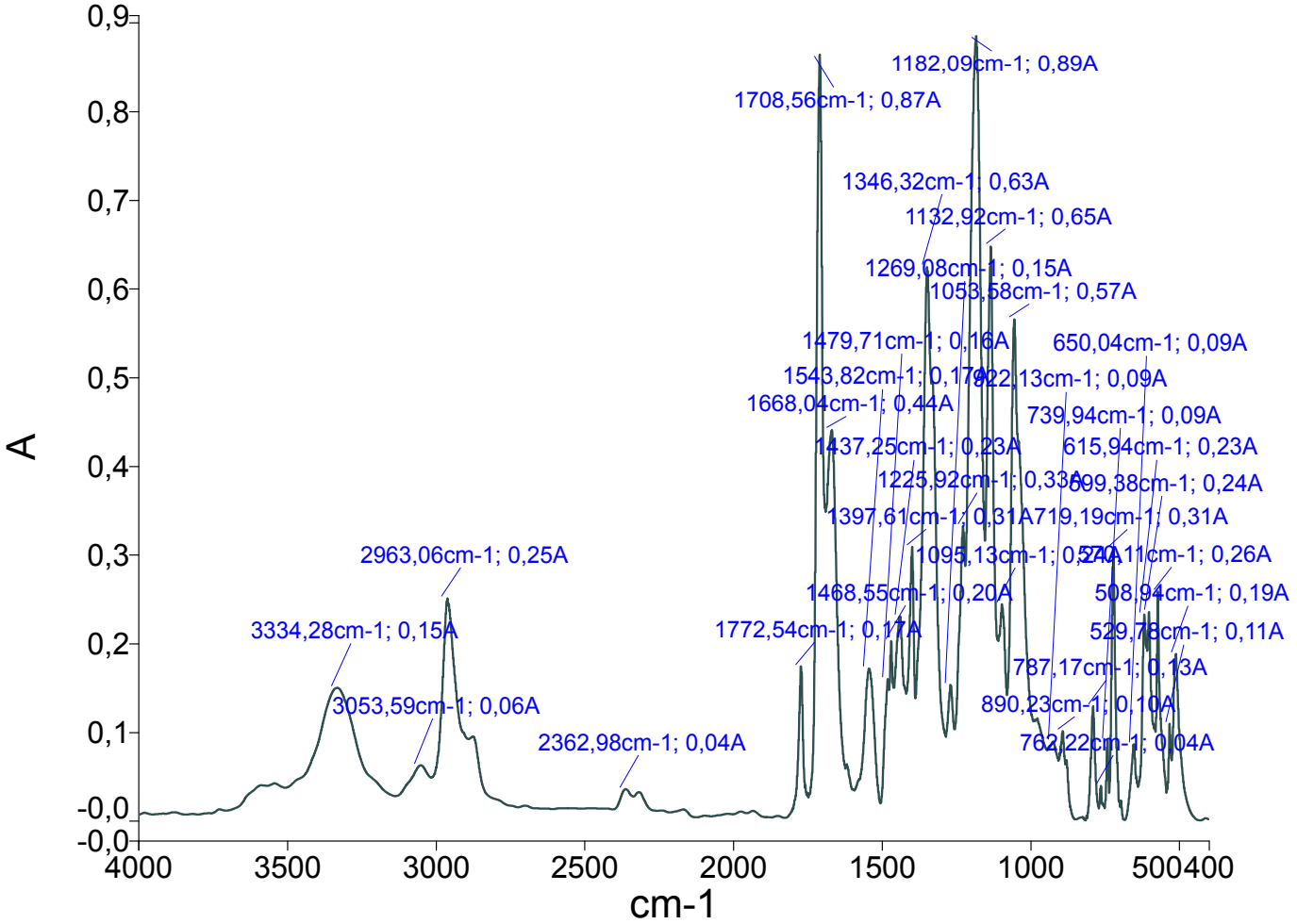

Fig. S176. IR spectrum of 5,11,17,23-tetra-*tert*-butyl-25,26,27,28-tetrakis[(N-(2'-methyl-2',2'-diethyl)ammoniumethyl)carbomoylmethoxy]-2,8,14,20-tetrathiacalix[4]arene tetra[bis(trifluoromethylsulfonyl)imide] (*cone* **48**)

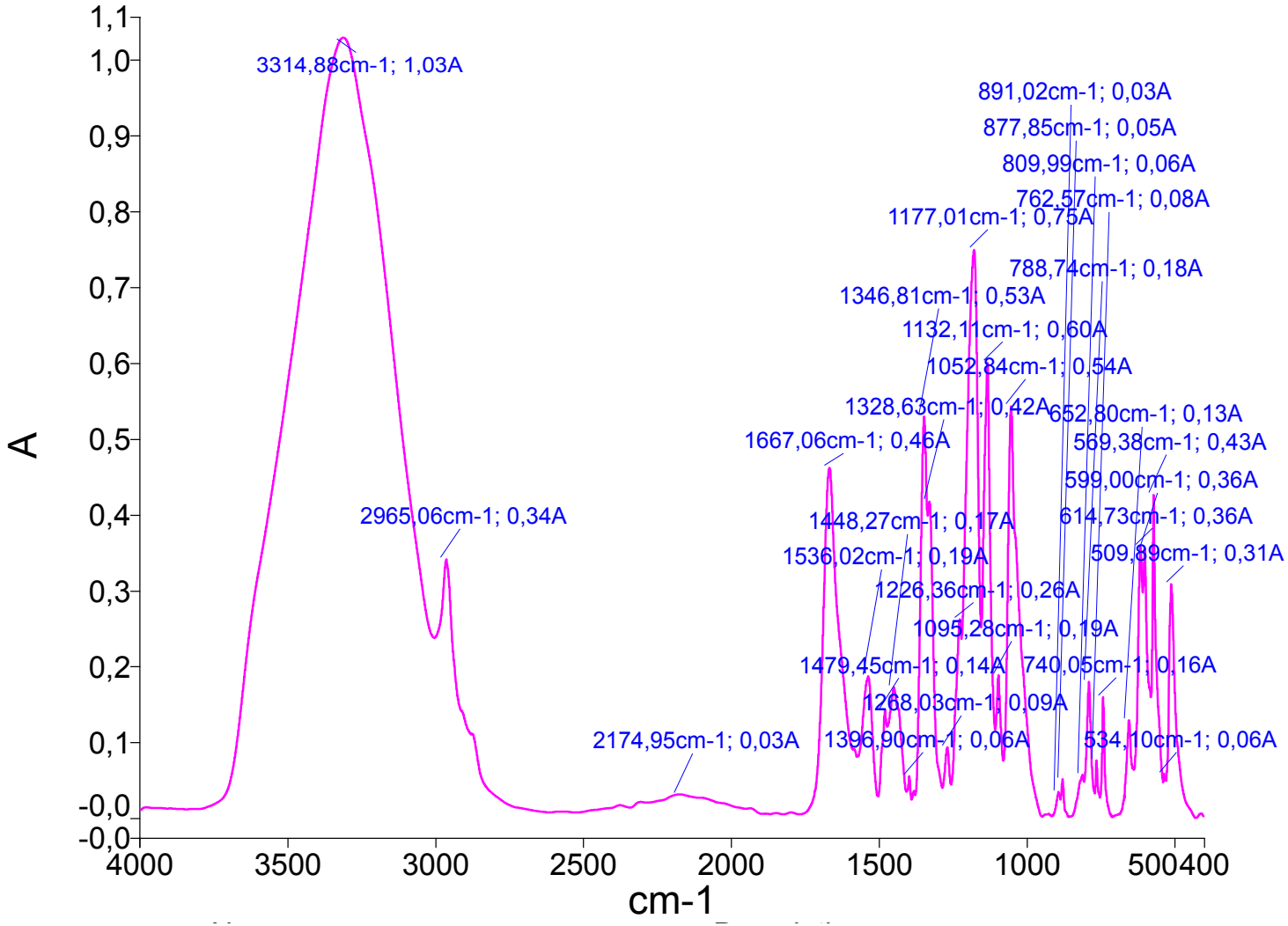

Fig. S177. IR spectrum of 5,11,17,23-tetra-*tert*-butyl-25,26,27,28-tetrakis[(N-(2',2',2'-triethyl)ammoniumethyl)carbomoylmethoxy]-2,8,14,20-tetrathiacalix[4]arene tetra[bis(trifluoromethylsulfonyl)imide] (*cone* **49**)

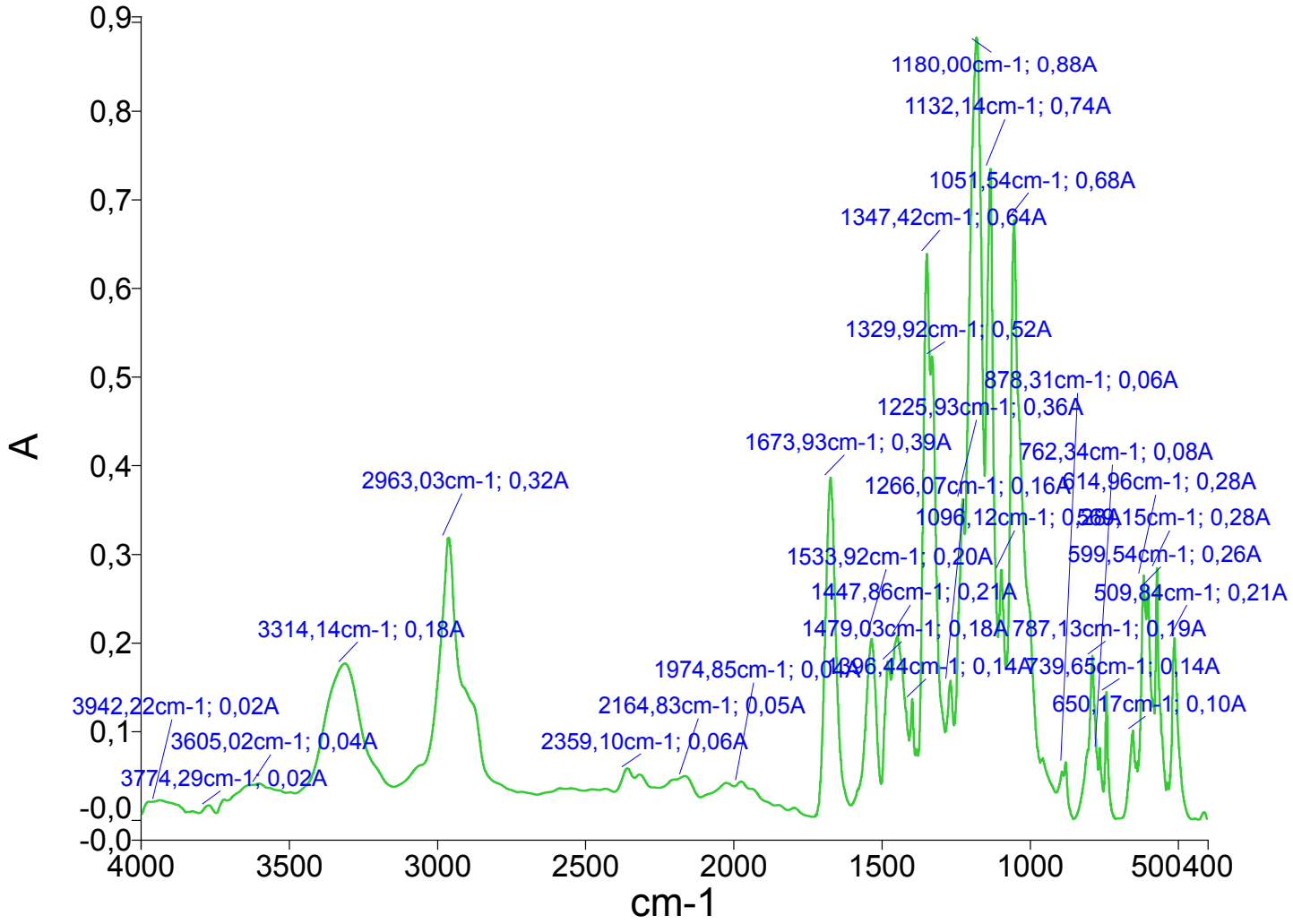

Fig. S178. IR spectrum of 5,11,17,23-tetra-*tert*-butyl-25,26,27,28-tetrakis[(N-(2',2'-diethyl-2'–benzyl)ammoniumethyl)carbomoylmethoxy]-2,8,14,20-tetrathiacalix[4]arene tetra[bis(trifluoromethylsulfonyl)imide] (*cone* **50**)

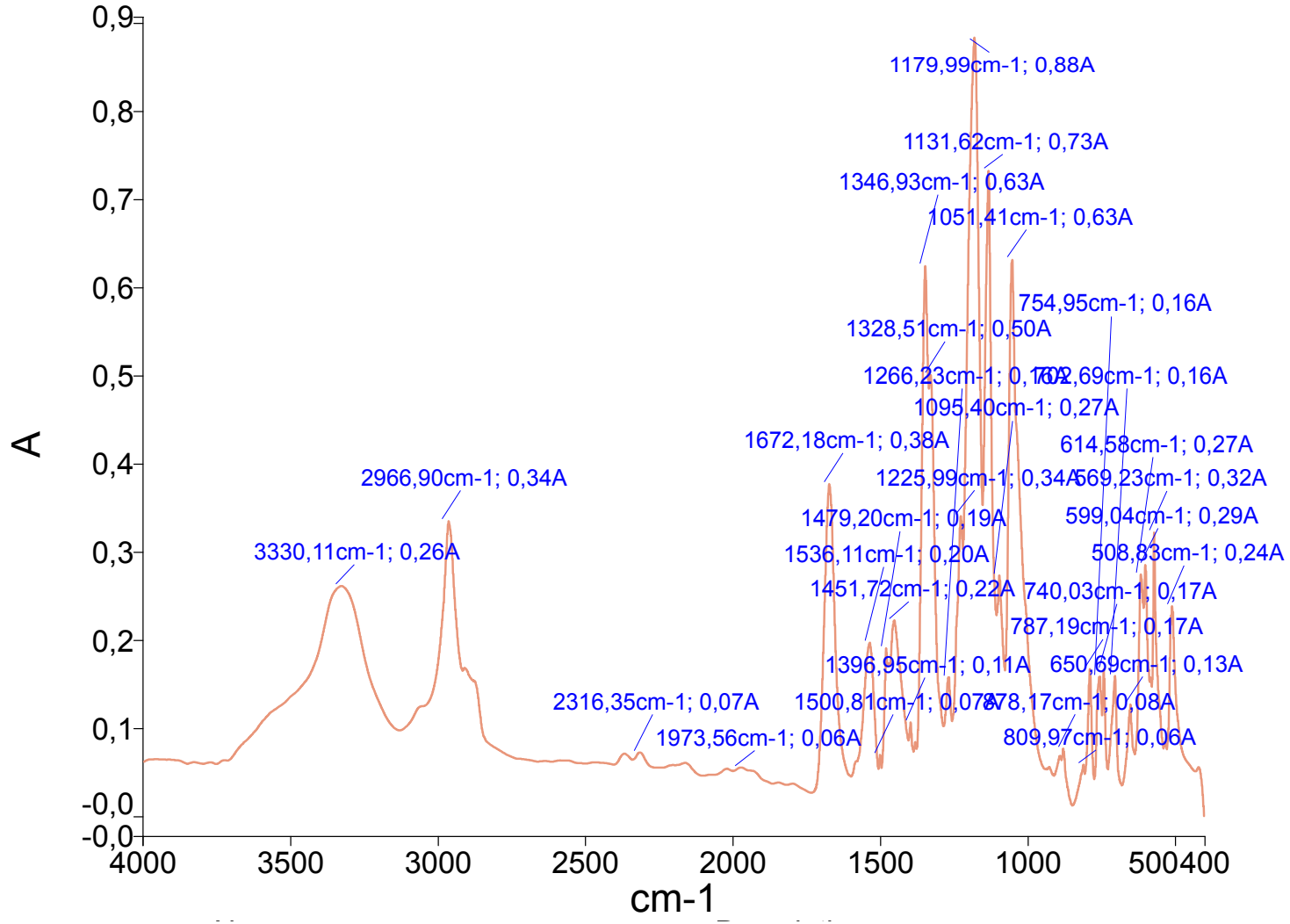

Fig. S179. IR spectrum of 5,11,17,23-tetra-*tert*-butyl-25,26,27,28-tetrakis[(N-(2',2'-diethyl-2'-(ethoxycarbonylmethyl)ammoniumethyl)-carbomoylmethoxy]-2,8,14,20-tetrathiacalix[4]arene tetra[bis(trifluoromethylsulfonyl)imide] (*cone* **51**)

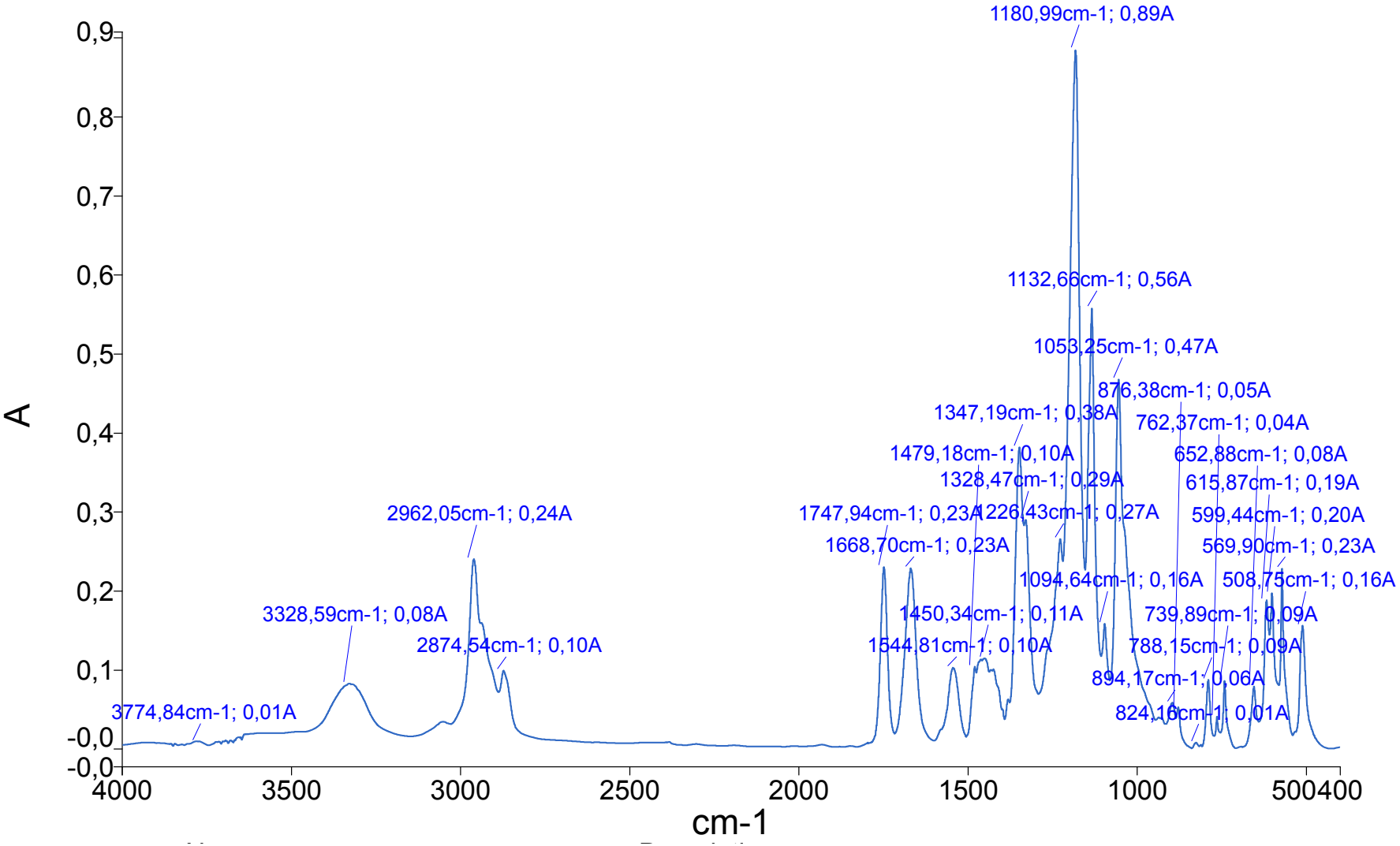

Fig. S180. IR spectrum of 5,11,17,23-tetra-*tert*-butyl-25,26,27,28-tetrakis[(N-(2',2'-diethyl-2'-(pentoxycarbonylmethyl)ammoniumethyl)-carbomoylmethoxy]-2,8,14,20-tetrathiacalix[4]arene tetra[bis(trifluoromethylsulfonyl)imide] (*cone* **52**)

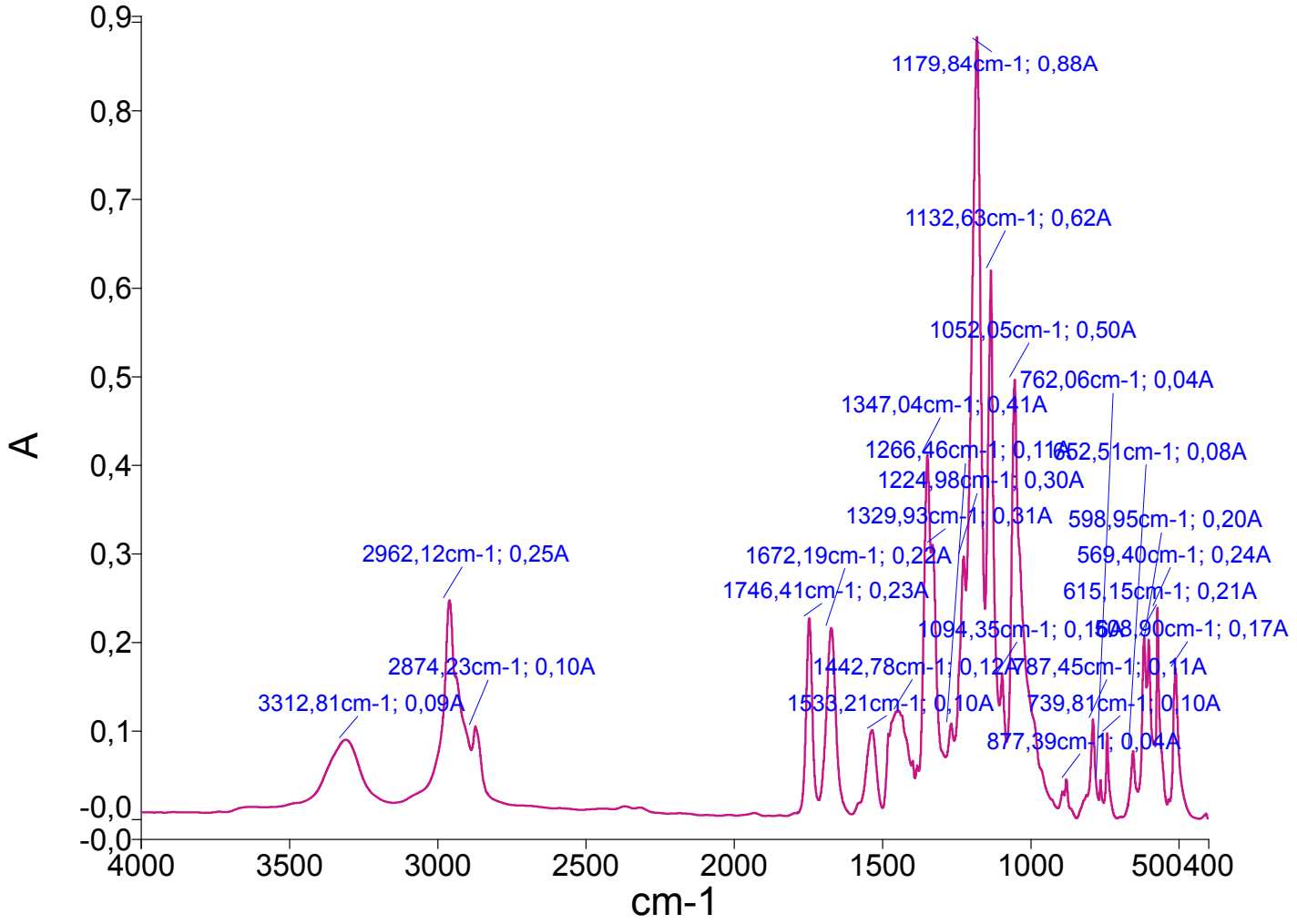

Fig. S181. IR spectrum of 5,11,17,23-tetra-*tert*-butyl-25,26,27,28-tetrakis[(N-(2',2'-diethyl-2'-{(ethoxycarbonylmethyl)amidocarbonylmethyl})-ammoniumethyl)carbomoylmethoxy]-2,8,14,20-tetrathiacalix[4]arene tetra[bis(trifluoromethylsulfonyl)imide] (*cone* **53**)

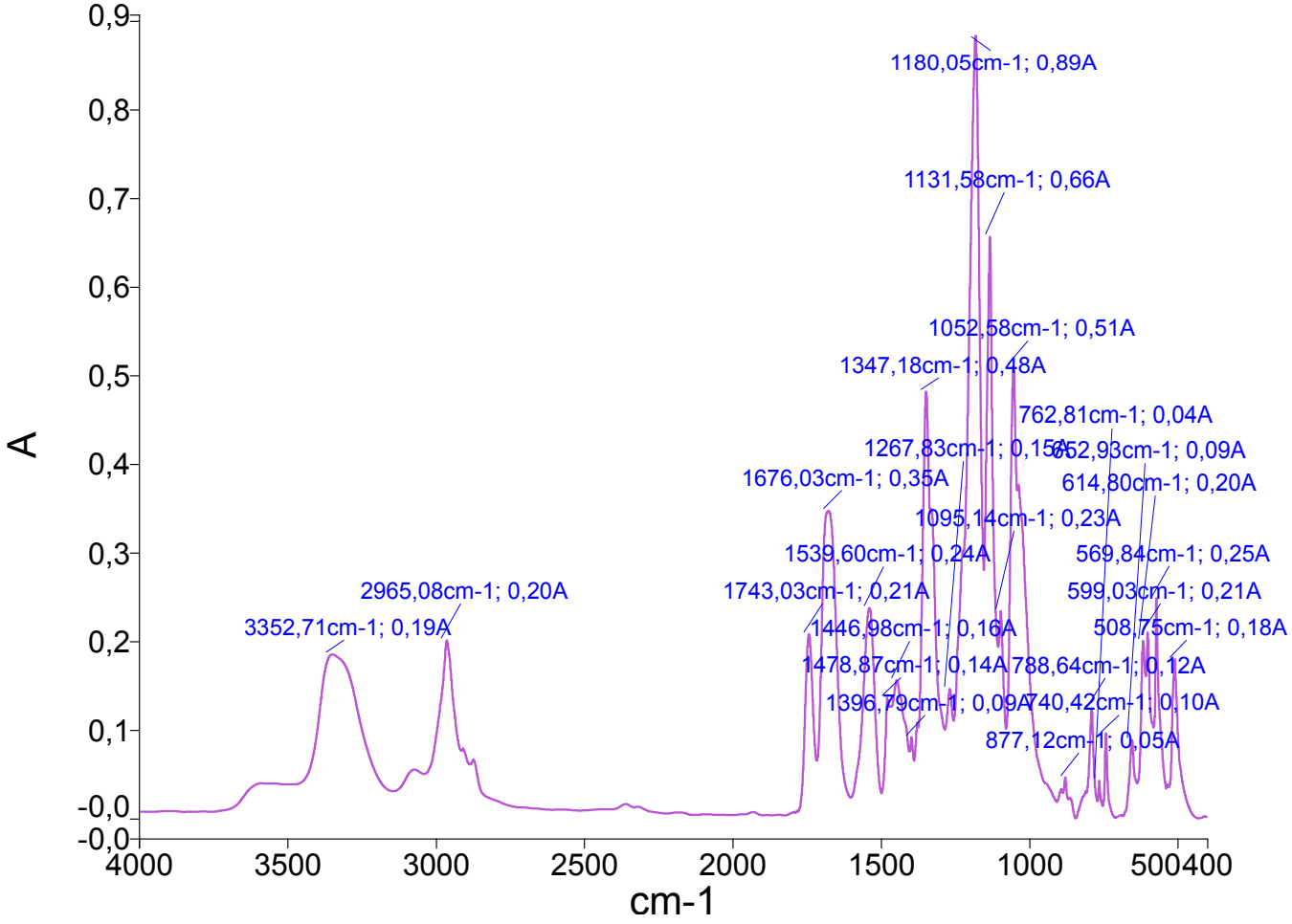

Fig. S182. IR spectrum of 5,11,17,23-tetra-*tert*-butyl-25,26,27,28-tetrakis[(N-(2',2'-diethyl-2'-{([ethoxycarbonylmethyl]-amidocarbonylmethyl)amidocarbonylmethyl}ammoniumethyl)carbomoylmethoxy]-2,8,14,20-tetrathiacalix[4]arene tetra[bis(trifluoromethylsulfonyl)imide] (*cone* **54**)

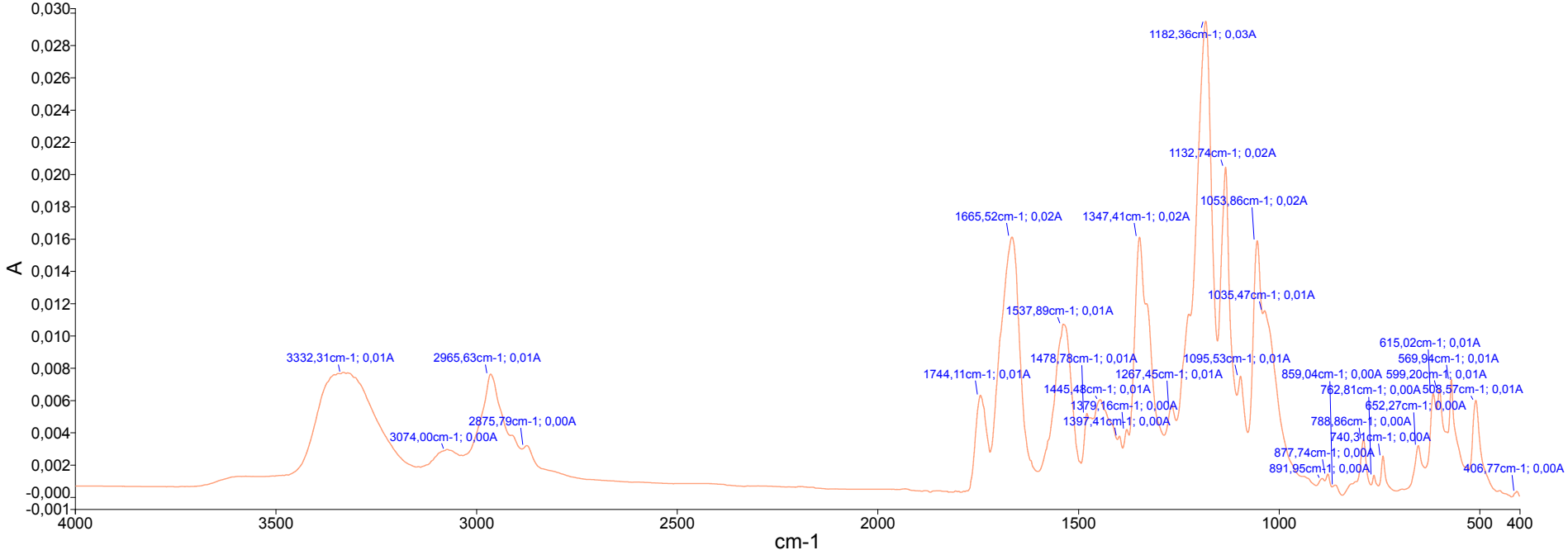

Fig. S183. IR spectrum of 5,11,17,23-tetra-*tert*-butyl-25,26,27,28-tetrakis[(N-(2',2'-diethyl-2'-{(ethoxycarbonyl[S-methyl]methyl)amidocarbonylmethyl}ammoniumethyl)carbomoylmethoxy]-2,8,14,20-tetrathiacalix[4]arene tetra[bis(trifluoromethylsulfonyl)imide] (*cone* **55**)

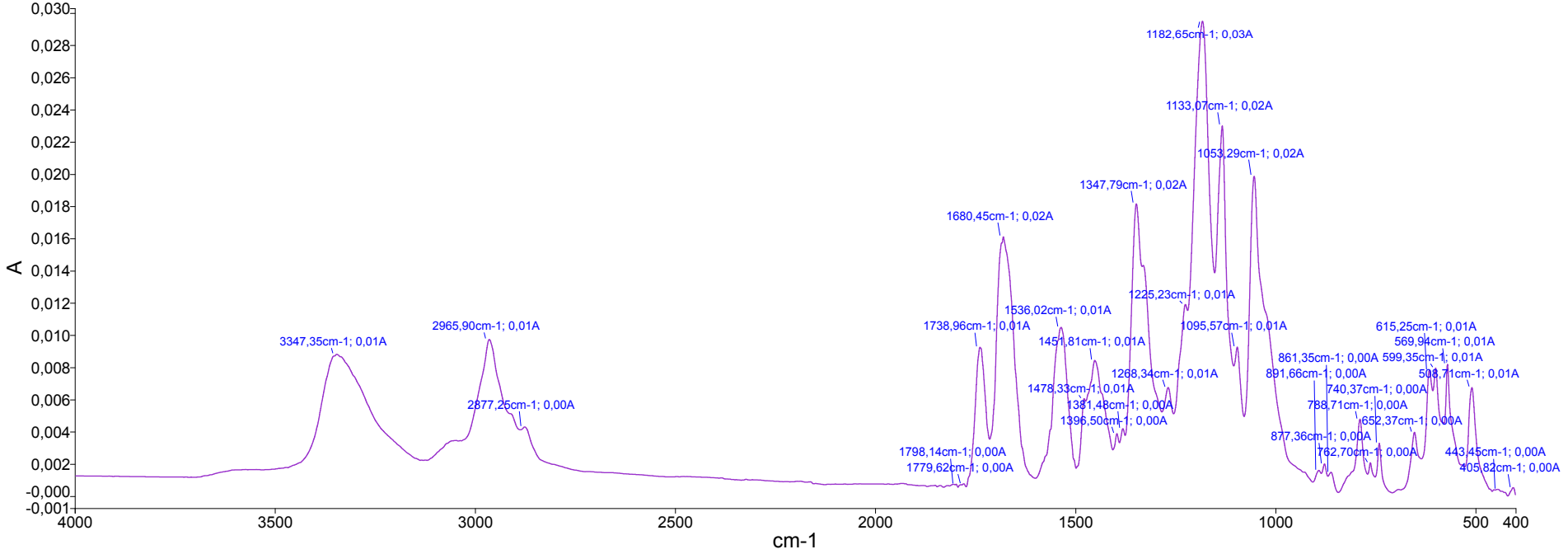

Fig. S184. IR spectrum of 5,11,17,23-tetra-*tert*-butyl-25,26,27,28-tetrakis[(N-(3',3',3'-trimethyl)ammoniumpropyl)carbomoylmethoxy]-2,8,14,20-tetrathiacalix[4]arene tetra[bis(trifluoromethylsulfonyl)imide] (*1,3-alternate* **56**)

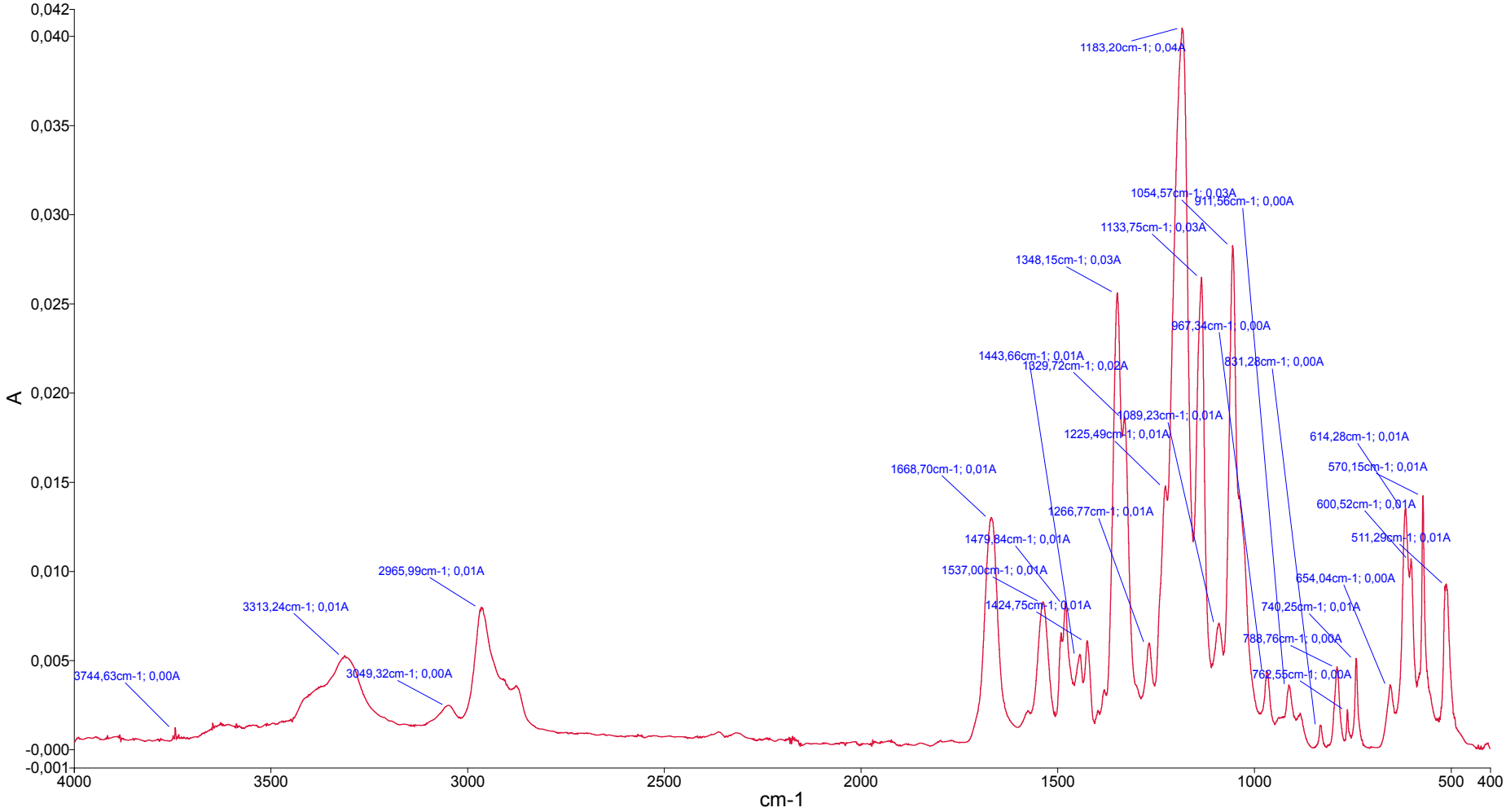

Fig. S185. IR spectrum of 5,11,17,23-tetra-*tert*-butyl-25,26,27,28-tetrakis[(N-(3',3'-dimethyl-3'-ethyl)ammoniumpropyl)carbomoylmethoxy]-2,8,14,20-tetrathiacalix[4]arene tetra[bis(trifluoromethylsulfonyl)imide] (*1,3-alternate* **57**)

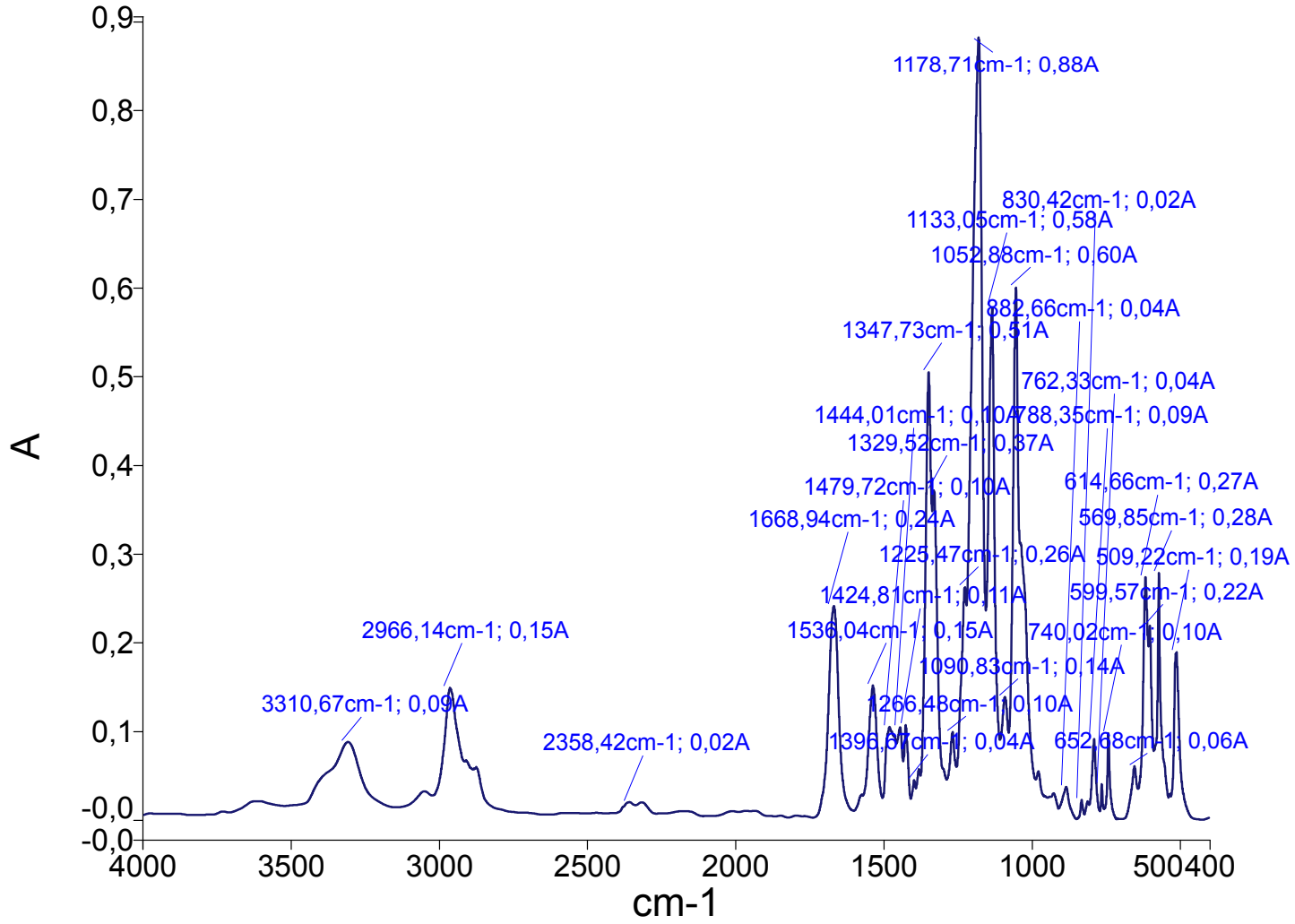

Fig. S186. IR spectrum of 5,11,17,23-tetra-*tert*-butyl-25,26,27,28-tetrakis[(N-(3',3'-dimethyl-3'-benzyl)ammoniumpropyl)carbomoylmethoxy]-2,8,14,20-tetrathiacalix[4]arene tetra[bis(trifluoromethylsulfonyl)imide] (*1,3-alternate* **58**)

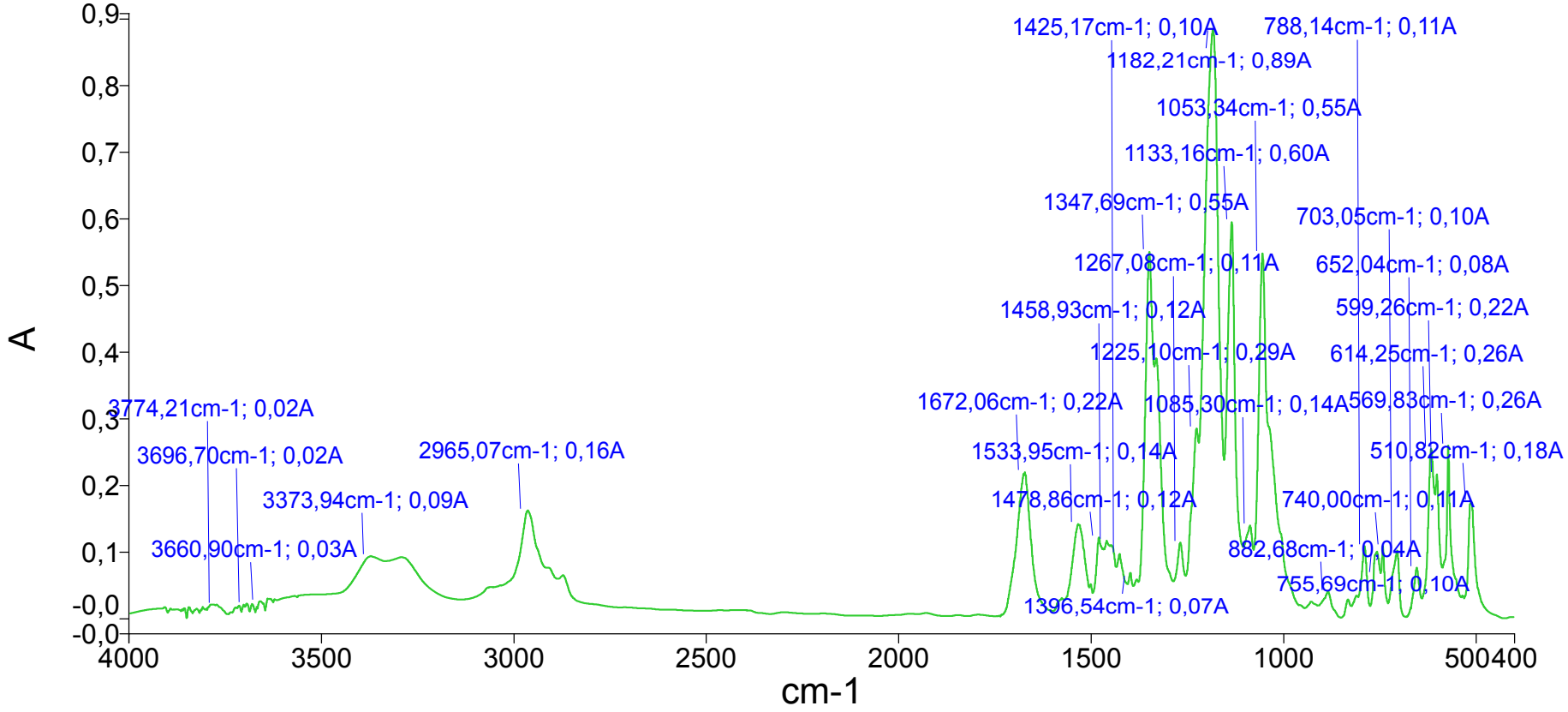

Fig. S187. IR spectrum of 5,11,17,23-tetra-*tert*-butyl-25,26,27,28-tetrakis[(N-(3',3'-dimethyl-3'-(ethoxycarbonylmethyl)ammoniumpropyl)-carbomoylmethoxy]-2,8,14,20-tetrathiacalix[4]arene tetra[bis(trifluoromethylsulfonyl)imide] (*1,3-alternate* **59**)

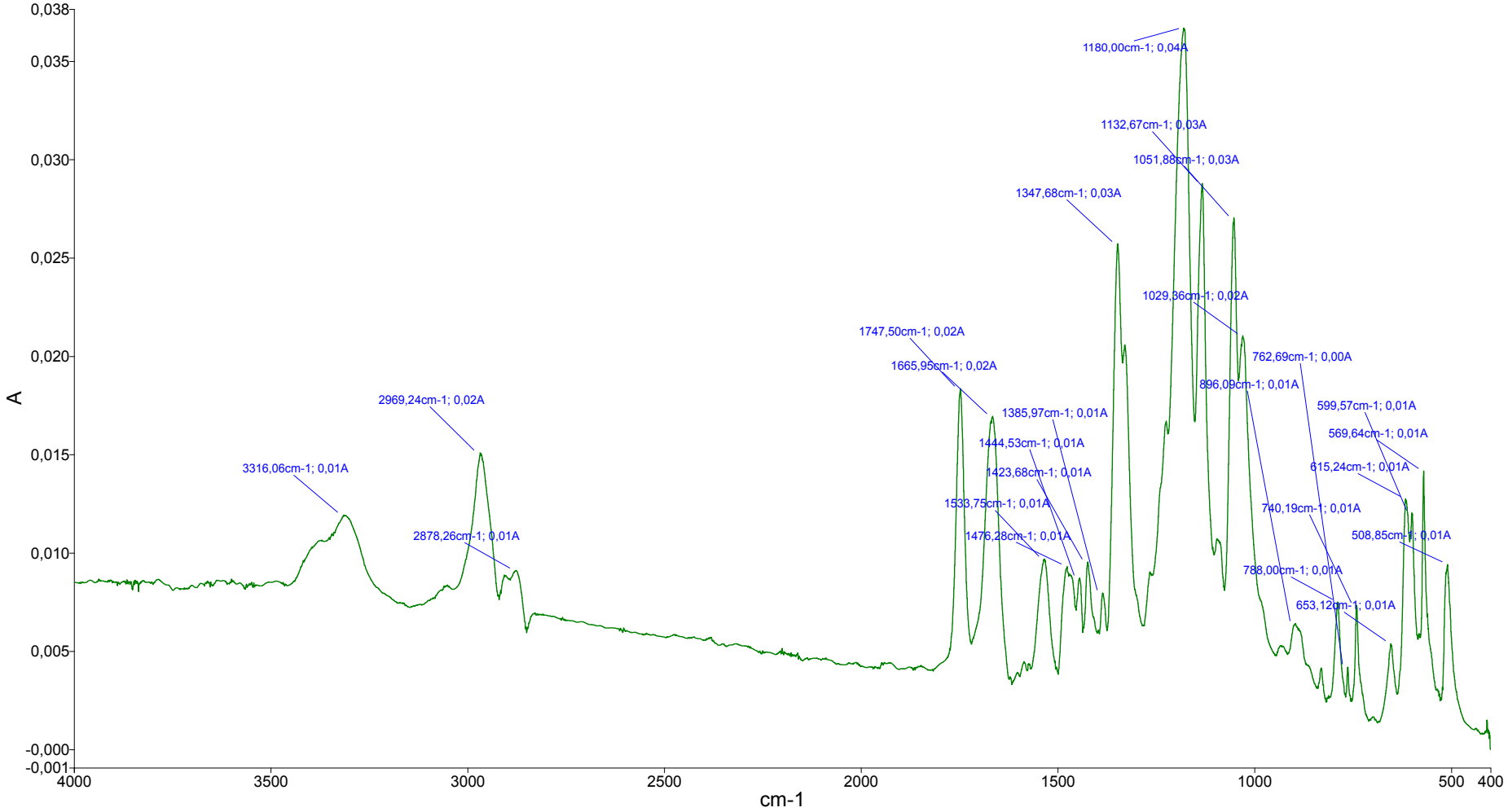

Fig. S188. IR spectrum of 5,11,17,23-tetra-*tert*-butyl-25,26,27,28-tetrakis[(N-(3',3'-dimethyl-3'-(pentoxycarbonylmethyl)ammoniumpropyl)-carbomoylmethoxy]-2,8,14,20-tetrathiacalix[4]arene tetra[bis(trifluoromethylsulfonyl)imide] (*1,3-alternate* **60**)

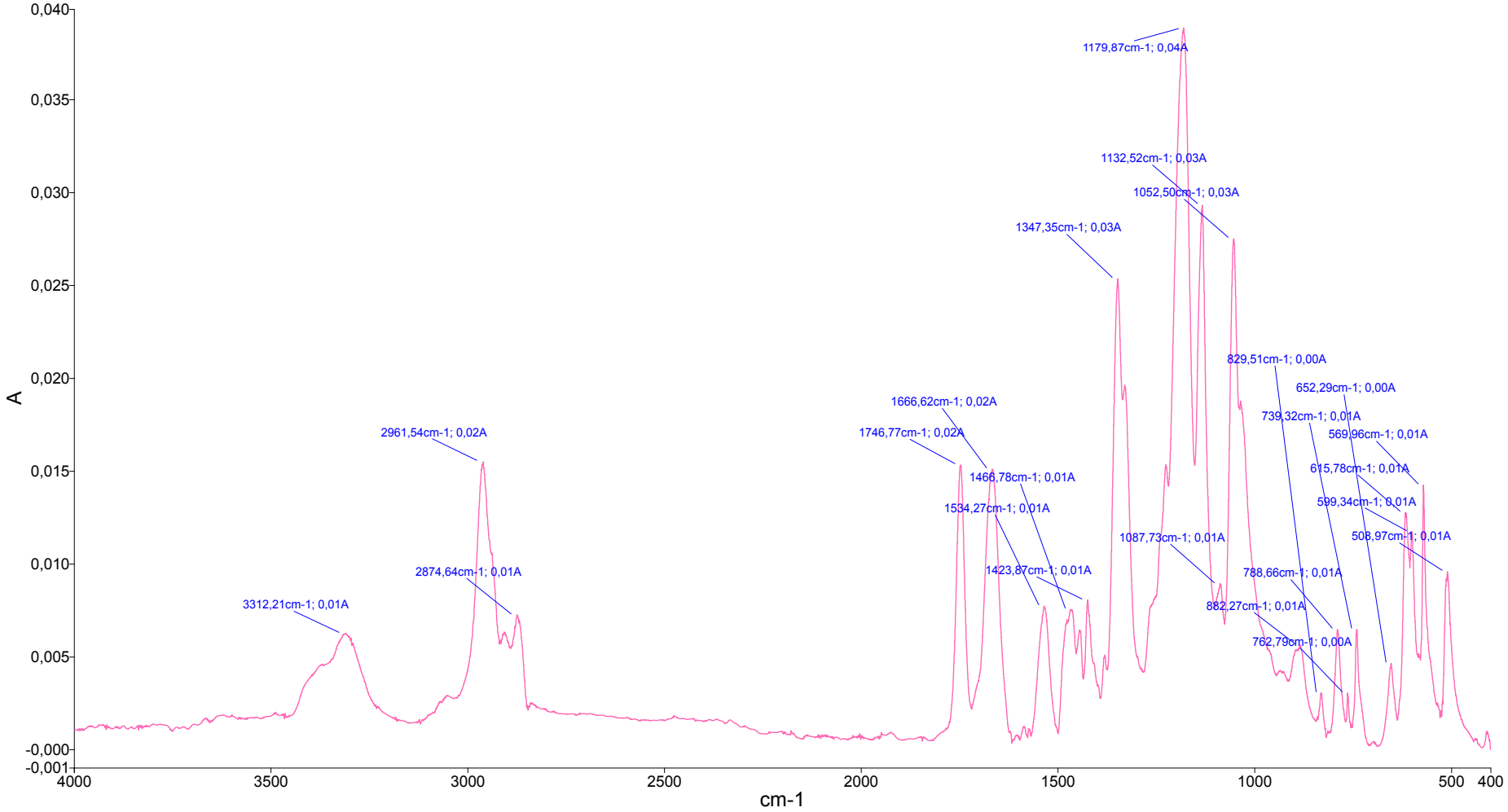

Fig. S189. IR spectrum of 5,11,17,23-tetra-*tert*-butyl-25,26,27,28-tetrakis[(N-(3',3'-dimethyl-3'-{(ethoxycarbonylmethyl)amidocarbonylmethyl}-ammoniumpropyl)carbomoylmethoxy]-2,8,14,20-tetrathiacalix[4]arene tetra[bis(trifluoromethylsulfonyl)imide] (*1,3-alternate* **61**)

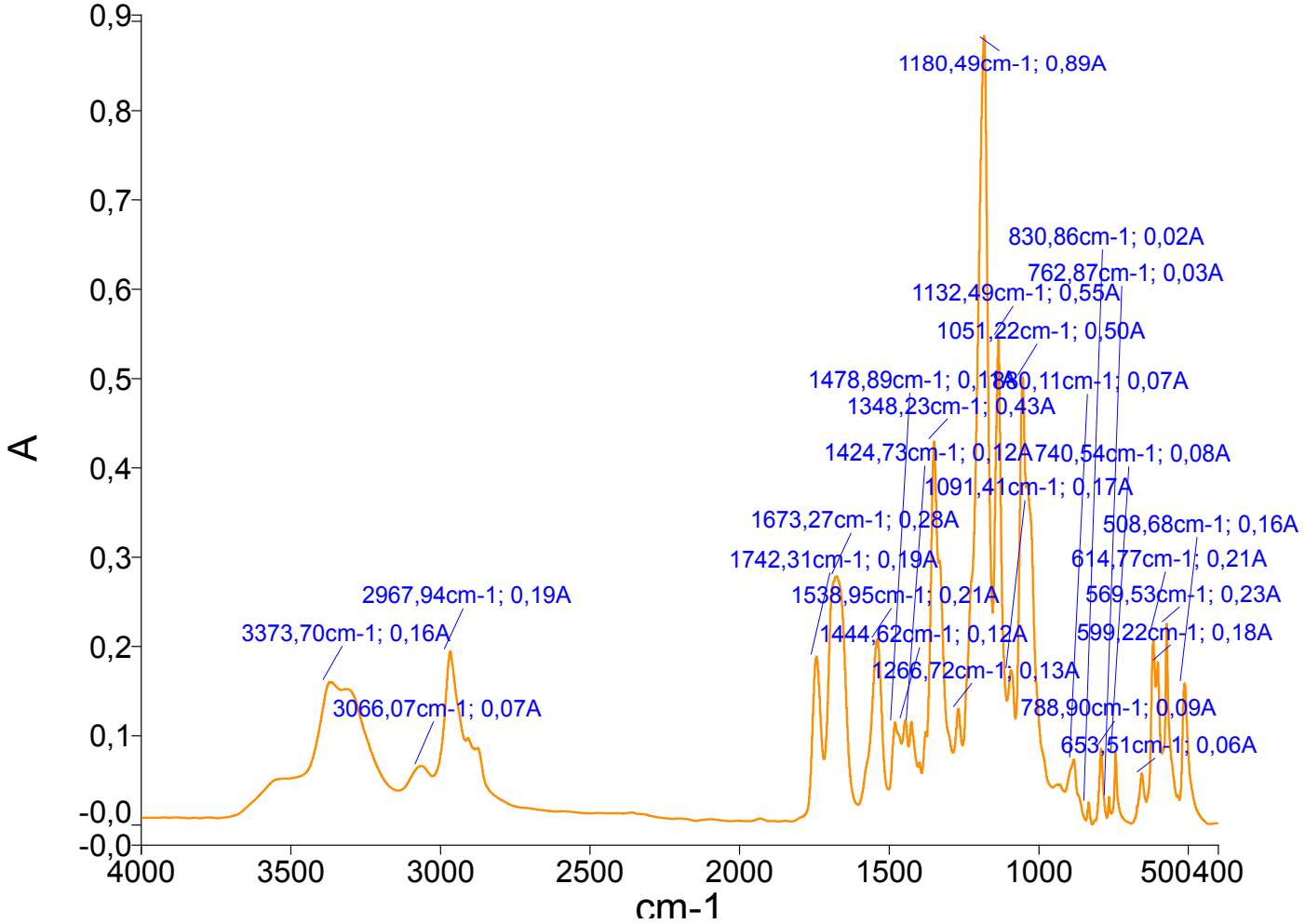

Fig. S190. IR spectrum of 5,11,17,23-tetra-*tert*-butyl-25,26,27,28-tetrakis[(N-(3',3'-dimethyl-3'-{([ethoxycarbonylmethyl]amidocarbonylmethyl)amidocarbonylmethyl}ammoniumpropyl)carbomoylmethoxy]-2,8,14,20-tetrathiacalix[4]arene tetra[bis(trifluoromethylsulfonyl)imide] (*1,3-alternate* **62**)

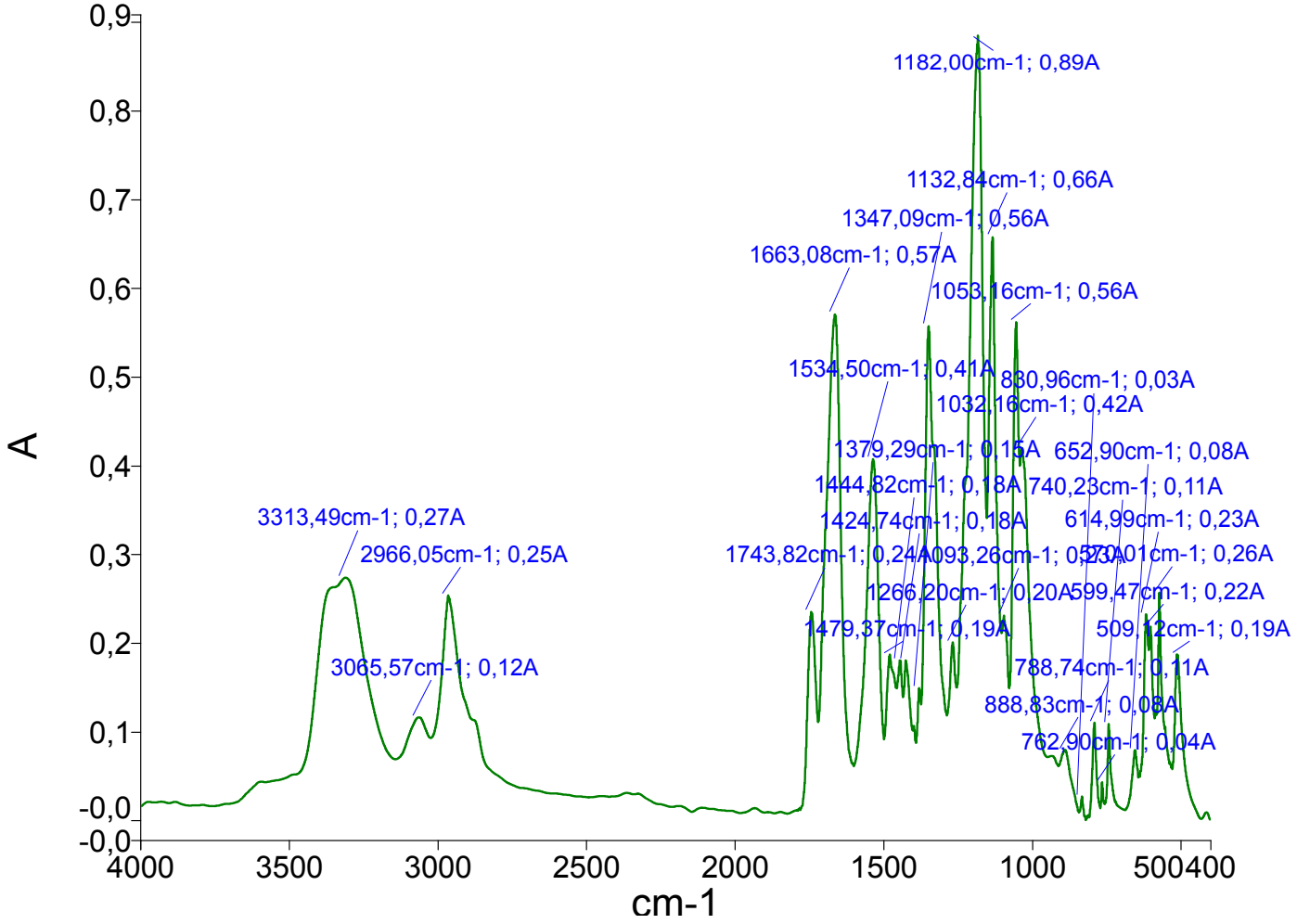

Fig. S191. IR spectrum of 5,11,17,23-tetra-*tert*-butyl-25,26,27,28-tetrakis[(N-(3',3'-dimethyl-3'-{(ethoxycarbonyl[S-methyl]methyl)amidocarbonylmethyl}ammoniumpropyl)carbomoylmethoxy]-2,8,14,20-tetrathiacalix[4]arene tetra[bis(trifluoromethylsulfonyl)imide] (*1,3-alternate* **63**)

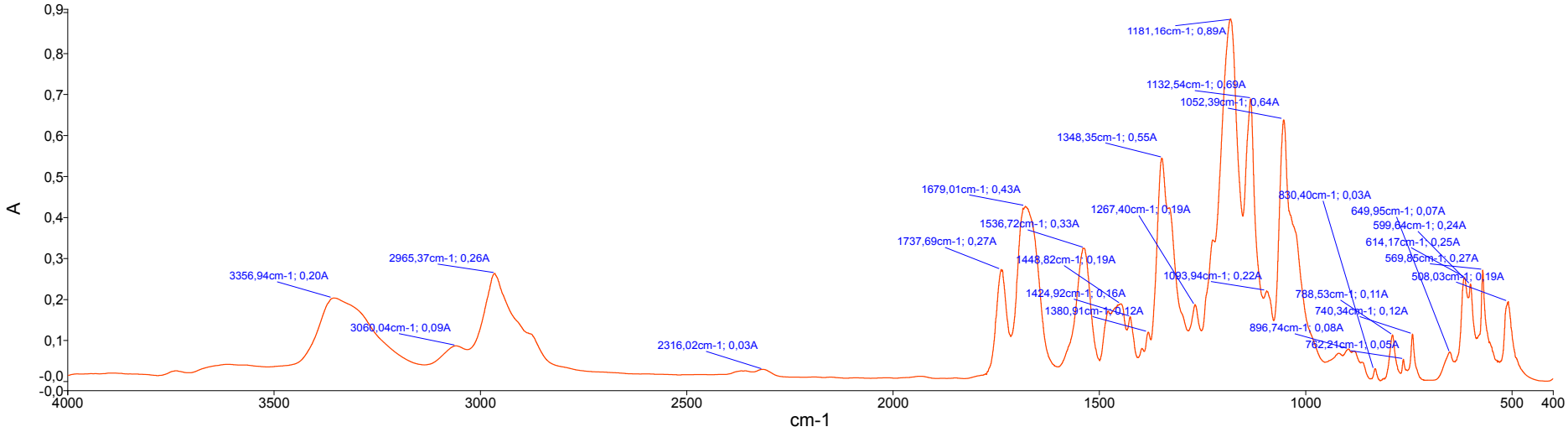

Fig. S192. IR spectrum of 5,11,17,23-tetra-*tert*-butyl-25,26,27,28-tetrakis[(N-(3',3'-dimethyl-3'-{3''-propylphtalimide}ammoniumpropyl)-carbomoylmethoxy]-2,8,14,20-tetrathiacalix[4]arene tetra[bis(trifluoromethylsulfonyl)imide] (*1,3-alternate* **64**)

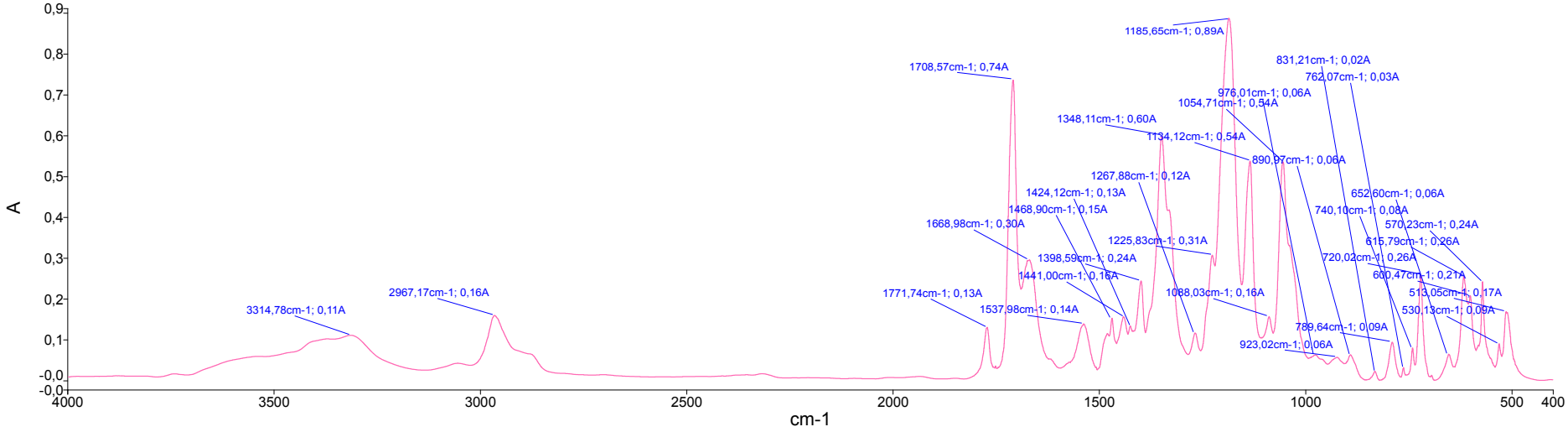

Fig. S193. IR spectrum of 5,11,17,23-tetra-*tert*-butyl-25,26,27,28-tetrakis[(N-(2'-methyl-2',2'-diethyl)ammoniumethyl)carbomoylmethoxy]-2,8,14,20-tetrathiacalix[4]arene tetra[bis(trifluoromethylsulfonyl)imide] (*1,3-alternate* **65**)

Fig. S194. IR spectrum of 5,11,17,23-tetra-*tert*-butyl-25,26,27,28-tetrakis[(N-(2',2',2'-triethyl)ammoniumethyl)carbomoylmethoxy]-2,8,14,20-tetrathiacalix[4]arene tetra[bis(trifluoromethylsulfonyl)imide] (*1,3-alternate* **66**)

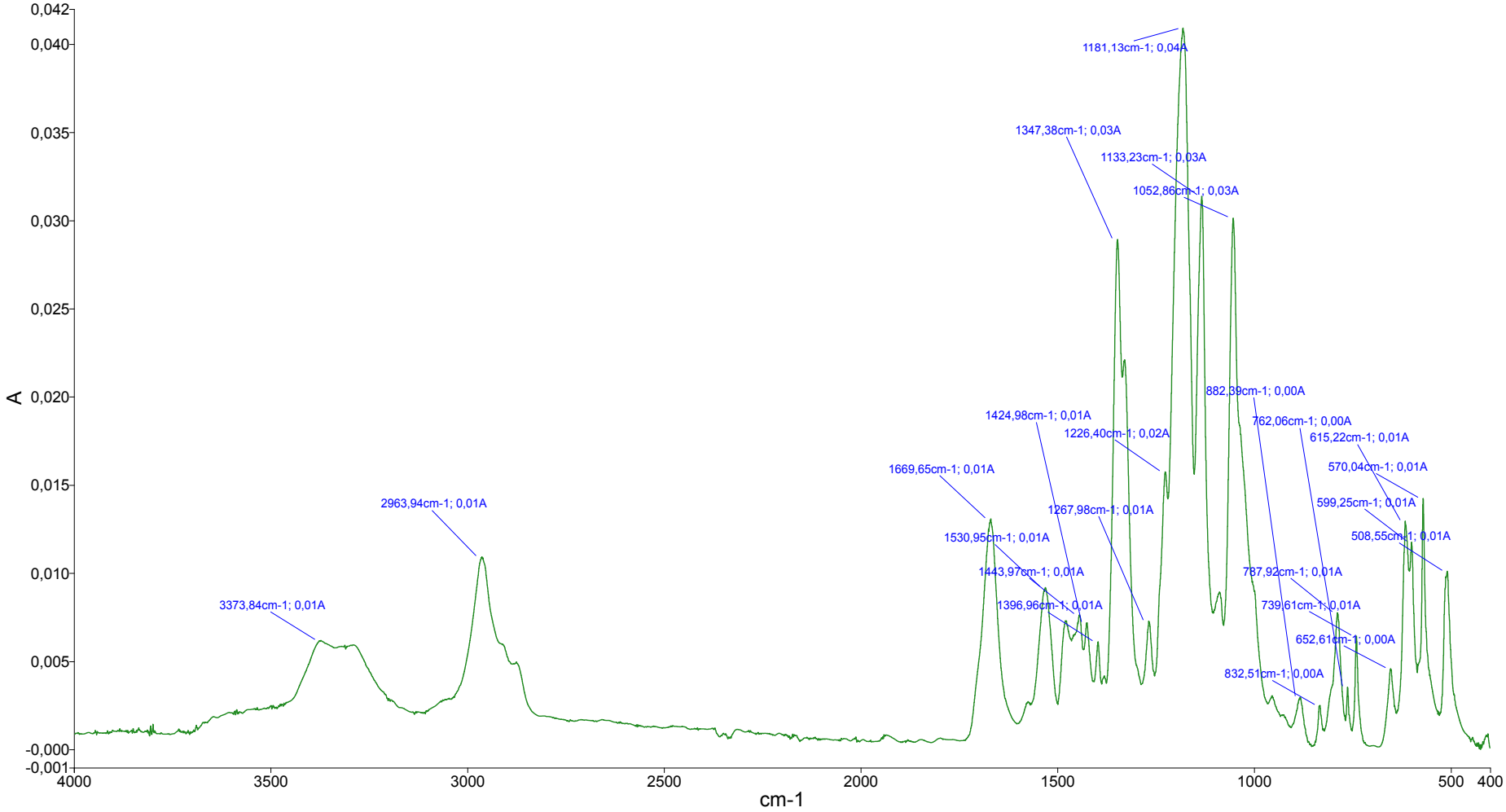

Fig. S195. IR spectrum of 5,11,17,23-tetra-*tert*-butyl-25,26,27,28-tetrakis[(N-(2',2'-diethyl-2'-benzyl)ammoniumethyl)carbomoylmethoxy]-2,8,14,20-tetrathiacalix[4]arene tetra[bis(trifluoromethylsulfonyl)imide] (*1,3-alternate* **67**)

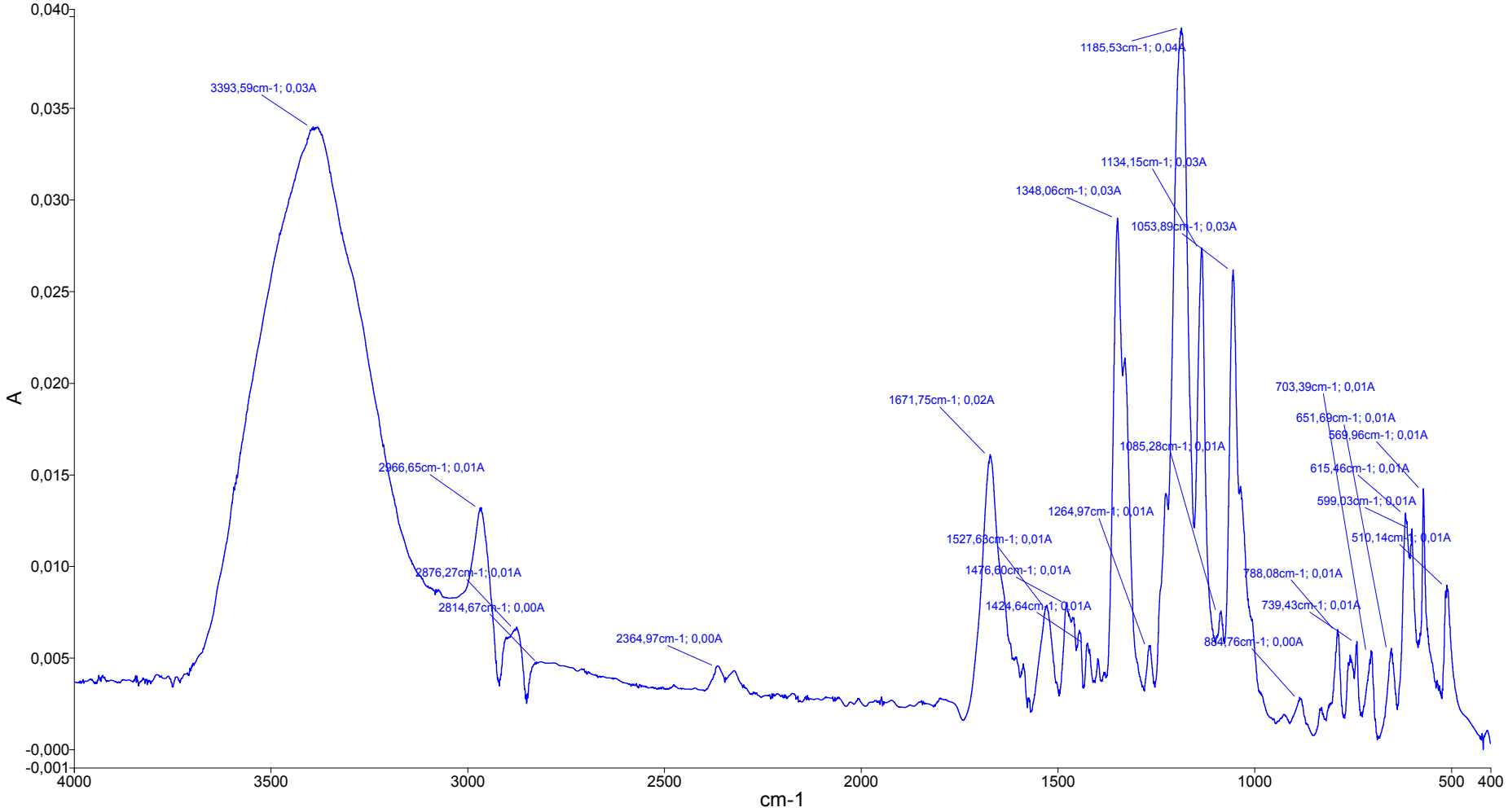

Fig. S196. IR spectrum of 5,11,17,23-tetra-*tert*-butyl-25,26,27,28-tetrakis[(N-(2',2'-diethyl-2'-(ethoxycarbonylmethyl)ammoniumethyl)-carbomoylmethoxy]-2,8,14,20-tetrathiacalix[4]arene tetra[bis(trifluoromethylsulfonyl)imide] (*1,3-alternate* **68**)

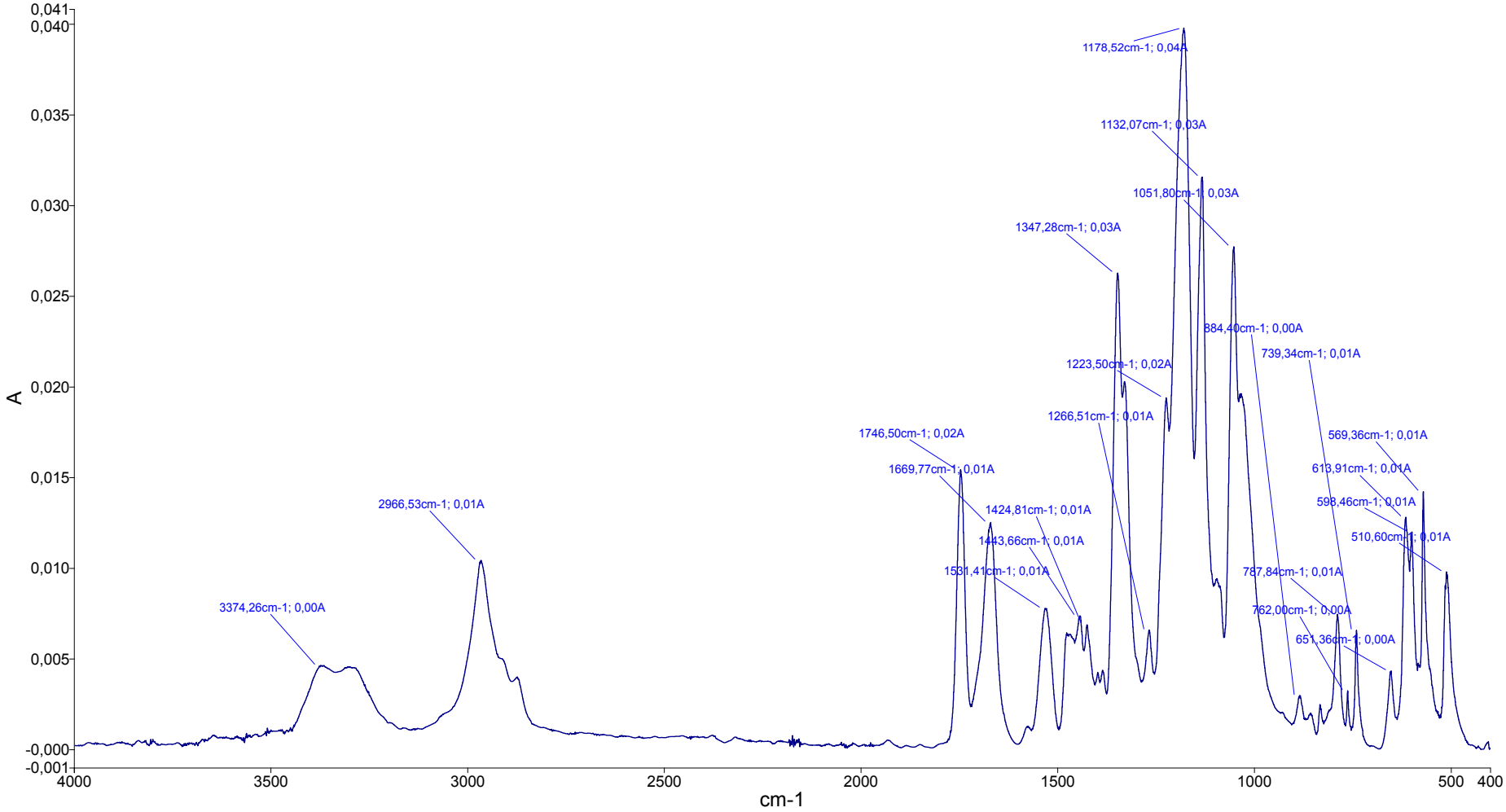

Fig. S197. IR spectrum of 5,11,17,23-tetra-*tert*-butyl-25,26,27,28-tetrakis[(N-(2',2'-diethyl-2'-(pentoxycarbonylmethyl)ammoniumethyl)-carbomoylmethoxy]-2,8,14,20-tetrathiacalix[4]arene tetra[bis(trifluoromethylsulfonyl)imide] (*1,3-alternate* **69**)

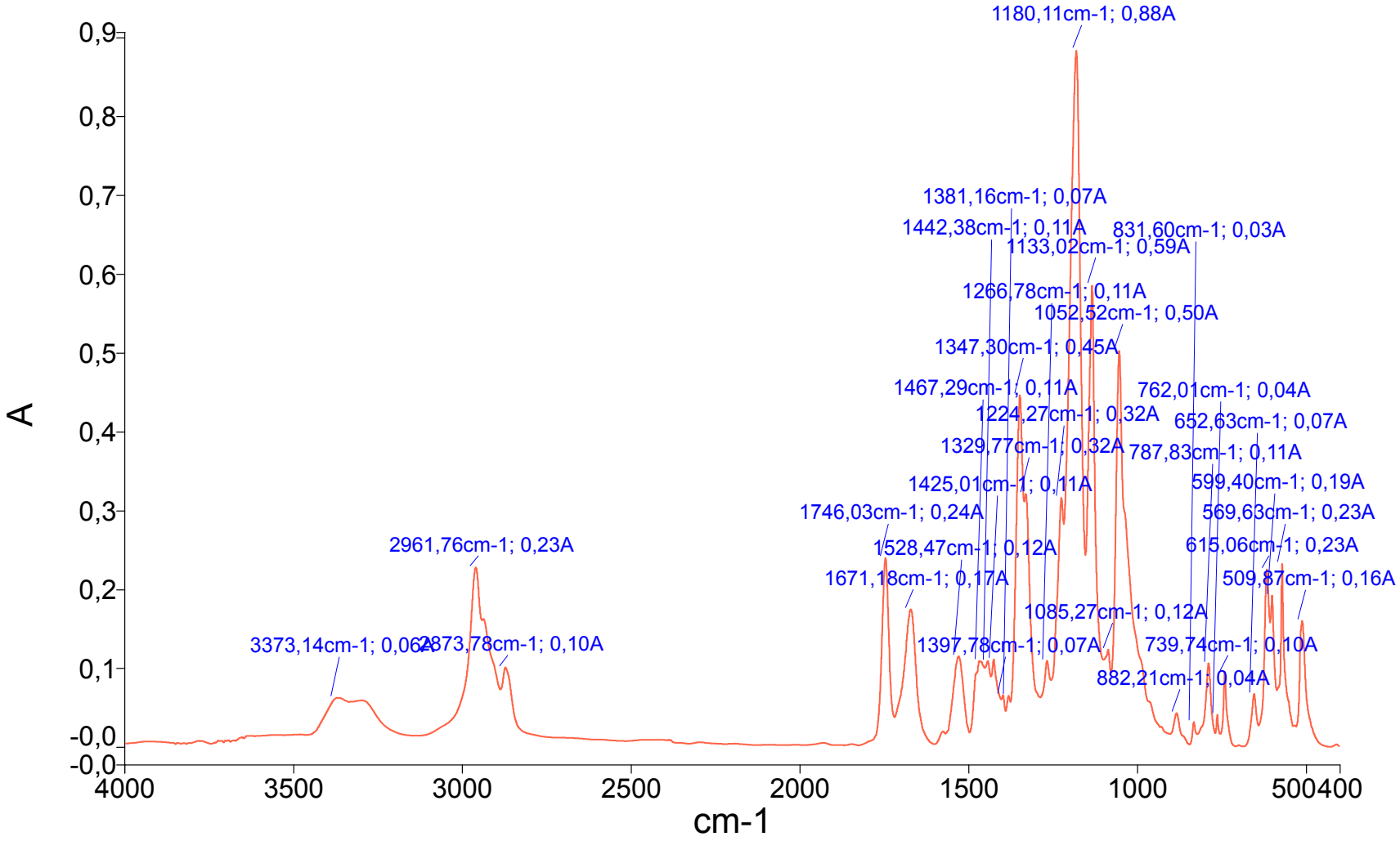

Fig. S198. IR spectrum of 5,11,17,23-tetra-*tert*-butyl-25,26,27,28-tetrakis[(N-(2',2'-diethyl-2'-{(ethoxycarbonylmethyl)amidocarbonylmethyl})-ammoniumethyl)carbomoylmethoxy]-2,8,14,20-tetrathiacalix[4]arene tetra[bis(trifluoromethylsulfonyl)imide] (*1,3-alternate* **70**)

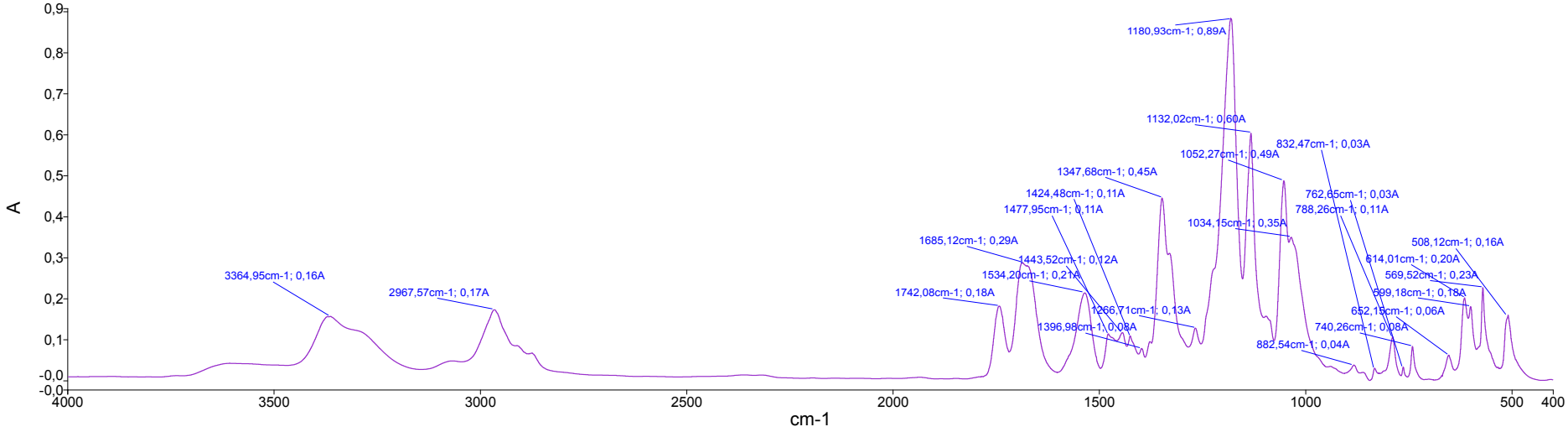

Fig. S199. IR spectrum of 5,11,17,23-tetra-*tert*-butyl-25,26,27,28-tetrakis[(N-(2',2'-diethyl-2'-{([ethoxycarbonylmethyl]amidocarbonylmethyl)-amidocarbonylmethyl}ammoniumethyl)carbomoylmethoxy]-2,8,14,20-tetrathiacalix[4]arene tetra[bis(trifluoromethylsulfonyl)imide] (*1,3-alternate* **71**)

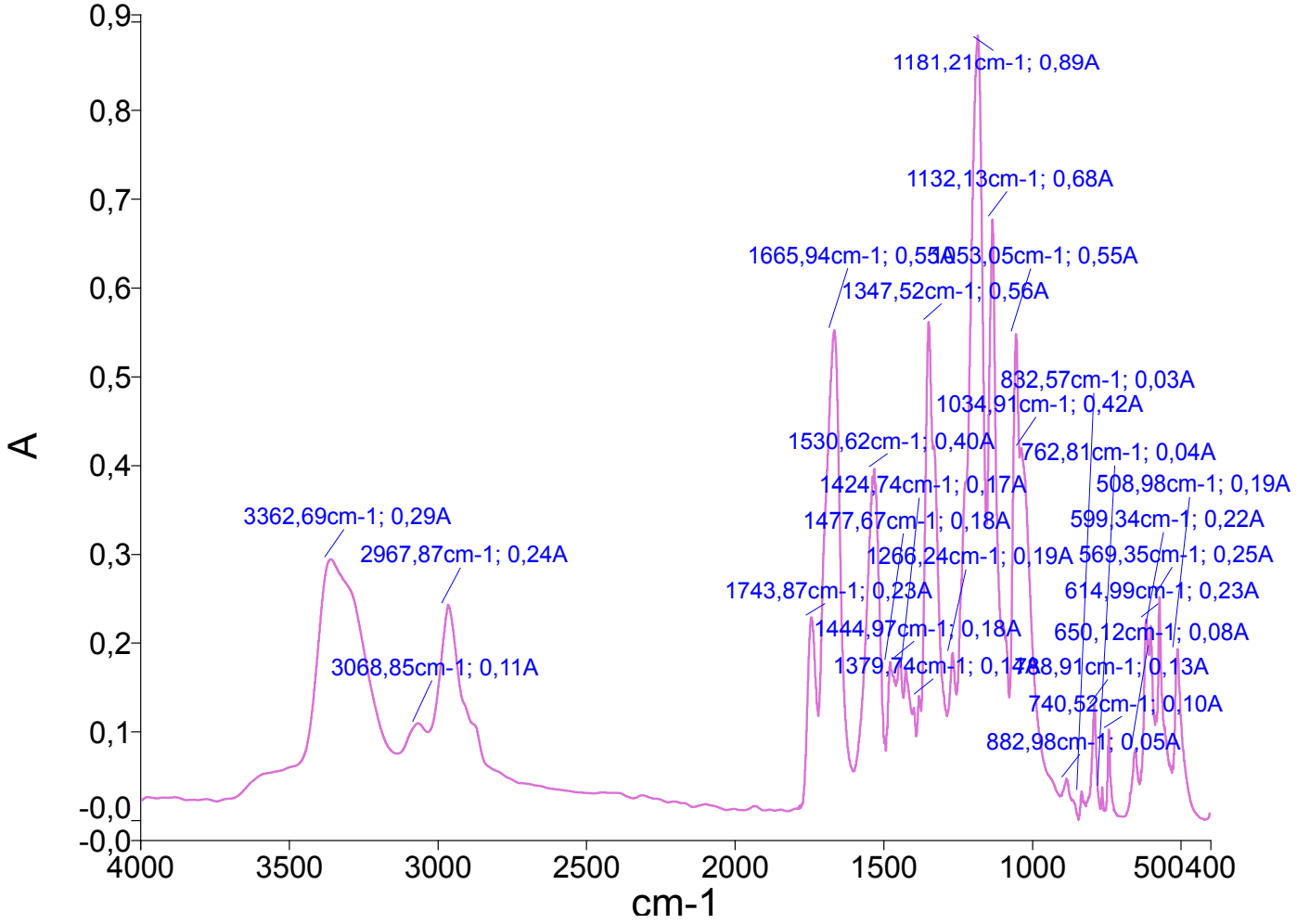

Fig. S200. IR spectrum of 5,11,17,23-tetra-*tert*-butyl-25,26,27,28-tetrakis[(N-(2',2'-diethyl-2'-{(ethoxycarbonyl[S-methyl]methyl)amidocarbonylmethyl}ammoniumethyl)carbomoylmethoxy]-2,8,14,20-tetrathiacalix[4]arene tetra[bis(trifluoromethylsulfonyl)imide] (*1,3-alternate* **72**)

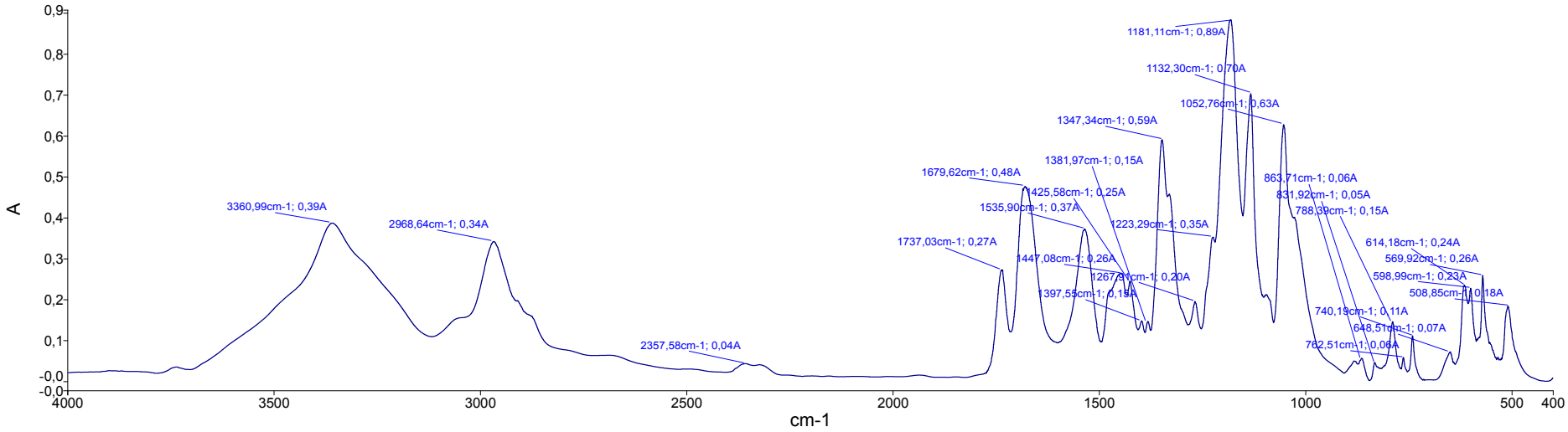

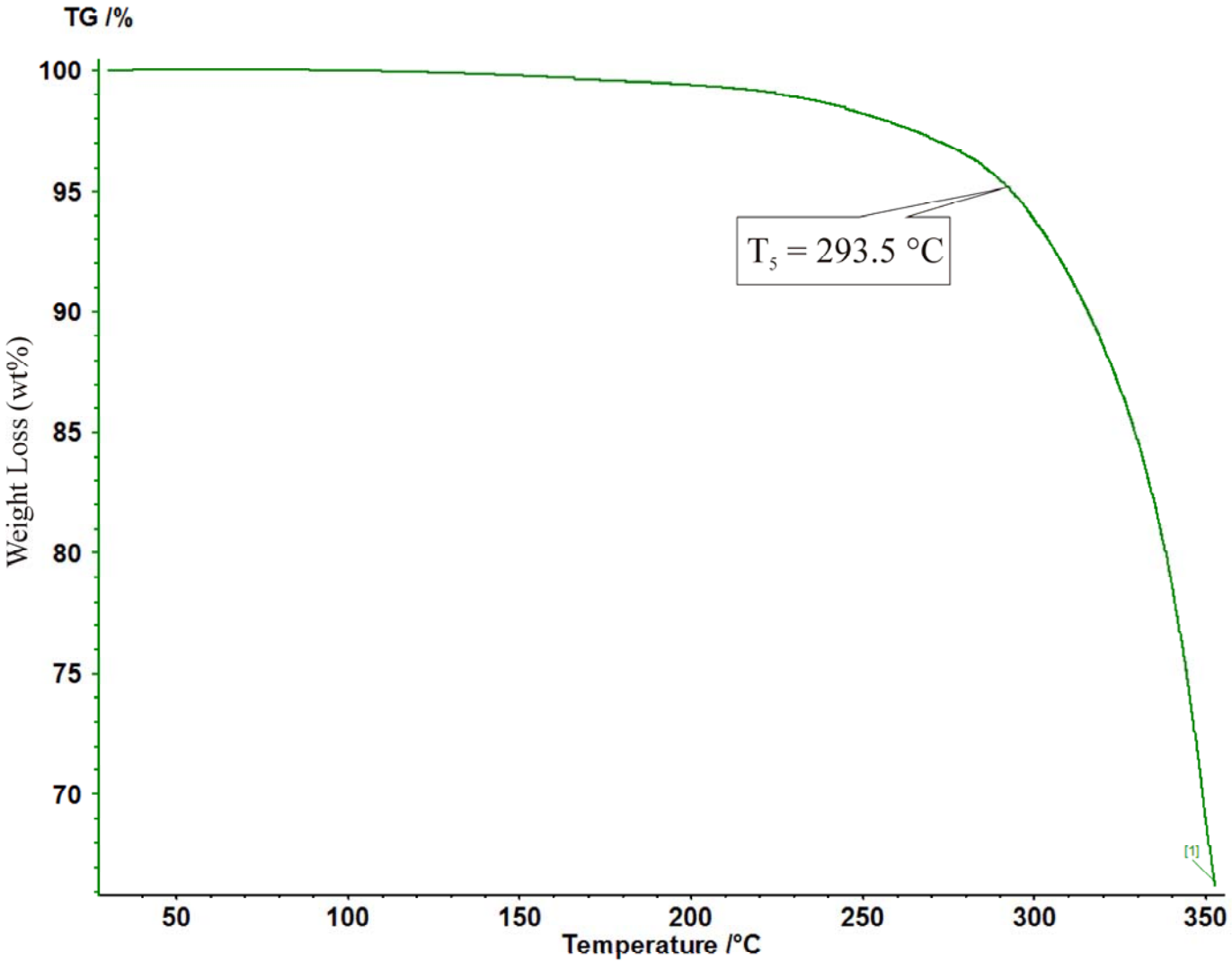

Fig. S201. Thermogravimetric analysis of the compound cone-**43**.